Fundamental Limitations on Plasma Fusion Systems Not in Thermodynamic Equilibrium

by

Todd Harrison Rider

S.M., Nuclear Engineering, MIT, 1994
S.M., Electrical Engineering and Computer Science, MIT, 1991
S.B., Electrical Engineering, MIT, 1991

Submitted to the Department of Electrical Engineering and Computer Science
in partial fulfillment of the requirements for the degree of

Doctor of Philosophy

at the

MASSACHUSETTS INSTITUTE OF TECHNOLOGY

June 1995

© Todd Harrison Rider 1995

The author hereby grants to MIT permission to reproduce
and to distribute publicly paper and electronic copies
of this thesis document in whole or in part.

Signature of Author_____
Department of Electrical Engineering and Computer Science
May 19, 1995

Certified by_____
Lawrence M. Lidsky
Professor of Nuclear Engineering
Thesis Supervisor

Accepted by_____
Frederic R. Morgenthaler
Chairman, Department Committee on Graduate Students

MASSACHUSETTS INSTITUTE
OF TECHNOLOGY

JUL 17 1995 ARCHIVES

LIBRARIES

Fundamental Limitations on Plasma Fusion Systems Not in Thermodynamic Equilibrium

by

Todd Harrison Rider

Submitted to the Department of Electrical Engineering and Computer Science
on May 19, 1995, in partial fulfillment of the
requirements for the degree of
Doctor of Philosophy

Abstract

Although there have been a few proposals for fusion reactors employing plasmas far out of thermodynamic equilibrium (such as migma and inertial-electrostatic confinement), there has never been a broad, systematic study of the entire possible range of such devices. This research fills that gap by deriving fundamental power limitations which apply to virtually any possible type of fusion reactor that uses a grossly nonequilibrium plasma. Two main categories of nonequilibrium plasmas are considered: (1) systems in which the electrons and/or fuel ions possess a significantly non-Maxwellian velocity distribution, and (2) systems in which at least two particle species, such as electrons and ions or two different species of fuel ions, are at radically different mean energies. These types of plasmas would be of particular interest for overcoming bremsstrahlung radiation losses from advanced aneutronic fuels (eg. ^{3}He-^{3}He, p-^{11}B, and p-^{6}Li) or for reducing the number of D-D side reactions in D-^{3}He plasmas. Analytical Fokker-Planck calculations are used to determine accurately the minimum recirculating power that must be extracted from undesirable regions of the plasma's phase space and reinjected into the proper regions of the phase space in order to counteract the effects of collisional scattering events and keep the plasma out of equilibrium. In virtually all cases, this minimum recirculating power is substantially larger than the fusion power, so barring the discovery of methods for recirculating the power at exceedingly high efficiencies, reactors employing plasmas not in thermodynamic equilibrium will not be able to produce net power. Consequently, the advanced aneutronic fuels cannot generate net power in any foreseeable reactor operating either in or out of equilibrium. Moreover, D-^{3}He can only produce net power when burned in thermodynamic equilibrium, which means that in any possible D-^{3}He reactor, the neutrons and tritium produced by D-D side reactions cannot be reduced below a certain level, which is calculated.

Thesis Supervisor: Lawrence M. Lidsky
Title: Professor of Nuclear Engineering

Acknowledgements

Yet each man kills the thing he loves,
  By each let this be heard,
Some do it with a bitter look,
  Some with a flattering word,
The coward does it with a kiss,
  The brave man with a sword!

Oscar Wilde, "The Ballad of Reading Gaol"
Part I, Stanza 7 (1898) [1]

For the record, the author would like to apologize for apparently killing some of the most attractive types of fusion reactors which have been proposed. He advises future graduate students working on their theses to avoid accidentally demolishing the area of research in which they plan to work after graduation.

The author is deeply indebted to P.J. Catto, who for no reason other than sheer niceness provided invaluable assistance in getting started on the analytical Fokker-Planck calculations, contributed some of the original work presented in Chapter 2, taught the author how to keep journal articles to tolerable lengths, and generally served as a very useful sounding board and sanity-checker for the rest of the thesis research.

L.M. Lidsky is to be thanked for suggesting that it might actually be possible to find fundamental limits on nonequilibrium fusion systems (rather than simply limits on particular types of nonequilibrium fusion systems) in a reasonable amount of time; that suggestion has made all the difference. On several occasions he also provided valuable services as a bodyguard in preventing the author from getting sacked.

The calculations of recirculating power for non-Maxwellian velocity distributions owe their present form to the challenging questions of T.H. Dupree, who persisted in asking questions until the author could come up with a fairly reasonable and straightforward definition of the recirculating power. (If you think it's bad now, you should have seen it before...)

P.L. Hagelstein provided very useful input, including valuable suggestions regarding the choice of model velocity distribution functions to minimize the recirculating power in Chapter 3.

Many contributions were made by L.D. Smullin, who among other things helped to keep the author's flights of fancy from diverging too far from reality.

L.L. Wood offered very helpful advice and perspective in the early stages of this work, and of course he also deserves credit for being one of the very first researchers to point out

the attractions of advanced aneutronic fuels and to propose highly innovative approaches to their use.

J.D. Galambos graciously provided a copy of his original Fokker-Planck code results for the purpose of comparison with the analytical results of Chapter 2.

Useful conversations with W.M. Nevins and D.C. Barnes are also gratefully acknowledged. These folks have offered several excellent suggestions about strange pieces of the research ranging from wave-particle interactions to the effects of anisotropic velocity distributions.

Boatloads of gratitude for proofreading and general moral support go to K.E. Wilson, C.S. Trotter Wilson, D.M. Spetman, V.M. Luchangco, and A.C. Powell.

Portions of this thesis are based on two of the author's papers, "Modification of Classical Spitzer Ion-Electron Energy Transfer Rate for Large Ratios of Ion to Electron Temperatures" and "A General Critique of Inertial-Electrostatic Confinement Fusion Systems," both of which are currently scheduled to appear in the June 1995 issue of *Physics of Plasmas*. Material from these papers has been used with the permission of the American Institute of Physics.

The author has been supported by graduate fellowships from the Office of Naval Research and the MIT Department of Electrical Engineering and Computer Science.

Finally, the author would like to acknowledge his parents, without whom he would not have been possible.

Contents

List of Figures

List of Tables

Chapter 1

Introduction

In order to make candidate fusion reactors more acceptable to the public and the electric utility industry, it has been suggested to use advanced fusion fuels instead of the traditional deuterium-tritium (D-T) or pure deuterium (D-D) cycles [2−21]. Advanced-fuel reactions of interest include deuterium–helium-3 (D-^{3}He), helium-3–helium-3 (^{3}He-^{3}He), proton–boron-11 (p-^{11}B), and proton–lithium-6 (p-^{6}Li); these fuels would produce much less neutron radiation and involve much smaller total radioactive inventories than D-T and D-D. Also, since virtually all of these fuels' reaction products would be charged, it may be possible to convert the fusion product energy directly into electrical energy at very high efficiencies (> 80%) instead of having to do the conversion with a thermal cycle at only about 30-40% efficiency.

Unfortunately, plasmas in or fairly close to thermodynamic equilibrium are not able to reduce the undesirable D-D side reactions from a D-^{3}He plasma below a certain level [11, 12], and equilibrium plasmas are not even able to produce net power with the more advanced aneutronic fuels [12, 22]. Because the properties of plasmas far out of thermodynamic equilibrium (ie. with highly non-Maxwellian velocity distributions or particle species at radically different mean energies) have not been systematically studied in the

past, the principal object of the present investigation is to determine the fundamental limitations which apply to all types of reactors employing nonequilibrium plasmas and then to examine whether it is feasible to improve the performance of D-^{3}He or advanced aneutronic fuel reactors by utilizing plasmas not in thermodynamic equilibrium.

1.1 Background Information

Considering the complexity of the fusion problem and the long and difficult history of fusion research, fusion reactors will probably be much more technologically sophisticated than fission reactors and thus may have trouble competing on a solely economic basis. Because of this likely disadvantage, it would be best if fusion reactors could boast of better performance than fission reactors in terms of virtually all other characteristics. One of the most important of these characteristics is neutron production, since neutrons can activate structural materials, degrading them and ultimately converting them into high-level radioactive waste, which necessitates difficult and costly removal and disposal practices [13, 14, 23]. The neutrons from a fusion reactor could also be used to make weapons-grade nuclear material, rendering such types of fusion reactors serious nuclear proliferation hazards. A related problem is the presence of radioactive elements such as tritium in the plasma, either as fuel for or as products of the nuclear reactions; substantial quantities of radioactive elements would not only pose a general health risk, but tritium in particular would also be another proliferation hazard. The problems of neutron radiation and radioactive element production are especially interconnected because both would result from D-D fusion (roughly half of the fusion events would lead to a neutron-producing branch and the other half would result in a tritium-producing branch).

Therefore, one figure of merit for the performance of a fusion reactor is the percentage of its total power which is produced as neutron kinetic energy, as compared with the amount of a fission reactor's total power which is produced in the form of neutrons. On average the fission of ^{235}U yields approximately 210 MeV, of which about 5 MeV is neutron

kinetic energy [24]. Thus for fission, the neutron power fraction is $P_{neutrons}/P_{total} \approx$ 2%. It would be highly desirable for fusion reactors to achieve a neutron power fraction substantially smaller than this value. While this is not the only or even necessarily the primary criterion to use in evaluating fusion approaches, it is certainly an important item to consider.

Because of the twin considerations of neutrons and radioactive elements, it has been felt for some time that D-T and D-D fusion reactors may not be sufficiently attractive for the public and the electric utility industry [13, 14]. Both fuel mixtures produce neutrons in such copious quantities ($P_{neutrons}/P_{total} \approx 80\%$ for D-T and at least approximately 40% for D-D [12]) that the central components of reactors employing these fuels might have to be replaced quite often [23], at great inconvenience and cost. In addition, these reactors would involve the presence of large amounts of tritium, since D-T reactions run on it and D-D reactions produce it.

D-^{3}He, ^{3}He-^{3}He, p-^{11}B, and p-^{6}Li fuels have all been proposed as much cleaner alternatives [2, 3, 10, 11, 12, 14], but because they require higher ion temperatures than D-T, the performance of reactors using these fuels is subject to much tighter constraints. The most important factor which limits the performance of these fuels in equilibrium plasmas is the bremsstrahlung radiation from the electrons, which is caused by electrons colliding with ions or with other electrons. Energy losses due to escaping particles can theoretically be rendered manageable by improving the confinement system. Similarly, synchrotron radiation losses can in principle be limited to acceptable levels by choosing magnetic field geometries which avoid the use of strong magnetic fields within most of the inner volume of the plasma (eg. configurations with multipoles [10], strong plasma diamagnetism [18], or ring magnets [25]), as well as by reflecting the synchrotron radiation back into the plasma and reabsorbing it there. In contrast, little can be done about bremsstrahlung losses from plasmas in thermodynamic equilibrium (apart from attempting to convert the radiation into electric power at low thermal efficiencies), since the frequency range of the radiation is not conducive to reflection or efficient direct electric conversion, and

both magnetic fusion and inertial confinement fusion plasmas are optically thin to the bremsstrahlung they emit.

The impact of bremsstrahlung losses on equilibrium fusion plasmas may be seen by performing a simple calculation. (For more details of this calculation, see Chapters 6 and 7.) The rate of energy transfer between ions and electrons, P_{ie}, may be determined by using a modified version of the usual Spitzer rate [26, 27],

$$P_{ie} = 7.61 \cdot 10^{-28} n_e \sum_i \frac{Z_i^2 n_i \ln \Lambda}{\mu_i T_e^{3/2}} \left(1 + \frac{m_e}{m_i}\frac{T_i}{T_e}\right)^{-3/2} \left(1 + \frac{0.3T_e}{m_e c^2}\right) (T_i - T_e) \, \frac{\text{Watts}}{\text{cm}^3} \, , \tag{1.1}$$

which accounts for relativistic effects [11, 28, 29] and the possibility that the ion energies may be much larger than the electron energies. The conventions which have been used in the above formula are that temperatures T and the electron rest energy $m_e c^2$ are in eV, the ion mass $m_i \equiv \mu_i m_p$ has been expressed in terms of the proton mass m_p, and the density n is in cm^{-3}. The Coulomb logarithm is given by $\ln \Lambda \approx [24 - \ln(\sqrt{n_e}/T_e)]$ (see [30]) and varies from about 5 for inertial confinement fusion (ICF) plasmas up to approximately 20 for some magnetic confinement plasmas.

For the purposes of making an optimistic calculation of the minimum power loss, sources of electron heating other than Coulomb friction with the ions will be neglected. One should realize, however, that in a realistic reactor, the electrons would also be heated by external heating systems, friction with fusion products, and other sources. As a result, the electron temperatures and bremsstrahlung radiation losses will be larger than are computed below.

The bremsstrahlung loss power density, including relativistic corrections [12, 31], is

$$P_{brem} = 1.69 \cdot 10^{-32} n_e^2 \sqrt{T_e} \left\{ \frac{\sum_i Z_i^2 n_i}{n_e} \left[1 + .7936 \frac{T_e}{m_e c^2} + 1.874 \left(\frac{T_e}{m_e c^2}\right)^2\right] + \frac{3}{\sqrt{2}} \frac{T_e}{m_e c^2} \right\} \frac{\text{Watts}}{\text{cm}^3} \, . \tag{1.2}$$

If there is no other energy loss mechanism for the electrons, the minimum loss incurred by them will be due to bremsstrahlung radiation, so one may set $P_{ie} = P_{brem}$ to find the equilibrium electron temperature T_e. (Because of these assumptions, the reactor plasma will be in what has previously been described as the "hot ion mode" [32].) The resulting value for the bremsstrahlung loss may be compared with the fusion power P_{fus} for the case in which there are two fuel ion species $i1$ and $i2$ with $Z_{i1} \equiv 1$ and $x \equiv n_{i1}/n_{i2}$:

$$\begin{aligned} P_{fus} &= 1.602 \cdot 10^{-19} n_{i1} n_{i2} \langle \sigma v \rangle_{fus} E_{fus} \frac{\text{Watts}}{\text{cm}^3} \\ &= 1.602 \cdot 10^{-19} \frac{x}{(x + Z_{i2})^2} n_e^2 \langle \sigma v \rangle_{fus} E_{fus} \frac{\text{Watts}}{\text{cm}^3} , \end{aligned} \tag{1.3}$$

where $\langle \sigma v \rangle_{fus}$ is the average fusion reactivity (fusion cross section times net collision velocity) in cm^3/sec and E_{fus} is the energy (in eV) released per fusion event.

If there is only one ion species then in Eq. (1.3) one should make the substitution,

$$\frac{x}{(x + Z_{i2})^2} \rightarrow \frac{1}{2Z_i^2} . \tag{1.4}$$

Thus it is found that the bremsstrahlung losses for various fuels under approximately optimum conditions are as given in Table 1.1.

Fuel mixture	T_i	T_e	$\langle \sigma v \rangle_{fus}$ (in 10^{-16} cm^{-3}/s)	E_{fus}	$\frac{P_{neutrons}}{P_{fus}}$	$\frac{P_{brem}}{P_{fus}}$
D-T (1:1)	50 keV	42 keV	8.54	17.6 MeV	0.80	0.007
D-^{3}He (1:1)	100 keV	73 keV	1.67	18.3 MeV	0.01	0.19
D-D	500 keV	209 keV	1.90	3.7 MeV	0.36	0.35
^{3}He-^{3}He	1 MeV	274 keV	1.25	12.9 MeV	–	1.39
p-^{11}B (5:1)	300 keV	137 keV	2.39	8.7 MeV	–	1.74
p-^{6}Li (3:1)	800 keV	256 keV	1.60	4.0 MeV	–	4.81

Table 1.1: Bremsstrahlung losses for various fusion fuels with $\ln \Lambda = 15$ and fusion cross section data drawn from references [33], [34], [35], and [36].

From the results shown in the table, one may see that the bremsstrahlung loss under optimum conditions is insignificant for D-T, but it becomes appreciable for D-^{3}He and D-D and is prohibitively large for the advanced aneutronic fuels. The Coulomb logarithm was chosen to be 15, which is the smallest value which can reasonably be expected in a magnetic fusion device, although variations of the Coulomb logarithm over its entire range (5-20) only affect the electron temperatures and bremsstrahlung loss fractions by a fairly small amount. (See Chapters 6 and 7 for more detailed calculations.)

In the table it has been assumed that the fusion products are somehow removed before they undergo any further reactions, in order to prevent possible neutron production from reactions of daughter nuclei. Leaving the fusion products in the plasma would appreciably alter the performance of only three of the fuels. The results for D-^{3}He would be improved slightly and the performance of D-D would be improved to a much greater extent by burning up the T and ^{3}He produced by D-D reactions, but then considerable numbers of very unpleasant 14-MeV neutrons would be generated by D-T reactions in the plasma for both D-^{3}He and D-D fuels. Similarly, the performance of p-^{6}Li would be improved considerably by burning the produced ^{3}He with the ^{6}Li or with exogenous D, but even so the system would not be able to break even against realistic losses. (Complete burnup of the ^{3}He produced by p-^{6}Li could effectively increase the value of E_{fus} in Table 1.1 by $\sim 17 - 18$ MeV [12], which in an absolutely ideal system would enable the fusion power to exceed the bremsstrahlung slightly; however, for the operation of a realistic system with many other power loss mechanisms, one would need the bremsstrahlung loss to be substantially less than the total fusion power.)

D-^{3}He would be a fairly attractive fuel for fusion reactors, since for a 1:1 fuel mixture D-D side reactions would cause only about 1% of the total fusion power to be produced in neutrons and would produce tritium at only a fairly modest rate. Of course, since this neutron power fraction is still comparable to that of fission reactors, it would be desirable to reduce the problems associated with the D-D side reactions even further if possible, but this cannot be accomplished in a plasma in thermodynamic equilibrium. By the very

equilibrium nature of the plasma, the deuteron temperature cannot be made substantially lower than the helium-3 temperature in order to cut down on the D-D reactions. Furthermore, although the D-D reactions could be significantly reduced by operating with a large excess of ^{3}He, this technique would unfortunately cause the bremsstrahlung radiation losses and other losses to exceed the fusion power.

The advanced aneutronic fuels, ^{3}He-^{3}He, p-^{11}B, and p-^{6}Li, would be even more attractive for use in reactors, as they would produce essentially no neutrons through direct reactions (although one would still have to consider low-level neutron production via photo-ejection or fast-fusion-product-induced ejection of neutrons from reactor structural materials). The unfortunate fact that the advanced aneutronic fuels cannot produce net power when burned in thermodynamic equilibrium, as illustrated in Table 1.1, was first observed over a decade ago [12, 22].

Because plasmas in thermodynamic equilibrium cannot burn advanced aneutronic fuels or reduce the D-D side reactions in D-^{3}He systems below a certain level, there have been several proposals to use reactors in which the ions and/or electrons are significantly non-Maxwellian or in which the mean energies of two particle species in the plasma (eg. ions and electrons or two species of fuel ions) are significantly different from each other. Particular proposals for such nonequilibrium fusion systems include inertial-electrostatic confinement fusion [18, 19, 37], migma [15, 16, 38, 39], and other ideas [4, 13, 40, 41]. While the specific details of the proposed schemes vary, it is worthwhile to explore the general limitations imposed on systems which deviate from thermodynamic equilibrium in these ways; the properties and limitations of these types of systems have not previously been examined in much detail, let alone in a broad, systematic fashion. After finding the general constraints on nonequilibrium plasma systems, it will be determined whether reactors operating within those limits can offer significantly improved performance with D-^{3}He or advanced aneutronic fuels.

1.2 Simplifying Assumptions and Conventions Used in the Thesis

Certain simplifying assumptions are made for the purpose of performing this analysis. The assumptions, together with the reasons why they are made, are outlined below, and they are utilized throughout the thesis except where explicitly noted otherwise.

- In comparing collisional scattering effects, fusion, and bremsstrahlung with each other, the density, spatial density profiles, and plasma volume do not matter, since all of these phenomena are two-body effects and thus are proportional to $\int d^3\mathbf{x}[n(\mathbf{x})]^2$ (neglecting the weak density dependence of the Coulomb logarithm).

- The regions of the plasma which have values of $\int d^3\mathbf{x}[n(\mathbf{x})]^2$ large enough to be of interest are approximately isotropic. If they are anisotropic, one must deal with counterstreaming [42], Weibel [43, 44], and other instabilities, so it is preferred to avoid significant anisotropy in these regions. (However, the potential utility of anisotropic systems, assuming that they can somehow actually avoid instabilities, will be examined later in the thesis.)

- Although instabilities can prove to be a serious concern even in nonthermal plasmas which are essentially isotropic, the effects of instabilities will not be taken into account in any of the calculations. Because of this choice, the results represent an optimistic bound on the performance of plasma fusion systems which operate out of thermodynamic equilibrium. Due to instabilities and other defects not considered here, actual nonequilibrium systems will be more difficult to maintain and will offer poorer performance.

- Spatial variations of temperature and energy may be neglected in the regions of significant $\int d^3\mathbf{x}[n(\mathbf{x})]^2$. (The potential usefulness of systems which violate this assumption will also be checked eventually.)

- In calculating bremsstrahlung rates, the plasma is assumed to be quasineutral and optically thin to bremsstrahlung. (The thesis will later return to these assumptions and consider systems which violate them.)

- The functional dependence of $\langle \sigma v \rangle_{fus}$ on the mean ion energy $\langle E_i \rangle$ will be assumed to be approximately independent of the precise shape of the ion velocity distribution function (Maxwellian, monoenergetic, etc.) provided that the distributions are isotropic and the two ion species (if there are in fact two separate fuel ion species) both have that same mean energy. This assumption is justified, as shown explicitly in Appendix A for particular distribution shapes. Even if the distributions are not Maxwellian (because of nuclear elastic scattering [10], active shaping of the velocity distributions, or other phenomena), the fusion reactivity must still be averaged over all angles, a process which leads to very nearly the same answer as averaging over Maxwellian distributions.

Fusion fuels other than those listed in Table 1.1 will not be considered in the calculations presented in this thesis, although the calculations could readily be performed for other fuels if desired. The three most commonly suggested fuels which are not examined, together with the reasons why they are not investigated here, are as follows:

- **D-^{6}Li** – This fuel is roughly as difficult to burn as p-^{11}B [12], yet it produces substantially more neutrons, both from D-D side reactions and also certain D-^{6}Li reactions which directly produce neutrons.

- **p-^{7}Li** – The cross section for this reaction is far too low except possibly for $T_i > 1$ MeV [34], but at such high temperatures an endothermic, direct neutron-producing reaction also becomes very significant [30].

- **p-^{9}Be** – Not only is this fuel mixture very difficult to burn, but also ^{9}Be is infamous for the ease with which it can be induced to disintegrate into a neutron plus two alpha particles. (See [12] and [34] for more information.)

By convention, all quantities in the thesis are in cgs units, with energies and temperatures both measured in ergs, unless otherwise stated. Temperatures and energies will frequently be converted into eV, but it will be noted when this is done.

In order for it to be explicitly obvious that certain portions of the work apply to non-Maxwellian distributions as well as Maxwellian distributions, ions and electrons will often be characterized by mean particle energies rather than temperatures. For comparisons with prior experience, the reader may find it preferable in these cases to think in terms of a "temperature" of $T \equiv 2\langle E \rangle /3$, where $\langle E \rangle$ is the mean particle energy.

Ion masses m_i will frequently be given in terms of the proton mass m_p, so that $\mu_i \equiv m_i/m_p$.

1.3 Overview of Material to be Presented

The presentation of material will commence with the consideration of methods for reducing the rate of energy transfer between ions and electrons in order to lower the mean electron energy and bremsstrahlung losses. Since on average an ion colliding with an electron will give energy to the electron only when the electron is moving more slowly than the ion, one obvious method of reducing ion-electron energy transfer is to deplete electrons in the low-speed part of the electron distribution function. To some extent this effect happens in a "passive" natural manner because the slow electrons that directly receive energy from ions are thereby promoted to higher velocities; this phenomenon becomes more pronounced as the ion temperature T_i becomes much greater than the electron temperature T_e.

A simple calculation of this effect was done by Rosenbluth for the case of electrons in the presence of one Maxwellian ion species with $T_i \sim T_e$ [45, 46]. However, Rosenbluth's calculation does not apply to cases in which $T_i \gg T_e$, more than one ion species is present, or the ions are significantly non-Maxwellian. Because this effect provides a "no cost" method of reducing ion-electron energy transfer (provided that the ions are substantially

more energetic than the electrons) and the magnitude of the potential benefit from the effect for $T_i \gg T_e$ has not previously been determined, a detailed analytical treatment of the problem will be presented in Chapter 2. The derivation of Chapter 2 will extend to those cases not covered by Rosenbluth's derivation, namely situations involving $T_i \gg T_e$, multiple ion species, and non-Maxwellian ion distributions. The material in Chapter 2 will also serve as an introduction to the analytical Fokker-Planck methods to be employed again in Chapter 3.

Chapter 3 is really the centerpiece of this entire thesis. In it will be derived the minimum power requirements imposed on any system which attempts to actively (rather than passively, as in Chapter 2) deplete the slow electrons and thus reduce the ion-electron energy transfer rate. However, the machinery set up in Chapter 3 can also be applied to other problems involving non-Maxwellian distribution functions, and so the chapter will explore one of the most important of these other issues, specifically the minimum power requirements of any system which maintains ions or electrons in an isotropic but beamlike state with a given thermal velocity spread.

An overall evaluation of the effectiveness of various methods to "decouple" the ion and electron energies and lower the mean electron energy will be given in Chapter 4. These methods include the passive and active depletion of slow electrons discussed in Chapters 2 and 3 respectively, along with all other techniques that have been proposed to date.

Chapter 5 will deal with energy decoupling between two fuel ion species. Such an effect would be particularly useful, for instance, for suppressing D-D side reactions from D-^{3}He plasmas by keeping the deuterons at lower energies than the helium-3 ions. As another example, decoupling between ion species might also be useful for boosting the fusion rate in p-^{11}B plasmas by using high-energy protons and very low-energy boron ions to operate within the narrow maximum resonance peak of the reaction cross section. The effectiveness of all known techniques for possibly maintaining two fuel ion species at substantially different mean energies will be examined.

Once the general constraints on nonequilibrium plasma systems have been determined,

the potential usefulness of such systems for improving the performance of D-^{3}He or the advanced aneutronic fuels will be examined. For example, if it were possible to keep the electrons of an advanced aneutronic fuel plasma at much lower energies than they would otherwise have, fuels like p-^{11}B and ^{3}He-^{3}He would be able to produce net power despite bremsstrahlung losses; this issue will be confronted in Chapter 6. Furthermore, devices capable of maintaining nonequilibrium plasmas might allow the D-D side reactions in D-^{3}He reactors to be greatly suppressed by either reducing the bremsstrahlung losses from ^{3}He-rich plasmas or by permitting the deuterons to be kept at much lower energies than the ^{3}He ions. This problem will be addressed in Chapter 7.

One of the most striking features of Dante's *Inferno* [47] (apart from its big-name cast) was the extreme temperature differences between the different circles of hell. As the ultimate goal of this project is to maintain similarly large temperature differences between the ions and electrons or between two ion species within the plasma in order to improve the performance of aneutronic fuels, the project has been dubbed INFERNO – Interspecies Nonclassical Flow of Energy for Reduced Neutron Output. (The name also alludes to the painful difficulty of the task and the calculations involved.)

Chapter 2

Modification of Ion-Electron Energy Transfer Rate For Large Ratios of Ion to Electron Temperatures

Rosenbluth [45, 46] has shown that natural interactions of electrons with ions tend to cause a passive depletion of some of the slow electrons which promote ion-electron energy transfer, thereby decreasing the ion-electron energy transfer rate from its classical Spitzer value [26, 27]. However, Rosenbluth's derivation assumed that the ions were Maxwellian, the electrons were nearly Maxwellian, and the ion thermal velocity was much less than the electron thermal velocity. The object of this chapter is to broaden the scope of the derivation to cover even highly non-Maxwellian distribution functions and temperature regimes in which the mean ion velocity starts to approach the average electron velocity.

In addition to being a useful addition to the fundamental plasma physics knowledge regarding ion-electron energy transfer, a better understanding of this phenomenon has im-

portant practical applications. If the ion-electron energy transfer could be reduced appreciably from the classical Spitzer value, the electron temperature, and thus bremsstrahlung and synchrotron radiation losses, would be substantially reduced, and as a result the performance of fusion reactors (especially advanced fuel reactors) would be significantly improved.

Before the main results of the paper are presented, Section 2.1 will offer a brief and fairly intuitive look at the ion-electron energy transfer problem. Then Section 2.2 will present much more detailed and rigorous calculations which should give a good description of the problem under a wide array of possible conditions (eg. various types of ion velocity distributions, temperature ranges, etc.). Finally, Sections 2.3 and 2.4 will apply these general results to the specific cases in which the ion distributions are Maxwellian and monoenergetic, respectively, and derive simple approximate answers as well as more accurate analytical results.

2.1 Preliminary Estimate of the Effect

Before presenting a detailed analysis of the ion-electron energy transfer problem, it is worthwhile to consider the more qualitative results offered by a much simpler model.

The energy exchange time between a test particle of velocity v and background particles with a Maxwellian velocity distribution characterized by the thermal velocity $v_t' \equiv \sqrt{2T'/m'}$ is defined [27] as

$$t_E \equiv \frac{m^2 v^3}{16\pi Z^2 Z'^2 e^4 n' \ln\Lambda} \frac{(v/v_t')^2}{[\mathrm{erf}\,(v/v_t') - (v/v_t')\mathrm{erf}'\,(v/v_t')]}\,, \tag{2.1}$$

in which the error function is

$$\mathrm{erf}(w) \equiv \frac{2}{\sqrt{\pi}} \int_0^w e^{-y^2} dy\,, \tag{2.2}$$

the definition $\mathrm{erf}'(x) \equiv d[\mathrm{erf}(x)]/dx$ has been made, and in all other cases the primes denote the background particles as opposed to the test particle.

One finds the following electron-ion collision time t_E^{ei} and electron-electron collision time t_E^{ee} for electrons of velocity v in the limit $v_{ti} \ll v \ll v_{te}$:

$$t_E^{ei} \equiv \frac{m_e^2 v^3}{16\pi Z_i^2 e^4 n_i \ln\Lambda} \frac{v^2}{v_{ti}^2} ; \tag{2.3}$$

$$t_E^{ee} \equiv \frac{m_e^2 v^3}{16\pi e^4 n_e \ln\Lambda} \frac{3\sqrt{\pi} v_{te}}{4v} . \tag{2.4}$$

In the case of electrons for which $t_E^{ei} < t_E^{ee}$, collisions with the ions will tend to have a greater effect than collisions with the faster electrons. As may be seen from the energy exchange times, this constraint is satisfied for electrons whose speeds are less than a certain critical velocity v_c,

$$v^3 < \frac{3\sqrt{\pi}}{4} \frac{Z_i^2 n_i}{n_e} v_{ti}^2 v_{te} \equiv v_c^3 . \tag{2.5}$$

Now the form of the modification to the Spitzer heat transfer rate may be obtained in a straightforward and intuitive manner. The power transferred from the ions to the electrons is essentially proportional to the number of electrons moving more slowly than the ions. Since it is assumed that $v_{ti} \ll v_{te}$, the energy transfer rate P_{ie} will be proportional to $f_e(0)$, the value of the electron velocity distribution at $v = 0$.

For $v > v_c$ electron-electron collisions dominate and the electron distribution assumes what is essentially its usual Maxwellian distribution,

$$f_e(v) \propto \exp\left(-\frac{v^2}{v_{te}^2}\right) \qquad (\text{for } v > v_c) . \tag{2.6}$$

On the other hand, below the critical velocity the dominance of collisions with ions tends to upscatter some of the electrons to higher energies and thereby flatten out the

electron distribution at a constant value, namely its value at the critical velocity:

$$f_e(v) \propto \exp\left(-\frac{v_c^2}{v_{te}^2}\right) \qquad \text{(for } v < v_c\text{)}. \tag{2.7}$$

Since $P_{ie} \propto f_e(0)$, one may see that the actual heat transfer rate in comparison with its classical Spitzer value is

$$\begin{aligned} \frac{P_{ie}}{(P_{ie})_{Spitzer}} &= \exp\left(-\frac{v_c^2}{v_{te}^2}\right) \\ &= \exp\left\{-\left(C\frac{Z_i^2 n_i}{n_e}\frac{m_e}{m_i}\frac{T_i}{T_e}\right)^{2/3}\right\}. \end{aligned} \tag{2.8}$$

While the above calculation yields a value of $C = 3\sqrt{\pi}/4$, the true value of C cannot be found from this simple calculation. This limitation is caused by the uncertainty in the precise velocity at which the electron distribution may be considered to flatten out. All that can be said for now is that C appears to be a constant of order unity.

Having taken this first enlightening look at the problem, one may now appeal to more detailed calculations to ascertain the accuracy of this initial computation, determine the actual value of C, and extend the analysis to other cases not covered in this simple example.

It should be remarked from the outset that only collisional interspecies energy transfer will be considered. Various instabilities which might be driven by substantial deviations of the plasma from thermodynamic equilibrium and which would further promote energy transfer will be ignored; thus these calculations will serve to set a lower bound on the ion-electron energy transfer rate.

2.2 General Description of Interspecies Energy Transfer

In this section will be presented a description of how the Fokker-Planck collision operator may be applied to the present problem in order to obtain the equilibrium particle distribution functions and the interspecies energy exchange rate.

2.2.1 Rosenbluth Potentials for General Isotropic Distributions

Consider the distribution function f_α for a given particle species α; the distribution function is normalized such that

$$\int d^3\mathbf{v} f_\alpha(\mathbf{v}) = n_\alpha \, . \tag{2.9}$$

As presented by Rosenbluth [48, 49], the collisionally induced evolution of the particle distribution functions is governed by the Fokker-Planck equation,

$$\frac{\partial f_\alpha}{\partial t} + \mathbf{v}\cdot\nabla_{\mathbf{x}} f_\alpha + \frac{Z_\alpha e}{m_\alpha}\left(\mathbf{E} + \frac{1}{c}\mathbf{v}\times\mathbf{B}\right)\cdot\nabla_{\mathbf{v}} f_\alpha = \left(\frac{\partial f_\alpha}{\partial t}\right)_{col} \, . \tag{2.10}$$

The Fokker-Planck collision operator in the above equation is given by

$$\begin{aligned}\left(\frac{\partial f_\alpha}{\partial t}\right)_{col} &= -\sum_\beta \Gamma_{\alpha\beta}\nabla_{\mathbf{v}}\cdot\left[f_\alpha\nabla_{\mathbf{v}}h_{\alpha\beta} - \frac{1}{2}\nabla_{\mathbf{v}}\cdot\left(f_\alpha\nabla_{\mathbf{v}}\nabla_{\mathbf{v}}g_{\alpha\beta}\right)\right] \\ &\equiv \sum_\beta C_{\alpha\beta} \equiv -\nabla_{\mathbf{v}}\cdot\sum_\beta \mathbf{J}_{\alpha\beta} \, ,\end{aligned} \tag{2.11}$$

in which $C_{\alpha\beta}$ is the collision operator just between two species α and β, $\mathbf{J}_{\alpha\beta}$ is the collisional velocity-space particle flux, the sums over all β include $\beta = \alpha$,

$$\Gamma_{\alpha\beta} \equiv \frac{4\pi Z_\alpha^2 Z_\beta^2 e^4 \ln\Lambda}{m_\alpha^2}, \tag{2.12}$$

and the Rosenbluth potentials $h_{\alpha\beta}$ and $g_{\alpha\beta}$ are defined as:

$$h_{\alpha\beta}(\mathbf{v}) \equiv \frac{m_\alpha + m_\beta}{m_\beta}\int d^3\mathbf{u}\frac{f_\beta(\mathbf{u})}{|\mathbf{v}-\mathbf{u}|} \, ; \tag{2.13}$$

$$g_{\alpha\beta}(\mathbf{v}) \equiv \int d^3\mathbf{u} f_\beta(\mathbf{u})|\mathbf{v}-\mathbf{u}| \,, \tag{2.14}$$

with the useful relation

$$h_{\alpha\beta} = \left(\frac{m_\alpha + m_\beta}{2m_\beta}\right) \nabla_v^2 g_{\alpha\beta} \,. \tag{2.15}$$

For isotropic velocity distributions, the Rosenbluth potentials (2.13) and (2.14) may be integrated over all angles in velocity space as follows (θ is the angle between $\mathbf{u}$ and $\mathbf{v}$) [50]:

$$\begin{aligned} h_{\alpha\beta}(\mathbf{v}) &= 2\pi \frac{m_\alpha + m_\beta}{m_\beta} \int \frac{f_\beta(u) u^2 \sin\theta \, du \, d\theta}{\sqrt{u^2+v^2-2uv\cos\theta}} \\ &= 2\pi \frac{m_\alpha + m_\beta}{m_\beta} \left[\int \frac{du u^2 f_\beta(u) \sqrt{u^2+v^2-2uv\cos\theta}}{uv} \right]_0^\pi \\ &= \frac{m_\alpha + m_\beta}{m_\beta} \int_0^\infty (du 4\pi u^2) f_\beta(u) \left[\frac{u\Theta(v-u) + v\Theta(u-v)}{uv} \right] \\ &= 4\pi \left(\frac{m_\alpha + m_\beta}{m_\beta}\right) \left[\int_0^v du f_\beta(u) \left(\frac{u^2}{v} - u\right) + \int_0^\infty du f_\beta(u) u \right] \,, \end{aligned} \tag{2.16}$$

in which $\Theta(x)$ is the Heaviside unit step function.

Similarly, one finds that

$$\begin{aligned} g_{\alpha\beta}(\mathbf{v}) &= 2\pi \int f_\beta(u) \sqrt{u^2+v^2-2uv\cos\theta} u^2 \sin\theta du d\theta \\ &= 2\pi \left[\int \frac{du u^2 f_\beta(u) (u^2+v^2-2uv\cos\theta)^{3/2}}{3uv} \right]_0^\pi \\ &= \frac{1}{3} \int_0^\infty (du 4\pi u^2) f_\beta(u) \left[\frac{u(u^2+3v^2)\Theta(v-u) + v(v^2+3u^2)\Theta(u-v)}{uv} \right] \\ &= \frac{4\pi}{3} \left[\int_0^v du f_\beta(u) \left(\frac{u^4}{v} + 3u^2 v - 3u^3 - uv^2 \right) + \int_0^\infty du f_\beta(u) (uv^2 + 3u^3) \right] \,. \end{aligned} \tag{2.17}$$

The following derivatives of the Rosenbluth potentials are also needed for the calcu-

lations presented in this paper:

$$\frac{\partial h_{\alpha\beta}}{\partial v} = -4\pi \left(\frac{m_\alpha + m_\beta}{m_\beta} \right) \frac{1}{v^2} \int_0^v du f_\beta(u) u^2 \; ; \tag{2.18}$$

$$\begin{aligned} \frac{\partial^2 g_{\alpha\beta}}{\partial v^2} &= \frac{\partial}{\partial v} \frac{4\pi}{3} \left[\int_0^v du f_\beta(u) \left(3u^2 - \frac{u^4}{v^2} - 2uv \right) + 2v \int_0^\infty du f_\beta(u) u \right] \\ &= \frac{8\pi}{3} \left[\frac{1}{v^3} \int_0^v du f_\beta(u) u^4 + \int_v^\infty du f_\beta(u) u \right] . \end{aligned} \tag{2.19}$$

2.2.2 Interspecies Energy Transfer Rate

The rate of energy transfer per volume from the α species to the β species is defined to be $P_{\alpha\beta}$:

$$P_{\alpha\beta} = - \int d^3\mathbf{v} \left(\frac{1}{2} m_\alpha v^2 \right) C_{\alpha\beta} \, . \tag{2.20}$$

By using the definition of the Fokker-Planck collision operator and integrating by parts, one finds

$$\begin{aligned} P_{\alpha\beta} &= \frac{1}{2} m_\alpha \Gamma_{\alpha\beta} \int d^3\mathbf{v} v^2 \nabla_\mathbf{v} \cdot \left[f_\alpha \nabla_\mathbf{v} h_{\alpha\beta} - \frac{1}{2} \nabla_\mathbf{v} \cdot (f_\alpha \nabla_\mathbf{v} \nabla_\mathbf{v} g_{\alpha\beta}) \right] \\ &= -\frac{1}{2} m_\alpha \Gamma_{\alpha\beta} \int d^3\mathbf{v} \left[f_\alpha \nabla_\mathbf{v} v^2 \cdot \nabla_\mathbf{v} h_{\alpha\beta} - \frac{1}{2} \nabla_\mathbf{v} v^2 \cdot \nabla_\mathbf{v} \cdot (f_\alpha \nabla_\mathbf{v} \nabla_\mathbf{v} g_{\alpha\beta}) \right] \\ &= -\frac{1}{2} m_\alpha \Gamma_{\alpha\beta} \int d^3\mathbf{v} \left[2 f_\alpha \mathbf{v} \cdot \nabla_\mathbf{v} h_{\alpha\beta} - \mathbf{v} \cdot \nabla_\mathbf{v} \cdot (f_\alpha \nabla_\mathbf{v} \nabla_\mathbf{v} g_{\alpha\beta}) \right] \\ &= -\frac{1}{2} m_\alpha \Gamma_{\alpha\beta} \int d^3\mathbf{v} \left[2 f_\alpha \mathbf{v} \cdot \nabla_\mathbf{v} h_{\alpha\beta} + f_\alpha \nabla_v^2 g_{\alpha\beta} \right] \\ &= -m_\alpha \Gamma_{\alpha\beta} \int d^3\mathbf{v} f_\alpha \left[\mathbf{v} \cdot \nabla_\mathbf{v} h_{\alpha\beta} + \left(\frac{m_\beta}{m_\alpha + m_\beta} \right) h_{\alpha\beta} \right] . \end{aligned} \tag{2.21}$$

For isotropic velocity distributions the energy transfer becomes

$$
\begin{aligned}
P_{\alpha\beta} &= -m_\alpha \Gamma_{\alpha\beta} \int_0^\infty (dv 4\pi v^2) f_\alpha \left[v \frac{\partial h_{\alpha\beta}}{\partial v} + \left(\frac{m_\beta}{m_\alpha + m_\beta} \right) h_{\alpha\beta} \right] \\
&= -16\pi^2 m_\alpha \Gamma_{\alpha\beta} \int_0^\infty dv v^2 f_\alpha \left[-\left(\frac{m_\alpha + m_\beta}{m_\beta} \right) \frac{1}{v} \int_0^v du f_\beta(u) u^2 + \frac{1}{v} \int_0^v du f_\beta(u) u^2 \right. \\
&\qquad \left. + \int_v^\infty du f_\beta(u) u \right] \\
&= 64\pi^3 Z_\alpha^2 Z_\beta^2 e^4 \ln\Lambda \int_0^\infty dv v^2 f_\alpha \left[\frac{1}{m_\beta} \frac{1}{v} \int_0^v du f_\beta(u) u^2 - \frac{1}{m_\alpha} \int_v^\infty du f_\beta(u) u \right] .
\end{aligned}
\tag{2.22}
$$

2.2.3 Equilibrium Distribution Functions

With the aid of Eq. (2.15), the collision operator between two species may be rewritten as

$$
C_{\alpha\beta} = \Gamma_{\alpha\beta} \nabla_{\mathbf{v}} \cdot \left[\frac{1}{2} (\nabla_{\mathbf{v}} f_\alpha) \cdot \nabla_{\mathbf{v}} \nabla_{\mathbf{v}} g_{\alpha\beta} - \frac{m_\alpha}{m_\alpha + m_\beta} f_\alpha \nabla_{\mathbf{v}} h_{\alpha\beta} \right] . \tag{2.23}
$$

For isotropic distribution functions the collision operator is

$$
\begin{aligned}
C_{\alpha\beta} &= \Gamma_{\alpha\beta} \frac{1}{v^2} \frac{\partial}{\partial v} v^2 \left[\frac{1}{2} \frac{\partial f_\alpha}{\partial v} \frac{\partial^2 g_{\alpha\beta}}{\partial v^2} - \frac{m_\alpha}{m_\alpha + m_\beta} f_\alpha \frac{\partial h_{\alpha\beta}}{\partial v} \right] \\
&= \frac{16\pi^2 Z_\alpha^2 Z_\beta^2 e^4 \ln\Lambda}{m_\alpha^2} \frac{1}{v^2} \frac{\partial}{\partial v} v^2 \left\{ \frac{\partial f_\alpha}{\partial v} \frac{1}{3} \left[\frac{1}{v^3} \int_0^v dv' f_\beta(v') v'^4 + \int_v^\infty dv' f_\beta(v') v' \right] \right. \\
&\qquad \left. + f_\alpha \frac{m_\alpha}{m_\beta} \frac{1}{v^2} \int_0^v dv' f_\beta(v') v'^2 \right\} .
\end{aligned}
\tag{2.24}
$$

The collision operator between two species which was given in Eq. (2.24) may not seem immediately familiar, so it will now be explicitly shown that this expression for the collision operator reduces to a previously published result. Calculating the divergence in

Eq. (2.24), one finds

$$
\begin{aligned}
C_{\alpha\beta} &= \frac{16\pi^2 Z_\alpha^2 Z_\beta^2 e^4 \ln\Lambda}{m_\alpha^2 v^2}\frac{\partial}{\partial v}\left(v^2\left\{\frac{\partial f_\alpha}{\partial v}\frac{1}{3}\left[\frac{1}{v^3}\int_0^v du f_\beta(u)u^4 + \int_v^\infty du f_\beta(u)u\right]\right.\right. \\
&\qquad \left.\left. + f_\alpha\frac{m_\alpha}{m_\beta}\frac{1}{v^2}\int_0^v du f_\beta(u)u^2\right\}\right) \\
&= \frac{16\pi^2 Z_\alpha^2 Z_\beta^2 e^4 \ln\Lambda}{m_\alpha^2 v^2}\frac{\partial}{\partial v}\left\{f_\alpha\frac{m_\alpha}{m_\beta}\int_0^v du f_\beta(u)u^2\right. \\
&\qquad \left. + \frac{\partial f_\alpha}{\partial v}\frac{1}{3}\left[\frac{1}{v}\int_0^v du f_\beta(u)u^4 + v^2\int_0^\infty du f_\beta(u)u - v^2\int_0^v du f_\beta(u)u\right]\right\} \\
&= \frac{16\pi^2 Z_\alpha^2 Z_\beta^2 e^4 \ln\Lambda}{3m_\alpha^2}\left\{\frac{\partial^2 f_\alpha}{\partial v^2}\left[\frac{1}{v^3}\int_0^v du f_\beta(u)u^4 + \int_v^\infty du f_\beta(u)u\right]\right. \\
&\qquad + \frac{\partial f_\alpha}{\partial v}\left[\int_0^v du f_\beta(u)\left(3\frac{m_\alpha}{m_\beta}\frac{u^2}{v^2} - \frac{u^4}{v^4}\right) + \frac{2}{v}\int_v^\infty du f_\beta(u)u\right] \\
&\qquad \left. + 3\frac{m_\alpha}{m_\beta}f_\alpha(v)f_\beta(v)\right\} . \qquad (2.25)
\end{aligned}
$$

For like particles Eq. (2.25) becomes

$$
\begin{aligned}
C_{\alpha\alpha} &= \frac{16\pi^2 Z_\alpha^4 e^4 \ln\Lambda}{3m_\alpha^2}\left\{\frac{\partial^2 f_\alpha}{\partial v^2}\left[\frac{1}{v^3}\int_0^v du f_\alpha(u)u^4 + \int_v^\infty du f_\alpha(u)u\right]\right. \\
&\qquad \left. + \frac{\partial f_\alpha}{\partial v}\left[\int_0^v du f_\alpha(u)\left(3\frac{u^2}{v^2} - \frac{u^4}{v^4}\right) + \frac{2}{v}\int_v^\infty du f_\alpha(u)u\right] + 3\left[f_\alpha(v)\right]^2\right\} \\
&= \frac{8\pi^2 Z_\alpha^4 e^4 \ln\Lambda}{m_\alpha^2}\left\{\frac{2}{3}\frac{\partial^2 f_\alpha}{\partial v^2}\left[\frac{1}{v^3}\int_0^v du f_\alpha(u)u^4 + \int_v^\infty du f_\alpha(u)u\right] + 2\left[f_\alpha(v)\right]^2\right. \\
&\qquad \left. + \frac{4}{3v}\frac{\partial f_\alpha}{\partial v}\left[\int_0^\infty du f_\alpha(u)u - \int_0^v du f_\alpha(u)u\left(1-\frac{u}{v}\right)^2\left(1+\frac{u}{2v}\right)\right]\right\} . \\
&\qquad (2.26)
\end{aligned}
$$

This last expression for $C_{\alpha\alpha}$ matches Eq. (1) of Reference [49].

The collisional velocity-space particle flux from Eq. (2.11) is found to be

$$\mathbf{J}_{\alpha\beta} = -\frac{16\pi^2 Z_\alpha^2 Z_\beta^2 e^4 \ln\Lambda}{m_\alpha^2}\left\{\frac{\partial f_\alpha}{\partial v}\frac{1}{3}\left[\frac{1}{v^3}\int_0^v dv' f_\beta(v')v'^4 + \int_v^\infty dv' f_\beta(v')v'\right]\right.$$
$$\left. + f_\alpha \frac{m_\alpha}{m_\beta}\frac{1}{v^2}\int_0^v dv' f_\beta(v')v'^2\right\}\hat{\mathbf{v}}\,, \qquad (2.27)$$

where $\hat{\mathbf{v}}$ denotes the "radial" direction in velocity space.

Assuming that there are no external forces or spatial gradients, for f_α to be in equilibrium one must have $(\partial f_\alpha/\partial t)_{col.} = 0$. For isotropic velocity distributions, this requirement reduces to $\sum_\beta \mathbf{J}_{\alpha\beta} = 0$, or equivalently

$$\frac{\partial f_\alpha(v)}{\partial v} = -f_\alpha(v)\frac{3\sum_\beta\left[Z_\beta^2(m_\alpha/m_\beta)(1/v^2)\int_0^v dv' f_\beta(v')v'^2\right]}{\left[(1/v^3)\int_0^v dv'\sum_\beta Z_\beta^2 f_\beta(v')v'^4 + \int_v^\infty dv'\sum_\beta Z_\beta^2 f_\beta(v')v'\right]}\,. \qquad (2.28)$$

For the case of electrons interacting with ions, the electron distribution function will acquire a quasi-equilibrium shape while its mean energy is still in the process of changing due to energy exchange with the ion species. Therefore one may use Eq. (2.28) to find the electrons' "equilibrium" distribution function f_α, which may then be used in Eq. (2.22) to arrive at the rate of interspecies energy transfer.

Note that $f_\alpha(v)$ cannot increase with increasing v in any range of velocity space if the distribution is to be held in equilibrium (or quasi-equilibrium) solely by collisions with other species (even if those other species have fixed and/or non-Maxwellian distribution functions). Thus, one cannot "dig a well" in the electron distribution to cause a radical depletion of the slow-moving electrons which draw energy away from ions, unless one resorts to particle sources and sinks, externally applied electromagnetic fields, transient operating conditions, etc.

2.3 Ion-Electron Energy Transfer for Maxwellian Ions

In this section the general ion-electron energy transfer formulas of the previous section will be applied to the specific case in which the various ion species which are present have Maxwellian velocity distributions.

2.3.1 General Heat Transfer for Maxwellian Ions

For Maxwellian ions with thermal velocity $v_{ti} \equiv \sqrt{2T_i/m_i}$, the distribution function is

$$f_i(v) = \frac{n_i}{\pi^{3/2} v_{ti}^3} \exp\left(-\frac{v^2}{v_{ti}^2}\right). \tag{2.29}$$

It is assumed for the time being that different ion species in the plasma may have different temperatures.

Substituting Eq. (2.29) into the expression for the ion-electron heat transfer, Eq. (2.22), and integrating by parts, one finds that the power per volume transferred from the ions to the electrons is

$$P_{ie} = 16\pi^2 e^4 \ln\Lambda \int_0^\infty dv v^2 f_e(v) \sum_i \frac{Z_i^2 n_i}{m_i} \left[\frac{2}{\sqrt{\pi}} \frac{m_i}{m_e} \frac{1}{v_{ti}} \exp\left(-\frac{v^2}{v_{ti}^2}\right) - \frac{1}{v} \mathrm{erf}\left(\frac{v}{v_{ti}}\right)\right]. \tag{2.30}$$

Now one needs to find the equilibrium electron distribution function $f_e(v)$ to use in Eq. (2.30) for the heat transfer. By substituting (2.29) into Eq. (2.28) and again employing integration by parts, the differential equation determining $f_e(v)$ reduces to

$$\begin{aligned} \frac{\partial f_e}{\partial v} \Bigg\{ & \frac{1}{3v} \int_0^v dv' f_e(v') v'^4 - \frac{v^2}{3} \int_0^v dv' f_e(v') v' + \frac{v^2}{3} \int_0^\infty dv' f_e(v') v' \\ & + \sum_i \frac{Z_i^2 n_i v_{ti}^2}{4\pi^{3/2} v} \left[\frac{\sqrt{\pi}}{2} \mathrm{erf}\left(\frac{v}{v_{ti}}\right) - \frac{v}{v_{ti}} \exp\left(-\frac{v^2}{v_{ti}^2}\right)\right] \Bigg\} \\ & + f_e(v) \left\{ \int_0^v dv' f_e(v') v'^2 + \sum_i \frac{Z_i^2 n_i}{2\pi^{3/2}} \frac{m_e}{m_i} \left[\frac{\sqrt{\pi}}{2} \mathrm{erf}\left(\frac{v}{v_{ti}}\right) - \frac{v}{v_{ti}} \exp\left(-\frac{v^2}{v_{ti}^2}\right)\right] \right\} = 0 \end{aligned} \tag{2.31}$$

for the case of electrons in the presence of multiple Maxwellian ion species.

If Eq. (2.31) is solved numerically and its solution for the equilibrium $f_e(v)$ used with Eq. (2.30), one will find the exact value for the heat transfer to electrons from Maxwellian ions for any choice of parameters. However, to obtain useful analytical expressions and simplified numerical results, further approximations are required.

One should also note that by using Eq. (2.30) and assuming that the electrons remain perfectly Maxwellian (and allowing the ratio of ion and electron temperatures to remain arbitrary), the result first found by Spitzer [26, 27] may be obtained:

$$(P_{ie})_{Spitzer} = \frac{4\sqrt{2\pi m_i m_e} Z_i^2 e^4 n_i n_e \ln\Lambda}{(m_i T_e + m_e T_i)^{3/2}} (T_i - T_e) \ . \tag{2.32}$$

This classical Spitzer energy transfer rate will serve as a useful basis for comparison with the modified rate described by Eqs. (2.30) and (2.31).

2.3.2 Modification of Spitzer Ion-Electron Heat Transfer

If the electrons moving more slowly than the ions are partially depleted due to energy upscattering from the ions, the heat transfer rate will be less than the Spitzer result. To examine this effect, it will be assumed that the ions are Maxwellian and are moving significantly more slowly that the electrons, but the electron distribution will not be assumed to be Maxwellian. This calculation will produce a modification factor to the Spitzer heat transfer rate which will reduce to the answer obtained by Rosenbluth [45, 46] in the proper limit.

Relationship Between Slow Electron Depletion and Reduction of Ion-Electron Heat Transfer

Before proceeding with the main line of the derivation, one of the key arguments used in the more intuitive analysis of Section 2.1 will now be confirmed; in particular, it will be shown that the ion-electron heat transfer rate is essentially proportional to the number of electrons moving more slowly than the ions, or in other words approximately proportional to $f_e(v=0)$.

For $v_{te} \gg v_{ti}$ one may assume that the electron distribution shape is governed by electrons with velocities v such that $v \gg v_{ti}$; therefore Eq. (2.30) becomes

$$P_{ie} \approx \frac{16\pi^2 Z_i^2 e^4 n_i \ln\Lambda}{m_i}\left[\frac{T_i}{m_e} f_e(0) - \int_0^\infty dv f_e(v) v\right] . \tag{2.33}$$

For Maxwellian electrons Eq. (2.33) reduces to:

$$\begin{aligned} P_{ie} &\approx \frac{16\pi^2 Z_i^2 e^4 n_i \ln\Lambda}{m_i m_e}(T_i - T_e)\,[f_e(0)]_{Maxwellian} \\ &\approx (P_{ie})_{Spitzer} . \end{aligned} \tag{2.34}$$

Equation (2.34) is clearly the $v_{te} \gg v_{ti}$ limiting form of the full Spitzer result of Eq. (2.32). Assuming that the electrons do not deviate too much from a Maxwellian distribution, then one may use

$$\int_0^\infty dv v f_e(v) \approx \frac{T_e}{m_e} f_e(0) \tag{2.35}$$

in Eq. (2.33). Dividing the resulting expression by Eq. (2.34) produces the result

$$\frac{P_{ie}}{(P_{ie})_{\text{Spitzer}}} \approx \frac{\frac{T_i}{m_e} f_e(0) - \frac{T_e}{m_e} f_e(0)}{\frac{(T_i - T_e)}{m_e}[f_e(0)]_{Maxwellian}} = \frac{f_e(0)}{[f_e(0)]_{Maxwellian}} . \tag{2.36}$$

Because substantially non-Maxwellian electron distributions will arise only when $T_i \gg$

T_e (causing interactions with ions to interfere strongly with the electron distribution), the correction to the Spitzer rate will reduce to (2.36) even when the assumption underlying Equation (2.35) breaks down:

$$\frac{P_{ie}}{(P_{ie})_{\text{Spitzer}}} \approx \frac{\frac{T_i}{m_e} f_e(0)}{\frac{T_i}{m_e}[f_e(0)]_{Maxwellian}} = \frac{f_e(0)}{[f_e(0)]_{Maxwellian}} . \tag{2.37}$$

Therefore when the electron distribution function is altered so that fewer than the Maxwellian number of electrons have very slow speeds, the heat transfer rate is reduced accordingly.

Derivation of Electron Distribution and Energy Transfer

Attention will now be directed to electrons with velocity v such that $v_{ti} \ll v \ll v_{te}$. In this case one may make the approximations $\exp(-v^2/v_{ti}^2) \to 0$ and $\text{erf}(v/v_{ti}) \to 1$ in Eq. (2.31).

Using these approximations, the differential equation for the electron distribution becomes

$$\frac{\partial f_e}{\partial v}\left[\sum_i \frac{Z_i^2 n_i}{4\pi v^3}\frac{T_i}{m_i} + \frac{1}{3}\int_0^\infty dv' f_e(v')v'\right] + f_e(v)\frac{1}{v^2}\left[\frac{v^3}{3}f_e(0) + \sum_i \frac{Z_i^2 n_i}{4\pi}\frac{m_e}{m_i}\right] = 0 . \tag{2.38}$$

Assuming that the electrons are nearly Maxwellian so that Maxwellian values may be used for the electron-related quantities within the brackets, one obtains

$$\frac{\partial f_e}{\partial v}\frac{T_e}{m_e}\left[v^3 + 3\sqrt{\frac{\pi}{2}}\sum_i \frac{Z_i^2 n_i}{n_e}\frac{T_i}{m_i}\sqrt{\frac{T_e}{m_e}}\right] + v f_e\left[v^3 + 3\sqrt{\frac{\pi}{2}}\sum_i \frac{Z_i^2 n_i}{n_e}\frac{m_e}{m_i}\left(\frac{T_e}{m_e}\right)^{3/2}\right] = 0 . \tag{2.39}$$

The form of Eq. (2.39) suggests that one define a critical velocity v_c for the electrons

as

$$v_c^3 \equiv 3\sqrt{\frac{\pi}{2}} \sum_i \frac{Z_i^2 n_i}{n_e} \frac{T_i}{m_i} \sqrt{\frac{T_e}{m_e}} = \frac{3\sqrt{\pi}}{4} \sum_i \frac{Z_i^2 n_i}{n_e} v_{ti}^2 v_{te} \,. \tag{2.40}$$

This definition is the same critical velocity which was found in the introductory section. By using the critical velocity and assuming that all of the ion species are at the same temperature T_i, Eq. (2.39) may be solved to find $f_e(v)$ [51]:

$$f_e(v) = f_e(0) \exp\left\{ -\frac{m_e}{T_e} \int_0^v \frac{dv' v' \left(v'^3 + \frac{T_e}{T_i} v_c^3 \right)}{(v'^3 + v_c^3)} \right\} . \tag{2.41}$$

One may find $f_e(0)$ from the normalization condition in Eq. (2.9). It should be realized that the derivation of this distribution function assumed that $v_{ti} \ll v \ll v_{te}$.

The integral in the exponent may be evaluated [52]:

$$\begin{aligned} \int_0^v \frac{dv' v' \left(v'^3 + \frac{T_e}{T_i} v_c^3 \right)}{(v'^3 + v_c^3)} &= \frac{1}{2} v^2 - \left(1 - \frac{T_e}{T_i} \right) v_c^3 \int_0^v \frac{dv' v'}{(v'^3 + v_c^3)} \\ &= \frac{1}{2} v^2 + \left(1 - \frac{T_e}{T_i} \right) \frac{v_c^2}{3} \left\{ \frac{1}{2} \ln \left[\frac{(v + v_c)^2}{v^2 - v v_c + v_c^2} \right] \right. \\ &\qquad \left. - \sqrt{3} \tan^{-1} \left(\frac{1}{\sqrt{3}} \right) - \sqrt{3} \tan^{-1} \left(\frac{2v - v_c}{\sqrt{3} v_c} \right) \right\} . \end{aligned} \tag{2.42}$$

It is clear from Equation (2.42) that in the classical limit ($v_c \to 0$) the distribution function becomes the usual Maxwellian.

Now the electron distribution function found above may be used in the expression from Eq. (2.30) for ion-electron energy transfer in the presence of Maxwellian ion species. Making this substitution and dividing by the Spitzer energy transfer rate from Eq. (2.32),

one obtains

$$\frac{P_{ie}}{(P_{ie})_{\text{Spitzer}}} \approx \frac{\sqrt{\pi}}{2}\frac{T_e}{(T_i-T_e)}\left(1+\frac{m_e}{m_i}\frac{T_i}{T_e}\right)^{3/2} \times\left\{\int_0^\infty dvv^2\exp\left[-\frac{m_e}{T_e}\int_0^v\frac{dv'v'\left(v'^3+\frac{T_e}{T_i}v_c^3\right)}{(v'^3+v_c^3)}\right] \times\left[\frac{2}{\sqrt{\pi}}\left(\frac{m_i}{m_e}\right)^{3/2}\sqrt{\frac{T_e}{T_i}}\exp\left(\frac{-v^2}{v_{ti}^2}\right)-\frac{v_{te}}{v}\text{erf}\left(\frac{v}{v_{ti}}\right)\right]\right\} \times\left[\int_0^\infty dvv^2\exp\left\{-\frac{m_e}{T_e}\int_0^v\frac{dv'v'\left(v'^3+\frac{T_e}{T_i}v_c^3\right)}{(v'^3+v_c^3)}\right\}\right]^{-1}. \tag{2.43}$$

Note that $v\sim v_{ti}$ corrections have been retained so that the correct Spitzer rate will be recovered for $v_c^3\to 0$.

Useful Approximate Answer

A simplified answer can be extracted from Eq. (2.43) by analytical means [53].

In the first integral of Eq. (2.43), the integrand is appreciable only for v of the order of v_{ti} or smaller, so one may assume that v and v' are of the order v_{ti} and thus much smaller than v_c. In this limit the integral becomes

$$\begin{aligned}\int_0^\infty dvv^2\exp\left[-\frac{m_e}{T_e}\int_0^v\frac{dv'v'\left(v'^3+\frac{T_e}{T_i}v_c^3\right)}{(v'^3+v_c^3)}\right]\frac{2}{\sqrt{\pi}}\left(\frac{m_i}{m_e}\right)^{3/2}\sqrt{\frac{T_e}{T_i}}\exp\left(\frac{-v^2}{v_{ti}^2}\right)&\\ \approx\int_0^\infty dvv^2\exp\left[-\left(1+\frac{m_e}{m_i}\right)\frac{v^2}{v_{ti}^2}\right]\frac{2}{\sqrt{\pi}}\left(\frac{m_i}{m_e}\right)^{3/2}\sqrt{\frac{T_e}{T_i}}&\\ \approx v_{te}\frac{T_i}{m_e}.&\end{aligned} \tag{2.44}$$

The integrands of the remaining integrals in Eq. (2.43) are not restricted to the $v\sim v_{ti}$ velocity range (they do not have the $\exp(-v^2/v_{ti}^2)$ term), so in general the electron velocity

v in these integrals extends to the order of v_{te}, or much larger than v_c. In this limit, the integral in the exponentials of these terms may be approximated by using Eq. (2.42), so that

$$\int_0^v \frac{dv'v'\left(v'^3+\frac{T_e}{T_i}v_c^3\right)}{(v'^3+v_c^3)} \approx \frac{1}{2}v^2-\left(1-\frac{T_e}{T_i}\right)v_c^2\frac{2\pi}{3\sqrt{3}}. \tag{2.45}$$

Therefore the remaining integrals in Eq. (2.43) may be approximated as

$$\begin{aligned}\int_0^\infty dv\, v\, v_{te}\,\mathrm{erf}\left(\frac{v}{v_{ti}}\right)\exp\left\{-\frac{m_e}{T_e}\int_0^v\frac{dv'v'\left(v'^3+\frac{T_e}{T_i}v_c^3\right)}{(v'^3+v_c^3)}\right\}&\\ \approx v_{te}\exp\left\{\frac{2\pi}{3\sqrt{3}}\left(1-\frac{T_e}{T_i}\right)\frac{m_ev_c^2}{T_e}\right\}\int_0^\infty dvv\exp\left\{-\frac{m_ev^2}{2T_e}\right\}&\\ \approx v_{te}\frac{T_e}{m_e}\exp\left\{\frac{2\pi}{3\sqrt{3}}\left(1-\frac{T_e}{T_i}\right)\frac{m_ev_c^2}{T_e}\right\};&\end{aligned} \tag{2.46}$$

$$\begin{aligned}\int_0^\infty dv\, v^2\exp\left\{-\frac{m_e}{T_e}\int_0^v\frac{dv'v'\left(v'^3+\frac{T_e}{T_i}v_c^3\right)}{(v'^3+v_c^3)}\right\}&\\ \approx \exp\left\{\frac{2\pi}{3\sqrt{3}}\left(1-\frac{T_e}{T_i}\right)\frac{m_ev_c^2}{T_e}\right\}\int_0^\infty dvv^2\exp\left\{-\frac{m_ev^2}{2T_e}\right\}&\\ \approx \sqrt{\frac{\pi}{2}}\left(\frac{T_e}{m_e}\right)^{3/2}\exp\left\{\frac{2\pi}{3\sqrt{3}}\left(1-\frac{T_e}{T_i}\right)\frac{m_ev_c^2}{T_e}\right\}.&\end{aligned} \tag{2.47}$$

Using these approximations, Eq. (2.43) becomes

$$\frac{P_{ie}}{(P_{ie})_{\text{Spitzer}}} \approx \left(1+\frac{m_e}{m_i}\frac{T_i}{T_e}\right)^{3/2}\exp\left\{-\left(\frac{2\pi^2}{3^{5/4}}\sum_i\frac{Z_i^2n_i}{n_e}\frac{m_e}{m_i}\frac{T_i}{T_e}\right)^{2/3}\right\}, \tag{2.48}$$

where some corrections of order v_{ti}^2/v_{te}^2 have been neglected in the asymptotic evaluation of the integrals.

For the case in which only one ion species is present ($Z_in_i=n_e$) and the temperature ratio T_i/T_e remains moderate, this expression clearly reduces to precisely the answer

obtained by Rosenbluth [46]:

$$\frac{(P_{ie})_{Rosenbluth}}{(P_{ie})_{Spitzer}} \approx 1 - \left(\frac{2\pi^2}{3^{5/4}} Z_i \frac{m_e}{m_i} \frac{T_i}{T_e}\right)^{2/3} . \tag{2.48}$$

It is useful to realize that $2\pi^2/3^{5/4} \approx 5.000$.

Now the significance of this work may be seen. While Rosenbluth's answer is just an expansion valid for T_i not much larger than T_e (and indeed takes on a nonphysical negative value if one chooses T_i/T_e to be sufficiently large), the result presented in Eq. (2.43) and even the more approximate one of Eq. (2.48) are considerably more accurate, and they give sensible answers even for large T_i/T_e. The accuracy of Eq. (2.43) will next be demonstrated by numerically integrating this expression and comparing the result with the output of a Fokker-Planck code for a wide range of T_i/T_e values.

More Accurate Answer via Numerical Integration

Mathematica [54] has been used to plot the normalized distribution function from Eq. (2.41) for various values of T_i/T_e (with $Z_i \equiv 1$ and $A \equiv 1$ for all of the curves). Figure 2-1 shows the plots for T_i/T_e =1, 10, 100, and 1000. As may be seen in the figure, the flattening of the electron distribution at small velocities becomes more pronounced as the temperature ratio increases, as expected. (Some of the approximations made in obtaining Eq. (2.41) begin to break down for T_i/T_e=1000, but the general appearance of the distribution function at these parameters is still highly revealing.)

The correction to the Spitzer rate as described by Eq. (2.43) has been calculated via numerical integration with Mathematica. The resulting graphs are shown in Figures 2-2 through 2-4 for the cases in which the plasma consists of pure light hydrogen, pure deuterium, and pure helium-3. These results for the case of Maxwellian ions are contrasted in the graphs with the results for the case of monoenergetic ions, which will be derived in the next section.

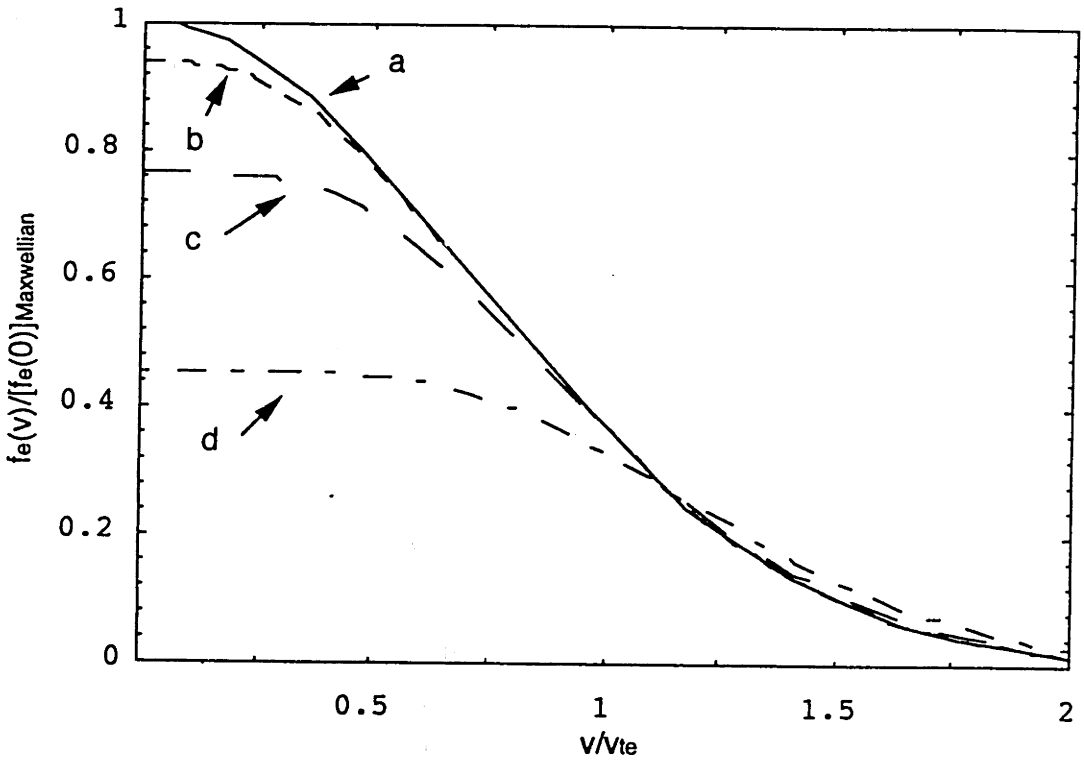

Figure 2-1: Electron distribution for a pure hydrogen (^{1}H) plasma with T_i/T_e=1 (a), 10 (b), 100 (c), and 1000 (d).

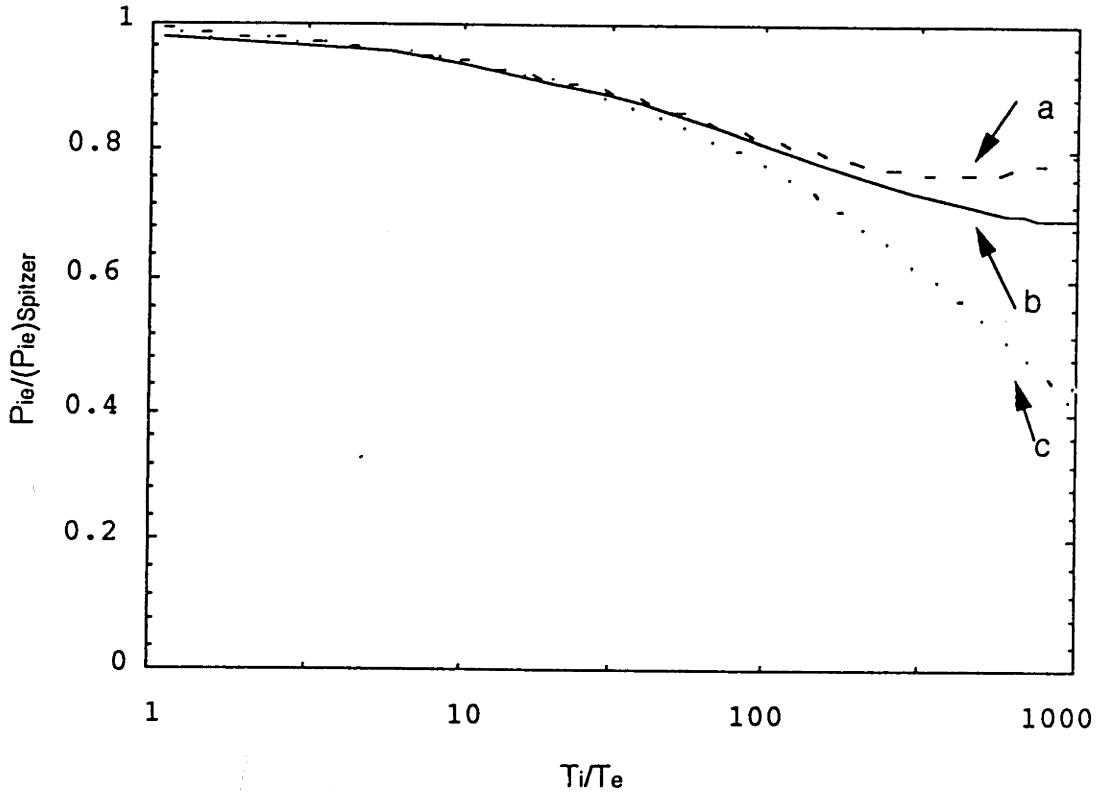

Figure 2-2: Correction factor to the Spitzer ion-electron energy transfer rate for a pure hydrogen (^{1}H) plasma as a function of T_i/T_e: a) monoenergetic ions, b) Maxwellian ions, c) approximate answer from Eq. (2.50).

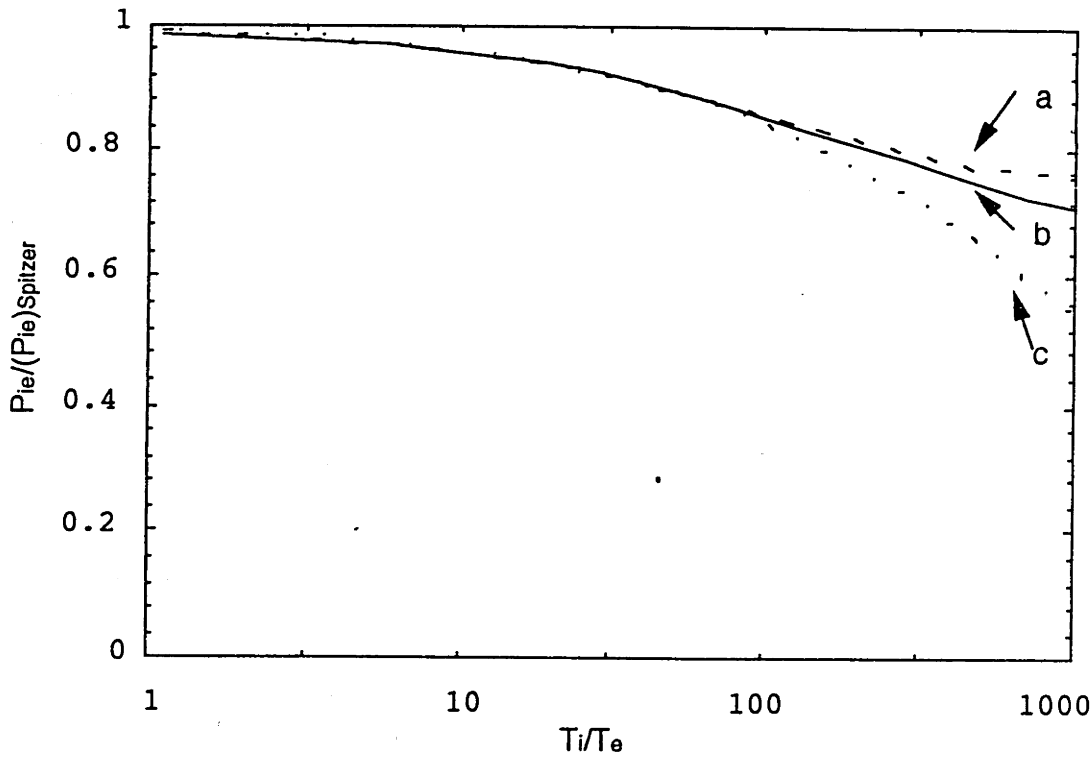

Figure 2-3: Correction factor to the Spitzer ion-electron energy transfer rate for a pure deuterium plasma as a function of T_i/T_e: a) monoenergetic ions, b) Maxwellian ions, c) approximate answer from Eq. (2.50).

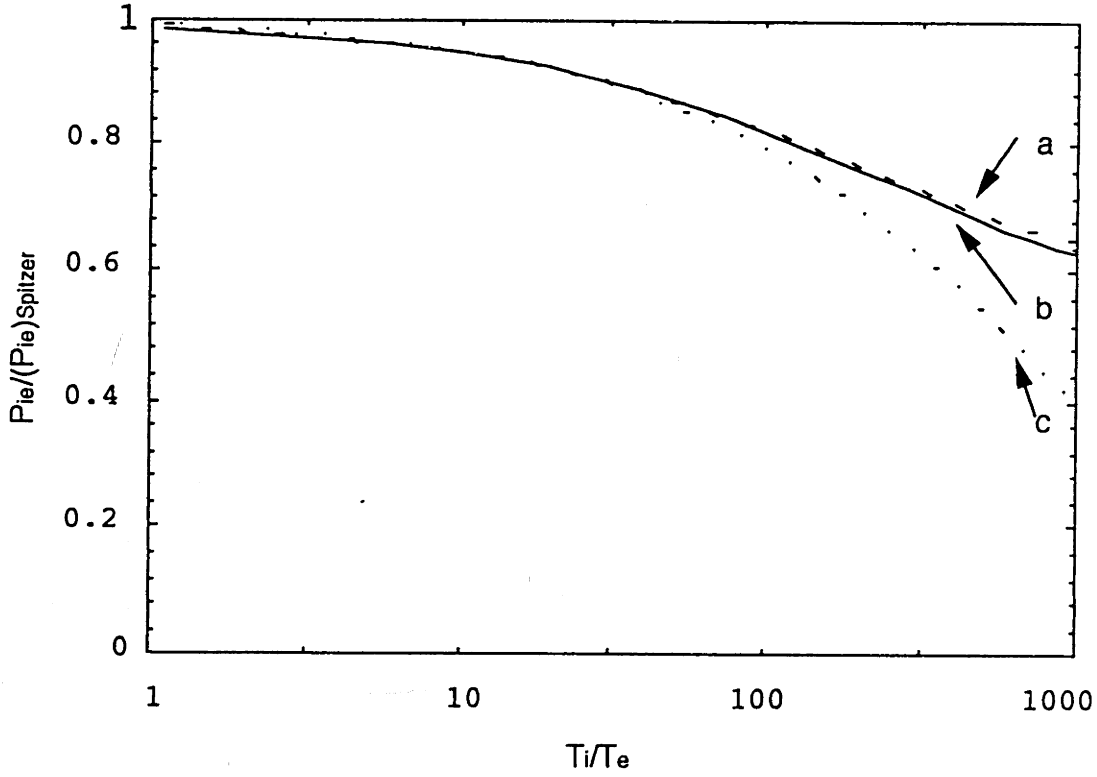

Figure 2-4: Correction factor to the Spitzer ion-electron energy transfer rate for a pure helium-3 plasma as a function of T_i/T_e: a) monoenergetic ions, b) Maxwellian ions, c) approximate answer from Eq. (2.50).

As may be seen in the graphs, the correction factor begins to level off for large T_i/T_e. This behavior is to be expected, for if one continues to hold the ion distribution perfectly Maxwellian and redefines T_e to be 2/3 of the mean electron energy (even when the electron distribution becomes non-Maxwellian), the ion-electron heat transfer should return toward the $T_i/T_e \to \infty$ Spitzer rate for extremely large values of T_i/T_e (when $v_{ti}^2 \gg v_{te}^2$, so the ion velocity is the dominant determinant of the relative collision velocity). At $T_i/T_e = 1000$, this upward return back toward the Spitzer formula has not yet begun (except for the case of light hydrogen with monoenergetic ions, as shown by curve (a) of Figure 2-2), but the correction factor is beginning to level off in preparation for the upward turn.

Along with the plots based on Eq. (2.43), Figures 2-2 through 2-4 also present graphs of the more approximate but more readily useable answer,

$$\frac{P_{ie}}{(P_{ie})_{\text{Spitzer}}} \approx \left(1 + \frac{m_e}{m_i}\frac{T_i}{T_e}\right)^{3/2} \exp\left\{-\left(3.5\sum_i \frac{Z_i^2 n_i}{n_e}\frac{m_e}{m_i}\frac{T_i}{T_e}\right)^{2/3}\right\} . \qquad (2.50)$$

Note that the coefficient in the exponent has been changed from the previous approximate value of 5.00 to the present value of 3.5 in order to match the complete results more accurately over a wider range of values of T_i/T_e. As one may see in the graphs, this approximate answer matches the full analytical results quite well for temperature ratios such that

$$1 \le \sum_i \frac{Z_i^2 n_i}{n_e}\frac{m_p}{m_i}\frac{T_i}{T_e} \le 50 , \qquad (2.51)$$

in which m_p is the proton mass.

Figure 2-5 again shows the numerically integrated result for the case of deuterium with a Maxwellian ion distribution, but now that curve is compared with the results obtained by Galambos [55, 56] using the FPPAC Fokker-Planck code [57, 58]. It may be seen that there is fairly good agreement between the present analytical results and the code results for the heat transfer rate. Methods for obtaining even more precise analytical expressions for the energy exchange rate will now be presented.

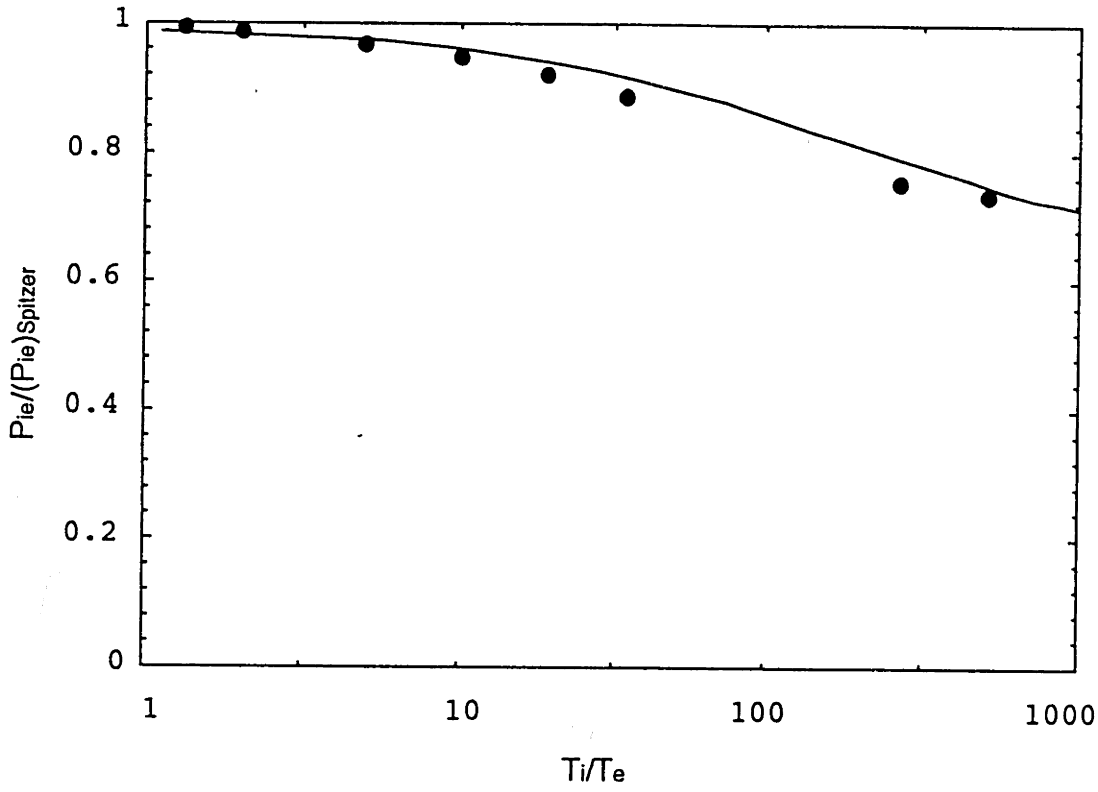

Figure 2-5: Comparison of analytical result from Eq. (2.43) (line) with code results (points) from [55, 56] for a pure deuterium plasma with a Maxwellian ion distribution.

2.3.3 Toward Even More Accurate Analytical Results

It should be possible to obtain an even more accurate answer by returning to the full nonlinear first-order differential equation for the electron distribution function in the presence of Maxwellian ions, Eq. (2.31). This first-order equation for f_e may be iterated, so that the coefficients are found by using a less accurate expression for the distribution, which will be denoted f_e^*:

$$\frac{\partial f_e}{\partial v}\left\{\frac{1}{3v}\int_0^v dv' f_e^*(v')v'^4 + \frac{v^2}{3}\int_v^\infty dv' f_e^*(v')v' + \sum_i \frac{Z_i^2 n_i v_{ti}^2}{4\pi^{3/2}v}\left[\frac{\sqrt{\pi}}{2}\mathrm{erf}\left(\frac{v}{v_{ti}}\right) - \frac{v}{v_{ti}}\exp\left(-\frac{v^2}{v_{ti}^2}\right)\right]\right\}$$
$$+ f_e(v)\left\{\int_0^v dv' f_e^*(v')v'^2 + \sum_i \frac{Z_i^2 n_i}{2\pi^{3/2}}\frac{m_e}{m_i}\left[\frac{\sqrt{\pi}}{2}\mathrm{erf}\left(\frac{v}{v_{ti}}\right) - \frac{v}{v_{ti}}\exp\left(-\frac{v^2}{v_{ti}^2}\right)\right]\right\} = 0\,. \tag{2.52}$$

Solving this equation, the iterated solution for the distribution function expressed in terms of the previous iteration's solution is

$$f_e(v) = f_e(0)\exp\left\{-\int_0^v\left[dv'v'\left\{3\int_0^{v'} dv'' f_e^*(v'')v''^2 + \sum_i \frac{3Z_i^2 n_i}{2\pi^{3/2}}\frac{m_e}{m_i}\left[\frac{\sqrt{\pi}}{2}\mathrm{erf}\left(\frac{v'}{v_{ti}}\right) - \frac{v'}{v_{ti}}\exp\left(-\frac{v'^2}{v_{ti}^2}\right)\right]\right\}\right.\right.$$
$$\left.\left.\times\left\{\int_0^{v'} dv'' f_e^*(v'')v''^4 + v'^3\int_{v'}^\infty dv'' f_e^*(v'')v'' + \sum_i \frac{3Z_i^2 n_i v_{ti}^2}{4\pi^{3/2}}\left[\frac{\sqrt{\pi}}{2}\mathrm{erf}\left(\frac{v'}{v_{ti}}\right) - \frac{v'}{v_{ti}}\exp\left(-\frac{v'^2}{v_{ti}^2}\right)\right]\right\}^{-1}\right]\right\}\,. \tag{2.53}$$

One may then find $f_e(0)$ directly from the normalization condition as usual.

If one begins the iteration process by assuming that $f_e^*(v)$ is Maxwellian and charac-

terized by the thermal velocity v_{te}, then the distribution function of Eq. (2.53) becomes

$$f_e(v) = f_e(0)\exp\left\{-2\int_0^v\left[\frac{dv'v'}{v_{te}^2}\left\{\frac{3}{2}\left[\frac{\sqrt{\pi}}{2}\mathrm{erf}\left(\frac{v'}{v_{te}}\right)-\frac{v'}{v_{te}}\exp\left(-\frac{v'^2}{v_{te}^2}\right)\right]\right.\right.\right.$$
$$\left.+\sum_i\frac{3\sqrt{\pi}}{4}\frac{Z_i^2n_i}{n_e}\frac{m_e}{m_i}\left[\mathrm{erf}\left(\frac{v'}{v_{ti}}\right)-\frac{2}{\sqrt{\pi}}\frac{v'}{v_{ti}}\exp\left(-\frac{v'^2}{v_{ti}^2}\right)\right]\right\}$$
$$\times\left\{\frac{3}{2}\left[\frac{\sqrt{\pi}}{2}\mathrm{erf}\left(\frac{v'}{v_{te}}\right)-\frac{v'}{v_{te}}\exp\left(-\frac{v'^2}{v_{te}^2}\right)\right]\right.$$
$$\left.\left.\left.+\sum_i\frac{3\sqrt{\pi}}{4}\frac{Z_i^2n_iv_{ti}^2}{n_ev_{te}^2}\left[\mathrm{erf}\left(\frac{v'}{v_{ti}}\right)-\frac{2}{\sqrt{\pi}}\frac{v'}{v_{ti}}\exp\left(-\frac{v'^2}{v_{ti}^2}\right)\right]\right\}^{-1}\right]\right\}. \tag{2.54}$$

Note that by using the series expansion for $v' < v_{te}$ one finds

$$\begin{aligned}\frac{\sqrt{\pi}}{2}\mathrm{erf}\left(\frac{v'}{v_{te}}\right)-\frac{v'}{v_{te}}\exp\left(-\frac{v'^2}{v_{te}^2}\right) &= \sum_{n=0}^{\infty}\frac{(-1)^n}{n!(2n+1)}\left(\frac{v'}{v_{te}}\right)^{2n+1}\\ &\quad-\left(\frac{v'}{v_{te}}\right)\sum_{n=0}^{\infty}\frac{(-1)^n}{n!}\left(\frac{v'}{v_{te}}\right)^{2n}\\ &= \sum_{n=0}^{\infty}\frac{(-1)^{n+1}}{n!}\left(\frac{2n}{2n+1}\right)\left(\frac{v'}{v_{te}}\right)^{2n+1}\\ &= \frac{2}{3}\left(\frac{v'}{v_{te}}\right)^3-\frac{2}{5}\left(\frac{v'}{v_{te}}\right)^5+\frac{1}{7}\left(\frac{v'}{v_{te}}\right)^7\\ &\quad-O\left\{\left(\frac{v'}{v_{te}}\right)^9\right\}+\ldots\end{aligned} \tag{2.55}$$

By taking just the first term of this expansion, making the approximation $v \gg v_{ti}$, and defining the critical velocity v_c as before, the distribution function of Eq. (2.54) reduces to the simpler form used in the previous section.

Even more accurate distribution functions could be found by using Eq. (2.54) or a simplified form of it as the basis for further iterations with Eq. (2.53).

Once a distribution function of the desired accuracy has been obtained, it can be used

to find the correction to the Spitzer ion-electron energy transfer rate,

$$\frac{P_{ie}}{(P_{ie})_{\text{Spitzer}}} \approx \frac{\sqrt{\pi}}{2}\frac{T_e}{(T_i - T_e)}\left(1 + \frac{m_e}{m_i}\frac{T_i}{T_e}\right)^{3/2}\int_0^\infty \left\{dv v^2 \frac{f_e(v)}{f_e(0)} \times \left[\frac{2}{\sqrt{\pi}}\left(\frac{m_i}{m_e}\right)^{3/2}\sqrt{\frac{T_e}{T_i}}\exp\left(\frac{-v^2}{v_{ti}^2}\right) - \frac{v_{te}}{v}\text{erf}\left(\frac{v}{v_{ti}}\right)\right]\right\} \times \left[\int_0^\infty dv v^2 \frac{f_e(v)}{f_e(0)}\right]^{-1} . \tag{2.56}$$

Another possible improvement involves refining the definition of the electron temperature. For the case of significantly non-Maxwellian electrons, it is desirable to accompany the heat transfer expression by a definition of the effective electron temperature $\Theta_e \equiv 2\langle E_e\rangle/3$, where $\langle E_e\rangle$ is the mean energy per electron. One finds that

$$\begin{aligned}\Theta_e &\equiv \frac{2}{3}\frac{1}{n_e}\int_0^\infty \left(dv 4\pi v^2\right)\left(\frac{1}{2}m_e v^2\right) f_e(v) \\ &= \frac{2}{3}T_e\frac{\int_0^\infty duu^4 f_e(u)}{\int_0^\infty duu^2 f_e(u)} ,\end{aligned} \tag{2.57}$$

in which $u \equiv v/v_{te}$.

Numerical integration with Mathematica revealed that using the distribution function of Eq. (2.54) produces only minute alterations in the graphs which were presented earlier. Likewise, plotting the heat transfer correction factor versus T_i/Θ_e (as opposed to T_i/T_e) only makes very slight alterations in the curves, since T_e and Θ_e only begin to diverge for large values of T_i/T_e, where the correction factor is nearly flat with respect to the temperature ratio.

More appreciable improvements might be gained from iterating the electron distribution function at least once more or by expressing all of the integrals in terms of Θ_e instead of T_e (being careful to maintain self-consistency with the new definition throughout the derivation), but these possibilities were not tested computationally, as the resulting expressions could not be numerically integrated within a reasonable time on the sort of computers presently available to the author (Macintosh Quadra 610).

2.4 Ion-Electron Energy Transfer for Monoenergetic Ions

Now the energy transfer rate will be calculated assuming that the ions all have velocity v_i, or energy $E_i = m_i v_i^2/2$. This calculation is relevant to the evaluation of fusion concepts such as those proposed by Bussard [18] and Maglich [38], which are intended to operate with nearly monoenergetic ion beams that have energies much greater than the mean electron energy.

(In spherically convergent systems of the type proposed by Bussard, the density generally varies as roughly $1/r^2$, where r is the radial distance from the center of the spherical plasma [18]. Therefore most of the collisions occur in the dense central region, where particles are coming from and returning to all directions, and so the assumption of isotropy made in the present calculations is valid. Anisotropy could be a more serious concern in Maglich's migma configuration [38], although the present isotropic calculation may be considered a first-order treatment of the plasma behavior in that device.)

2.4.1 Derivation of Electron Distribution and Energy Transfer

For isotropic but monoenergetic ions, the distribution function is

$$f_i(v) = \frac{n_i}{4\pi v_i^2}\delta(v - v_i) \; . \tag{2.58}$$

By substituting this distribution function in Eq. (2.22), the power per volume transferred from the ions to the electrons is found to be

$$P_{ie} \;=\; 16\pi^2 Z_i^2 e^4 n_i \ln\Lambda \left[\frac{1}{m_e v_i}\int_0^{v_i} dv' f_e(v') v'^2 - \frac{1}{m_i}\int_{v_i}^{\infty} dv' f_e(v') v'\right] \; . \tag{2.59}$$

Using the monoenergetic ion distribution together with the earlier general formula for

the equilibrium electron distribution function, Eq. (2.28), one obtains

$$\frac{\partial f_e}{\partial v}\frac{1}{3}\left[\frac{1}{v^3}\int_0^v dv' f_e(v')v'^4 + \sum_i \frac{Z_i^2 n_i}{4\pi v^3}v_i^2\Theta(v-v_i) + \int_v^\infty dv' f_e(v')v' + \sum_i \frac{Z_i^2 n_i}{4\pi v_i}\Theta(v_i - v)\right]$$
$$+ f_e(v)\left[\frac{1}{v^2}\int_0^v dv' f_e(v')v'^2 + \sum_i \frac{Z_i^2 n_i}{4\pi}\frac{m_e}{m_i}\frac{1}{v^2}\Theta(v-v_i)\right] = 0\,. \qquad (2.60)$$

For v_i substantially smaller that v_{te}, the electron distribution will be governed by the equation for the overwhelming majority of the electrons which have $v > v_i$, so one may set $\Theta(v - v_i) = 1$ and $\Theta(v_i - v) = 0$ in Eq. (2.60) in order to find a good expression for $f_e(v)$. However, if v_i is comparable to v_{te}, phenomena occuring on both sides of $v = v_i$ must be taken into account.

2.4.2 Useful Approximate Answer

For electrons with $v_{te} \gg v > v_i$, Eq. (2.60) may be approximated by

$$\frac{\partial f_e}{\partial v}\left[\sum_i \frac{Z_i^2 n_i}{4\pi v^3}\frac{v_i^2}{3} + \frac{1}{3}\int_0^\infty dv' f_e(v')v'\right] + f_e\frac{1}{v^2}\left[\frac{v^3}{3}f_e(0) + \sum_i \frac{Z_i^2 n_i}{4\pi}\frac{m_e}{m_i}\right] = 0\,. \qquad (2.61)$$

Note that this equation for electrons interacting with monoenergetic ions is exactly the same as Eq. (2.38) for electrons interacting with Maxwellian ions in the corresponding velocity range ($v_{te} \gg v \gg v_{ti}$), provided that one uses $v_{ti}^2 \to 2v_i^2/3$, or $T_i \to 2E_i/3$.

Accordingly, the critical velocity for the electrons is now defined as

$$v_c^3 \equiv \sqrt{2\pi}\sum_i \frac{Z_i^2 n_i}{n_e}\frac{E_i}{m_i}\sqrt{\frac{T_e}{m_e}}\,. \qquad (2.62)$$

Similarly the electron distribution function is

$$f_e(v) = \frac{n_e}{4\pi}\exp\left\{-\frac{m_e}{T_e}\int_0^v \frac{dv'v'\left(v'^3 + \frac{3}{2}\frac{T_e}{E_i}v_c^3\right)}{(v'^3 + v_c^3)}\right\}$$
$$\times\left[\int_0^\infty dv' v'^2 \exp\left\{-\frac{m_e}{T_e}\int_0^{v'}\frac{dv''v''\left(v''^3 + \frac{3}{2}\frac{T_e}{E_i}v_c^3\right)}{(v''^3 + v_c^3)}\right\}\right]^{-1}\,. \qquad (2.63)$$

The power density transferred from the ions to the electrons may be approximated as

$$P_{ie} \approx \frac{16\pi^2 Z_i^2 e^4 n_i \ln\Lambda}{m_i}\left[\frac{2}{3}\frac{E_i}{m_e}f_e(0) - \int_0^\infty dv f_e(v) v\right] . \tag{2.64}$$

This expression is identical to Eq. (2.33) provided that one again makes the identification $T_i \to 2E_i/3$. Because of the exact correspondence between Eqs. (2.61) and (2.64) and their predecessors in the Maxwellian ion case, the Maxwellian results may be used here, provided the proper substitution is made for the ion temperature in each case.

By analogy with the earlier Maxwellian results, a useful approximation for the heat transfer is (taking the numerical coefficient in the exponential to be $3.5 \cdot 2/3 \approx 2.4$)

$$\frac{P_{ie}}{(P_{ie})_{\text{Spitzer}}} \approx \left(1 + \frac{2}{3}\frac{m_e}{m_i}\frac{E_i}{T_e}\right)^{3/2} \exp\left\{-\left(2.4\sum_i \frac{Z_i^2 n_i}{n_e}\frac{m_e}{m_i}\frac{E_i}{T_e}\right)^{2/3}\right\} . \tag{2.65}$$

2.4.3 More Accurate Answer

By using the electron distribution function of Eq. (2.63) in Eq. (2.59) and dividing by the Spitzer rate, a more accurate expression for the correction factor is found to be

$$\begin{aligned}\frac{P_{ie}}{(P_{ie})_{\text{Spitzer}}} \approx{}& \sqrt{\frac{\pi}{2}}\frac{T_e}{\left(\frac{2}{3}E_i - T_e\right)}\left(1 + \frac{2}{3}\frac{m_e}{m_i}\frac{E_i}{T_e}\right)^{3/2} \\ &\times\left[\frac{m_i}{m_e}\frac{1}{v_i}\int_0^{v_i} dv v^2 \exp\left\{-\frac{m_e}{T_e}\int_0^v \frac{dv' v'\left(v'^3 + \frac{3}{2}\frac{T_e}{E_i}v_c^3\right)}{(v'^3 + v_c^3)}\right\}\right. \\ &\left. - \int_{v_i}^\infty dv v \exp\left\{-\frac{m_e}{T_e}\int_0^v \frac{dv' v'\left(v'^3 + \frac{3}{2}\frac{T_e}{E_i}v_c^3\right)}{(v'^3 + v_c^3)}\right\}\right] \\ &\times\left[\sqrt{\frac{m_e}{T_e}}\int_0^\infty dv v^2 \exp\left\{-\frac{m_e}{T_e}\int_0^v \frac{dv' v'\left(v'^3 + \frac{3}{2}\frac{T_e}{E_i}v_c^3\right)}{(v'^3 + v_c^3)}\right\}\right]^{-1} .\end{aligned} \tag{2.66}$$

Mathematica was again employed in order to numerically integrate and graph this

improved expression for the ion-electron heat transfer rate in the case monoenergetic ions. The results are shown in Figures 2-2 through 2-4 (along with the results for the Maxwellian ion case) for plasmas consisting of pure light hydrogen, pure deuterium, and pure ^{3}He, respectively. In the graphs, the effective ion temperature has been defined as $T_i \equiv 2E_i/3$.

Since the most important feature about the interactions of the ions with the electrons is that the ion speeds are typically much smaller than the electron thermal speed, one would expect that the heat transfer rate would depend only on the mean ion energy and not the particular ion distribution shape (except at very large temperature ratios, $T_i/T_e \sim 1000$, when the mean ion and electron speeds start to become comparable). This behavior is indeed quite evident in the figures.

Based on the comparison with the analytical and code results for Maxwellian ions, this monoenergetic ion answer appears to be fairly accurate. However, techniques for obtaining an even more precise analytical answer for the monoenergetic ion case will now be discussed.

2.4.4 Toward Even More Accurate Analytical Results

As in the case of Maxwellian ions, an even more accurate answer may be obtained by returning to the full nonlinear first-order differential equation for the electron distribution function, Eq. (2.60), and iterating. The next iteration expression for f_e written in terms of the previous iteration's less accurate expression, f_e^*, is

$$f_e(v) = f_e(0)\exp\left\{-\int_0^v \left[dv'v'\left\{3\int_0^{v'} dv'' f_e^*(v'')v''^2 + \sum_i \frac{3Z_i^2 n_i}{4\pi}\frac{m_e}{m_i}\Theta(v'-v_i)\right\}\right.\right.$$
$$\times\left\{\int_0^{v'} dv'' f_e^*(v'')v''^4 + v'^3\int_{v'}^{\infty} dv'' f_e^*(v'')v''\right.$$
$$\left.\left.\left.+\sum_i \frac{Z_i^2 n_i}{4\pi}\left[v_i^2\Theta(v'-v_i) + \frac{v'^3}{v_i}\Theta(v_i-v')\right]\right\}^{-1}\right]\right\}. \tag{2.67}$$

As usual $f_e(0)$ is calculated directly from the normalization condition.

If one begins the iteration process by assuming that $f_e^*(v)$ is Maxwellian and characterized by the thermal velocity v_{te}, then the distribution function of Eq. (2.67) becomes

$$f_e(v) = f_e(0)\exp\left\{-2\int_0^v\left[\frac{dv'v'}{v_{te}^2}\left\{\frac{3}{2}\left[\frac{\sqrt{\pi}}{2}\mathrm{erf}\left(\frac{v'}{v_{te}}\right)-\frac{v'}{v_{te}}\exp\left(-\frac{v'^2}{v_{te}^2}\right)\right]\right.\right.\right.$$
$$\left.+\sum_i\frac{3\sqrt{\pi}}{4}\frac{Z_i^2n_i}{n_e}\frac{m_e}{m_i}\Theta(v'-v_i)\right\}$$
$$\times\left\{\frac{3}{2}\left[\frac{\sqrt{\pi}}{2}\mathrm{erf}\left(\frac{v'}{v_{te}}\right)-\frac{v'}{v_{te}}\exp\left(-\frac{v'^2}{v_{te}^2}\right)\right]\right.$$
$$\left.\left.\left.+\sum_i\frac{\sqrt{\pi}}{2}\frac{Z_i^2n_i}{n_e}\left[\frac{v_i^2}{v_{te}^2}\Theta(v'-v_i)+\frac{v'^3}{v_{te}^2v_i}\Theta(v_i-v')\right]\right\}^{-1}\right]\right\}. \tag{2.68}$$

Note that by using the series expansion for $v_i < v' \ll v_{te}$ this distribution function reduces to the simpler one found given in the previous section.

Even more accurate distribution functions could be found by using Eq. (2.68) or a simplified form of it as the basis for further iterations with Eq. (2.67).

Once a distribution function of the desired accuracy has been obtained, it can be used to find the correction to the Spitzer ion-electron energy transfer rate,

$$\frac{P_{ie}}{(P_{ie})_{\text{Spitzer}}} \approx \sqrt{\frac{\pi}{2}}\frac{T_e}{\left(\frac{2}{3}E_i-T_e\right)}\left(1+\frac{2}{3}\frac{m_e}{m_i}\frac{E_i}{T_e}\right)^{3/2}$$
$$\times\left[\frac{m_i}{m_e}\frac{1}{v_i}\int_0^{v_i}dvv^2\frac{f_e(v)}{f_e(0)}-\int_{v_i}^{\infty}dvv\frac{f_e(v)}{f_e(0)}\right]$$
$$\times\left[\sqrt{\frac{m_e}{T_e}}\int_0^{\infty}dvv^2\frac{f_e(v)}{f_e(0)}\right]^{-1}, \tag{2.69}$$

as well as the effective electron temperature, as given by Equation (2.57).

2.5 Summary

Corrections to the classical Spitzer rate of ion-electron energy exchange were calculated for the case of large T_i/T_e ratios. The results of these calculations are substantially more accurate and more broadly applicable than the original result of Rosenbluth [46].

A useful expression for the correction factor is

$$\frac{P_{ie}}{(P_{ie})_{\text{Spitzer}}} \approx \left(1+\frac{m_e}{m_i}\frac{T_i}{T_e}\right)^{3/2} \exp\left\{-\left(3.5\sum_i \frac{Z_i^2 n_i}{n_e}\frac{m_e}{m_i}\frac{T_i}{T_e}\right)^{2/3}\right\}. \qquad (2.70)$$

This result assumes that all of the ion species are Maxwellian and at the same temperature T_i. If the ions are non-Maxwellian, an effective ion temperature for use in the above equation may be defined in terms of the mean ion energy, $T_i \equiv 2\langle E_i\rangle/3$. Note that this simple approximation yields accurate results only for the temperature range

$$1 \le \sum_i \frac{Z_i^2 n_i}{n_e}\frac{m_p}{m_i}\frac{T_i}{T_e} < 50\,. \qquad (2.71)$$

For temperature ratios larger than this range, the approximate answer given above begins to underestimate the actual energy transfer rate, so in such cases one should use the results of one of the more sophisticated calculations presented in this chapter.

These more accurate analytical expressions for the correction factor were numerically integrated and graphed using Mathematica, and the results were summarized in graphs for plasmas of various compositions. The results generally agree with those obtained by Galambos [55, 56] with a Fokker-Planck code.

As was shown, iterative methods may be employed if one desires to obtain even more accurate analytical expressions for the correction factor for the two cases of Maxwellian ions and monoenergetic ions.

The correction factor derived in this chapter may be incorporated into calculations of

electron energy balance and bremsstrahlung radiation in order to improve the accuracy of those calculations; this will be done in Chapters 6 and 7.

Chapter 3

Power Requirements for Actively Maintaining Non-Maxwellian Velocity Distributions

The limitations on any system which actively maintains one or more particle species in substantially non-Maxwellian (but isotropic) velocity distributions will now be examined.

Figure 3-1 shows the most efficient system imaginable for maintaining a nonequilibrium plasma. Entropy generated by collisions in the plasma (at the rate $\dot{S}$) is pumped out of the plasma in the form of heat energy ($\dot{Q}$). Most of this heat energy is recycled by a heat engine (limited by the Carnot efficiency) and returned to the plasma as work input ($\dot{W}_{recirc}$); the remainder of the heat energy ($\dot{Q}_{loss}$) is exhausted to a low-temperature thermal reservoir.

This conceptual system for keeping the plasma out of thermodynamic equilibrium immediately shows that there will be two fundamental limitations. One limitation is the minimum power loss due to the heat energy that must be exhausted to the low-

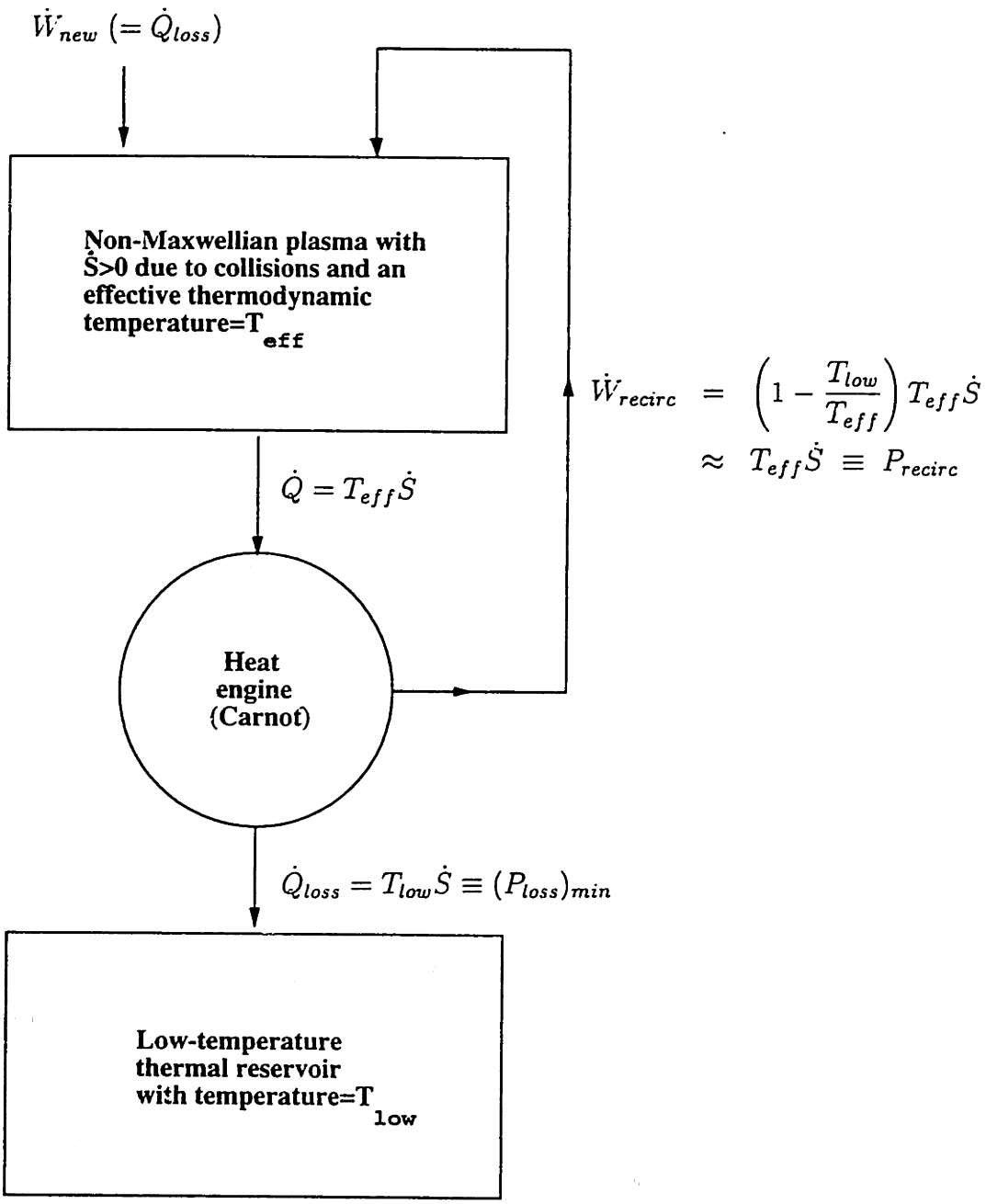

Figure 3-1: Maximally efficient system for maintaining a nonequilibrium plasma.

temperature reservoir; if this minimum power exceeds the fusion power, the reactor will clearly not be useful. The second limiting quantity is the minimum recirculating power, which for typical parameters should be much larger than the minimum power loss. As a practical constraint, if this recirculating power becomes much larger than the fusion power, the reactor will not be particularly desirable.

This basic picture will now be used to derive detailed limits on the performance of plasma fusion systems in which one or more particle species have substantially non-Maxwellian distributions.

There are two cases of particular interest. The first is that of a nearly monoenergetic but isotropic beam with a given thermal spread, such as the distributions that have been proposed for ions and/or electrons in inertial-electrostatic confinement fusion [19] and migma [38]. The second case is that of a nearly Maxwellian distribution in which virtually all of the slow particles have been depleted below some speed that is small in comparison with the "thermal" speed that characterizes the Maxwellian shape. This type of distribution would be desirable for electrons in advanced-fuel plasmas, since by depleting most of the electrons with speeds slower than the ion speeds, ion-electron energy transfer can be greatly reduced, thereby also substantially cutting the bremsstrahlung radiation losses.

Rough preliminary estimates of the power requirements for maintaining the particle distributions in these two important cases will be made in Section 3.1. After this brief and intuitive introduction to the problems which must be faced, a rigorous derivation of the power requirements will be given in Section 3.2. In Section 3.3, the results of the rigorous derivation will be applied to the calculation of the power requirements for a large number of different fusion fuels. Because all of these calculations will be performed assuming isotropy of the velocity distribution functions, Section 3.4 will estimate the impact that large deviations from isotropy would have on the calculations. Finally, Section 3.5 will discuss the categories of possible fusion approaches which can be ruled out on the basis of the calculations presented in this chapter.

3.1 Prelimary Estimates

Before performing a meticulous calculation of the requirements for maintaining non-Maxwellian velocity distributions, it would be useful to estimate the requirements (at least the recirculating power) for the two limiting cases just mentioned.

3.1.1 Beamlike Velocity Distribution with a Thermal Spread

Attention will first focus on an isotropic velocity distribution in which the particles are centered around a mean speed v_o with some "thermal" spread $v_t \ll v_o$ on each side of the mean speed. Due to collisions, a certain number (actually a certain density) of the particles n_{fast} will gain an amount of energy ΔE_{fast} on a timescale of τ_{fast}. If the width of the distribution is to be kept from spreading beyond the allowed v_t, then one must recirculate a power density P_{recirc} defined by

$$P_{recirc} = \frac{n_{fast}\,\Delta E_{fast}}{\tau_{fast}} \,. \tag{3.1}$$

According to Sivukhin [59], the parallel velocity-space diffusion coefficient for a particle with velocity v_{test} in the presence of isotropic, monoenergetic field particles of the same species with speed v_o is

$$\begin{aligned} D_{\|} &= \frac{4\pi (Ze)^4 n v_o^2 \ln\Lambda}{3m^2 v_{test}^3} \\ &= \frac{\sqrt{\pi}}{3\sqrt{6}} \left(\frac{v_o}{v_{test}}\right)^3 \frac{v_o^2}{\tau_{col}} \,, \end{aligned} \tag{3.2}$$

where the usual definition of the collision time [30] with $\langle E \rangle = (3/2)T \approx m v_o^2/2$,

$$\tau_{col} \equiv \frac{\sqrt{m}\,\langle E \rangle^{3/2}}{2\sqrt{3\pi}(Ze)^4 n \ln\Lambda} \,, \tag{3.3}$$

was used to rewrite the diffusion coefficient.

The time for a typical test particle to be collisionally upscattered from the velocity v_o to the maximum allowed velocity $v_{fast} \equiv v_o + v_t$ may be estimated as

$$\begin{aligned} \tau_{fast} &\approx \frac{v_t^2}{D_{\|}} \\ &\approx \frac{3\sqrt{6}}{\sqrt{\pi}} \left(\frac{v_t}{v_o}\right)^2 \tau_{col} \,, \end{aligned} \tag{3.4}$$

where only the largest term has been retained.

By likewise keeping only the largest term of ΔE_{fast} and using $\langle E \rangle \approx m v_o^2/2$, one finds the energy upscattering to be

$$\Delta E_{fast} = \frac{1}{2} m (v_{fast}^2 - v_o^2) \approx 2 \frac{v_t}{v_o} \langle E \rangle \ . \tag{3.5}$$

The final necessary assumption is that approximately half of the particles will be upscattered in energy and half will be downscattered, so $n_{fast} \approx n/2$. By putting all of this information together, the recirculating power required to hold the proper distribution shape despite self-collisions is found to be

$$\begin{aligned} P_{recirc} &\approx \frac{\sqrt{\pi}}{3\sqrt{6}} \frac{v_o}{v_t} \frac{n \langle E \rangle}{\tau_{col}} \\ &\approx 0.24 \frac{v_o}{v_t} \frac{n \langle E \rangle}{\tau_{col}} \,. \end{aligned} \tag{3.6}$$

One might wonder whether this rather crude technique for estimating the recirculating power is particularly precise, or even whether there may not be more complicated considerations which would greatly alter the answer. Yet as will be shown rigorously later in the chapter, this initial estimate is surprisingly accurate.

3.1.2 Nearly Maxwellian Distribution with Slow Particles Depleted

The other major type of distribution function of interest is one that is nearly Maxwellian but with essentially all of the very slow particles depleted. This situation would be especially desirable for the electron distribution in advanced-fuel plasmas, so that far fewer than the purely Maxwellian number of electrons would have speeds slower than the ions, thus resulting in a large reduction in the rate of energy transfer from the ions to the electrons.

For the purpose of a simple initial estimate, one may choose an electron distribution which looks superficially like a normal Maxwellian with a characteristic thermal velocity $v_{tf} \equiv \sqrt{2T_{of}/m_e}$ but has no particles at speeds below some velocity v_o, which is chosen such that it is comparable to (actually somewhat greater than) the ion thermal velocity and obeys the relation, $v_o \ll v_{tf}$.

The recirculating power which must be continually extracted from the tail of the electron distribution function and given to the slow electrons to boost their energies is

$$P_{recirc} = \frac{n_{slow}\,\Delta E_{slow}}{t_E^{ee}}\ , \tag{3.7}$$

where n_{slow} is the density of slow electrons that must continually be acted upon, ΔE_{slow} is the energy that must be given to each one of them, and t_E^{ee} is the collision time for slow electrons interacting with Maxwellian "field" electrons, as given in Eq. (2.4).

By using the overall electron-electron collision time from Eq. (3.3) with $\langle E \rangle \approx (3/2)T_{of} = (3/4)m_e v_{tf}^2$, t_E^{ee} from Eq. (2.4) may be rewritten as

$$t_E^{ee} \approx \frac{1}{4}\left(\frac{v_o}{v_{tf}}\right)^2 \tau_{col}\ . \tag{3.8}$$

Within a time period t_E^{ee}, the density of electrons which must be boosted in energy to prevent them from occupying the depleted region below $v = v_o$ will be comparable to the

normal Maxwellian population of that region of velocity space,

$$n_{slow} \sim \left(\frac{n_e}{\pi^{3/2} v_{tf}^3}\right)\left(\frac{4}{3}\pi v_o^3\right) = \frac{4}{3\sqrt{\pi}} n_e \left(\frac{v_o}{v_{tf}}\right)^3 . \tag{3.9}$$

If the distribution were allowed to relax for a time t_E^{ce}, the number of slow electrons would approach this equilibrium value but would still be less than it, so n_{slow} will actually be somewhat less than the value on the right-hand side of Eq. (3.9).

Naively one might think that the required ΔE_{slow} to restore each electron that had been about to become slower than v_o to its proper place would be comparable to $m_e v_o^2/2$. However, while one group of electrons with $v \approx v_o$ is attempting to diffuse lower in velocity space, another group of electrons is following "on their heels" at a slightly higher velocity but still with a net downward movement in velocity. To intercept electrons attempting to cross the $v = v_o$ line and return them to a velocity just above that value would cause the downward velocity space flux to coalesce into a large undesirable spike in the distribution there. Because of this reason, intercepted slow electrons must be boosted up much higher in the distribution function to some "continental divide" from which they are free to diffuse either lower or higher in velocity space. The exact amount of energy which they must be given is not readily apparent in this simple model, but it should be comparable to the mean electron energy: $\Delta E_{slow} \sim \langle E \rangle$.

Putting all of this information together, one arrives at the conclusion that

$$P_{recirc} \sim \frac{v_o}{v_{tf}} \frac{n \langle E \rangle}{\tau_{col}} . \tag{3.10}$$

The proper numerical coefficient by which this expression should be multiplied cannot be determined from this simple model, and to discover it, one will have to await the much more rigorous calculations of Section 3.2.5.

3.2 Limitations on Isotropic Non-Maxwellian Distributions

Now that preliminary estimates have been made, the requirements needed to maintain isotropic but non-Maxwellian velocity distributions will be calculated in a rigorous fashion. For simplicity, only the effects of like-particle collisions will be considered.

3.2.1 Model Distribution Function

The particle distribution function is chosen to be non-Maxwellian but isotropic, specifically the distribution shown in Figure 3-2,

$$f(v) = \begin{cases} nK_1\{\exp[-(v-v_o)^2/v_{ts}^2] + \exp[-(v+v_o)^2/v_{ts}^2]\} & \text{for } v < v_o \\ nK_1\{\exp[-(v-v_o)^2/v_{tf}^2] + \exp[-(v+v_o)^2/v_{ts}^2]\} & \text{for } v \geq v_o, \end{cases} \tag{3.11}$$

in which K_1 is a constant included to normalize the distribution and the "thermal velocities" on the fast (subscript f) and slow (subscript s) sides of $v = v_o$ may be expressed in terms of "temperatures," so that $v_{ts} \equiv \sqrt{2T_{os}/m}$ and $v_{tf} \equiv \sqrt{2T_{of}/m}$. Of course, in the spherical velocity coordinates convenient for studying isotropic plasmas, one only needs to be concerned with the distribution for $v \geq 0$.

This distribution function has many virtues. It can be set to a Maxwellian by the choice $v_o = 0$, and even for other choices of v_o it goes to the Maxwellian limit for large v. By varying the relative values of v_o, v_{ts}, and v_{tf}, a wide variety of distribution shapes may be studied. Yet despite this high degree of flexibility, the particular form of the distribution function allows one to obtain exact expressions for quantities such as the mean particle energy and the collision operator. Furthermore, the $\exp[-(v+v_o)^2/v_{ts}^2]$ term of the distribution function, which describes the decay of the (not explicitly seen) peak on the negative side of $v = 0$, ensures that the derivative with respect to velocity will be continuous across $v = 0$ and equal to zero.

While the precise non-Maxwellian distribution function produced by a certain system

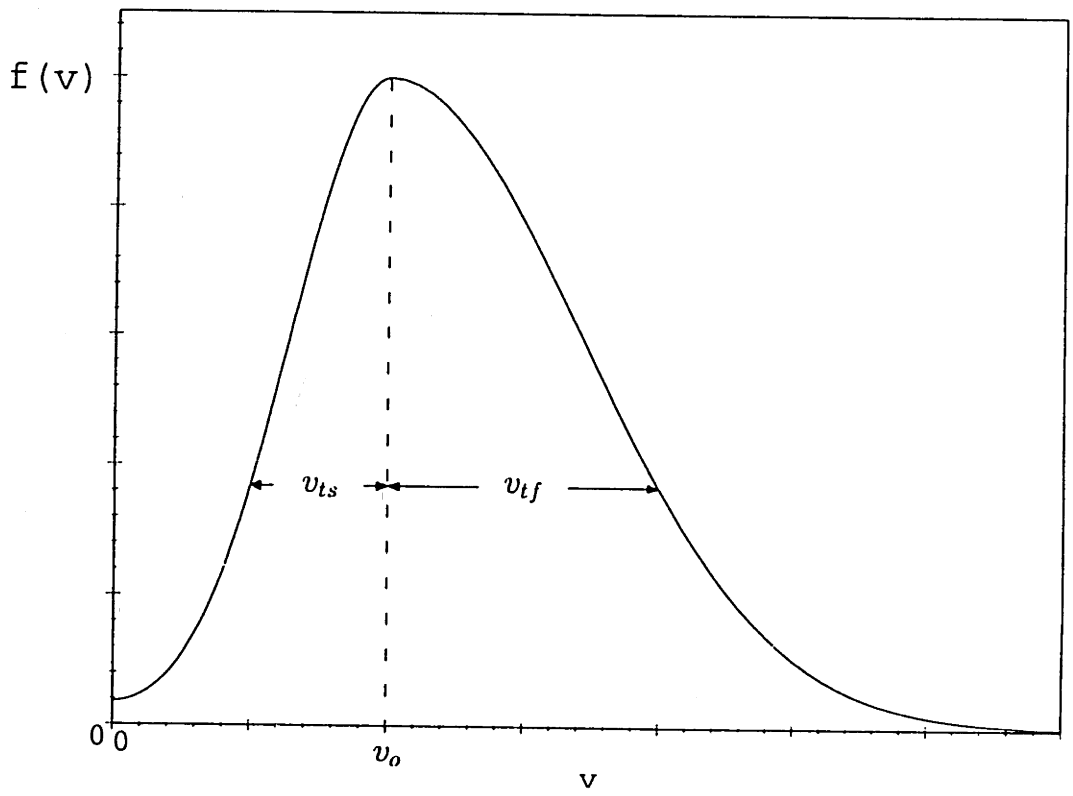

Figure 3-2: Model isotropic particle velocity distribution function.

may differ somewhat from this particular functional form (depending on the methods used to create and maintain the distribution shape), calculations involving the distribution of Eq. (3.11) should yield answers which are broadly applicable (at least approximately) to any system with a non-Maxwellian distribution function that is isotropic, peaks at a certain velocity v_o, and possesses characteristic widths on the fast and slow sides of $v = v_o$.

The two cases of particular interest which have already been mentioned can easily be explored using this model distribution function. By setting $v_{ts} = v_{tf} \equiv v_t$, $f(v)$ becomes suitable for describing a beamlike velocity distribution with a thermal spread. The second case, that of a nearly Maxwellian distribution in which there is a steep hole at very low speeds, may be investigated by choosing $v_{ts} \ll v_o \ll v_{tf}$.

(It should be briefly remarked that if one wished to study distributions in which $v_{ts} \gg v_{tf}$ and $v_{ts} \gg v_o$, Eq. (3.11) would have to be modified so that the $\exp[-(v+v_o)^2/v_{ts}^2]$ term would be cut off for $v > v_o$; a suitable modification of the distribution function would be

$$f(v) = \begin{cases} nK_1'\{\exp[-(v-v_o)^2/v_{ts}^2] + \exp[-(v+v_o)^2/v_{ts}^2]\} & \text{for } v < v_o \\ nK_1'\left[\exp\left(-4\frac{v_o^2}{v_{ts}^2}\right)+1\right]\exp\left[-\frac{(v-v_o)^2}{v_{tf}^2}\right] & \text{for } v \geq v_o, \end{cases} \tag{3.12}$$

Otherwise the exponential decay for $v > v_o$ would be dominated by the decay term from the peak on the negative side of $v = 0$ rather than by the desired fast decay velocity v_{tf}. This problem is not of concern in the present calculations, which only involve distribution functions for which Eq. (3.11) is perfectly adequate as it is.)

One may find K_1 from the normalization condition (with the unnormalized distribution function defined as $f_{un}(v) \equiv f(v)/nK_1$ and with ample use made of the integrals given in Appendix B):

$$K_1 = \left[\int_0^\infty dv 4\pi v^2 f_{un}(v)\right]^{-1}$$

$$= \frac{1}{\pi\left(2v_o^2v_{ts}\sqrt{\pi}+v_{ts}^3\sqrt{\pi}-4v_{ts}^2v_o+2v_o^2v_{tf}\sqrt{\pi}+v_{tf}^3\sqrt{\pi}+4v_{tf}^2v_o\right)} \frac{1}{\pi\left(2v_o^2v_{ts}\sqrt{\pi}+v_{ts}^3\sqrt{\pi}-4v_{ts}^2v_o+2v_o^2v_{tf}\sqrt{\pi}+v_{tf}^3\sqrt{\pi}+4v_{tf}^2v_o\right)} . \quad (3.13)$$

For $v_{ts} = v_{tf} \equiv v_t$, K_1 is greatly simplified:

$$K_1 = \frac{1}{2} \frac{1}{\pi^{3/2}v_t(2v_o^2+v_t^2)} . \quad (3.14)$$

It may be seen that in the Maxwellian limit ($v_o = 0$), the distribution function, including K_1, reduces to a properly normalized Maxwellian with temperature T_{of}.

In the opposite limiting case, that of nearly monoenergetic particles with a thermal spread $v_t \equiv v_{ts} = v_{tf}$ such that $v_o/v_t \gg 1$, the distribution function becomes

$$f(v) = \frac{n}{4\pi v_o^2} \frac{1}{\sqrt{\pi}\,v_t} \exp\left[-\frac{(v-v_o)^2}{v_t^2}\right] . \quad (3.15)$$

As $v_t \to 0$ for truly monoenergetic particles, this expression for the distribution function assumes its proper limiting form,

$$f(v) \to \frac{n}{4\pi v_o^2}\delta(v-v_o) . \quad (3.16)$$

3.2.2 Mean Particle Energy

The mean energy of the particles in the plasma is (see the integrals in Appendix B)

$$\begin{aligned}\langle E\rangle \equiv{}& \frac{1}{n}\int_0^\infty dv 4\pi v^2 \left(\frac{1}{2}mv^2\right) f(v) \\ ={}& \frac{m}{4}\left(3\sqrt{\pi}v_{tf}^4+16v_{tf}^3v_o-3v_{tf}^3v_{ts}\sqrt{\pi}+12v_{tf}^2v_o^2\sqrt{\pi}-16v_{tf}^2v_{ts}v_o+3v_{tf}^2\sqrt{\pi}v_{ts}^2\right. \\ &+16v_{tf}v_o^3-12v_{tf}v_o^2v_{ts}\sqrt{\pi}+16v_{tf}v_{ts}^2v_o-3v_{tf}v_{ts}^3\sqrt{\pi}+4v_o^4\sqrt{\pi}-16v_{ts}v_o^3 \\ &\left.+12v_{ts}^2v_o^2\sqrt{\pi}-16v_{ts}^3v_o+3\sqrt{\pi}v_{ts}^4\right) \\ &\Big/\left(\sqrt{\pi}v_{tf}^2+4v_{tf}v_o-v_{tf}v_{ts}\sqrt{\pi}+2v_o^2\sqrt{\pi}-4v_{ts}v_o+\sqrt{\pi}v_{ts}^2\right) . \end{aligned} \quad (3.17)$$

For $v_{ts} = v_{tf} \equiv v_t$, the mean energy simplifies to

$$\langle E \rangle = \frac{1}{4} \frac{m\left(4v_o^4 + 12v_t^2 v_o^2 + 3v_t^4\right)}{2v_o^2 + v_t^2} \,. \tag{3.18}$$

It is satisfying to note that in the Maxwellian limit, $v_o = 0$, the energy reduces to its usual value, $\langle E \rangle = \frac{3}{2} T_{of}$. Similarly, in the monoenergetic limit ($v_{ts},\ v_{tf} \to 0$) the energy also assumes its expected value, $\langle E \rangle = \frac{1}{2} m v_o^2 \equiv E_o$.

The mean energy may be used in the definition of the like-particle collision time, Eq. (3.3).

3.2.3 Depletion of Slow Particles

It is useful to note how heavily populated the slow-velocity region of the distribution function is compared with the case of a Maxwellian distribution with the same mean particle energy. (In other words, the Maxwellian with which the non-Maxwellian distribution is being compared has a temperature $T_{Maxw.} \equiv 2\langle E \rangle / 3$, where $\langle E \rangle$ is the mean particle energy of the non-Maxwellian distribution.) Dividing the non-Maxwellian distribution function by the Maxwellian one, it is found that

$$\begin{aligned}
\frac{f(v=0)}{f_{Maxwellian}(v=0)} &= \left(\frac{4}{3}\pi \frac{\langle E \rangle}{m}\right)^{3/2} \frac{f(0)}{n} \\
&= \frac{2\sqrt{\pi}}{3\sqrt{3}} \Big[\Big(3\sqrt{\pi} v_{tf}^4 + 16 v_{tf}^3 v_o - 3 v_{tf}^3 v_{ts}\sqrt{\pi} + 12 v_{tf}^2 v_o^2 \sqrt{\pi} \\
&\quad - 16 v_{tf}^2 v_{ts} v_o + 3 v_{tf}^2 \sqrt{\pi} v_{ts}^2 + 16 v_{tf} v_o^3 - 12 v_{tf} v_o^2 v_{ts}\sqrt{\pi} \\
&\quad + 16 v_{tf} v_{ts}^2 v_o - 3 v_{tf} v_{ts}^3 \sqrt{\pi} + 4 v_o^4 \sqrt{\pi} - 16 v_{ts} v_o^3 \\
&\quad + 12 v_{ts}^2 v_o^2 \sqrt{\pi} - 16 v_{ts}^3 v_o + 3\sqrt{\pi} v_{ts}^4\Big) \\
&\quad \Big/\Big(\sqrt{\pi} v_{tf}^2 + 4 v_{tf} v_o - v_{tf} v_{ts}\sqrt{\pi} + 2 v_o^2 \sqrt{\pi} - 4 v_{ts} v_o + \sqrt{\pi} v_{ts}^2\Big)\Big]^{3/2} \\
&\quad \times\Big(2 v_o^2 v_{ts}\sqrt{\pi} + v_{ts}^3 \sqrt{\pi} - 4 v_{ts}^2 v_o + 2 v_o^2 v_{tf}\sqrt{\pi} + v_{tf}^3 \sqrt{\pi} + 4 v_{tf}^2 v_o\Big)^{-1} \\
&\quad \times e^{\left(-v_o^2/v_{ts}^2\right)} \,.
\end{aligned} \tag{3.19}$$

For $v_{ts} = v_{tf} = v_t$, this expression becomes

$$\frac{f(0)}{f_{Maxw.}(0)} = \frac{(4v_o^4 + 12v_t^2v_o^2 + 3v_t^4)^{3/2}}{3^{3/2}v_t(2v_o^2 + v_t^2)^{5/2}} e^{(-v_o^2/v_t^2)} . \tag{3.20}$$

A graph of $f(0)/f_{Maxw.}(0)$ vs. v_o/v_t is given in Figure 3-3. Some important values should be noted. Half of the slow particles have been depleted when $v_o/v_t = 0.8606$; 90% of them have been depleted when $v_o/v_t = 1.506$, and 99% of the slow particles have been depleted when $v_o/v_t = 2.1432$.

This ratio is important, because for ion-electron energy transfer in which the electron distribution function is nearly constant down in the range of velocities comparable to the ion velocities, one may write (see Eq. (2.36))

$$\frac{P_{ie}}{(P_{ie})_{Spitzer}} = \frac{f(0)}{f_{Maxw.}(0)} . \tag{3.21}$$

In Eq. (3.21), energy transfer from electrons back to ions has been neglected.

However, a more general but more complex relation must be used when the electron distribution possesses fine structure in the ion velocity range. For the particular case of Maxwellian ions interacting with electrons which have an isotropic but otherwise arbitrary distribution function, it is found from Eqs. (2.30) and (2.32) that

$$\frac{P_{ie}}{(P_{ie})_{Spitzer}} = \frac{m_e}{(T_i - T_e)} \left(1 + \frac{m_e}{m_i}\frac{T_i}{T_e}\right)^{3/2} \int_0^\infty dv v^2 \frac{f_e(v)}{f_e^{Maxw.}(0)} \times \left[\frac{2}{\sqrt{\pi}}\frac{m_i}{m_e}\frac{1}{v_{ti}} \exp\left(-\frac{v^2}{v_{ti}^2}\right) - \frac{1}{v}\mathrm{erf}\left(\frac{v}{v_{ti}}\right)\right] . \tag{3.22}$$

One should recall that $T_e \equiv 2\langle E_e \rangle /3$ for non-Maxwellian electrons.

For the electron distribution in which $v_{ts} \ll v_o \ll v_{tf} \approx v_{te}$ with $v_o > v_{ti}$, Eq. (3.22) reduces to

$$\frac{P_{ie}}{(P_{ie})_{Spitzer}} \approx \frac{\frac{1}{\sqrt{\pi}}\left[(v_{ti}/v_o) + 2(v_o/v_{ti})\right] \exp\left(-v_o^2/v_{ti}^2\right) T_i - T_e}{T_i - T_e} . \tag{3.23}$$

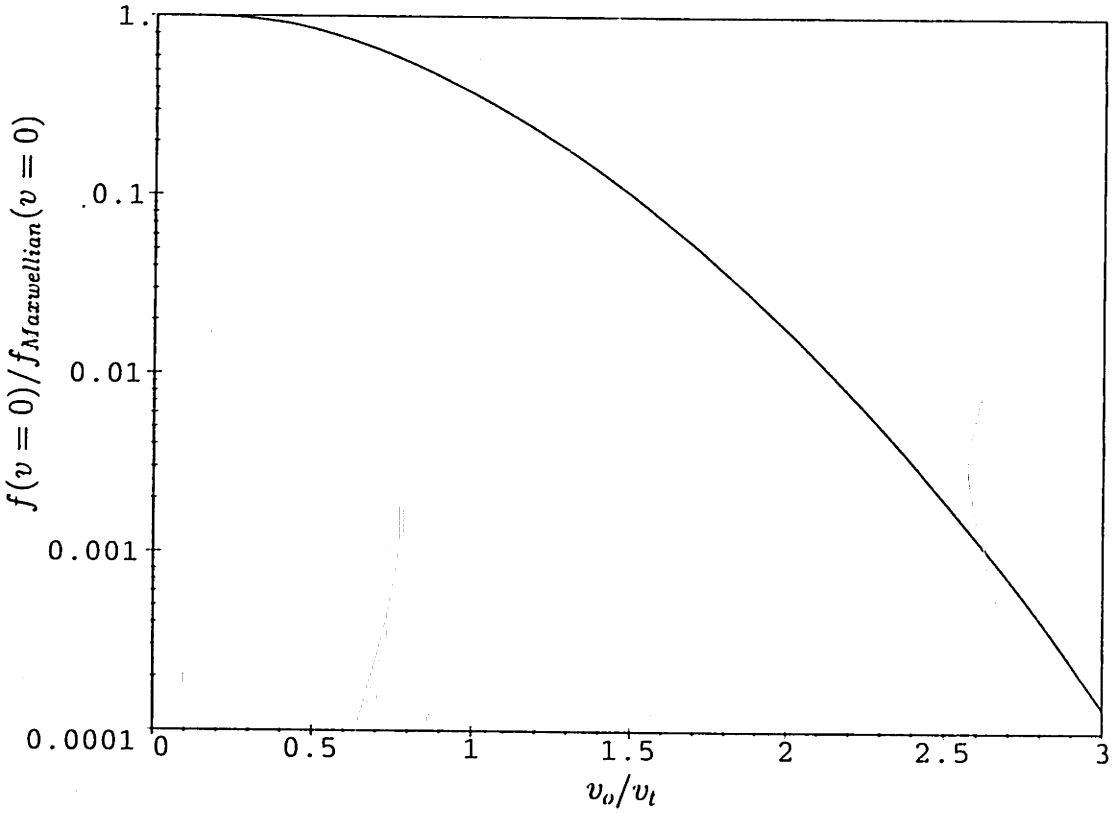

Figure 3-3: Slow particle depletion as a function of the exact shape of a beamlike distribution function with a thermal velocity spread.

For the purposes of future calculations with advanced fuels, it is useful to note that for $T_i \approx 10T_e$, the ion-electron energy transfer rate of Eq. (3.23) approaches zero for $v_o \approx \sqrt{3}v_{ti}$.

3.2.4 Collision Operator

The Fokker-Planck collision operator for collisions among like particles with an isotropic velocity distribution was given in Eq. (2.26) and may be rewritten as

$$\begin{aligned}\left(\frac{\partial f}{\partial t}\right)_{col.} &= \frac{8\pi^2(Ze)^4 \ln\Lambda}{m^2}\left\{\frac{2}{3}\frac{\partial^2 f}{\partial v^2}\left[\frac{1}{v^3}\int_0^v dv' f(v')v'^4 + \int_v^\infty dv' f(v')v'\right] + 2\left[f(v)\right]^2\right. \\ &\quad \left. + \frac{4}{3v}\frac{\partial f}{\partial v}\left[\int_0^\infty dv' f(v')v' - \int_0^v dv' f(v')v'\left(1-\frac{v'}{v}\right)^2\left(1+\frac{v'}{2v}\right)\right]\right\} \\ &= \frac{n}{\tau_{col.}}\left(\frac{4}{3}\pi\frac{\langle E\rangle}{m}\right)^{3/2} K_1^2\left\{\frac{\partial^2 f_{un}}{\partial v^2}\left[\frac{1}{v^3}\int_0^v dv' f_{un}(v')v'^4 + \int_v^\infty dv' f_{un}(v')v'\right]\right. \\ &\quad + \frac{\partial f_{un}}{\partial v}\left[\int_0^v dv' f_{un}(v')\left(3\frac{v'^2}{v^2} - \frac{v'^4}{v^4}\right) + \frac{2}{v}\int_v^\infty dv' f_{un}(v')v'\right] \\ &\quad \left. + 3\left[f_{un}(v)\right]^2\right\} . \end{aligned} \tag{3.24}$$

Using Eq. (3.24), an exact analytical solution for the collision operator with the distribution function from Eq. (3.11) may be found, but it is far too long (and unenlightening to superficial inspection) to give here, so it has been hidden in Appendix C. Appendix C also contains graphs of the collision operator for certain sets of parameters.

In the Maxwellian limit with $v_o = 0$, $(\partial f/\partial t)_{col.} = 0$ for all v, as expected; a Maxwellian distribution is a stationary solution of the Fokker-Planck equation. The collision operator for the more general distribution with $v_o \neq 0$ also conserves particles and energy when integrated over all velocities, as may be shown by numerical integration.

It should be mentioned that since the collision operator involves a $\partial^2 f/\partial v^2$ term, it develops a discontinuity across $v = v_o$ for $v_{ts} \neq v_{tf}$. Because the discontinuity is finite and because no derivatives of the collision operator have to be taken in this paper, this behavior

should not pose any mathematical difficulties. The discontinuity could be removed by replacing the sharp "step function" boundary in Eq. (3.11) with a smooth function such as that used for Butterworth low-pass filters [60], $1/[1 + (v/v_o)^{2n}]$ (with n a sufficiently large integer), or for the Fermi-Dirac function [61], $1/\{1 + \exp[(v - v_o)/\Delta v]\}$ (with Δv sufficiently small). However, when these low-pass filtering functions are made sufficiently sharp, one would simply recover the collision operator calculated in this paper (with the discontinuity replaced by an extremely rapid variation in the collision operator near $v = v_o$). Furthermore, the replacement of the step function with smooth low-pass filtering functions such as these would prevent the problem from being at all analytically tractable, or even readily computed numerically, considering the complexity of the calculations. For these reasons, the discontinuity in the collision operator is tolerated in these calculations.

3.2.5 Minimum Recirculating Power

The minimum recirculating power required to maintain the non-Maxwellian distribution may be found by using the method illustrated in Figure 3-4.

As shown in Figure 3-4, a certain number of the particles (N_{slow}) have lost energy as a result of collisions and have become too slow. The minimum energy required to restore these particles to their proper place in the distribution function is the energy difference between the total energy of all of the particles in the slow group and the total energy represented by the first N_{slow} vacated states (in order of increasing energy) in the desired non-Maxwellian distribution function. This amount of energy must be given to the particles every time they are downscattered in energy (a continual process), so it really represents a power. Rather than injecting this much fresh power into the plasma, in the ideal case the energy may be obtained by selectively extracting energy from those particles which have become too fast as the result of collisions. The "dividing velocity" v_d, which separates the first N_{slow} vacated states in the desired distribution function from

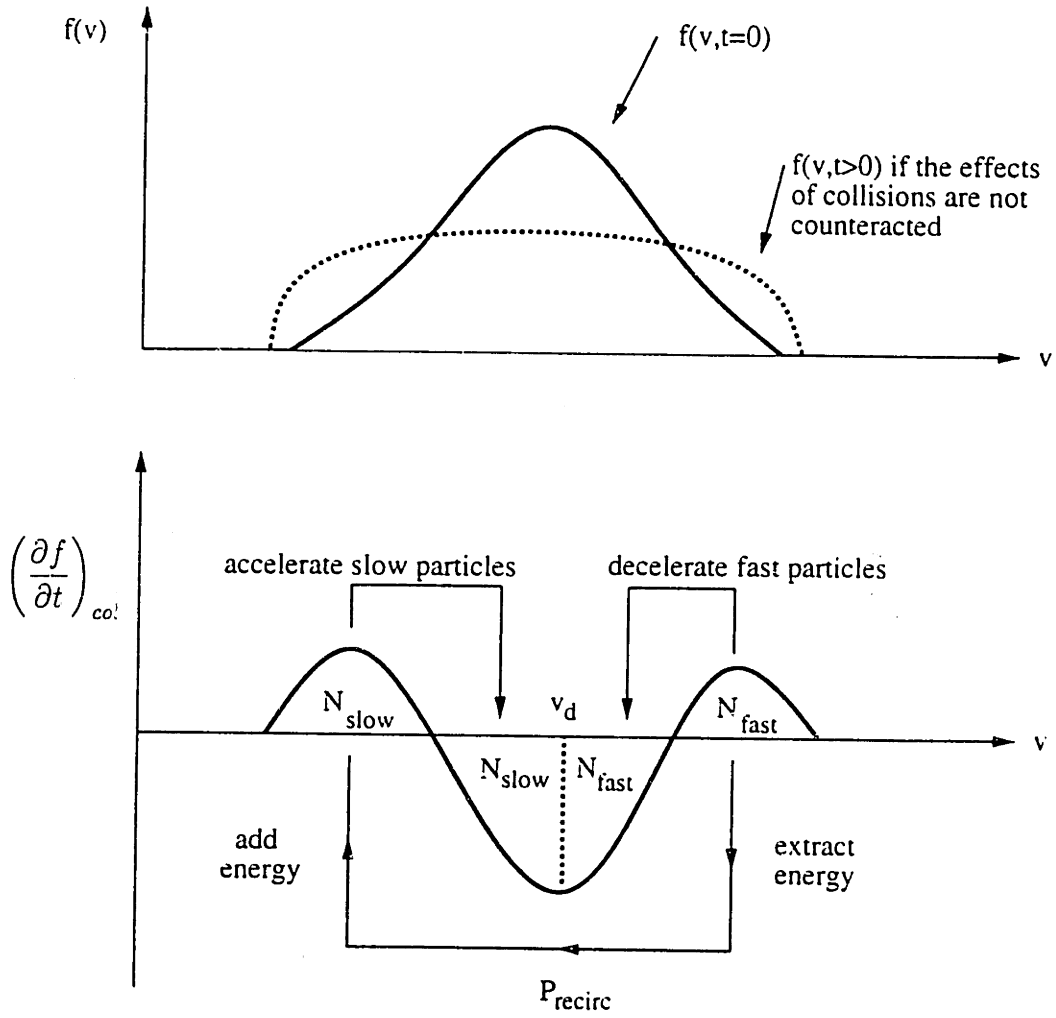

Figure 3-4: Method of calculating the minimum recirculating power necessary in order to hold the desired non-Maxwellian velocity distribution shape.

higher-energy vacated states, is defined as being finite and satisfying the relation:

$$\int_0^{v_d} \left(dv 4\pi v^2\right) \left(\frac{\partial f}{\partial t}\right)_{col} = 0 \,. \tag{3.25}$$

By expressing the collision operator for like-particle collisions in terms of the flux of particles in velocity space, $(\partial f/\partial t)_{col} = -\nabla_{\mathbf{v}} \cdot \mathbf{J}$, and then employing Gauss's divergence theorem, it may be seen that the dividing velocity is the finite velocity at which

$$\mathbf{J}(v_d) = 0 \,. \tag{3.26}$$

With the aid of the explicit form of the velocity-space particle flux from Eq. (2.27), this definition of the dividing velocity becomes

$$\left.\frac{\partial f}{\partial v}\right|_{v=v_d} \frac{1}{3}\left[\frac{1}{v_d^3}\int_0^{v_d} du f(u) u^4 + \int_{v_d}^{\infty} du f(u) u\right] + \frac{1}{v_d^2} f(v_d) \int_0^{v_d} du f(u) u^2 = 0 \,. \tag{3.27}$$

Insertion of the model distribution function from Eq. (3.11) yields an implicit equation for v_d (in which v_d appears in the arguments of exponentials and error functions). Either this resulting equation or Eq. (3.25) may be solved numerically to find the value of the dividing velocity for given values of v_{ts}, v_{tf}, and v_o in the model distribution function. (See Appendix D for the results of some test cases.)

The power which is found using the method outlined in Figure 3-4 is the minimum recirculating power needed to keep the non-Maxwellian distribution function constant, and it is defined as

$$P_{recirc} \equiv -\int_0^{v_d} \left(dv 4\pi v^2\right) \left(\frac{1}{2} m v^2\right) \left(\frac{\partial f}{\partial t}\right)_{col} \,. \tag{3.28}$$

By again relating the collision operator to the velocity-space flux, integrating by parts, and noting that $\mathbf{J} = 0$ at the $|\mathbf{v}| = v_d$ surface, the recirculating power may be rewritten

as

$$
\begin{aligned}
P_{recirc} &= -\int_0^{v_d} \left(dv 4\pi v^2\right)\, J\, mv \\
&= \frac{64\pi^3 Z^4 e^4 \ln\Lambda}{3m} \int_0^{v_d} dv \left\{ \frac{\partial f}{\partial v} \left[\int_0^v du f(u) u^4 + v^3 \int_v^\infty du f(u) u \right] \right. \\
&\qquad \left. + 3v f(v) \int_0^v du f(u) u^2 \right\} . \qquad (3.29)
\end{aligned}
$$

The first line of Eq. (3.29) reveals a somewhat different way of looking at the definition of the recirculating power. The flux in velocity space is essentially the net acceleration or deceleration of particles in a certain region of velocity space due to collisions; when multiplied by the mass that appears in the equation, this quantity can be pictured as a force. The power given to a particle by a force is the product of the force and the particle's velocity, so the above definition of the recirculating power is equivalent to the total power which is removed from decelerating particles (characterized by a negative or inward flux **J** in velocity space) and given to accelerating particles (characterized by a positive or outward flux in velocity space) in the course of the collisional process.

With this insight, it is now possible to generalize the definition of the recirculating power so that it also covers cases in which more than one dividing velocity is present. For an isotropic but otherwise arbitrary non-Maxwellian distribution function, collisional relaxation may create multiple, unconnected regions in which there is a net deceleration of particles (negative particle flux in velocity space); likewise, there may be multiple, unconnected regions in which there is a net acceleration of particles (positive particle flux). At the boundaries where the flux changes sign, $\mathbf{J} = 0$, or in other words, the boundaries occur at dividing velocities. If the non-Maxwellian distribution is to be maintained, power must be extracted from all of the regions with net acceleration due to collisions ($\mathbf{J} > 0$) and given to all of the regions with net deceleration ($\mathbf{J} < 0$). Assuming that no energy is lost from the distribution via radiation or other mechanisms, the total power which must be extracted is equal to the total power which must be added, so that each power

is equivalent to the recirculating power:

$$\begin{aligned} P_{recirc} &\equiv \int_0^\infty \left(dv 4\pi v^2\right)\left(\frac{1}{2}mv^2\right)\left(\frac{\partial f}{\partial t}\right)_{col}\Theta[J(v)] \\ &= \frac{1}{2}\int_0^\infty \left(dv 4\pi v^2\right)\left(\frac{1}{2}mv^2\right)\left(\frac{\partial f}{\partial t}\right)_{col}\mathrm{sign}\left[J(v)\right] \ . \end{aligned} \tag{3.30}$$

When only one dividing velocity is present, Eq. (3.30) reduces to the definition in Eq. (3.28).

(It should be observed that systems which recirculate power by extracting particles that have strayed in phase space, directly converting their full kinetic energy into electrical energy, and providing that energy to fresh particles which are then injected into the proper region of phase space will have a substantially larger recirculating power, which is given by

$$\begin{aligned} P_{recirc} &\equiv \int_0^\infty \left(dv 4\pi v^2\right)\left(\frac{1}{2}mv^2\right)\left(\frac{\partial f}{\partial t}\right)_{col}\Theta\left[\left(\frac{\partial f}{\partial t}\right)_{col}\right] \\ &= \frac{1}{2}\int_0^\infty \left(dv 4\pi v^2\right)\left(\frac{1}{2}mv^2\right)\left|\left(\frac{\partial f}{\partial t}\right)_{col}\right| \ . \end{aligned} \tag{3.31}$$

This recirculating power is much larger than that of Eq. (3.28), since here all of the energy of errant particles must be recycled, whereas in Eq. (3.28) only the discrepancy between stray particles' actual and desired energy had to be handled by the power recirculation system.)

As was stated earlier, one case of particular interest is that of an electron distribution which is essentially Maxwellian with the exception that a steep hole has been cut in the distribution function at low velocities. The collision operator for such a distribution is somewhat more complicated than that shown in Figure 3-4, but it can be shown that the definition of the recirculating power in Eq. (3.28) still applies. By using Maple [62] to integrate Eq. (3.28) numerically for the general distribution function of Eq. (3.11) and then examining the results for distributions of this particular type ($v_{ts} \ll v_o \ll v_{tf}$, raw data given in Appendix D), one finds that the recirculating power may be expressed in a

useful empirical form:

$$P_{recirc} = R_0(v_o/v_{tf}) \left(\frac{v_o}{v_{tf}}\right) \frac{n\langle E\rangle}{\tau_{col}} , \tag{3.32}$$

where $R_0(v_o/v_{tf})$ is a slowly varying function (at least for $v_o/v_{tf} \ll 1$) as given in Table 3.1. The functional dependence of this result agrees with that of the simple estimate made in Eq. (3.10).

v_o/v_{tf}	$R_0(v_o/v_{tf})$		v_o/v_{tf}	$R_0(v_o/v_{tf})$
1/60	0.0637		1/6	0.0749
1/30	0.0644		1/3	0.0957
1/10	0.0687		1	0.183

Table 3.1: Selected values of the function $R_0(v_o/v_{tf})$ in Eq. (3.32) for the recirculating power required to deplete the slow particles in an otherwise essentially Maxwellian distribution.

The particular value of v_o/v_{ts} used for each entry in Table 3.1 is 10, but the results are essentially independent of v_o/v_{ts} provided that it is much greater than 1 (at least 3 or so; see the data in Appendix D for more details).

The other major case of interest is that of an isotropic beamlike distribution with a given thermal velocity spread. Upon numerical integration of Eq. (3.28) for the distribution of Eq. (3.11) with $v_{ts} = v_{tf} \equiv v_t$ (see the raw data in Appendix D), it is found that the recirculating power may be expressed as

$$P_{recirc} = R_1(v_o/v_t) \left(\frac{v_o}{v_t}\right) \frac{n\langle E\rangle}{\tau_{col}} , \tag{3.33}$$

where $R_1(v_o/v_t)$ is a slowly varying (for $v_o/v_t > 1$) function as given in Table 3.2. Quite remarkably this rigorous calculation of the recirculating power agrees almost perfectly with the rough estimate made in Section 3.1.1 for $v_o/v_t \gg 1$.

Clearly the statement that R_1 is a slowly varying function breaks down for $v_o \ll v_t$, where the power dependence of P_{recirc} on v_o/v_t changes; in this nearly Maxwellian regime

v_o/v_t	R_1		v_o/v_t	R_1
0.01	$5.81 \cdot 10^{-7}$		3	0.148
0.1	$5.63 \cdot 10^{-4}$		4	0.168
0.5	0.0365		5	0.183
1	0.0854		10	0.221
1.5	0.107		30	0.253
2	0.122		100	0.265

Table 3.2: Selected values of the function $R_1(v_o/v_t)$ in Eq. (3.33) for the recirculating power required to maintain an isotropic, beamlike distribution.

of $v_o \ll v_t$, a more descriptive expression for P_{recirc} is

$$P_{recirc} \approx 0.6 \left(\frac{v_o}{v_t}\right)^4 \frac{n\langle E\rangle}{\tau_{col}} . \tag{3.34}$$

For simplicity, the recirculating power will by default be expressed for the case in which $v_{ts} = v_{tf} = v_t$, except where otherwise stated. To apply the formulas which are to follow to the case $v_{ts} \ll v_o \ll v_{tf}$, one should make the substitution,

$$R_1(v_o/v_t)\left(\frac{v_o}{v_t}\right) \rightarrow R_0(v_o/v_{tf})\left(\frac{v_o}{v_{tf}}\right) . \tag{3.35}$$

Putting the results obtained thus far into more readily useable form, the minimum recirculating power required to keep species "a" non-Maxwellian despite self-collisions is

$$P_{recirc} = 8.55 \cdot 10^{-25} R_1(v_o/v_t)\left(\frac{v_o}{v_t}\right)\sqrt{\frac{m_e}{m_a}}\,\frac{Z_a^4 n_a^2 \ln\Lambda}{\sqrt{\langle E_{a,\,eV}\rangle}}\ \frac{\mathrm{W}}{\mathrm{cm}^3} . \tag{3.36}$$

As any realistic reactor will have non-negligible losses associated with the recirculating power, it is important that the recirculating power not be much greater than the fusion power (and preferably even less than the fusion power).

Dividing the recirculating power by the fusion power from Eq. (1.3), one finds

$$\frac{P_{recirc}}{P_{fus}} = 5.34 \cdot 10^{-6} R_1 (v_o/v_t) \left(\frac{v_o}{v_t}\right) \sqrt{\frac{m_e}{m_a}} \frac{(x + Z_{i2})^2}{x} \frac{Z_a^4 n_a^2}{n_e^2} \times \frac{\ln \Lambda}{\langle \sigma v \rangle_{fus} E_{fus,\,eV} \sqrt{\langle E_{a,\,eV} \rangle}} . \quad (3.37)$$

If only one ion species is present, the substitution of Eq. (1.4) should be made.

3.2.6 Temporary Energy Down-Shifting

One might wonder how the recirculating power requirement presented in this chapter would be affected by having a plasma in which the particles circulate between different regions where they have different energies. As a concrete example, an electrostatic potential might be applied between two regions. In comparison with the second region, the first section of the plasma will be assumed to have relatively high particle energies and a large value of $\int n^2 d^3\mathbf{x}$, so the first region is where most of the deleterious scattering effects will occur. One might think that it would be easier to "repair" the particle velocity distribution when the particles circulate into the second region and have lower energies than they did in the first. Yet it can be shown that the recirculating power requirement is completely independent of the region in which the velocity distribution is repaired.

For a simple method of seeing why the recirculating power remains the same even when the particles are temporarily "down-shifted" in energy, one may consider the estimate of the recirculating power from Section 3.1.1, $P_{recirc} \approx n_{fast} \Delta E_{fast} / \tau_{fast}$. The number of particles which have become faster than desired, n_{fast}, remains the same even if the particles are temporarily moved up a potential hill so that they all slow down. Likewise, τ_{fast}, the timescale on which the particles become too fast, is also unaffected by the potential gradient, since it is determined solely by the rate of collisions in the dense first region. Finally, since the vacated "proper" states of the particles and the overpopulated "improper" particle states lose the same amount of kinetic energy in moving up the

potential gradient, the difference ΔE_{fast} between them remains the same. Thus the recirculating power requirement is unaffected.

A more rigorous way to demonstrate that temporary energy shifts have no effect on the power requirements is to write the formal definition of the recirculating power in terms of particle kinetic energies (E) instead of particle velocities:

$$P_{recirc} = -\int_0^{E_d} dE\, E \left(\frac{\partial f(E)}{\partial t}\right)_{col} . \tag{3.38}$$

For simplicity it has been assumed that there is only one dividing energy $E_d \equiv mv_d^2/2$, although this proof could easily be extended to the general case in which there are multiple dividing energies.

If the particle distribution is downshifted in kinetic energy by an amount ΔE (without bumping into $E = 0$ and losing particles) so that the new energy is $E' \equiv E - \Delta E$, the recirculating power needed to counteract collisional effects will be

$$\begin{aligned} P'_{recirc} &= -\int_0^{E_d - \Delta E} dE'\, E' \left(\frac{\partial f(E' + \Delta E)}{\partial t}\right)_{col} \\ &= -\int_0^{E_d} dE\, (E - \Delta E) \left(\frac{\partial f(E)}{\partial t}\right)_{col} \\ &= -\int_0^{E_d} dE\, E \left(\frac{\partial f(E)}{\partial t}\right)_{col} + \Delta E \int_0^{E_d} dE \left(\frac{\partial f(E)}{\partial t}\right)_{col} . \end{aligned} \tag{3.39}$$

The first integral in Eq. (3.39) is just the original value of P_{recirc}, while the second integral is zero by the definition of the dividing energy. Therefore the result of this more rigorous analysis is also that the recirculating power is unaltered by temporary energy downshifting of the particle distribution:

$$P'_{recirc} = P_{recirc} . \tag{3.40}$$

3.2.7 Entropy Generation Rate

The entropy density of a given particle species is [61, 63, 64, 65]:

$$S \equiv -\int d^3\mathbf{v} f(\mathbf{v}) \ln[f(\mathbf{v})] \,. \tag{3.41}$$

Thus the rate of entropy generation per volume due to particle collisions is

$$\begin{aligned} \frac{dS}{dt} &= -\int d^3\mathbf{v} \ln[f(\mathbf{v})] \left(\frac{\partial f}{\partial t}\right)_{col} - \int d^3\mathbf{v} \left(\frac{\partial f}{\partial t}\right)_{col} \\ &= -\int d^3\mathbf{v} \ln[f(\mathbf{v})] \left(\frac{\partial f}{\partial t}\right)_{col} , \end{aligned} \tag{3.42}$$

where the second term resulting from the time derivative was zero because of conservation of particles in collisions.

For the isotropic distributions of interest, the entropy generation per volume is

$$\frac{dS}{dt} = -\int_0^\infty dv 4\pi v^2 \ln[f(v)] \left(\frac{\partial f}{\partial t}\right)_{col} . \tag{3.43}$$

Since the entropy is only a well-defined quantity for near-equilibrium systems, the entropy generation rate of Eq. (3.43) may not be strictly valid for highly non-Maxwellian plasmas, but it should at least serve to make useful estimates.

Equation (3.43) was integrated numerically for the distribution function of Eq. (3.11) with $v_t = v_{ts} = v_{tf}$. The result of the numerical calculation (see the raw data in Appendix D) is that the entropy production may be described by the equation,

$$\frac{dS}{dt} = R_2(v_o/v_i) \left(\frac{v_o}{v_t}\right)^2 \frac{n}{\tau_{col}} , \tag{3.44}$$

in which $R_2(v_o/v_t)$ is a slowly varying (for $v_o/v_t > 1$) function whose values are given in Table 3.3.

v_o/v_t	R_2		v_o/v_t	R_2
0.01	$2.23 \cdot 10^{-10}$		5	0.332
0.03	$5.45 \cdot 10^{-9}$		10	0.390
0.1	$6.87 \cdot 10^{-6}$		30	0.447
0.5	$2.40 \cdot 10^{-2}$		100	0.471
1	0.138		300	0.479
1.5	0.207		1000	0.481
2	0.241		3000	0.482
3	0.282		10000	0.482
4	0.310		30000	0.482

Table 3.3: Selected values of the function $R_2(v_o/v_t)$ in Eq. (3.44) for the entropy generation rate of an isotropic, beamlike distribution.

For $v_o \ll v_t$ the functional dependence of dS/dt on v_o/v_t changes. While dS/dt in this regime is not strictly proportional to a given power of the velocity ratio, a rough estimate of the dependence for $v_o/v_t \ll 1$ is

$$\frac{dS}{dt} \sim \left(\frac{v_o}{v_t}\right)^6 \frac{n}{\tau_{col}} . \tag{3.45}$$

3.2.8 Minimum Power Loss

The minimum theoretical power density loss required to maintain the non-Maxwellian distribution (as shown in Figure 3-1) is

$$(P_{\rm loss})_{\rm min} \equiv \frac{dS}{dt} T_{\rm low} . \tag{3.46}$$

This relationship, which is familiar from classical thermodynamics, also holds true here, despite the highly nonequilibrium character of the plasma which is generating the entropy. The reason why the relationship is still valid is that although the usual connection [61] between temperature, energy, and entropy,

$$\frac{1}{T} = \frac{\partial S}{\partial E} , \tag{3.47}$$

is ill defined in the context of the nonequilibrium plasma, it may still be safely applied to the low-temperature thermal reservoir. Provided that the expression for dS/dt is indeed the actual entropy production rate, the rate of energy increase in the low-temperature thermal reservoir associated with receiving that much entropy will be the power given in Eq. (3.46).

$T_{\rm low}$ for terrestrial reactors will be roughly 270-300°K, or about 0.025 eV. (For space reactors the heat is radiated away to the vacuum, so theoretically $T_{\rm low}$ could essentially be arbitrarily low. In practice, however, there will be a minimum practical T_{low} even for a space-based reactor, since the required area of the radiator is inversely proportional to the radiated power flux, $\sigma_{SB}T_{\rm low}^4$, where σ_{SB} is the Stefan-Boltzmann constant.) With this value for T_{low}, the minimum power loss required to keep species "a" in a beamlike velocity distribution characterized by v_o/v_t is

$$\begin{aligned}(P_{\rm loss})_{\rm min} &\approx R_2(v_o/v_t)\left(\frac{v_o}{v_t}\right)^2 \frac{n}{\tau_{col}}\, 0.025 \text{ eV} \\ &\approx 2.14\cdot 10^{-26} R_2(v_o/v_t)\left(\frac{v_o}{v_t}\right)^2 \sqrt{\frac{m_e}{m_a}}\, \frac{Z_a^4 n_a^2 \ln\Lambda}{\langle E_{a,\,eV}\rangle^{3/2}}\, \frac{\rm W}{\rm cm^3}\,. \end{aligned} \tag{3.48}$$

Clearly the loss power density must be kept to some fraction of the fusion power density if the reactor is to be self-supporting.

Dividing the minimum power loss by the fusion power, one finds:

$$\begin{aligned}\frac{(P_{\rm loss})_{\rm min}}{P_{fus}} &\approx 1.33\cdot 10^{-7} R_2(v_o/v_t)\left(\frac{v_o}{v_t}\right)^2 \frac{(x+Z_{i2})^2}{x}\frac{Z_a^4 n_a^2}{n_e^2}\sqrt{\frac{m_e}{m_a}} \\ &\quad \times \frac{\ln\Lambda}{\langle\sigma v\rangle_{fus}\, E_{fus,\,eV}\,\langle E_{a,\,eV}\rangle^{3/2}}\,. \end{aligned} \tag{3.49}$$

Recall that if there is only one ion species, one should make the substitution in Equation (1.4).

The constraint that $(P_{\rm loss})_{\rm min} \leq P_{\rm fus}$ implies that

$$R_2(v_o/v_t)\left(\frac{v_o}{v_t}\right)^2 \leq 7.49\cdot 10^6 \frac{x}{(x+Z_{i2})^2}\frac{n_e^2}{Z_a^4 n_a^2}\sqrt{\frac{m_a}{m_e}}\frac{\langle\sigma v\rangle_{fus}\, E_{fus,\,eV}\,\langle E_{a,\,eV}\rangle^{3/2}}{\ln\Lambda}\,. \quad (3.50)$$

3.2.9 Effective Thermodynamic Temperature

One possible point of confusion regarding the maintenance of non-Maxwellian velocity distributions should be cleared up. As was remarked earlier, Eq. (3.47) is not particularly useful for defining the effective thermodynamic temperature of the non-Maxwellian distribution. This unfortunate fact arises because both the entropy and the energy depend on multiple parameters, and they do so in different ways, so that the differentials of the various parameters do not cancel when one takes the ratio of Eq. (3.47).

On the other hand, a different and more readily calculable definition of the effective thermodynamic temperature of the non-Maxwellian distribution can be constructed based on the picture of Figure 3-1:

$$T_{eff} \equiv \frac{P_{recirc}}{dS/dt}\,. \quad (3.51)$$

However, this temperature is not a readily identifiable (let alone useful) quantity, even in the Maxwellian limit. The reason for this problem is that a non-Maxwellian distribution function may be viewed as a sum of Maxwellian distributions with different temperatures, where each Maxwellian has been multiplied by a coefficient (which may actually be negative, further complicating the physical interpretation). Energy and particles flow between the different Maxwellians, giving rise to both the entropy production and the minimum recirculating power required to sustain the overall non-Maxwellian distribution. Thus the effective temperature defined in Eq. (3.51) is a complicated function of the temperatures and coefficients of the various Maxwellian components of the distribution, and it cannot be expected to correspond to the temperature of the "dominant" Maxwellian component even in the limit of an overall velocity distribution which is nearly Maxwellian.

These sorts of complications illustrate why it is necessary to calculate the recirculating power directly from the collision operator via the method of Figure 3-4, rather than by attempting to guess correctly the effective temperature of the plasma and then multiply that temperature by the entropy generation rate to arrive at the recirculating power.

3.3 Results for Isotropic Non-Maxwellian Distributions

Now the equations derived in the previous section will be explicitly applied to certain specific cases of interest.

3.3.1 Nearly Maxwellian Electron Distributions with Slow Electrons Actively Depleted

Ion-electron energy transfer is mediated by electrons moving more slowly than the ions, so in order to drastically cut the energy transfer rate, lower the electron temperature, and reduce the bremsstrahlung radiation losses from advanced fuel plasmas, it would be highly desirable to actively deplete all of the slow electrons. To keep the required amount of recirculating power to a minimum, the rest of the electron distribution function should be left essentially in equilibrium (apart from the nonequilibrium effects caused by receiving the "refugee" electrons displaced from lower velocities). Thus the requirements of nearly total depletion of slow electrons and minimization of recirculating power lead one to consider electron distribution function such as that of Eq. (3.11) with $v_{ts} \ll v_o \ll v_{tf}$, where v_o is chosen to be on the order of the ion thermal velocity and v_{tf} is found from the mean electron energy, $\langle E_e \rangle \approx 3T_f/2 = (3/4)m_e v_{tf}^2$.

By using a "blanket" value of $R_0 = 0.069$ and choosing $v_o \equiv \sqrt{3}v_{ti1}$ (for the reasons given in Section 3.2.3), where the i1 ion species is defined to be the lower-mass species if two fuel ion species are present, the recirculating power needed to maintain a narrow,

steep hole in the electron distribution is found to be

$$\frac{P_{recirc}}{P_{fus}} \approx 1.5 \cdot 10^{-8} \, \frac{(x + Z_{i2})^2}{x} \, \frac{\sqrt{\langle E_{i,\,eV} \rangle} \ln \Lambda}{\sqrt{\mu_{i1}} \, \langle \sigma v \rangle_{fus} \, E_{fus,\,eV} \, \langle E_{e,\,eV} \rangle} \, , \tag{3.52}$$

in which $\mu_{i1} \equiv m_{i1}/m_p$.

The recirculating power is inversely proportional to the mean electron energy, so it would seem advantageous to operate with $\langle E_e \rangle$ as large as possible. Unfortunately, another factor must be considered; as the energy increases, the bremsstrahlung radiation loss increases at least as rapidly as the square root of $\langle E_e \rangle$, as shown in Eq. (1.2). Therefore the electron energy must be kept sufficiently low to limit the bremsstrahlung power loss to a reasonable level.

The results of Eq. (3.52) for specific cases are given in Table 3.4 (where $\ln \Lambda = 15$ was assumed). In the table, the mean electron energies for the advanced aneutronic fuels were chosen so that the bremsstrahlung losses would not exceed half of the fusion power. For the other two fuels (D-^{3}He and D-D), the mean electron energy was chosen so that the bremsstrahlung losses would be no more than half as large as they would be in the equilibrium case (as calculated in Chapter 1). If the electron energies are lower than the values given, the bremsstrahlung losses will be lower but the recirculating power levels will be higher (note the "$\leq$" and "$\geq$" signs in the table). The calculation was not done for D-T since bremsstrahlung losses can be made negligibly small for D-T without at all altering the electron distribution from a Maxwellian shape (see the results for D-T in Chapter 7). (Values for the average fusion reactivity $\langle \sigma v \rangle_{fus}$ for ions with a mean energy $\langle E_i \rangle = (3/2)T_i$ are given in Table 1.1.)

From Table 3.4, it appears that for fusion plasmas using any of these fuels, the electrons cannot be maintained in a significantly non-Maxwellian state without using a recirculating power that is considerably larger than the fusion power. Since the slow electrons cannot be significantly depleted without resorting to unreasonably large recirculating power levels, ion-electron energy transfer will proceed at essentially its normal Spitzer-type rate.

Fuel	$\langle E_i \rangle$	$\langle E_e \rangle$	$\frac{P_{brem}}{P_{fus}}$	$\frac{P_{recirc}}{P_{fus}}$
D-^{3}He (1:1)	150 keV	$\leq$ 39 keV	≤ 0.093	≥ 4.7
D-D	750 keV	$\leq$ 170 keV	≤ 0.18	≥ 2.3
^{3}He-^{3}He	1.5 MeV	$\leq$ 160 keV	≤ 0.50	≥ 5.0
p-^{11}B (5:1)	450 keV	$\leq$ 35 keV	≤ 0.50	≥ 42
p-^{6}Li (3:1)	1.2 MeV	$\leq$ 22 keV	≤ 0.50	≥ 210

Table 3.4: P_{recirc}/P_{fus} for nearly Maxwellian electron distributions with the slow electrons depleted and $\ln \Lambda = 15$.

3.3.2 Further Optimization of Nearly Maxwellian Electron Distributions with Slow Electrons Actively Depleted

As one of the principal objects of this study is to determine whether any plausible system can maintain usefully non-Maxwellian electron velocity distributions and thereby ignite advanced aneutronic fuels, it is very important to investigate how well suited the chosen model distribution function is for this purpose.

In order to take into account all the necessary details of ion and electron behavior, a specific case will be chosen, namely a plasma of pure ^{3}He (which is the closest to ignition out of all the advanced aneutronic fuels) with an ion temperature of 1 MeV and $\ln \Lambda = 20$. From the equations presented in Chapter 1, it is found that if the ion-electron energy transfer rate is reduced from its classical value by two orders of magnitude ($P_{ie}/(P_{ie})_{Spitzer} = 0.01$), the equilibrium electron "temperature" (defined as $(2/3)\langle E_e \rangle$ for non-Maxwellian distributions) will be 49 keV, and the corresponding bremsstrahlung power loss fraction will be $P_{brem}/P_{fus} = 0.28$ (probably the largest which could realistically be tolerated when one includes other losses, as well as limited electric conversion efficiencies).

Thus the problem becomes to optimize the distribution function shape subject to the constraints that $\langle E_e \rangle = (3/2) \cdot 49$ keV$= 73.5$ keV and $P_{ie}/(P_{ie})_{Spitzer} = 0.01$. This optimization has been performed for the model distribution function of Eq. (3.11), as well

as for a more general distribution function.

Optimization of the Model Distribution from Eq. (3.11)

The model velocity distribution function of Eq. (3.11) contains three independently adjustable parameters: v_o, v_{ts}, and v_{tf}. By using the conditions on $\langle E_e \rangle$ and P_{ie}, two of these independent velocity variables may be eliminated. The remaining independent variable has been chosen to be v_o, and for ease of interpretation, all electron velocities have been expressed in terms of the ion thermal velocity v_{ti}, where $v_{ti} \equiv \sqrt{2T_i/m_i}$.

Figure 3-5 shows the behavior of the recirculating power requirement as v_o is varied. The minimum recirculating power subject to the constraints which have been noted occurs when $v_o \approx 1.91 v_{ti}$. At this value of v_o, v_{ts} must be equal to zero in order to reduce the ion-electron energy transfer rate by the necessary factor of 100; for smaller values of v_o, it would not be possible to reduce the energy transfer rate enough (the electron distribution would overlap too much with the ion distribution). From the constraint on mean electron energy, it is found that for $v_o \approx 1.91 v_{ti}$, $v_{tf} \approx 15.68 v_{ti}$. (For a completely Maxwellian electron distribution at $T_e = 49$ keV, the electron thermal velocity would be $v_{te} \approx 16.43 v_{ti}$.) As v_o is increased, v_{ts} also increases to prevent P_{ie} from dropping below 1/100 of the Spitzer value, while v_{tf} decreases to keep the mean energy constant.

For the optimum operating point of $v_o = 1.91 v_{ti}$, the recirculating power is $P_{recirc} \approx 8.75 \cdot 10^{-3} n_e \langle E_e \rangle / \tau_{col,\, e}$, which corresponds to $P_{recirc}/P_{fus} \approx 17.1$. This result is larger than the recirculating power value for ^{3}He which was found in the previous section, primarily because here the mean electron energy is being held much lower ($\langle E_e \rangle = 73.5$ keV vs. 160 keV) in order to reduce the bremsstrahlung losses further ($P_{brem}/P_{fus} = 0.28$ vs. 0.50). (There are also minor differences between the results of this section and those of the previous section due to different assumptions about $\ln \Lambda$ and the relative values of v_o, v_{tf}, and v_{ti}. Here the Coulomb logarithm has been chosen to be 20, which for magnetic fusion reactors is probably a more realistic value than the highly optimistic choice of $\ln \Lambda = 15$

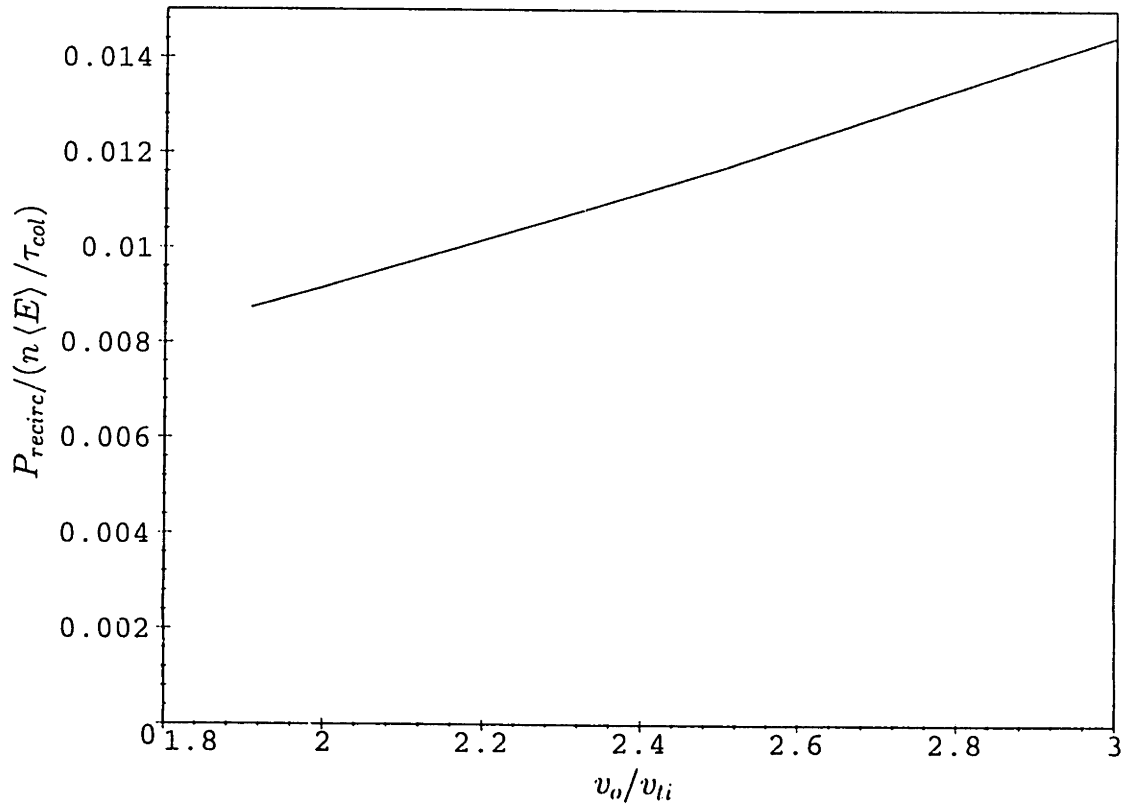

Figure 3-5: Optimization of v_o, v_{tf}, and v_{ts} from Eq. (3.11) for electrons in a pure ^{3}He plasma ($T_i = 1$ MeV and $\ln\Lambda = 20$) subject to the constraints that $\langle E_e\rangle = (3/2)\cdot 49$ keV$= 73.5$ keV and $P_{ie}/(P_{ie})_{Spitzer} = 0.01$.

which was made in the previous section.)

The physical interpretation of the results graphed in Figure 3-5 is that there is no power cost incurred to keep the lower edge of the distribution arbitrarily sharp ($v_{ts} \rightarrow 0$) provided that potential instabilities are ignored, as they are here. By contrast, there is a power cost to maintain more of the electron distribution in a non-Maxwellian shape (recall that $P_{recirc}/(n\langle E\rangle/\tau_{col}) \sim v_o/v_{tf}$ for $v_{ts} \ll v_o \ll v_{tf}$). Therefore, the optimum distribution function is a nearly Maxwellian shape in which all of the electrons up to a certain velocity have been depleted and in which that velocity (v_o) is as small as is allowed by the constraint on the ion-electron energy transfer rate.

In conclusion, this calculation justifies the particular form of the distribution function ($v_{ts} \ll v_o \ll v_{tf}$) which was used in the previous section.

Optimization of a More General Distribution Function

Now attention will be turned to determining the impact of using a velocity distribution function which is more general than can be described using Eq. (3.11). The particular distribution function which was chosen was

$$f(v) = \begin{cases} nK_1 \exp[-(v-v_{o1})^2/v_{ts}^2] & \text{for } v < v_o \\ nK_1\{(1-A)\exp[-(v-v_{o1})^2/v_{tf1}^2] + A\exp[-(v-v_{o2})^2/v_{tf2}^2]\} & \\ & \text{for } v \geq v_o. \end{cases} \tag{3.53}$$

This new distribution function has six independently adjustable parameters: v_{o1}, v_{o2}, v_{ts}, v_{tf1}, v_{tf2}, and A. It is assumed that $v_{o2} \geq v_{o1}$. Based on the optimization of the earlier model distribution function, one can safely choose to set $v_{ts} = 0$. The conditions on $\langle E_e\rangle$ and P_{ie} can again be used in order to eliminate two more of the variables, so that only three independently adjustable parameters are left.

Two local minima of the recirculating power have been found; for one A is small and

positive (corresponding to a relatively small positive perturbation of the model distribution function which was previously used), while for the other, A is small and negative (corresponding to a small negative perturbation of the previously used distribution function).

The minimum recirculating power with a positive perturbation (subject to the noted constraints) occurs for $v_{o1} \approx v_{o2} \approx 1.923 v_{ti}$, $v_{tf1} \approx 15.788 v_{ti}$, $v_{tf2} \approx 8.8 v_{ti}$, and $A \approx 0.0883$. The recirculating power for these parameters is $P_{recirc} \approx 3.39 \cdot 10^{-3} n_e \langle E_e \rangle / \tau_{col,\,c}$, or $P_{recirc}/P_{fus} \approx 6.63$. The effects of variations about this optimum are shown in Figures 3-6 through 3-8, where the three independent parameters have been chosen to be v_{tf1}, v_{tf2}, and τ_2.

While this power is still much too large to be practical, it is a substantial decrease from the minimum recirculating power which was found with the earlier model distribution function, and so it should be carefully explained. For the particular parameter values which have been cited, the new distribution function (with $v_{tf1} \approx 15.788 v_{ti}$) is essentially equivalent to the old distribution function (which had $v_{tf} \approx 15.68 v_{ti}$) plus a relatively small ($A/(1-A) \sim 0.1$) perturbation which has a qualitatively similar shape but a much smaller value of v_{tf} ($v_{tf2} \approx 8.8 v_{ti}$). The total number of electrons in the perturbation is roughly one order of magnitude greater than the total number of electrons which have been displaced from the region $v < v_o$ as compared with a perfect Maxwellian of the same mean energy.

What appears to be happening is that the displaced electrons "prefer" (energetically speaking) to remain relatively close to the velocity region from which they have been removed; however, if the displaced electrons are trying to diffuse back downward in velocity into the relatively small depleted region, there must also be a considerable number of electrons which will diffuse upward in velocity into the (much larger) velocity space volume which surrounds the perturbation. Thus it is reasonable that the optimum of the new distribution function occurs when the perturbation is fairly concentrated at small velocities and contains several times the number of displaced slow electrons.

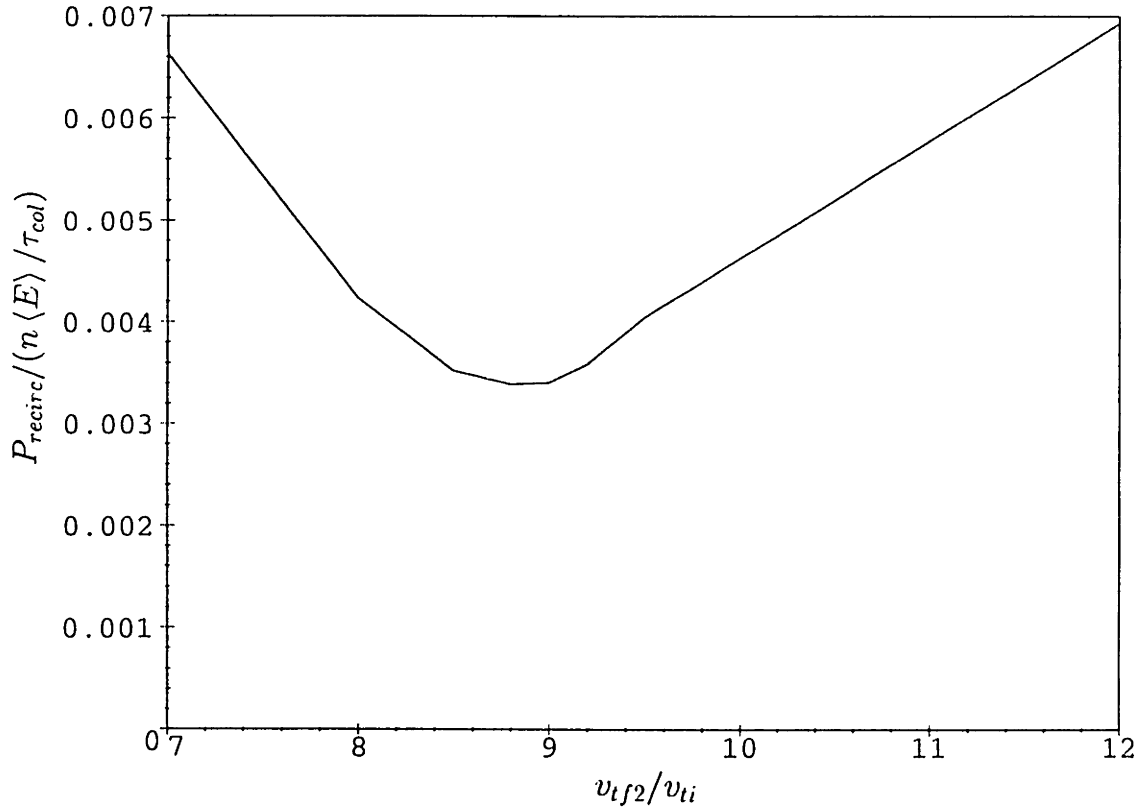

Figure 3-6: Optimization of v_{tf2} of the improved model distribution function with a positive perturbation (see Eq. (3.53)) in order to minimize P_{recirc} for electrons in a pure ^{3}He plasma ($T_i = 1$ MeV and $\ln\Lambda = 20$) subject to the constraints that $v_{tf1} = 15.788 v_{ti}$, $v_{o2} = v_{o1}$, $\langle E_e\rangle = 73.5$ keV, and $P_{ie}/(P_{ie})_{Spitzer} = 0.01$.

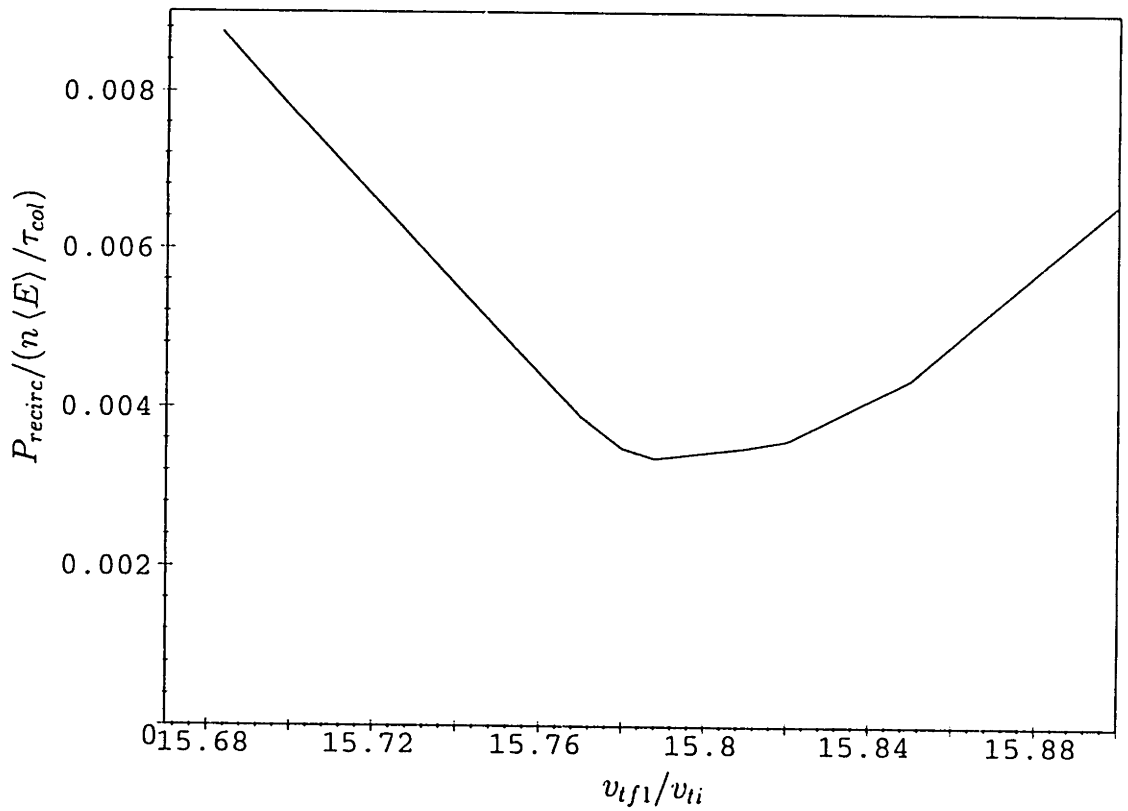

Figure 3-7: Optimization of v_{tf1} of the improved model distribution function with a positive perturbation (see Eq. (3.53)) in order to minimize P_{recirc} for electrons in a pure ^{3}He plasma ($T_i = 1$ MeV and $\ln\Lambda = 20$) subject to the constraints that $v_{tf2} = 8.8v_{ti}$, $v_{o2} = v_{o1}$, $\langle E_e\rangle = 73.5$ keV, and $P_{ie}/(P_{ie})_{Spitzer} = 0.01$.

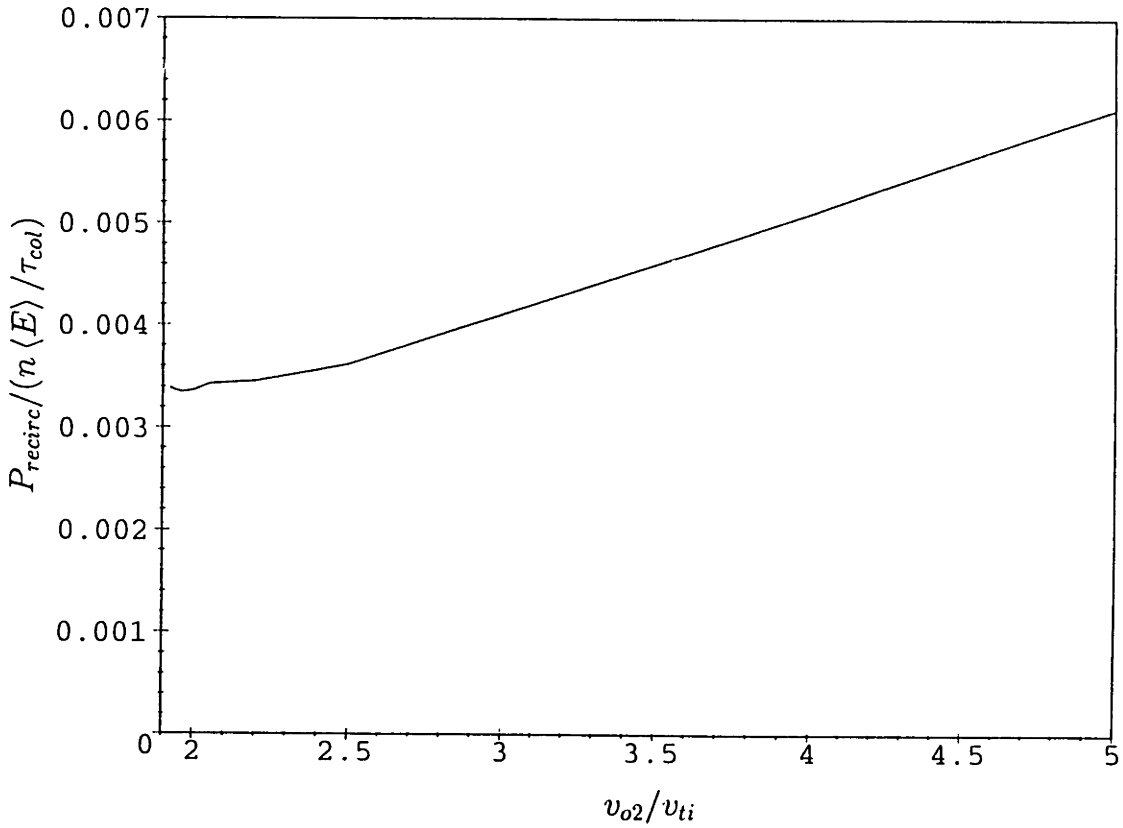

Figure 3-8: Optimization of v_{o2} of the improved model distribution function with a positive perturbation (see Eq. (3.53)) in order to minimize P_{recirc} for electrons in a pure ^{3}He plasma ($T_i = 1$ MeV and $\ln\Lambda = 20$) subject to the constraints that $v_{tf1} = 15.788v_{ti}$, $v_{tf2} = 8.8v_{ti}$, $\langle E_e\rangle = 73.5$ keV, and $P_{ie}/(P_{ie})_{Spitzer} = 0.01$.

The minimum recirculating power for the case of a negative perturbation is comparable to but slightly larger than the minimum with a positive perturbation. The minimum occurs for $v_{o1} \approx 1.926 v_{ti}$, $v_{o2} \approx 12 v_{ti}$, $v_{tf1} \approx 15.683 v_{ti}$, $v_{tf2} \approx 10.912 v_{ti}$, and $A \approx -0.05$. For these parameters, the recirculating power is $P_{recirc} \approx 3.83 \cdot 10^{-3} n_e \langle E_e \rangle / \tau_{col,\,e}$, or $P_{recirc}/P_{fus} \approx 7.49$. The effects of variations about this optimum are shown in Figures 3-9 through 3-11, where the three independent parameters have been chosen to be v_{02}, v_{tf1}, and A.

With an even more general distribution function, one could probably reduce the recirculating power somewhat further. This route was not taken in the present research because of the limitations of the computational methods employed; the calculations were performed with Maple on Sun Sparc Classic and Sparc 5 computers, and this method was not able to calculate the recirculating power for distributions more general than that of Eq. (3.53) in a reasonable amount of time. (Mathematica also showed similar limitations.) A complicating factor is that as the distribution is made more general, the number of independently variable parameters increases. Consequently, the parameter phase space over which P_{recirc} must be minimized (still subject to the noted constraints) gains more dimensions, and the parameter phase space volume which must be searched in order to find the global minimum of P_{recirc} becomes dauntingly large (especially when it can take several tens of minutes to calculate P_{recirc} for just one data point, as is presently the case). If the issue of more general distribution functions is taken up again in the future, it may be profitable to resort to more powerful numerical methods, such as those outlined in [66].

Yet even though the presently employed methods have not found the absolute optimum distribution function shape, there is good reason to believe that the results are sufficiently valid to meet the intended purpose, which was to determine the feasibility of advanced fuel reactors operating with non-Maxwellian electrons. The distribution of Eq. (3.53) has allowed the perturbation to assume its preferred magnitude and width in velocity space, so further corrections are likely to be smaller. Furthermore, the recirculating power for

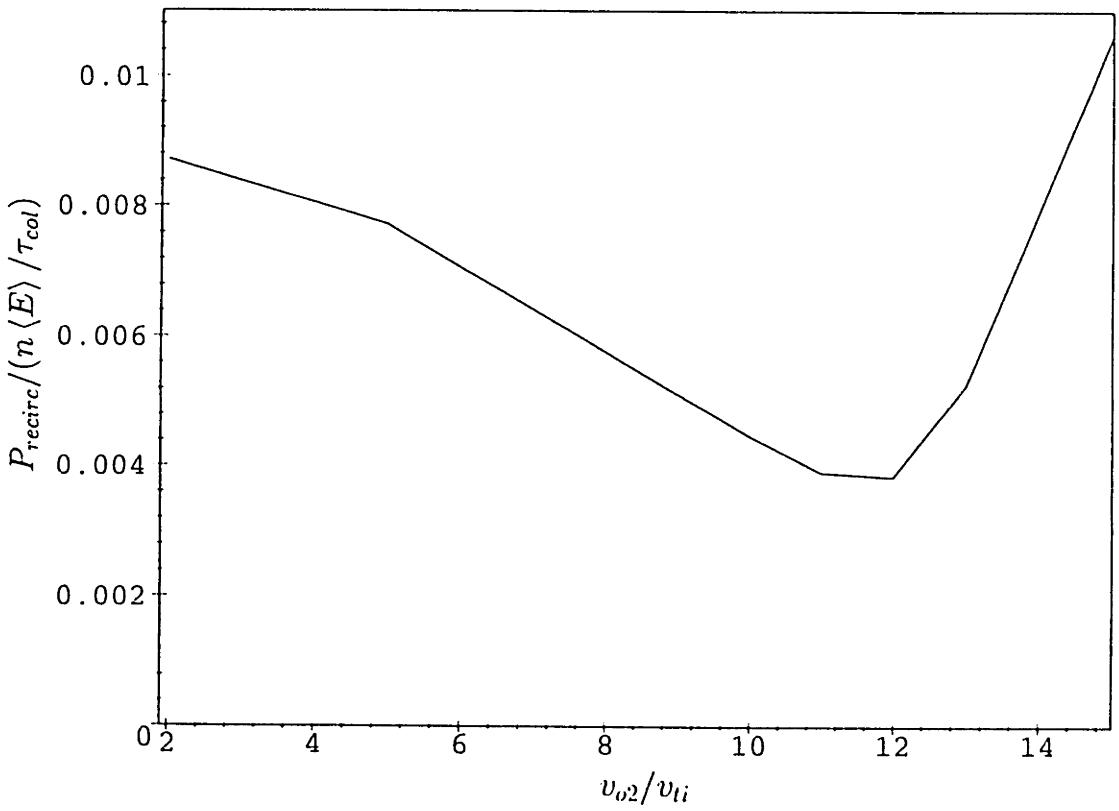

Figure 3-9: Optimization of v_{02} of the improved model distribution function with a negative perturbation (see Eq. (3.53)) in order to minimize P_{recirc} for electrons in a pure ^{3}He plasma ($T_i = 1$ MeV and $\ln\Lambda = 20$) subject to the constraints that $v_{tf1} = 15.683 v_{ti}$, $A = -0.05$, $\langle E_e\rangle = 73.5$ keV, and $P_{ie}/(P_{ie})_{Spitzer} = 0.01$.

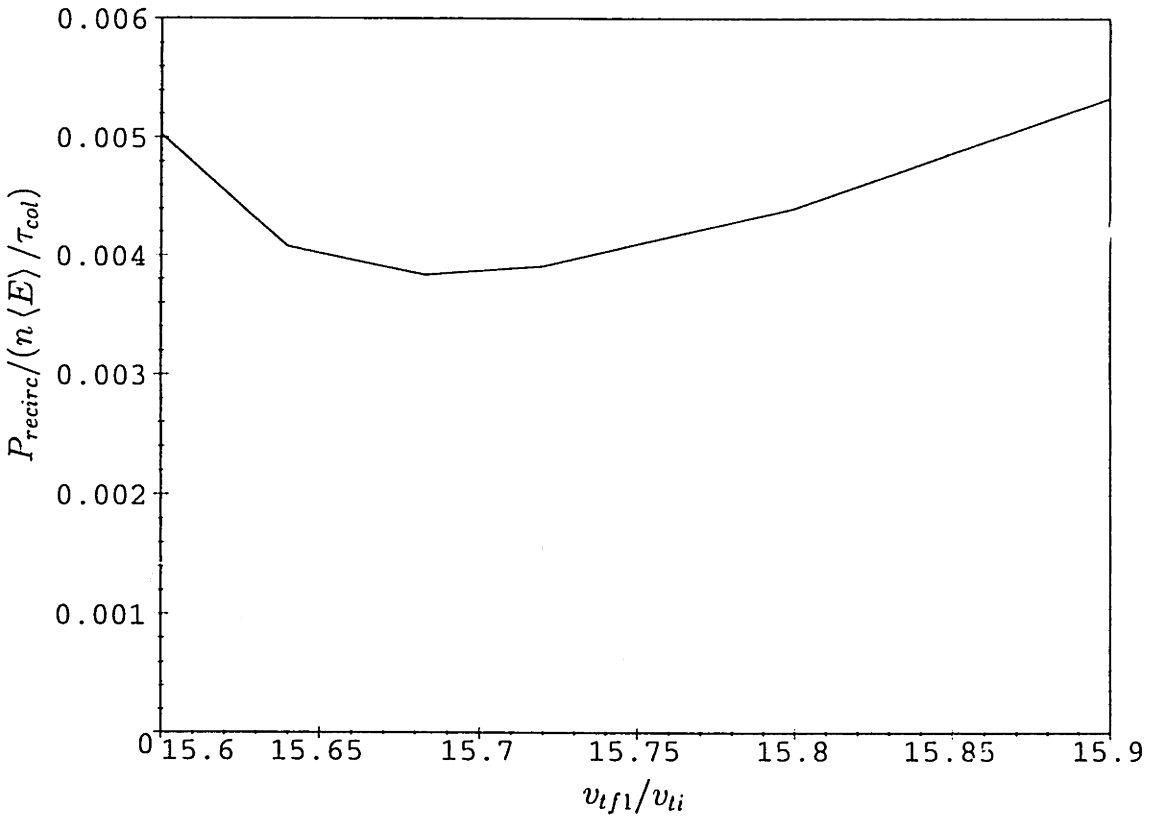

Figure 3-10: Optimization of v_{tf1} of the improved model distribution function with a negative perturbation (see Eq. (3.53)) in order to minimize P_{recirc} for electrons in a pure ^{3}He plasma ($T_i = 1$ MeV and $\ln\Lambda = 20$) subject to the constraints that $v_{02} = 12$, $A = -0.05$, $\langle E_e\rangle = 73.5$ keV, and $P_{ie}/(P_{ie})_{Spitzer} = 0.01$.

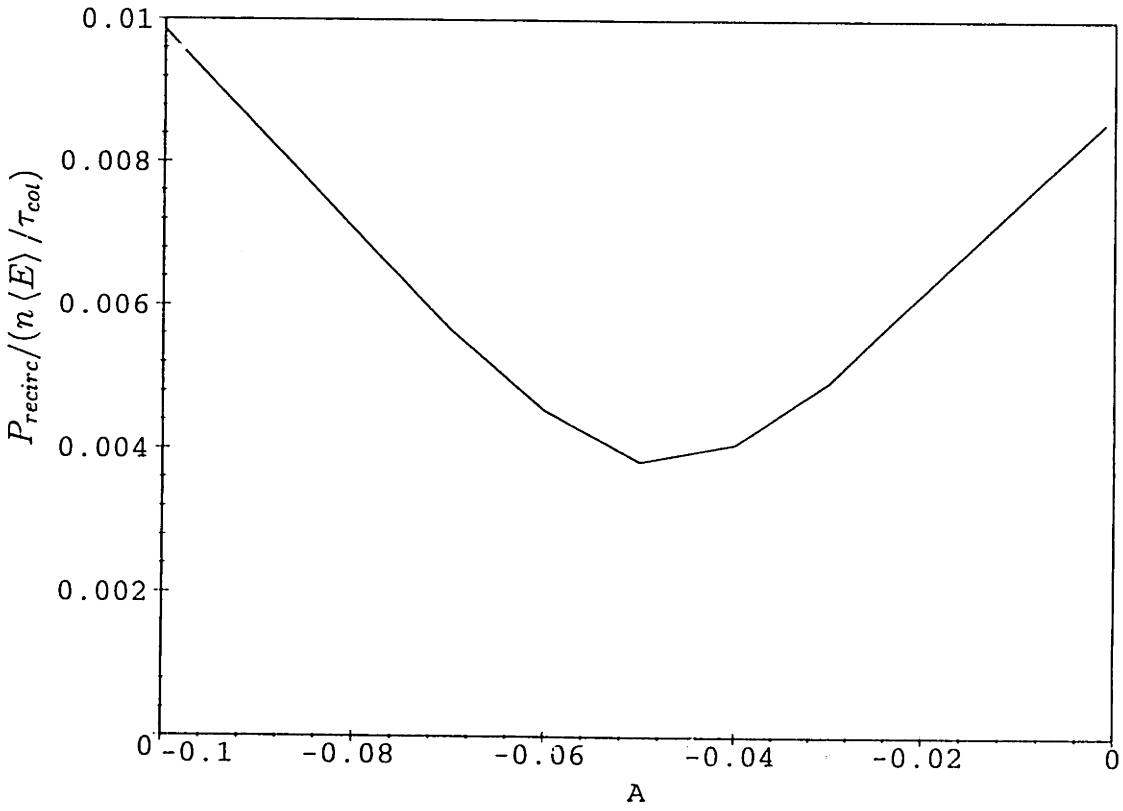

Figure 3-11: Optimization of A of the improved model distribution function with a negative perturbation (see Eq. (3.55)) in order to minimize P_{recirc} for electrons in a pure ^{3}He plasma ($T_i = 1$ MeV and $\ln\Lambda = 20$) subject to the constraints that $v_{tf1} = 15.683 v_{ti}$, $v_{o2} = 12 v_{ti}$, $\langle E_e\rangle = 73.5$ keV, and $P_{ie}/(P_{ie})_{Spitzer} = 0.01$.

electrons of this distribution shape in a ^{3}He plasma is still almost seven times the fusion power.

Several highly optimistic assumptions and choices have been made in doing these calculations, including the following: the quoted power is the recirculating power required of a maximally efficient entropy extraction and power recirculation system (as opposed to a much lower-efficiency, more realistic system), the bremsstrahlung losses assumed here are still quite large in comparison with realistic reactor designs (large bremsstrahlung losses accompany the high mean electron energies which have been chosen to reduce the recirculating power), and ^{3}He was chosen because at least in the ideal reactors under consideration, it is the closest to ignition of all the advanced aneutronic fuels, in spite of its extremely high necessary ion temperatures. Despite these and other optimistic choices, the recirculating power requirement is still much too large.

For these reasons, it is highly doubtful that sufficiently large gains in performance could be made by moving to more precisely tailored electron distribution functions.

3.3.3 Beamlike Electrons with a Thermal Spread

Because a beamlike distribution is further from thermodynamic equilibrium than the nearly Maxwellian distributions with the low-velocity holes which were considered above, one would expect the recirculating power required to maintain beamlike electrons to be even larger than the values summarized in Table 3.4. This will now be shown to be the case.

For electrons with $v_t = v_{ts} = v_{tf}$, the ratio of recirculating power to fusion power is

$$\frac{P_{recirc}}{P_{fus}} = 5.34 \cdot 10^{-6} R_1 (v_o/v_t) \left(\frac{v_o}{v_t}\right) \frac{(x + Z_{i2})^2}{x} \frac{\ln \Lambda}{\langle \sigma v \rangle_{fus} E_{fus,\,eV} \sqrt{\langle E_{e,\,eV} \rangle}} . \quad (3.54)$$

The minimum recirculating power needed to maintain a given value of v_o/v_t for the

electrons with various fuels under approximately optimum conditions is given in Table 3.5. (Here it has been assumed that $\ln \Lambda = 15$, and the fusion reactivity $\langle \sigma v \rangle_{fus}$ has been taken from the entries in Table 1.1 for ions with the same mean energies. The electron energies for the first three fuels have been chosen to be less than or equal to the equilibrium mean electron energies computed in Chapter 1, while the electron energies for the last three fuels have been selected so that the bremsstrahlung losses will not exceed half of the fusion power.):

Fuel mixture	$\langle E_i \rangle$	$\langle E_e \rangle$	$\frac{P_{brem}}{P_{fus}}$	$\frac{P_{recirc}}{P_{fus}}$ for $v_o/v_t = 1$	$\frac{P_{recirc}}{P_{fus}}$ for $v_o/v_t = 2$	$\frac{P_{recirc}}{P_{fus}}$ for $v_o/v_t = 10$
D-T (1:1)	75 keV	$\leq$ 63 keV	≤ 0.007	≥ 7.3	≥ 21	≥ 190
D-^{3}He (1:1)	150 keV	$\leq$ 108 keV	≤ 0.19	≥ 61	≥ 180	≥ 1600
D-D	750 keV	$\leq$ 315 keV	≤ 0.35	≥ 35	≥ 99	≥ 900
^{3}He-^{3}He	1.5 MeV	$\leq$ 158 keV	≤ 0.50	≥ 85	≥ 240	≥ 2200
p-^{11}B (5:1)	450 keV	$\leq$ 34.8 keV	≤ 0.50	≥ 350	≥ 1000	≥ 9100
p-^{6}Li (3:1)	1.2 MeV	$\leq$ 21.6 keV	≤ 0.50	≥ 870	≥ 2500	≥ 23000

Table 3.5: P_{recirc}/P_{fus} for beamlike electrons with $\ln \Lambda = 15$.

Clearly in terms of the recirculating power requirement it is easier to maintain the electrons in a nearly Maxwellian distribution with only the slow electrons depleted than to keep the whole electron distribution in a significantly beamlike state. Yet either way, the recirculating power is too large to be feasible in currently foreseeable systems.

Nevertheless, if one did have a mechanism for recirculating the power at very high efficiencies and in a practical manner, the minimum power loss (as limited by the second law of thermodynamics) could theoretically be made quite small. To demonstrate how much less stringent this minimum power loss condition is in comparison with the recirculating power requirement, the case of beamlike electrons with $(P_{\rm loss})_{\rm min} \leq P_{\rm fus}$ will be considered. For this case, one finds that

$$R_2(v_o/v_t) \left(\frac{v_o}{v_t}\right)^2 \leq 7.49 \cdot 10^6 \frac{x}{(x + Z_{i2})^2} \frac{\langle \sigma v \rangle_{fus} E_{fus,\,eV} \langle E_{e,\,eV} \rangle^{3/2}}{\ln \Lambda} . \qquad (3.55)$$

The maximum allowable values of v_o/v_t subject to the constraint that $(P_{loss})_{min} \leq P_{fus}$ are given in Table 3.6.

Fuel mixture	$\langle E_i \rangle$	$\langle E_e \rangle$	P_{brem}/P_{fus}	v_o/v_t
D-T (1:1)	75 keV	$\leq$ 63 keV	$\leq$ 0.007	$\leq$ 250
D-^{3}He (1:1)	150 keV	$\leq$ 108 keV	$\leq$ 0.19	$\leq$ 110
D-D	750 keV	$\leq$ 315 keV	$\leq$ 0.35	$\leq$ 250
^{3}He-^{3}He	1.5 MeV	$\leq$ 158 keV	$\leq$ 0.50	$\leq$ 120
p-^{11}B (5:1)	450 keV	$\leq$ 34.8 keV	$\leq$ 0.50	$\leq$ 27
p-^{6}Li (3:1)	1.2 MeV	$\leq$ 21.6 keV	$\leq$ 0.50	$\leq$ 15

Table 3.6: Maximum allowable v_o/v_t for beamlike electrons with $(P_{loss})_{min} \leq P_{fus}$ and $\ln \Lambda = 15$.

As may be seen from Table 3.6, the constraint that the minimum theoretical power loss must be less than the fusion power would still permit the electron distribution to be nearly monoenergetic with a very small thermal spread. The primary limitation on how far the electrons can be kept from thermodynamic equilibrium is therefore the difficulty of handling the vast amounts of recirculating power in an efficient and practical manner.

3.3.4 Beamlike Ions with a Thermal Spread

These calculational techniques may also be applied to non-Maxwellian ion populations. For isotropic ion distributions in which the two fuel ion species (if there are indeed two different types of fuel ions) have the same mean energy, the fusion reactivity is essentially independent of the precise ion velocity distribution shape (Maxwellian, monoenergetic, etc.), since ion-ion collisions must still be averaged over all angles. This fact is shown explicitly in Appendix A. Therefore non-Maxwellian ion distributions are not of interest for boosting the fusion rate. However, they might be desirable for helping to maintain the proper radial focusing in inertial-electrostatic confinement fusion [67] or for other purposes, so it is worthwhile to investigate the minimum recirculating power levels needed to sustain such distributions.

For beamlike ions ($v_t = v_{ts} = v_{tf}$) with only one ion species present, the recirculating power as compared with the fusion power is

$$\frac{P_{recirc}}{P_{fus}} \approx 2.49 \cdot 10^{-7} R_1 (v_o/v_t) \left(\frac{v_o}{v_t}\right) \frac{Z_i^4}{\sqrt{\mu_i}} \frac{\ln \Lambda}{\langle \sigma v \rangle_{fus} E_{fus,\,eV} \sqrt{\langle E_{i,\,eV} \rangle}} . \qquad (3.56)$$

For simplicity, even when the ion distributions are nearly monoenergetic, Maxwellian-averaged values of $\langle \sigma v \rangle_{fus}$ will be used in the calculations below. As shown in Appendix A, this substitution is accurate to within 20% or so, depending on the specific fuel and parameters. This degree of accuracy is perfectly acceptable for the purpose of these calculations.

An exact calculation of the recirculating power required when two non-Maxwellian fuel ion species are present would require considerably more work than has been done so far, since both like-particle and unlike-particle collisions would have to be taken into account, and the differences in the charge and mass of the two ion species would affect the collision operators for the two different types of collisions. As a simpler alternative, one may use the present expressions, which should be quite accurate for single ion species, to estimate the results for two different ion species, at least when the charge and mass of the two ion species are not extremely different. Accordingly, approximate answers are calculated below for D-T and D-^{3}He (but not p-^{11}B or p-^{6}Li).

(Aside: If one were going to perform a much more accurate calculation of the recirculating power required to maintain non-Maxwellian ion or electrons, one might wish also to include the effects of ion-electron collisions. Ion-electron collisions were neglected in all of the calculations in this chapter because they should constitute a fairly small effect in comparison with ion-ion and electron-electron collisions. Neglecting energy differences between the species, the ratio of the relevant electron-electron, ion-ion, and ion-electron collision timescales $\tau_{ee} : \tau_{ii} : \tau_{ie}$ is roughly like $1 : \sqrt{m_i/m_e} : (m_i/m_e)$ [27], so entropy should be generated at a much slower rate by ion-electron collisions.)

The minimum recirculating power to keep ions in a modestly beamlike state (with

$v_o/v_t = 2$ or 10) is given in Table 3.7 for a variety of fuels under approximately optimum conditions:

Fuel	$\langle E_i \rangle$	P_{recirc}/P_{fus} for $v_o/v_t = 2$	P_{recirc}/P_{fus} for $v_o/v_t = 10$
D-T (1:1)	75 keV	0.3	3
D-^{3}He (1:1)	150 keV	4	40
D-D	750 keV	1.1	9.6
^{3}He-^{3}He	1.5 MeV	4.3	38

Table 3.7: P_{recirc}/P_{fus} for beamlike ions with $\ln \Lambda = 15$.

Although answers for p-^{11}B and p-^{6}Li were not calculated, judging from the trends of previous calculations the performance of these fuels should be worse than that of ^{3}He-^{3}He and the other fuels for which the present calculation was performed.

The maximum allowable values of v_o/v_t for the ions subject to the constraint that $(P_{loss})_{min} \leq P_{fus}$ may be found from the formula,

$$R_2(v_o/v_t)\left(\frac{v_o}{v_t}\right)^2 \leq 1.61 \cdot 10^8 \frac{\sqrt{\mu_i}\,\langle \sigma v \rangle_{fus}\, E_{fus,\,eV}\, \langle E_{i,\,eV} \rangle^{3/2}}{Z_i^4 \ln \Lambda}\,, \tag{3.57}$$

and they are given in Table 3.8.

Fuel mixture	$\langle E_i \rangle$	v_o/v_t
D-T (1:1)	75 keV	≤ 3000
D-^{3}He (1:1)	150 keV	≤ 1000
D-D	750 keV	≤ 3800
^{3}He-^{3}He	1.5 MeV	≤ 2700

Table 3.8: Maximum allowable v_o/v_t for beamlike ions with $(P_{loss})_{min} \leq P_{fus}$ with $\ln \Lambda = 15$.

Just as was shown earlier for the electrons, for the ions the minimum theoretical power loss is a far less serious concern than the recirculating power.

Because of the vast recirculating power requirements, the ability of a system to keep the ions in a non-Maxwellian state is severely limited. D-T and perhaps also D-D can theoretically be maintained in a modestly beamlike state *if* one has an efficient mechanism for actually recirculating the power, but for the other fuels the ion velocity distributions cannot be kept even reasonably non-Maxwellian unless a practical mechanism for recirculating the power at extraordinarily high efficiencies can be found.

3.4 Estimate of Limitations on Highly Anisotropic Distributions

Up until this point it has generally been assumed that the particle velocity distributions are isotropic. It has been suggested [68] that strongly anisotropic distributions might considerably slow the collisional relaxation process, so the assumption of isotropy will now be lifted, and the maximum extent to which anisotropy might affect the recirculating power will be estimated by considering highly anisotropic distributions. For simplicity it will be assumed that only one particle species is present.

For the purposes of making an estimate which can be compared with the results for isotropic distributions, the case of two cold, counter-propagating linear beams (which are presumed to have equal densities and other properties) will be examined. It will be assumed that each beam is centered around some drift velocity ($\pm v_o \hat{\mathbf{x}}$) in the lab frame. This preferred $\hat{\mathbf{x}}$ axis will also be referred to as the parallel direction. The $\hat{\mathbf{y}}$ and $\hat{\mathbf{z}}$ axes will then be denoted as perpendicular directions. In the reference frame of each beam's drift velocity, that beam possesses a spheroidal, Maxwellian shape in velocity space; in such a reference frame, the beam may have significantly different parallel and perpendicular temperatures, $T_{\|}$ and $T_{\perp}$.

Because each beam, in its own reference frame, possesses a Maxwellian shape in each direction, the only effect of collisions between particles within the same beam will be to

drive $T_\parallel$ and $T_\perp$ toward equilibrium with each other. This relaxation is described by the relation [69]:

$$\frac{dT_\perp}{dt} = -\frac{1}{2}\frac{dT_\parallel}{dt} = -\frac{(T_\perp - T_\parallel)}{\tau_\theta} , \tag{3.58}$$

in which the inverse relaxation time is

$$\frac{1}{\tau_\theta} \equiv \frac{2\sqrt{\pi}n'(Ze)^4 \ln\Lambda}{\sqrt{m}} \int_{-1}^{1} \frac{d\mu\mu^2(1-\mu^2)}{[(1-\mu^2)T_\perp + \mu^2 T_\parallel]^{3/2}} . \tag{3.59}$$

For simplicity, $n' = n/2$ has been used to denote just the density of the one beam in question, not the combined density n of both beams.

For $T_\perp$ between the two limiting values, $T_\perp = T_\parallel$ and $T_\perp \gg T_\parallel$, the respective bounds on the relaxation time are

$$\frac{15\sqrt{m}T_\perp^{3/2}}{8\sqrt{\pi}n'(Ze)^4 \ln\Lambda} \geq \tau_\theta \geq \frac{\sqrt{m}T_\perp^{3/2}}{\pi^{3/2}n'(Ze)^4 \ln\Lambda} . \tag{3.60}$$

With $T_\perp \equiv \frac{1}{2}mv_{t\perp}^2$, the upper bound on the relaxation time between the temperatures of the different directions is

$$\tau_\theta \leq \frac{15m^2 v_{t\perp}^3}{16\sqrt{2\pi}n'(Ze)^4 \ln\Lambda} . \tag{3.61}$$

Collisions between the two beams will have other effects. Specifically, interbeam collisions will cause a slowing down of each beam (decrease in v_o), transverse velocity diffusion of each beam (increase in $v_{t\perp}$), and longitudinal velocity diffusion of each beam (increase in $v_{t\parallel}$, where $T_\parallel \equiv mv_{t\parallel}^2/2$). As a convenient perspective for the analysis, the situation may be viewed in the frame of one of the beams; the case is then identical to the situation in which a nearly monoenergetic, very high-energy beam (with velocity $v_o' \equiv 2v_o$) is interacting with a fairly cold background plasma with zero average velocity. Relevant formulas for beam-plasma interactions [50] may then be used in the present calculations.

Perpendicular velocity diffusion due to interbeam collisions may be described by

$$\frac{\partial v_{t\perp}^2}{\partial t} = \frac{v_o'}{\tau_{D\perp}} , \tag{3.62}$$

where

$$\tau_{D\perp} \equiv \frac{m^2 v_o'^2}{8\pi n'(Ze)^4 \ln\Lambda} . \tag{3.63}$$

Likewise, parallel velocity diffusion due to interbeam collisions may be described by

$$\frac{\partial v_{t\parallel}^2}{\partial t} = \frac{v_o'}{\tau_{D\parallel}} , \tag{3.64}$$

in which

$$\begin{aligned} \tau_{D\parallel} &\equiv \frac{m^2 v_o'^5}{4\pi v_t^2 n'(Ze)^4 \ln\Lambda} \\ &= 8\left(\frac{v_o}{v_t}\right)^2 \tau_{D\perp} \gg \tau_{D\perp} . \end{aligned} \tag{3.65}$$

The "average" thermal velocity v_t of each beam is defined as $v_t \equiv \sqrt{2T_{avg}/m}$, where $T_{avg} \equiv (2T_\perp + T_\parallel)/3$.

Thus perpendicular velocity diffusion will occur much more rapidly than parallel diffusion (which is why $T_\perp \geq T_\parallel$ was assumed in examining relaxation due to collisions within the same beam).

The third effect of interbeam collisions, the slowing down of the average beam velocity, is given by the relation

$$\frac{\partial v_o'}{\partial t} = -\frac{v_o'}{\tau_s} , \tag{3.66}$$

where

$$\tau_s \equiv \frac{m^2 v_o'^2}{8\pi n'(Ze)^4 \ln\Lambda} = \tau_{D\perp} \,. \tag{3.67}$$

Equation (3.62) allows the increase in perpendicular temperature due to interbeam collisions to be expressed as

$$\frac{\partial T_\perp}{\partial t} = \frac{T_\perp}{\tau_\perp} \,, \tag{3.68}$$

in which

$$\tau_\perp \equiv \frac{m^2 v_o v_{t\perp}^2}{4\pi n'(Ze)^4 \ln\Lambda} \,. \tag{3.69}$$

Taking the ratio of this time with the intrabeam relaxation time, one finds that

$$\frac{\tau_\perp}{\tau_\theta} \sim \frac{v_o}{v_{t\perp}} \gg 1 \,. \tag{3.70}$$

As a result of this ratio, each beam will stay approximately "round" in velocity space, or equivalently $T_\parallel \approx T_\perp$. Hence for simplicity, the definition $v_t \equiv v_{t\perp}$ will be made.

From these findings, one can see that the physical picture of the effects of collisions on the beams is that initially fast (large v_o) beams, which are each characterized by a spherical "radius" of v_t, begin to slow down. Part of the kinetic energy which had been initially associated with the highly ordered counterpropagating drift velocities of the beams is transferred via collisions to become random thermal energy of each beam, so that as v_o decreases, the radius v_t of each beam increases.

The equation for slowing down of the beams, Eq. (3.66), can be rewritten to give the time τ_{slow} which is required for the beam particles to lose an amount of velocity equal to

v_t and become slower than would be desirable:

$$\frac{\partial v_o}{\partial t} = -\frac{v_t}{\tau_{slow}} , \tag{3.71}$$

in which the time to become too slow has been defined as

$$\tau_{slow} \equiv \frac{m^2 v_o^2 v_t}{\pi n' (Ze)^4 \ln \Lambda} . \tag{3.72}$$

To prevent the beams from slowing down and spreading out, the minimum amount of power which must be recirculated is

$$P_{recirc} \equiv \frac{n_{slow} \Delta E_{slow}}{\tau_{slow}} , \tag{3.73}$$

where n_{slow} is the density of the particles which become too slow on the above timescale and ΔE_{slow} is the average amount of energy those slow particles have lost.

Using $n_{slow} \approx n$ and $\Delta E_{slow} \approx (1/2) m [v_o^2 - (v_o - v_t)^2] \approx m v_o v_t$, one finds that

$$P_{recirc} \approx \frac{\sqrt{\pi}}{4\sqrt{6}} \frac{n \langle E \rangle}{\tau_{col}} . \tag{3.74}$$

This result for a "one-dimensional" highly anisotropic beamlike distribution may be compared with the equivalent result for a "three-dimensional" isotropic beamlike distribution from Eq. (3.6):

$$\frac{(P_{recirc})_{1D\ beamlike}}{(P_{recirc})_{3D\ beamlike}} \approx \frac{3}{4} \frac{v_t}{v_o} . \tag{3.75}$$

Because of the fact that $v_t / v_o \ll 1$ for a beamlike distribution, the one-dimensional beamlike distribution requires considerably less recirculating power to maintain than does the three-dimensional beamlike distribution. If the ions are anisotropic and colliding head-on, the value of $\langle \sigma v \rangle_{fus}$ may also be increased over its Maxwellian-averaged value by a

factor of roughly 2 to 4 (see Appendix A).

However, the highly optimistic assumptions which have been made here must be kept in mind. It has been assumed that instabilities are not of concern in calculating the recirculating power, when in reality they would be a very great concern for such nonequilibrium distributions; instabilities would also be much more of a problem for highly anisotropic distributions than for approximately isotropic ones. Instabilities could greatly increase the recirculating power requirements or even prevent the task from being accomplished at all. Furthermore, it has been assumed that the collisionally generated entropy can be extracted from the plasma and the power can be recirculated from the thermal spread (v_t) to the ordered beam motion (v_o) with the maximum possible efficiency. Realistic systems would have a much harder time removing entropy, and consequently the recirculating power levels and power losses would be much larger.

Yet even if the full advantage of Eq. (3.75) could actually be realized, the improvement would be great enough to help only some of the more reactive, lower-Z_i fuels (eg. D-T and D-D). More advanced fusion fuel ions, as well as electrons in all types of fusion plasmas, would still require too much recirculating power to be maintained in a beamlike velocity distribution.

In conclusion, even if strong anisotropy could somehow be maintained without intolerable instability problems, it would not be able to sufficiently reduce the minimum recirculating power which is required in order to hold a particle velocity distribution in a particular desired nonequilibrium shape (except for ion beams in D-T reactors, since the reactivity of D-T is so high [70]).

3.5 Non-Maxwellian Fusion Systems Ruled Out

3.5.1 Systems Ruled Out So Far

In this chapter it has been shown that to maintain a non-Maxwellian velocity distribution or to keep two particle species at radically different mean energies would entail a recirculating power substantially larger than the fusion power. In all presently known types of systems, it would be necessary to have one mechanism for extracting the required amount of power from undesirable regions of the plasma's phase space and a different mechanism for returning the power to the proper region of the plasma's phase space. Realistically each of these mechanisms (and perhaps also the power transmission system linking them) would have non-negligible losses. Moreover, if these mechanisms could not tightly focus on the correct regions of plasma phase space and extract or add just the right amount of power there without substantially affecting other parts of phase space as well, then the mechanisms might have to recirculate far more than the theoretical minimum recirculating power just to get the job done. Even if nearly ideal power extraction and reinjection systems existed, it would be undesirable from an engineering and economic standpoint to have a fusion reactor which must continually extract vast amounts of power from the plasma, process the power, and re-inject it back into the plasma. For these reasons, systems with recirculating power levels substantially larger than the fusion power were deemed inviable.

In order to emphasize the broad extent and powerful implications of these findings, some specific examples of non-Maxwellian fusion systems which have been ruled out by this work should be given. In particular, the following systems cannot maintain particularly non-Maxwellian ion or electron distributions without having to recirculate a prohibitively large amount of power in comparison with the fusion power:

- Systems without explicit means of keeping the particles highly non-Maxwellian despite Coulomb collisions (eg. inertial-electrostatic confinement [19] and migma [38]).

- Systems involving removal and direct conversion of particles with improper velocities and reinjection of particles with the correct velocity (eg. multipolar traps with electrons removed before they thermalize [37]).
- Systems with selective heating of slow particles, even if the heating energy comes from a direct converter which selectively decelerates particles that are too fast.
- Transient nonequilibrium burning systems which try to produce enough fusion power before the particle distributions equilibrate (eg. ICF, bombs, and pulsed beam methods [71]).

Many other examples could also be given, but those presented above should serve as an indicator of the scope of the results which have been found in this chapter.

3.5.2 Demonstration That Virtually All Remaining Types of Systems Are Also Ruled Out

These objections to systems for maintaining nonequilibrium fusion plasmas might be circumvented if one possessed a hypothetical single mechanism which could both extract the power and also immediately reinject it properly and at exceedingly high efficiencies. With reference to Figure 3-1, this technique would allow the recirculation of the power not by an external heat engine, but rather by the plasma and the hypothetical mechanism acting in concert *as* the heat engine. Put in a slightly different way, the hypothetical mechanism would use the plasma as the "working fluid" of a heat engine and put the plasma through a closed thermodynamic cycle which would result in the net extraction of entropy from the plasma. This arrangement would be quite similar to a classical thermodynamic heat engine except that all of the states of the working fluid in the cycle would be far from thermodynamic equilibrium. As long as the entropy is indeed extracted (in the form of fairly low-temperature heat to limit the power losses) and work is added to the plasma (to compensate for the heat loss and keep the energy constant), such a system would not violate any fundamental physical tenets such as the laws of thermodynamics or

Liouville's theorem. The minimum power in heat energy which must be removed from the plasma and dumped to the outside world is $(P_{loss})_{min}$, which was calculated for several cases in this chapter and shown to be quite small in comparison with the fusion power.

Particle Interactions with Externally Applied and Self-Consistent Internal Electromagnetic Fields

The only apparent means of operating on the plasma in the required fashion is through the use of electromagnetic fields. Yet it can be shown that externally applied and self-consistent internal electric and magnetic fields cannot transport entropy to or from the plasma. Upon multiplying the Fokker-Planck equation, Eq. (2.10), by $(\ln f + 5/2)$ and integrating over all velocity space [72, 73], one arrives at the entropy conservation equation,

$$\begin{aligned} \frac{dS_{plasma}}{dt} &= \left(\frac{\partial S}{\partial t}\right)_{collisions} + \nabla_{\mathbf{x}} \cdot \left[\int d^3v \mathbf{v} f \ln f\right]_{\substack{spatial \\ entropy\ flux}} \\ &\quad + \left(\frac{\partial S}{\partial t}\right)_{\substack{particle\ sources \\ and\ sinks}} + \left(\frac{\partial S}{\partial t}\right)_{\substack{EM-plasma \\ interactions}}, \end{aligned} \tag{3.76}$$

in which the term corresponding to interactions between electromagnetic fields and the plasma is

$$\left(\frac{\partial S}{\partial t}\right)_{\substack{EM-plasma \\ interactions}} = -\frac{Ze}{m} \int d^3\mathbf{v} f \left(\ln f + \frac{3}{2}\right) \left[(\nabla_{\mathbf{v}} \cdot \mathbf{E}) - \frac{\mathbf{v}}{c} \cdot (\nabla_{\mathbf{v}} \times \mathbf{B})\right] = 0 . \tag{3.77}$$

This term is zero because the electric and magnetic fields do not depend on the velocities of the particles perceiving them (barring relativistic effects). Thus externally applied and internal self-consistent electric and/or magnetic fields cannot carry entropy away from the plasma or directly transfer entropy between different groups of particles.

This is a rather broad conclusion, but there are two loopholes which are worthy of notice; these potential loopholes will be considered in the following sections.

Wave-Particle Interactions

One might consider using electromagnetic or electrostatic waves to manipulate the plasma in the desired ways. As a very simple example, if a hot plasma emits photons as synchrotron or bremsstrahlung radiation, the plasma will cool down, and its entropy will be lowered; thus photons can in fact remove entropy from the plasma. It is possible that there could be other, more potentially useful situations in which the emission or absorption of photons (for electromagnetic waves) or even phonons (for other types of plasma waves) could alter plasma entropy in ways beneficial to maintaining systems out of thermodynamic equilibrium. This question leads one to consider devices employing wave-particle interactions.

There are several ways in which such techniques might be used to pump out the entropy at a very low temperature so that the power loss would be kept to a minimum. For instance, a wave with a certain energy might be injected into the plasma, and after interacting with the particles and removing their entropy, the wave would have the same energy but a broader frequency linewidth. The wave would then be direct-converted to recover nearly all of its energy, but due to the linewidth broadening a small fraction of the wave's energy could not be converted back into electrical energy and would have to be dissipated as heat in the wave-receiving system.

As a specific means of transferring entropy from the particles to the wave, one might wish to make the phase velocity of the wave equal to the desired optimum velocity of the particle distribution. If particles have not been too terribly affected by collisions since their last trip through the velocity-focusing device, their velocities should still be near the wave phase velocity. Particles which have been upscattered in energy by collisions would return that energy to the wave, while particles which have previously lost energy would be accelerated by "riding the wave" and would recover the necessary amount of energy from the traveling wave. Thus the wave would use Landau-damping-type processes [74] in order to serve as a sort of "Robin Hood" intermediary which would rob energy from the fast particles and return it to the slow particles from which it had been taken by

means of collisions. These sorts of wave-particle interactions are used in traveling-wave linear particle accelerators [75, 76, 77] as well as in free electron lasers [78]. If the wave really does remove entropy from the particles, then there will be an increase in the wave's entropy density, which is given by the formula [79],

$$S_{wave} = \sum_{\alpha} \int d^3\mathbf{k} \ln[N_\alpha(\mathbf{k})] \,, \tag{3.78}$$

where $N_\alpha(\mathbf{k})$ is the number of photons of a given mode α and wavevector $\mathbf{k}$ per volume.

Another example of a wave-based method of entropy extraction would be a system in which the electromagnetic waves are used to transfer the entropy from the high-energy fusion plasma particles to a much lower-energy group of particles which can be sacrificed (actually direct-converted at the best possible efficiencies) without causing an excessive energy loss.

Regrettably, the use of wave-particle interactions does not appear to be a useful way to proceed. Bremsstrahlung and synchrotron radiation could indeed extract entropy and energy from particles which have become too fast due to collisions, but an equivalent amount of outside energy would still have to be given to particles which have been collisionally down-scattered (unless there were significant amounts of inverse bremsstrahlung or cyclotron absorption in the right regions of phase space; see Appendix E for more details). One is therefore inevitably led back to the same value of the minimum recirculating power which has already been shown to be prohibitively large. (Bremsstrahlung radiation would also have the tremendous drawback that it is broad-band and very short-wavelength, and therefore essentially impossible to convert with any efficiency better than the relatively low efficiency of a thermal conversion cycle.)

The question of whether more general types of wave-particle interactions might be used to recirculate power efficiently within the plasma and to remove the collisionally generated entropy can be resolved by using a modified version of a derivation given by Swanson [80]. In quasilinear theory the change in the distribution function due to interactions with

waves may be written in terms of a diffusion tensor $\bar{\mathbf{D}}$:

$$\left(\frac{\partial f}{\partial t}\right)_{wave} = \frac{\partial}{\partial \mathbf{v}} \cdot \left(\bar{\bar{\mathbf{D}}} \cdot \frac{\partial f}{\partial \mathbf{v}}\right) . \tag{3.79}$$

By using this expression for the wave-particle interaction together with the definition of entropy from Eq. (3.41) and integrating by parts, one finds that

$$\begin{aligned} \frac{dS}{dt} &= -\int d^3\mathbf{v} \left(\frac{\partial f}{\partial t}\right)_{wave} \ln f \\ &= -\int d^3\mathbf{v} \ln f \, \frac{\partial}{\partial \mathbf{v}} \cdot \left(\bar{\bar{\mathbf{D}}} \cdot \frac{\partial f}{\partial \mathbf{v}}\right) \\ &= +\int d^3\mathbf{v} \frac{1}{f(v)} \frac{\partial f}{\partial \mathbf{v}} \cdot \bar{\bar{\mathbf{D}}} \cdot \frac{\partial f}{\partial \mathbf{v}} . \end{aligned} \tag{3.80}$$

With the diffusion tensor appropriate for electromagnetic waves [80], the change in entropy becomes

$$\begin{aligned} \frac{dS}{dt} = +\left(\frac{Ze}{m}\right)^2 \sum_{n=-\infty}^{\infty} \int d^3\mathbf{v} \frac{1}{f(v)} \int \frac{d^3\mathbf{k}}{(2\pi)^3} \left|\frac{\partial f}{\partial \mathbf{v}} \cdot \mathbf{a}_{n,\mathbf{k}}\right|^2 \\ \times \frac{\gamma_{\mathbf{k}}}{(\omega_{r\mathbf{k}} - \mathbf{k} \cdot \mathbf{v})^2 + \gamma_{\mathbf{k}}^2} , \end{aligned} \tag{3.81}$$

where n designates the wave mode, $\mathbf{a}_{n,\mathbf{k}}$ is essentially the polarization vector of the given wave mode (see the description in [80] for more details), $\omega_{r\mathbf{k}}$ is the real part of the frequency corresponding to wavevector $\mathbf{k}$, and $\gamma_{\mathbf{k}}$ is the growth rate.

Thus the change in particle entropy is non-negative for undamped waves ($\gamma_{\mathbf{k}} \geq 0$), since all factors other than the growth rate are manifestly non-negative. (As shown in Figure 3-1, the entropy would have to be extracted along with a small but non-negligible amount of energy, so the wave would have to be undamped if it were to work as intended.)

Similarly, the quasilinear diffusion tensor for particles interacting with electrostatic

waves [79] may be used to obtain the result,

$$\frac{dS}{dt} = +\left(\frac{Ze}{m}\right)^2 \sum_\alpha \int d^3\mathbf{v} \frac{1}{f(v)} \int d^3\mathbf{k} \left|\frac{\partial f}{\partial \mathbf{v}} \cdot \hat{\mathbf{k}}\right|^2 \times \frac{8\pi\gamma_\mathbf{k} U_k^\alpha}{(\omega_{r\mathbf{k}} - \mathbf{k}\cdot\mathbf{v})^2 + \gamma_\mathbf{k}^2}, \tag{3.82}$$

in which α designates the wave mode, U_k^α is the spectral energy density of the waves, and $\hat{\mathbf{k}}$ is the polarization vector of the given wave mode.

This quantity is also non-negative for undamped waves.

For both electromagnetic and electrostatic waves, the addition of a static magnetic field only affects wave-particle interactions and the diffusion tensor in ways [79, 80] which do not alter the fundamental conclusion that the plasma's entropy cannot decrease as a result of the wave-particle interactions.

Therefore, barring unforeseen benefits from highly nonlinear effects which cannot be adequately described by the quasilinear treatment above, these types of wave-particle interactions cannot be used to pump entropy out of the plasma and maintain non-Maxwellian velocity distributions.

Remaining Approaches

The second loophole in the proof about electromagnetic fields and entropy extraction is that at least hypothetically, fields might be able to modify the rate of collisional entropy generation (without also dampening the fusion rate too much) or the process of entropy transfer between different groups of particles without the fields themselves actually having to carry the entropy at any point.

This loophole has not yet been closed, so it remains an open, although admittedly quite distant, possibility. No current plasma systems can exploit such possible phenomena, but some novel concepts for doing so are suggested in Appendix E. Barring the success of one

of these "wild ideas," however, the outlook for non-Maxwellian plasma fusion systems is very bleak.

3.6 Summary

Without requiring much more recirculating power than fusion power: 1) electrons cannot be maintained in an appreciably non-Maxwellian state (even for D-T), and 2) ions can at best be kept only modestly non-Maxwellian, and even then only for D-T and perhaps also D-D.

Any potentially feasible approaches for recirculating the power *inside* the plasma and at exceedingly high efficiencies need to be more closely examined (and will be, in Appendix E).

Chapter 4

Energy Decoupling Between Ions and Electrons

Since bremsstrahlung radiation losses resulting from large mean electron energies are a serious difficulty for D-^{3}He and D-D reactors and are generally prohibitive for reactors employing advanced aneutronic fuels, it would be highly desirable to reduce the mean electron energies below their normal equilibrium values. If sources of electron heating other than Coulomb friction with the fuel ions are neglected, then the equilibrium electron energy is determined by equating the electron energy gain from friction with the ions and the total energy loss from bremsstrahlung radiation, synchrotron radiation, electron losses from the confinement system, etc. Methods of reducing the mean electron energy below this equilibrium value will be referred to as techniques for decoupling the electron energy from the ion energy.

Numerous methods of ion-electron decoupling have been examined, including the techniques presented in Chapters 2 and 3. Virtually all of these methods can be shown to fail for one reason or another; very few potentially useful directions of exploration for ion-electron decoupling approaches remain.

4.1 Failed Ideas for Ion-Electron Decoupling

Virtually all effects one might consider employing to accomplish the necessary decoupling simply do not work, or at least do not work well enough. A partial list of techniques which are insufficient includes the following ideas.

4.1.1 Active Cooling of Electrons

One way to lower the mean electron energy would be the "brute force" method of somehow actively cooling the electrons. Examples of possible electron cooling methods include synchrotron radiation and energetic particle removal, both of which would be coupled with direct electric conversion schemes in order to minimize the net power loss. In a maximally efficient system, virtually all of the energy extracted from the electrons could be returned to the ions. This concept leads to a minimum recirculating power $P_{recirc} = P_{ie}$. (If the system cannot return the extracted energy to the ions then this quantity becomes the loss power, not just the recirculating power.)

The ion-electron energy transfer rate of Eq. (1.1) for given ion and electron temperatures may be directly compared with the fusion rate from Eq. (1.3), yielding the result (with temperatures and energies in eV and all other quantities in cgs units),

$$\frac{P_{ie}}{P_{fus}} = 4.75 \cdot 10^{-9} \frac{(x+Z_{i2})^2}{x} \frac{1}{\langle \sigma v \rangle_{fus} E_{fus,\,eV}} \sum_i \frac{Z_i^2 n_i}{\mu_i n_e T_e^{3/2}} (T_i - T_e) \left[24 - \ln\left(\frac{\sqrt{n_e}}{T_e}\right) \right] \times \left(1 + \frac{0.3 T_e}{m_e c^2}\right) \exp\left[- \left(3.5 \sum_i \frac{Z_i^2 n_i}{n_e} \frac{m_e}{m_i} \frac{T_i}{T_e} \right)^{2/3} \right] \frac{\text{Watts}}{\text{cm}^3}, \tag{4.1}$$

where the corrections due to variations in the Coulomb logarithm [30] and ion-induced partial depletion of slow electrons (from Eq. (2.50)) have been included.

The electron temperature (or two-thirds of the mean electron energy if the electrons

are non-Maxwellian) must be kept low enough that bremsstrahlung losses are reduced to the desired levels. The maximum allowable electron temperature for a given amount of bremsstrahlung loss may be found by comparing the bremsstrahlung power from Eq. (1.2) with the fusion power from Eq. (1.3):

$$\frac{P_{brem}}{P_{fus}} = 1.06 \cdot 10^{-13} \frac{(x + Z_{i2})^2}{x} \frac{\sqrt{T_{e,eV}}}{< \sigma v >_{fus,cgs} E_{fus,eV}} \times \left\{ \frac{\sum_i Z_i^2 n_i}{n_e} \left[1 + .7936 \left(\frac{T_e}{m_e c^2} \right) + 1.874 \left(\frac{T_e}{m_e c^2} \right)^2 \right] + \frac{3}{\sqrt{2}} \left(\frac{T_e}{m_e c^2} \right) \right\}, \tag{4.2}$$

where all temperatures and energies (including the electron rest energy) are given in eV.

Table 4.1 presents the minimum recirculating power (as defined by the ion-electron energy transfer rate) required for a system which actively refrigerates the electrons in order to keep the bremsstrahlung at a certain level. The electron temperatures for D-D and D-^{3}He have been chosen to cut the bremsstrahlung losses in half from what they would be without active refrigeration, while the electron temperatures for the advanced aneutronic fuels have been chosen to limit the bremsstrahlung losses to half of the fusion power.

Fuel mixture	T_i	T_e	$\langle \sigma v \rangle_{fus}$ (in 10^{-16} cm^{-3}/s)	E_{fus}	$\frac{P_{brem}}{P_{fus}}$	$\frac{P_{recirc}}{P_{fus}}$
D-^{3}He (1:1)	100 keV	26 keV	1.67	18.3 MeV	0.093	2.0
D-D	500 keV	113 keV	1.90	3.7 MeV	0.18	1.1
^{3}He-^{3}He	1 MeV	106 keV	1.25	12.9 MeV	0.50	6.2
p-^{11}B (5:1)	300 keV	23 keV	2.39	8.7 MeV	0.50	33.6
p-^{6}Li (3:1)	800 keV	14 keV	1.60	4.0 MeV	0.50	325

Table 4.1: Recirculating power to actively refrigerate electrons (with $\ln \Lambda \approx 15$ and fusion cross section data drawn from references [33], [34], and [35]).

Therefore even in the best of circumstances (an electron cooling system which returns

virtually all of the extracted energy to the ions), a reactor would have to recirculate an amount of power greater than the fusion power in order to refrigerate the electrons to a useful degree. This approach is clearly not practical.

If the electron energy is to be successfully decoupled from that of the ions, it will be necessary actually to reduce the energy transfer rate from its usual value. (In the above calculation, the reduction due to the effect examined in Chapter 2 helps slightly, but it is far from being as large a reduction as is required.)

4.1.2 Particle Circulation Between Two Regions with $\langle E_i \rangle > \langle E_e \rangle$ and $\langle E_e \rangle > \langle E_i \rangle$

Another approach one might consider would be to design a system in which particles circulate between two (or more) regions in which the energies of the particles are significantly different. In particular, it might be possible to establish an electric potential difference between the two parts of the plasma, thus causing ions to lose energy and electrons to gain energy (or vice versa) in traveling between them. One of the regions would then have $\langle E_i \rangle > \langle E_e \rangle$ so that in it energetic ions would fuse and electrons would have energies too low to radiate strongly, while in the second region the situation would be reversed, $\langle E_e \rangle > \langle E_i \rangle$, and energy transferred from the ions to the electrons in the first region would be transferred back in the second.

This idea fails for a straightforward reason. In order for the energy transfer in the two regions to be comparable, the volume-integrated square of the density $\int d^3\mathbf{x}[n(\mathbf{x})]^2$ must be comparable for the two regions. Since the second part of the plasma has a higher mean electron energy than the first and also has a comparable $\int d^3\mathbf{x}[n(\mathbf{x})]^2$, bremsstrahlung losses from the second region will be larger than those from the first, and with lower ion energies, the second region will not even be able to compensate partially for these losses by producing substantial amounts of fusion power. Therefore such schemes are counterproductive.

4.1.3 Non-Maxwellian Electron Distributions

Since ion-electron energy transfer is directly mediated by slow electrons (electrons which move more slowly than the ions), it would be possible to achieve a large reduction in the energy transfer rate and bremsstrahlung loss by actively depleting the slow electrons, or in other words by creating and maintaining a non-Maxwellian electron velocity distribution. This was the motivation underlying the work presented in Chapter 3. Yet as was demonstrated in that chapter, the recirculating power needed for the active maintenance of such electron distributions in the presence of electron-electron collisions is substantially larger than the fusion power for all cases of interest (even when the electron distribution is nearly Maxwellian with only a narrow hole "cut out" in the low velocity range). This minimum recirculating power is independent of the specific mechanism used to keep the electrons non-Maxwellian (eg. systems with rapid throughput of electrons, selective energy extraction from fast electrons with selective energy donation to slow ones, etc.). For this reason, any readily foreseeable types of fusion reactors must make do with essentially Maxwellian electrons.

4.1.4 Non-Maxwellian Ion Distributions

Among other things, Chapter 2 demonstrated that even highly non-Maxwellian ion distributions such as a monoenergetic distribution will transfer energy to ions at almost exactly the same rate as Maxwellian ions with the same mean ion energy, even when there are very large energy differences between the ions and electrons.

In fact, as shown in Appendix A, isotropic but non-Maxwellian distributions would also have nearly the same fusion reactivity $\langle \sigma v \rangle$ (within 20% or so) as Maxwellian ions with the same mean energy, since ion-ion collisions must still be averaged over all angles (assuming that if there are two fuel ion species, their mean energies are the same, a problem which will be addressed in the next chapter). Thus a non-Maxwellian ion distribution could not even indirectly reduce the relative severity of the recirculating power requirements and

bremsstrahlung losses by boosting the fusion power.

Therefore, there is little to be gained in terms of ion-electron energy decoupling by attempting to keep the ion distributions non-Maxwellian (even if one could in spite of the recirculating power requirements to do so).

4.1.5 Effects of Anisotropy on Ion-Electron Energy Transfer

As this research has generally focused on isotropic systems, one might wonder whether anisotropy (if it could be sustained without instabilities) could help the situation. The effect of anisotropic ion and electron velocity distributions on the energy transfer rate may be derived as follows.

According to Sivukhin, the rate of energy transfer to a particle of species "a" from species "b" is [59]:

$$\left\langle \frac{dE_a}{dt} \right\rangle = -\frac{4\pi Z_a^2 Z_b^2 e^4 \ln\Lambda}{m_a m_b} \int d^3v_b f_b(\mathbf{v_b}) \frac{(m_a\mathbf{v_a} + m_b\mathbf{v_b}) \cdot (\mathbf{v_a} - \mathbf{v_b})}{|\mathbf{v_a} - \mathbf{v_b}|^3} , \tag{4.3}$$

in which the distribution function for species b has been taken to be completely arbitrary.

By applying this formula to ions and electrons and integrating over arbitrary distribution functions for both species (with θ defined to be the angle between the velocity $\mathbf{v_i}$ of an ion and the velocity $\mathbf{v_e}$ of an electron), it is found that

$$\begin{aligned} P_{ie} &= \frac{4\pi Z_i^2 e^4 \ln\Lambda}{m_i m_e} \int d^3v_i \int d^3v_e f_i(\mathbf{v_i}) f_e(\mathbf{v_e}) \frac{[m_i v_i^2 - m_e v_e^2 - m_i(\mathbf{v_i} \cdot \mathbf{v_e})]}{|\mathbf{v_i} - \mathbf{v_e}|^3} \\ &= \frac{4\pi Z_i^2 e^4 \ln\Lambda}{m_i m_e} \int d^3v_i \int d^3v_e \frac{f_i(\mathbf{v_i}) f_e(\mathbf{v_e}) [m_i v_i^2 - m_e v_e^2 - m_i v_i v_e \cos\theta]}{v_e^3 |1 + (v_i/v_e)^2 - 2(v_i/v_e)\cos\theta|^{3/2}} . \end{aligned} \tag{4.4}$$

This expression reduces to the "isotropic" P_{ie} equation if all ion velocities are perpendicular to the electron velocities ($\theta = 90^o$, as would be the case in an ideal migma configuration with electrons oscillating through the plane of the ion orbits [38, 39]).

Furthermore, it also reduces to the isotropic rate if the ion and/or electron velocity distributions are anisotropic but symmetric under inversion. In other words, if there is bi-directional flow, as would be needed for colliding ion beams to fuse, $\cos\theta$ will have a certain value just as often as it has the negative of that value.

Therefore anisotropy does not substantially alter ion-electron energy transfer for cases of interest.

4.1.6 Magnetic Fields

It was once suggested that magnetic fields might decrease the rate of energy transfer between ions and electrons by decreasing the effective value of the Coulomb logarithm [12, 81]. Unfortunately, detailed studies of this issue [55, 82, 83] revealed that magnetic fields actually increase the energy transfer rate. Of course, even if magnetic fields did in fact decrease the energy transfer, they would also cause synchrotron radiation losses, so it would still be highly undesirable to have strong magnetic fields throughout the bulk of the plasma. From the standpoint of radiation losses, it is best to limit strong magnetic confinement fields to the outer edges of the plasma by employing multipolar field geometries or by arranging for the plasma to exclude the field diamagnetically from most of its internal volume.

4.1.7 Operation Without Electrons

Because the root of the radiation loss problem is electrons, one obvious idea would be to eliminate or at least greatly reduce the number of electrons in the system by maintaining a grossly nonneutral plasma of positive fuel ions. However, space charge effects from the ions would limit the density of the plasma, in accordance with the Brillouin limit [84],

$$n_i < \frac{B^2/8\pi}{m_i c^2} \,. \tag{4.5}$$

Even for extremely large magnetic fields, the Brillouin-limited ion density is quite low. For example, for $B = 2 \cdot 10^5$ G (20 T), the ion density is limited to

$$n_i < \frac{1.1 \cdot 10^{12}\ \mathrm{cm}^{-3}}{\mu_i}\ , \tag{4.6}$$

where $\mu_i \equiv m_i/m_p$.

For a p-^{11}B plasma with fuel ion densities of $n_p < 10^{12}$ cm^{-3} and $n_B < 10^{11}$ cm^{-3}, the fusion power density is at most about 30 W/m^3, far too low to be of interest for fusion reactors of reasonable size.

One might try to exploit the fact that the Brillouin limit only applies to the overall average density by attempting to create a spherical ion focusing system with a dense fusion core [85], but unrealistically high fields would still be required, collisional scattering effects would rapidly degrade the particle velocity distributions needed to maintain proper focusing [86, 87], and the approach would not readily scale up to large (10^8-10^9 Watt) fusion reactors.

Thus the Brillouin-limited ion density is too low for the production of useful amounts of fusion power in a system without electrons.

4.1.8 Preferential Fusion Product Heating of Ions

Preferential fusion product heating of ions (without heating the electrons) via nuclear elastic scattering [10, 55, 88, 89, 90, 91, 92] or other mechanisms does not improve these calculations; it is already assumed that the ion energy distribution is held fixed and that the *only* source of electron heating is Coulomb friction with ions. In less idealized systems, the electrons would gain energy from the fusion products, from external heating beams, and from other sources, and the electron temperatures and bremsstrahlung radiation rates would be even higher than calculated in this thesis. Furthermore, since the fusion reactivity is nearly independent of the ion velocity distribution shape for a given mean

ion energy (as shown in Appendix A), enhancement of the fast tail of the ion distribution due to nuclear elastic scattering would not substantially alter the results given here.

4.1.9 Spatially Inhomogeneous Systems

Ion-electron energy transfer, fusion, and bremsstrahlung are all two-body collisional events, so they are all proportional to $\int d^3\mathbf{x}[n(\mathbf{x})]^2$. Therefore the relative magnitudes of these effects are not altered in spatially inhomogeneous sytems; the ratios of these quantities are independent of the densities and density profiles (apart from the weak density dependence of the Coulomb logarithm). Thus ion-electron decoupling cannot be faciliated by employing inhomogeneous plasmas.

4.1.10 Wave-Based Recirculation of Power from Electrons Back to Ions

A method of using waves to couple the energy of fusion products selectively and efficiently to current drive or fuel ion energy (without also coupling to electrons) has recently been suggested [93, 94, 95]. This idea leads one to contemplate the use of waves to recirculate the large amounts of power which would be required if a plasma's electron temperature were kept much below the equilibrium value determined from the ion temperature and the electron losses. Because of the large mass difference between ions and electrons, even if the ion energies were far larger than the electron energies, it would still be possible to have

$$v_e > v_{phase} > v_i \ , \tag{4.7}$$

where v_e and v_i are the characteristic electron and ion velocities, respectively, and v_{phase} is the phase velocity of the wave. Thus the electrons could give energy to the wave, which in turn would give it to the ions. This technique would operate entirely within the plasma itself and at least theoretically might have extremely high efficiencies, so at least

superficially it appears very attractive.

Unfortunately, this approach seems to be fatally flawed. Below the velocity v_{phase}, the electrons would have to be held in a highly non-Maxwellian distribution, or else the electrons would reabsorb the wave energy via Landau damping [74] instead of transmitting the energy to the ions. As was shown in Chapter 3, the maintenance of substantially non-Maxwellian velocity distributions would require prohibitively large recirculating power levels. Furthermore, even if the electron distribution could be held in the proper shape, it was explicitly demonstrated in Section 3.5 that wave-particle interactions cannot decrease the entropy of a particle species, barring highly nonlinear effects unforeseen by the quasi-linear calculation performed in that section. For these reasons, wave-based techniques of recirculating power from the electrons back to the ions do not appear to be a useful way to approach the problem.

4.1.11 Reabsorption of Bremsstrahlung Radiation Within the Plasma

While the reabsorption of bremsstrahlung radiation within the plasma would not constitute an ion-electron energy decoupling method, it would nonetheless solve (or at least alleviate) the problem of high-electron-temperature-induced radiation losses, so it will be considered here.

In order for most of the bremsstrahlung to be reabsorbed in the plasma, the plasma radius R must be comparable to or greater than the inverse of the bremsstrahlung reabsorption coefficient K as given in [96, 97]:

$$R \geq \frac{1}{K} = 1.7 \cdot 10^{37} \frac{T_{e,\,eV}^{7/2}}{Z_i n_e^2 \ln \Lambda} \text{ cm.} \tag{4.8}$$

If most of the bremsstrahlung is reabsorbed, the electron temperature will equilibrate to become approximately the same as the ion temperature.

Even for a very dense ($n_e = 10^{16}$ cm^{-3}) p-^{11}B magnetic fusion plasma with $T_e = 300,000$ eV, $Z_{i,\,effective} = 2$, and $\ln \Lambda = 20$, one finds $R \geq 6 \cdot 10^{20}$ meters. Thus magnetic fusion reactors clearly have no hope of retaining useful amounts of bremsstrahlung within the plasma.

Extremely dense ICF-type plasmas theoretically might be able to retain a substantial amount of bremsstrahlung, but for such fusion systems one must also consider another important quantity, namely the energy yield from the fusion of each pellet. The yield can be expressed in terms of the explosive energy of an equivalent amount of TNT:

$$\text{Yield} = \eta_{burn} E_{fus,\,eV} \frac{n_i}{2} \left(\frac{4}{3}\pi R^3\right) \left(\frac{1 \text{ ton TNT}}{2.6 \cdot 10^{28} \text{ eV}}\right) , \tag{4.9}$$

in which η_{burn} is the fraction of the ion pairs which are burned up in the reaction, $E_{fus,\,eV}$ is the energy in eV released per reaction, n_i is the total ion density, and R is the pellet radius. It has been assumed for simplicity that the fuel mixture is stoichiometric so that each ion can find a proper fusion partner.

A truly accurate inverse bremsstrahlung calculation for ultra-dense, high-energy plasmas of the type under consideration would require the incorporation of three-body effects, electron-electron collisional effects, and relativistic corrections. However, the above equations may be used at least to get some idea of the physical implications of bremsstrahlung reabsorption for fusion reactors.

Currently contemplated ICF reactors would achieve compressed plasma densities of about 10^3 times the density of uncompressed solid fuel [98]. By using the equations presented above, one finds that a fusion plasma of this density, or even one with a density a few orders of magnitude higher, would require a pellet radius large enough that even if the pellet could be ignited, the yield would be sufficient to destroy the reactor.

In order to bring the yield down to a reasonable level while retaining the bremsstrahlung within the plasma, the density would have to be increased until it is roughly 8 or so orders of magnitude larger than the density of the uncompressed solid fuel, or in other words

about 5 orders of magnitude greater than is currently considered for ICF fusion reactors. Even if such phenomenal amounts of compression could somehow be achieved, the cumulative bremsstrahlung losses during the compression of the plasma might become intolerably large before the plasma could attain a density high enough to retain further bremsstrahlung.

For these reasons, reabsorption of the bremsstrahlung within the fusion plasma does not appear to be a feasible or useful means of lowering the radiation losses of advanced aneutronic fuels to acceptable levels.

4.1.12 Direct Electric Conversion of Bremsstrahlung Radiation

As a final related note, it should be mentioned that even highly optimistic calculations regarding various proposed methods for directly converting bremsstrahlung radiation power into electrical power arrive at efficiencies which are not much greater than thermal conversion efficiencies [5]. (In thermal conversion approaches, the bremsstrahlung would be reabsorbed in a solid or liquid blanket surrounding the reactor, and then the heat deposited in the blanket would be used to drive a heat engine at Carnot-limited efficiencies.) Bremsstrahlung radiation is simply emitted at frequencies which are too high to permit radio-frequency-type conversion and too low to permit truly efficient conversion via the Compton effect [5].

4.2 Ion-Electron Decoupling Approaches Which Are Still Potentially Viable

When examined in terms of the removal of collisionally generated entropy, the problem of ion-electron decoupling is quite similar to the issue considered in Chapter 3, the maintenance of non-Maxwellian velocity distributions. An ion-electron decoupling system can also be described by Figure 3-1, and it is subject to the same stringent limitations noted

in Section 3.5. Likewise, the handful of approaches which were not ruled out in Chapter 3 could at least hypothetically be adapted to the problem of ion-electron decoupling. Possible directions of research which may yet prove fruitful for ion-electron decoupling will be discussed in more detail in Appendix E.

4.3 Summary

While it cannot be claimed that this is an exhaustive list of all possible ion-electron energy decoupling methods, at least all currently known potential ways to decouple the electrons have been examined and shown to fail because they would not work well enough or would not even work at all. Unless some of the highly speculative approaches such as those outlined in Appendix E meet with success, reactor designs which rely on ion-electron energy decoupling appear doomed to failure.

Chapter 5

Energy Decoupling Between Two Fuel Ion Species

It is worthwhile to check whether one ion species can be maintained at a significantly lower energy than the other ion species, or in other words whether two ion species can be decoupled in energy from each other. Such an energy decoupling would be useful for operating D-^{3}He plasmas with deuteron energies much lower than the ^{3}He energy in order to suppress D-D reactions. Decoupling between the two ion species in p-^{11}B and p-^{6}Li plasmas could also increase the fusion reaction rate by up to a factor of two or three by not "smearing out" the sharp resonance peaks in the reaction cross sections with a wide range of net collision velocities between the two types of ions.

5.1 Failed Ideas for Decoupling Between Ion Species

Several ideas for decoupling between ion species have been suggested, but unfortunately none of them can work sufficiently well to be of use. The principal proposed approaches, together with the reasons why they fail, are summarized below.

5.1.1 Degree of Passive Decoupling Due to Ion Loss Via Fusion Events

It has been proposed [18, 19] that it might be possible for the ions in a system to be lost to fusion events before the mean energies of the two fuel ion species have time to equilibrate. To investigate this issue, it will be assumed that the $i1$ species is more energetic than the $i2$ species and that the standard Spitzer expression for interspecies energy transfer may be applied to this problem. (As was shown in Chapter 3, the individual ion species cannot deviate substantially from Maxwellian distributions without requiring prohibitively large amounts of recirculating power; thus the standard formula may be employed here.)

Considering for the moment only the heating of the $i2$ species by the $i1$ species, the power density (in eV/sec-cm^3) transferred to the $i2$ ions will be [27, 30]:

$$P_{i1-i2} = \frac{3}{2} n_{i2} \frac{dT_{i2}}{dt} = 2.63 \cdot 10^{-19} \frac{\sqrt{m_{i1} m_{i2}} Z_{i1}^2 Z_{i2}^2 n_{i1} n_{i2} \ln \Lambda_{i1-i2}}{(m_{i1} T_{i2} + m_{i2} T_{i1})^{3/2}} (T_{i1} - T_{i2}) \,, \qquad (5.1)$$

in which the temperatures are in eV.

The cooling rate of $i2$ ions due to the replacement of fused ions is:

$$P_{cool} = \frac{3}{2} T_{i2} n_{i1} n_{i2} \langle \sigma v \rangle_{fus} \,. \qquad (5.2)$$

The equilibrium temperature of the $i2$ species is determined by setting the total amounts of heating and cooling equal to each other. Since both the heating and cooling expressions have the same dependence on the ion densities, integrating them over the spatial region of interest has no effect on the ratio between them. By defining the ion mass as a multiple of the proton mass m_p, $m_i \equiv \mu_i m_p$, and expressing the temperatures in eV, one arrives at an expression which is convenient for seeing the general range of permitted values for T_{i2}:

$$T_{i2} = T_{i1} \left[1 + \frac{7.40 \cdot 10^6 \langle \sigma v \rangle_{fus} (\mu_{i1} T_{i2,\,eV} + \mu_{i2} T_{i1,\,eV})^{3/2}}{\sqrt{\mu_{i1} \mu_{i2}} Z_1^2 Z_2^2 \ln \Lambda_{i1-i2}} \right]^{-1} \,. \qquad (5.3)$$

For all of the fuels of interest (D-T, D-^{3}He, p-^{11}B, etc.) utilized under any reasonable circumstances (see for example the parameters in Table 1-1), one finds from Eq. (5.3) that the temperature of the $i2$ species is constrained to be very close to that of the $i1$ species:

$$.95T_{i1} \leq T_{i2} \leq T_{i1} \; . \tag{5.4}$$

Therefore this evaluation shows that it is not possible to keep one ion species at a significantly lower temperature or energy than the other unless one provides an additional means of cooling the $i2$ species or of reducing the energy transfer rate between the species.

5.1.2 Active Refrigeration of One Ion Species

Now calculations will be performed for the case in which a large temperature difference between the ion species is maintained by somehow actively refrigerating one species. In a maximally efficient system, virtually all of the energy removed from the less energetic species would be returned to the more energetic species, making the interspecies power flow the minimum recirculating power. Less than ideal systems would require more recirculating power and/or incur sizeable losses each time the power was handled by the recirculation system.

It will be assumed that $T_{i1} \gg T_{i2}$, so that the collisions between the two ion species occur at a relative velocity $v \approx \sqrt{3T_{i1}/m_{i1}}$. Coulomb collisions will then transfer energy between the species at the rate calculated above. Dividing this energy transfer rate by the fusion power and putting T_{i1} and E_{fus} in eV, one obtains:

$$\frac{P_{i1-i2}}{P_{fus}} = 1.20 \cdot 10^{-13} \frac{m_{i1}}{m_{i2}} \frac{Z_{i1}^2 Z_{i2}^2 \ln \Lambda_{i1-i2}}{\sigma_{fus} E_{fus,\,eV} T_{i1,\,eV}} \; . \tag{5.5}$$

For a numerical estimate it is illustrative to use the case of p-^{11}B reactions, for which it would be desirable to have high-energy protons ($i1$ species) and low-energy boron ions ($i2$ species). The peak of the fusion cross section, $\sigma_{fus} \approx 8 \cdot 10^{-25}$ cm^2, occurs for a proton

energy of about 620,000 eV, or T_{i1} equal to two-thirds of that energy [35]. Estimating the Coulomb logarithm as approximately 15 and very optimistically assuming that all of the protons have the optimum energy of 620 keV, the power ratio is found to be:

$$\frac{P_{p-^{11}B}}{P_{fus}} \approx 1.4 \, . \tag{5.6}$$

As another example, D-^{3}He reactions may be considered. In order to suppress D-D side reactions, it would be desirable to keep all of the deuterons at very low energies. Assuming very optimistically that all of the ^{3}He ions can be kept at the optimum energy of 675 keV, the fusion cross section will be at its maximum, $\sigma_{fus} \approx 7.2 \cdot 10^{-25}$ cm^2 [33]. For $\ln \Lambda = 15$, this means that the power ratio is

$$\frac{P_{^3He-D}}{P_{fus}} \approx 2 \, . \tag{5.7}$$

Realistically it will not be possible to keep the energetic ion species in a nearly monoenergetic distribution, so there will be a large spread in the collision velocities and most will not occur at the peak cross section. Also, it may not be practical to support the required mean ion energies of over 600 keV. If the ions are essentially Maxwellian or if they are at a lower mean energy, the ratio of the interspecies energy transfer rate to the fusion power may be over an order of magnitude greater than the values calculated above for these two fuels.

Thus the recirculating power requirements imposed on a system which actively maintains two fuel ion species at very different mean energies appear to be too large to be practical unless a means can be found to reduce the interspecies energy transfer rate or to recirculate the power in an extremely efficient and relatively trouble-free manner.

5.1.3 Non-Maxwellian Ion Distributions

It has already been observed that highly non-Maxwellian ion distributions cannot be employed to reduce the energy transfer rate because they would necessitate the use of far too much recirculating power (see Chapter 3). Yet even if the power limitations were not a problem, non-Maxwellian ion velocity distributions would not be useful for decoupling the energies of two ion species, as will now be shown.

It will again be assumed that the $i1$ species is to be maintained at a much larger mean energy than the $i2$ species. By analogy with the case of ion-electron energy decoupling, the only way in which non-Maxwellian ion distributions would decrease the energy flow between the $i1$ and $i2$ species is if there were very few $i2$ ions "below" the $i1$ ions in velocity space. In other words, the mean $i2$ speed must be larger than the mean $i1$ speed. For $v_{i2} > v_{i1}$, the ratio of the ion energies must obey the relation,

$$\frac{\langle E_{i2} \rangle}{\langle E_{i1} \rangle} > \frac{m_{i2}}{m_{i1}} \,. \tag{5.8}$$

This sets a limit on the maximum difference in the ion energies.

Because of this requirement, such methods cannot be employed with p-^{11}B and p-^{6}Li plasmas. It is not possible to keep the protons at high energies ($>$ 600 keV in order to maximize the fusion rate) and the more massive ions at low energies while allowing the more massive ions to have higher velocities than the protons. Although it would be permissible to have the opposite situation with high-energy but relatively low-velocity ^{11}B or ^{6}Li and lower-energy but higher-velocity protons, there would be many unpleasant consequences. It would be desirable to hold the proton velocities to low enough values that they would not "smear" the peaks in the fusion cross section which one desired to exploit. However, if the ^{11}B or ^{6}Li velocities were then kept from exceeding the proton velocities, the net collision velocities would be limited to uninterestingly low values in terms of promoting nuclear reactions. On the other hand, if the boron or lithium ions were accelerated up to fusion velocities (regardless of the implications for the interactions

with the protons), the presence of such high-energy, relatively high-Z ions would cause the ion-electron energy transfer and bremsstrahlung radiation losses to be at least as bad as they were in the equilibrium case calculated in Chapter 1.

D-^{3}He plasmas could potentially make use of this effect, but only in a modest fashion. Because the masses of the two ion species are not very dissimilar, one would be limited to $\langle E_D \rangle / \langle E_{He-3} \rangle > 2/3$. Even if the recirculating power necessary to keep the deuterons non-Maxwellian with the slow ions depleted could be tolerated, the deuteron energy could not be made greatly lower than the helium ion energy, as would be required in order to suppress D-D side reactions to a worthwhile degree.

Thus, one concludes that the use of non-Maxwellian ion distributions is neither a feasible approach nor even a particularly desirable one in dealing with energy decoupling between ion species.

5.1.4 Wave-Mediated Recirculation of Power Between Ion Species

Just as Chapter 4 considered the possibility of using waves to recirculate power between ions and electrons, the possibility of using waves to recirculate power between two ion species which are at different energies will be considered here. In systems of the desired type, the waves would have a phase velocity v_{phase} between the velocities of the two ion species, so that $v_{i2} > v_{phase} > v_{i1}$, but the mean energies of the two ion species would obey the relation, $E_{i1} > E_{i2}$.

These relative orderings of the velocities and energies lead directly back to the arguments stated above for systems with non-Maxwellian ion distributions. Desirable types of p-^{11}B and p-^{6}Li plasmas cannot meet these requirements, and at best such systems could keep deuterons at only modestly lower energies than helium-3 ions, which is not enough to greatly reduce the D-D side reactions.

Even if this method could work, it would require the velocity distribution of the $i2$

species to have $\partial f_{i2}/\partial v > 0$ for a significant part of the distribution, or else the $i2$ distribution would reabsorb the waves it emits instead of transmitting them to the $i1$ species. This requirement leads back to the tremendous recirculating power levels which are necessitated by non-Maxwellian distributions.

The final argument against wave-based techniques is that all such methods which were examined in Section 3.5 were shown to be unable to remove entropy from the plasma, which is what would have to occur in order for the collisionally mediated transfer of energy between species to be counteracted.

5.1.5 Particle Circulation Between Two Regions with $\langle E_{i1} \rangle > \langle E_{i2} \rangle$ and $\langle E_{i2} \rangle > \langle E_{i1} \rangle$

Another way to handle the large amount of recirculating power in an essentially "hands-off" and efficient manner would be to pass all of the ions back and forth between two (or possibly more) regions with potential differences between them. If the two ion species have different charges (which they do in all cases of interest), it would then be possible to establish conditions such that $\langle E_{i1} \rangle > \langle E_{i2} \rangle$ in the main (fusion) region and $\langle E_{i2} \rangle > \langle E_{i1} \rangle$ in the other (but no significant rate of fusion reactions occurred there). Energy transferred between the species in one region would automatically be recirculated back in the other.

Even if this technique could be made to work, it will now be shown that it could not possibly help enough.

D-^{3}He

For a D-^{3}He plasma, it would be desirable to have a "fusion region" in which the ^{3}He ions have some energy $E_{optimum}$ and the deuterons are at a much lower energy, ϵ. In this region, energy will flow from the helium ions to the deuterons. Ideally, one would like to have the particles periodically circulate into a "restoration region" in which the D energy

is higher than the ^{3}He energy, so that the energy transferred between the species in the fusion region will be returned to its proper place.

In order to achieve this effect, one would have to create an electrostatic potential energy increase $\Delta\Phi$ in going from the fusion region to the restoration region. Since the helium ions will lose twice as much kinetic energy as the deuterons, it is possible to reverse the relative order of the ion species' energies as desired. Unfortunately, the constraints on the ion kinetic energies in the restoration region, $E_D > E_{He-3} \geq 0$, set a lower limit on the deuteron energy in the fusion region,

$$\epsilon \geq \frac{1}{2} E_{optimum} \cdot \tag{5.9}$$

The deuteron energy in the fusion region of the plasma is required to be at least half of the ^{3}He energy; this decrease in D energy is only sufficient to reduce the D-D neutrons by roughly a factor of 2, which is a far smaller reduction than would be desired. Furthermore, this result is predicated on the extremely optimistic assumption that such systems can actually be made to work.

p-^{11}B and p-^{6}Li

Now the use of these types of systems with p-^{11}B and p-^{6}Li will be considered. For the sake of generality, the two ion species in the plasma will be referred to as the protons and the $i2$ species.

If most of the fusion events could be made to occur near the peak of the fusion cross section, rather than over a wide range of net collisional energies, the average fusion reactivity could be substantially improved. For an isotropic system, this goal would require one of the ion species to be at a high energy and the other to be at an energy so low that it cannot greatly alter the relative collision velocity between the two types of ions.

It would not be useful to have a fusion region with high proton energies and very

low $i2$ energies (so that energy flows from protons to $i2$ ions in the fusion region) and then a restoration region at a different potential. If the potential change in going from the fusion to the restoration region were positive, the $i2$ species would lose more kinetic energy (due to its charge $Z_{i2} > 1$) than the protons, and thus energy flow between species would not be reversed in the restoration region (it would still go from protons to $i2$ ions). On the other hand, if there were a potential decrease so that the ions gained a substantial amount of kinetic energy upon entering the restoration region, both species would have high energies, causing the restoration region to have a high fusion rate with comparatively few of the collisions occurring near the peak of the cross section.

The opposite situation, in which the fusion region contains high-energy $i2$ ions (at some energy $E_{optimum}$) and low-energy protons (at an energy ϵ), would be only slightly more useful. The potential change in moving from the fusion region to the restoration region would have to be positive to cause a reversal of the energy flow between the ion species. The constraints on the particle energies in the restoration region, $E_p > E_{i2} \geq 0$, set a lower limit on ϵ, just as they did in the D-^{3}He case, so that

$$\epsilon \geq \frac{1}{Z_{i2}} E_{optimum} \cdot \tag{5.10}$$

Because of the mass difference between protons and $i2$ ions, even a fairly small amount of proton energy will correspond to a large proton velocity in comparison with the $i2$ velocities. Therefore, even if this method could be made to work as intended, proton energies in the fusion region would remain high enough to ensure that a large number of the proton-$i2$ collisions would happen at a net collision velocity far from the optimum collision velocity at which the peak of the fusion cross section occurs.

5.1.6 Counter-Propagating Ion Beams

The use of counter-propagating "cold" beams of the two different ion species with properly chosen energies would enable virtually all of the fusion reactions to occur at the optimum

collision velocity and essentially eliminate reactions between particles in the same beam (eg. D-D side reactions). Unfortunately, one would then have to cope with the recirculating power required to negate the effects of both parallel and perpendicular velocity-space diffusion, assuming that a specific mechanism for doing so even existed. As was shown in Chapter 3, the recirculating power entailed in choosing to operate with such beams would be prohibitively large for all fuels except possibly D-T and D-D, which are not of particular interest here. Weibel, counter-streaming, and other instabilities would also pose huge problems. For these reasons, this does not appear to be a useful approach to the problem.

5.1.7 Effects of Anisotropy in Beam-Plasma Systems

A less ambitious anisotropic system would be one in which a high-energy beam of $i1$ ions interacts with a low-energy, relatively stationary "target plasma" of $i2$ ions. It therefore becomes of interest to examine how the energy transfer rate between the ion species in such configurations would differ from the rate given in Eq. (5.5) for the isotropic case.

Again employing the result from Sivukhin [59] for energy transfer between two species, Eq. (4.3), the power flow between the ion species is

$$P_{i1-i2} = \frac{4\pi Z_{i1}^2 Z_{i2}^2 e^4 \ln\Lambda}{m_{i1} m_{i2}} \int d^3\mathbf{v_{i1}} \int d^3\mathbf{v_{i2}} f_{i1}(\mathbf{v_{i1}}) f_{i2}(\mathbf{v_{i2}}) \times \frac{(m_{i1}\mathbf{v_{i1}} + m_{i2}\mathbf{v_{i2}}) \cdot (\mathbf{v_{i1}} - \mathbf{v_{i2}})}{|\mathbf{v_{i1}} - \mathbf{v_{i2}}|^3} . \tag{5.11}$$

For $i1$ ions sufficiently fast that $v_{i1} \gg (m_{i2}/m_{i1})v_{i2}$ and $v_{i1} \gg v_{i2}$ (as would be needed to avoid blurring the resonance peak of the p-^{11}B fusion cross section or to strongly suppress D-D side reactions from D-^{3}He reactors), one finds that

$$\begin{aligned} P_{i1-i2} &\approx \frac{4\pi Z_{i1}^2 Z_{i2}^2 e^4 \ln\Lambda}{m_{i2}} \int d^3\mathbf{v_{i1}} \int d^3\mathbf{v_{i2}} f_{i1}(\mathbf{v_{i1}}) f_{i2}(\mathbf{v_{i2}}) \frac{1}{v_{i1}} \\ &\approx \frac{4\pi Z_{i1}^2 Z_{i2}^2 n_{i2} e^4 \ln\Lambda}{m_{i2}} \int d^3\mathbf{v_{i1}} f_{i1}(\mathbf{v_{i1}}) \frac{1}{v_{i1}} . \end{aligned} \tag{5.12}$$

Because of the assumption that the $i1$ ions are much faster than the $i2$ ions, the energy transfer rate no longer depends on the angle between the velocities of the two ion species. In other words, the energy transfer rate between the species reduces to that found in Eq. (5.5) regardless of any anisotropy in the velocity distribution of the $i1$ species. (Of course, even if there were some tangible benefit to this approach, one would still have to deal with the problems of instabilities, the recirculating power needed to maintain the ion beam against diffusive and decelerating effects, and heating of the electrons by the beam.)

5.2 Approaches to Decoupling Between Ion Species Which Are Still Potentially Viable

The problem of energy decoupling between ion species can be viewed in terms of Figure 3-1, just as could the problems of maintaining non-Maxwellian distributions and decoupling electrons from ions. Thus while all of the techniques which have been examined have been ruled out, there still remain a very small number of possible avenues for further exploration; these remaining routes are similar to those which could be considered for velocity distribution focusing and ion-electron decoupling, and they will be examined in more detail in Appendix E.

5.3 Summary

To hold the mean energy of one ion species substantially lower than that of the other would require a recirculating power considerably greater than the fusion power. All presently foreseeable methods of reducing the interspecies energy transfer rate or of recirculating the power efficiently and with little effort have been demonstrated to be inadequate or impractical. Barring a radical breakthrough in one of the directions outlined in Appendix E, it does not appear to be possible to decouple the energies of two fuel ion species in a

reactor.

Because of these findings, there is no apparent way to reduce the D-D side reactions of D-^{3}He plasmas by keeping the deuterons substantially colder than the helium ions. Futhermore, even if two ion species could be maintained with nearly monoenergetic velocity distributions (which they cannot, as shown in Chapter 3), the energies of the two species would have to be nearly equal; therefore the fusion reactivity $\langle \sigma v \rangle_{fus}$ would be averaged over all collision angles and would become essentially the Maxwellian-averaged quantity (to within 20% or so; see Appendix A for more details). This implies that one could not efficiently exploit the resonance peaks of fusion cross sections, such as the sharp peaks in the p-^{11}B cross section.

Chapter 6

Advanced Aneutronic Fuels

The three advanced aneutronic fuels which have been considered are ^{3}He-^{3}He, p-^{11}B, and p-^{6}Li. If it were possible to hold a plasma significantly out of thermodynamic equilibrium, one could greatly improve the performance of these three fuels over that which could be obtained if they were burned in thermodynamic equilibrium. The improvement in performance could be accomplished by decoupling the electron energy to lower the bremsstrahlung losses; the most effective method of decoupling the electrons would be to deplete most of the slow electrons which can drain energy from the ions. For the proton-based fuels, the performance could also be increased by decoupling the energies of the two ion species in the plasma, so that virtually all of the collisions between ions of the two species would occur at the optimum net collision velocity corresponding to the maximum fusion cross section.

Yet as has been shown in Chapters 3-5, to hold a plasma out of thermodynamic equilibrium in these ways would require prohibitively large amounts of recirculating power. It therefore becomes of interest to determine the best performance which can be obtained from each of these three advanced aneutronic fuels when they are burned in a plasma which is essentially in thermodynamic equilibrium. Chapter 1 presented a quick calculation of

the performance of equilibrium systems which use these fuels, but a more systematic analysis will now be performed. The analysis in this chapter will incorporate the results of Chapter 2 and optimize the net power production with respect to those parameters which can still be varied, such as the ion temperature and the fuel stoichiometry.

After some general remarks about the bremsstrahlung radiation loss calculations in Section 6.1, the remaining sections of this chapter will graphically illustrate the optimum performance of equilibrium ^{3}He-^{3}He, p-^{11}B, and p-^{6}Li systems.

6.1 Bremsstrahlung Radiation Losses

As was stated in Chapter 1, the bremsstrahlung losses have been evaluated by setting the ion-electron energy transfer rate, P_{ie}, equal to the bremsstrahlung power loss, P_{brem}, to find the equilibrium electron temperature. The bremsstrahlung losses caused by that electron temperature have been compared with the fusion power. In contrast with the results in Chapter 1, the calculations presented in this chapter also include the correction factor derived in Chapter 2. It is very important to note that these calculations are inherently optimistic, because in them the only source of energy to the electrons is Coulomb friction with the fuel ions. In more realistic systems, the electrons would also receive energy from external heating mechanisms, friction with the fusion products, etc., so the electron temperatures and bremsstrahlung losses would be even higher.

Of course, a realistic system would also have other losses, such as synchrotron radiation (see Appendix F) and particle losses, with which it would have to contend. Although it is true that these losses might help cool the electrons and lower the bremsstrahlung radiation power, that would simply be substituting one loss mechanism for another, so the incorporation of such losses into the calculations would not result in a better energy gain than is found here.

Because P_{ie} is proportional to the Coulomb logarithm, $\ln\Lambda$, there will be some dif-

ference in performance between reactor designs which have markedly different values for the Coulomb log. To illustrate the range of performance which might be expected, the calculations have been performed for the cases of $\ln \Lambda = 5$ (as in inertial confinement fusion [ICF] reactors) and $\ln \Lambda = 20$ (as in typical magnetic confinement fusion systems).

Reducing the Coulomb logarithm all the way down to $\ln \Lambda = 5$ improves the performance of the advanced fuels somewhat, but one should not be misled into optimism about achieving a net energy gain from any of these fuels via ICF. In the implosion of an ICF pellet, the electrons receive a considerable amount of energy in addition to energy they siphon from the ions, so the electron temperatures and bremsstrahlung losses of a realistic system would be substantially larger than those calculated here for the "ideal" case with $\ln \Lambda = 5$.

It is also necessary to realize that the importance of the bremsstrahlung power loss may actually be underestimated by simply considering the ratio P_{brem}/P_{fus}. It has recently been shown [99] that most proposed types of direct electric conversion schemes, such as electrostatic direct converters [100, 101], would not be suitable for directly converting the kinetic energy of charged fusion products into electricity. This unfortunate fact arises because of electrical arcing problems on the high-voltage conversion grids and also because confinement systems designed to let the fusion products escape will generally allow large numbers of the fuel ions and electrons to escape as well. Unless better methods of direct electric conversion can be found (such as the possibility of using traveling waves to convert the particle energy into electricity [102, 103, 104]), thermal conversion methods will have to be employed to convert the fusion power into electrical power.

For a reactor in which both the fusion power and the bremsstrahlung power are converted into electricity via thermal cycles with a typical efficiency of approximately 1/3, the net power loss due to bremsstrahlung will be $P_{loss} \approx (2/3)P_{brem}$. Similarly, the electrical power generated by the fusion reactions will be $P_{gen} \approx P_{fus}/3$. Therefore the net impact of the bremsstrahlung losses with respect to the electrical power generated by fusion will

be

$$\frac{P_{loss}}{P_{gen}} \approx 2\frac{P_{brem}}{P_{fus}} . \tag{6.1}$$

Thus unless the fusion power can be converted into electricity at very high efficiencies, the actual severity of the radiation losses will be approximately twice as high as one might be led to think by simply considering the ratio P_{brem}/P_{fus} which is calculated for various fuels in this chapter and Chapter 7.

In order to utilize nearly 100% of the fusion power, one might contemplate confining the fusion products enough that they could give essentially all of their energy to the fusion plasma. This technique would not be beneficial, though, since it would greatly increase the electron temperature and bremsstrahlung radiation losses in comparison with the results given in this chapter.

Preferential fusion product heating of ions (without heating the electrons) via nuclear elastic scattering [10, 55, 88, 89, 90, 91, 92] or other mechanisms does not improve these calculations; it is already assumed that the ion energy distribution is held fixed and that the *only* source of electron heating is Coulomb friction with ions. Furthermore, since the fusion reactivity is nearly independent of the ion velocity distribution shape for a given mean ion energy (as shown in Appendix A), enhancement of the fast tail of the ion distribution due to nuclear elastic scattering would not substantially alter the results given here.

For p-^{11}B and p-^{6}Li, one is free to vary the ratio of the two ion species in the plasma in order to minimize the relative severity of the bremsstrahlung losses in comparison with the fusion power. With the protons denoted as the $i1$ species and the boron or lithium ions designated as the $i2$ species, the fusion reaction rate per total number of electrons will be maximized for a fuel ratio $x \equiv n_{i1}/n_{i2} = Z_{i2}$ (see Eq. (1.3)). Provided that the effects of modest changes in the fuel ratio upon the equilibrium electron temperature and bremsstrahlung rate are not too severe, one would expect the ratio of bremsstrahlung

power to fusion power to be minimized near $x = Z_{i2}$, or $n_p/n_{B-11} = 5$ for p-^{11}B and $n_p/n_{Li-6} = 3$ for p-^{6}Li. This will be shown in fact to be the case.

6.2 ^{3}He-^{3}He

Pure ^{3}He has been proposed as the fuel for reactors based on the ^{3}He(^{3}He,2p)^{4}He reaction, which would release 12.9 MeV in energy. The main problem with this fuel is that the cross section for the reaction becomes significant only at very high ion temperatures ($T_i \sim 1$ MeV). At such ion temperatures, the electron temperature causes very large bremsstrahlung losses, as revealed in Figure 6-1. Cross section data was not available for $T_i > 1$ MeV, but as that temperature is approached, the bremsstrahlung loss is clearly leveling off at an intolerably large value. (Specifically, the bremsstrahlung losses for $T_i = 1$ MeV amount to $P_{brem}/P_{fus} = 1.56$ for $\ln\Lambda = 20$ and $P_{brem}/P_{fus} = 0.86$ for $\ln\Lambda = 5$.) Also, at $T_i = 1$ MeV, one is already putting 3 MeV of energy into each pair of ions in order to get 12.9 MeV of energy out of them when they react, so it would not be advisable to go to much higher ion temperatures.

Figure 6-2 graphically shows the equilibrium operating point at which the ion-electron energy transfer rate and bremsstrahlung loss power achieve a balance. Using this figure, one can see how much the electron temperature would have to lowered to bring the bremsstrahlung losses under control. As was discussed in Chapter 4, when T_e is low enough that bremsstrahlung losses are manageable, the ion-electron energy transfer rate is far too large to be counteracted by any known mechanism; this fact may also be seen from Figure 6-2.

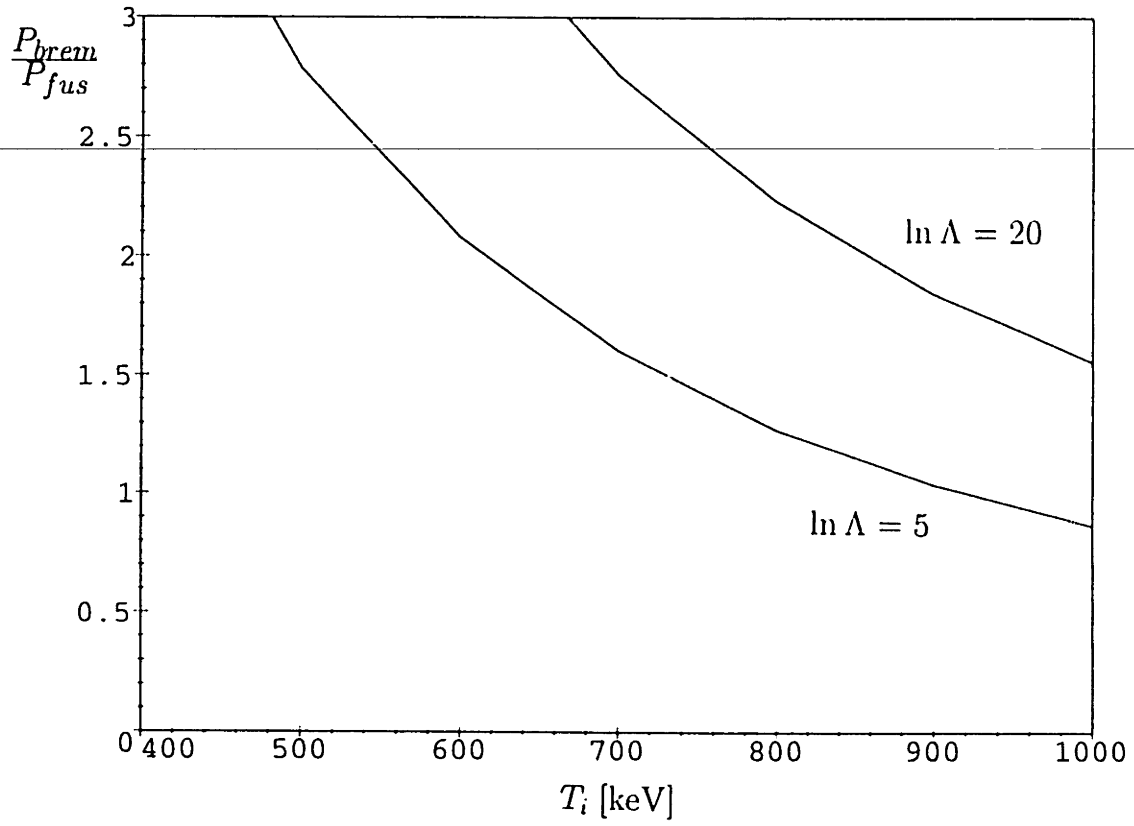

Figure 6-1: Ratio of bremsstrahlung losses to fusion power for ^{3}He-^{3}He with various ion temperatures. (T_e determined from energy balance equation, $P_{ie} = P_{brem}$.)

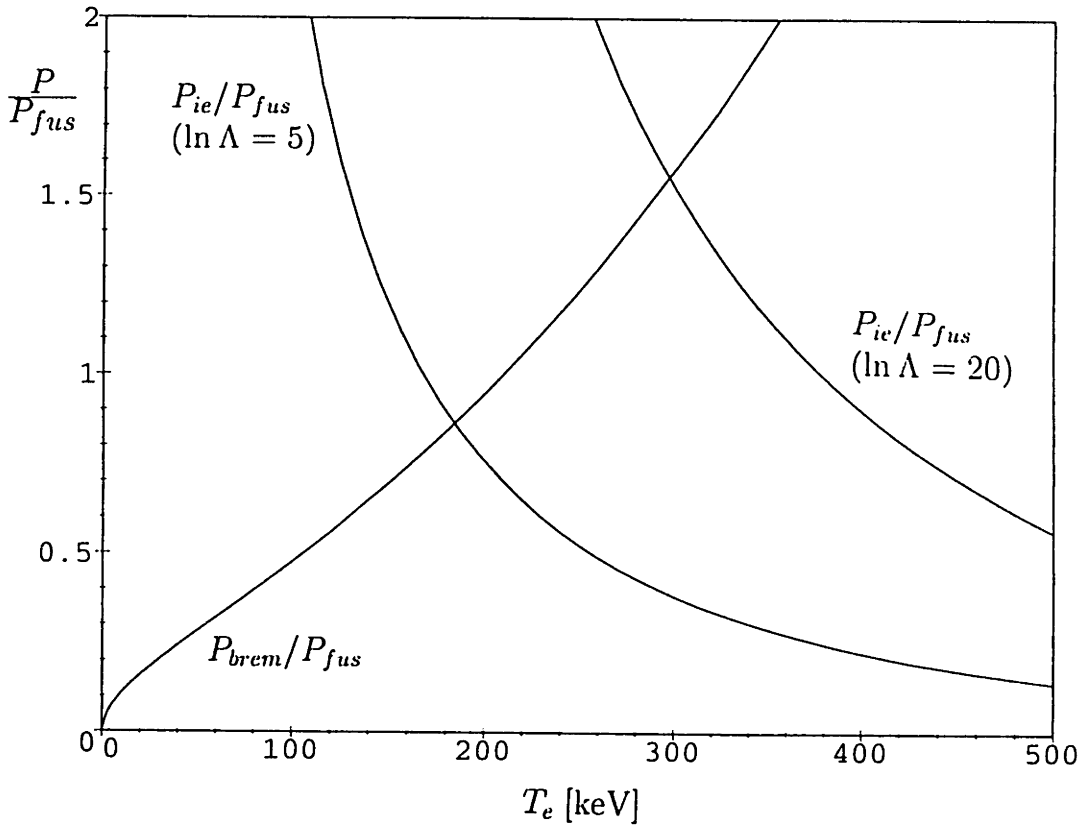

Figure 6-2: Ion-electron energy transfer and bremsstrahlung compared with fusion power for ^{3}He-^{3}He with various electron temperatures. (T_i = 1 MeV.)

6.3 p-^{11}B

Another long-time favorite candidate for advanced aneutronic fuel fusion reactors is the ^{11}B(p,2α)^{4}He reaction, which releases 8.7 MeV of energy.

As depicted in Figure 6-3, the performance is optimized for T_i between 300 keV and 400 keV, depending on the exact value of the Coulomb logarithm. The minimum bremsstrahlung loss fraction for $\ln\Lambda = 20$ occurs for $T_i = 300$ keV, at which point $P_{brem}/P_{fus} = 1.88$. For $\ln\Lambda = 5$, the minimum of $P_{brem}/P_{fus} = 1.20$ occurs at around $T_i = 400$ keV.

Figure 6-4 shows that when the fuel mixture is varied, the relative severity of the bremsstrahlung losses is indeed minimized for $n_p/n_{B-11} = 5$. Unfortunately, even at this optimum operating point, and even taking the very optimistic $\ln\Lambda = 5$ results, the bremsstrahlung loss power exceeds the fusion power.

Just as with the earlier figure for ^{3}He, the graphical depiction of the equilibrium between ion-electron energy transfer and bremsstrahlung radiation power shown in Figure 6-5 could be used to see how low T_e must be in order to limit the bremsstrahlung loss to a bearable value. The figure demonstrates that the ion-electron energy transfer for such low electron temperatures would be far in excess of the fusion power.

6.4 p-^{6}Li

The ^{6}Li(p,^{3}He)^{4}He reaction would produce approximately 4.0 MeV of energy. Because of this low energy output per reaction, the unimpressive cross section of the reaction, and the high temperatures that are required, p-^{6}Li cannot even begin to approach break-even. Although the product ^{3}He could be used to generate additional energy through reactions with the ^{6}Li or with added deuterons, even this measure would not enable break-even against realistic losses. This fact may be seen by assuming complete burnup of the ^{3}He

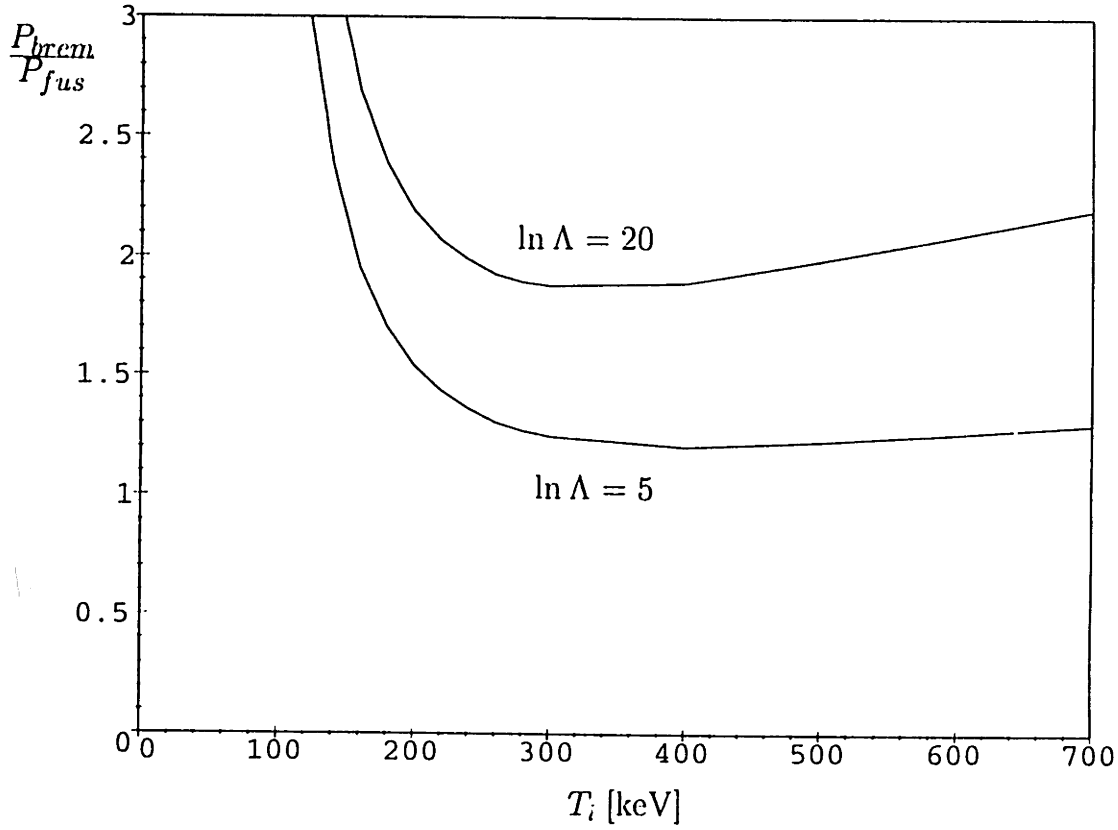

Figure 6-3: Ratio of bremsstrahlung losses to fusion power for p-^{11}B with various ion temperatures. (T_e determined from $P_{ie} = P_{brem}$; $n_p/n_{B-11} = 5$.)

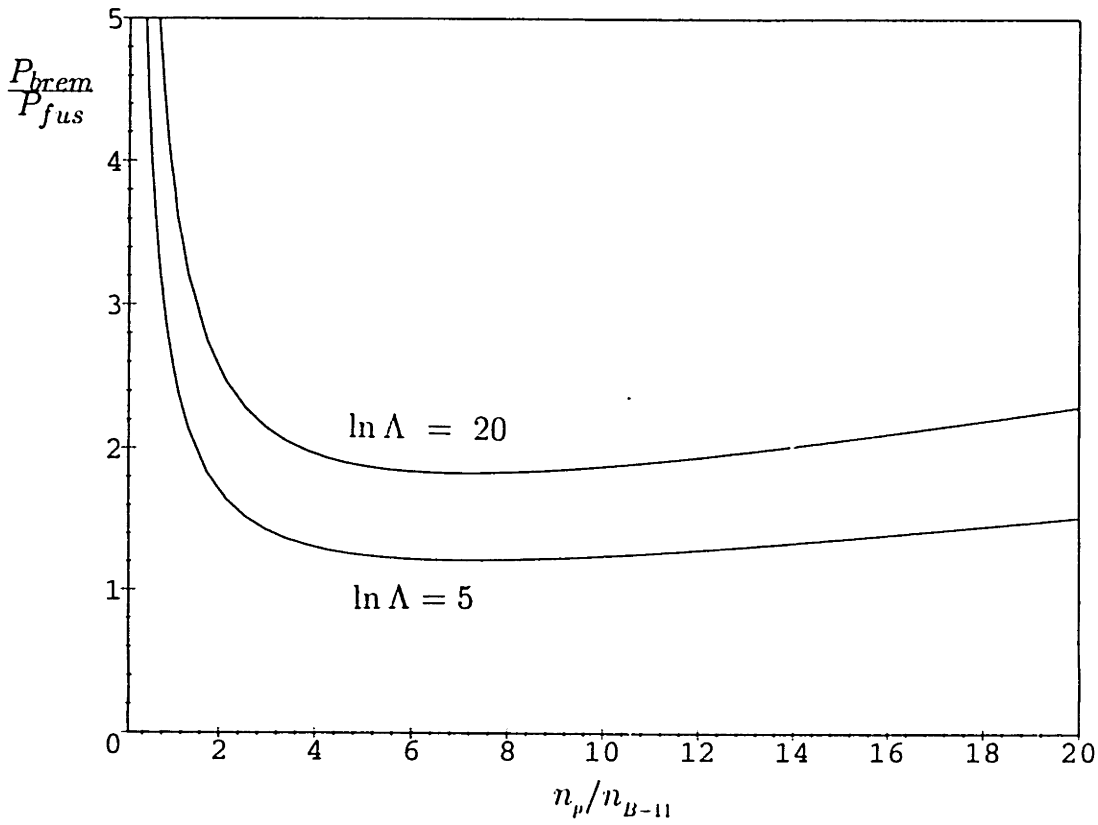

Figure 6-4: Ratio of bremsstrahlung losses to fusion power for p-^{11}B with various fuel mixtures. (T_i = 300 keV; T_e determined from $P_{ie} = P_{brem}$.)

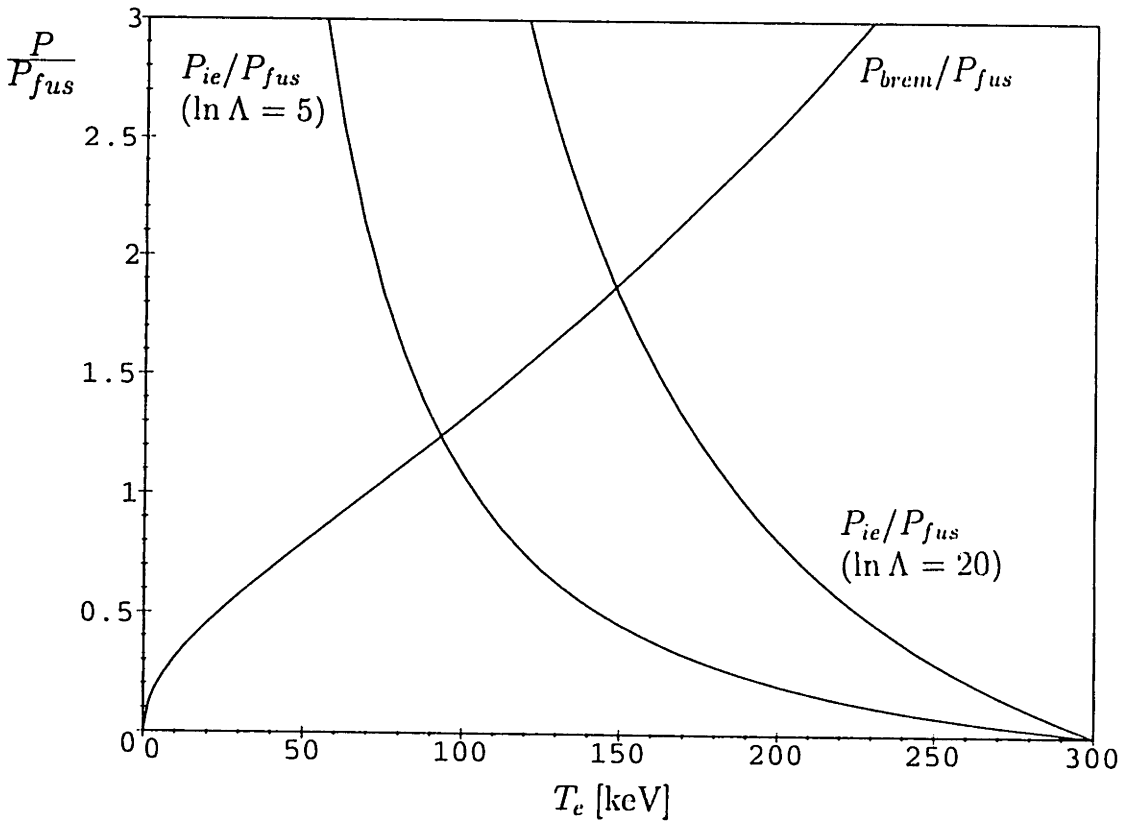

Figure 6-5: Ion-electron energy transfer and bremsstrahlung compared with fusion power for p-^{11}B with various electron temperatures. ($T_i = 300$ keV; $n_p/n_{B-11} = 5$.)

with exogenous deuterons (to release an additional 18.3 MeV of energy per reaction) and optimistically assuming that there are no further power losses attendant in such schemes. The values of P_{brem}/P_{fus} which are calculated here would then have to be multiplied by a factor of (4.0 MeV)/(4.0 MeV + 18.3 MeV)$\approx$ 0.18. The bremsstrahlung losses would still be comparable to the fusion power, even in this very idealized case.

The outlook for p-^{6}Li is illustrated in the graphs. Figure 6-6 shows that the optimum ion temperature is around 800 keV, and Figure 6-7 confirms that the optimum fuel mixture is in the vicinity of $n_p/n_{Li-6} = 3$, but even at these optimum parameters the bremsstrahlung loss power is several times the fusion power. To cite specific numbers, the minimum of the $\ln\Lambda = 20$ curve in Figure 6-6 is $P_{brem}/P_{fus} = 5.36$ and occurs at $T_i = 800$ keV; the $\ln\Lambda = 5$ curve levels off at a value of $P_{brem}/P_{fus} = 3.00$ at $T_i = 1$ MeV.

In agreement with the results for the other advanced aneutronic fuels, if the electron temperature is kept low enough to limit the bremsstrahlung losses to reasonable levels, the ion-electron energy transfer will be far greater than the fusion power, as demonstrated in Figure 6-8.

6.5 Summary

The outlook for the advanced aneutronic fuels is best summarized in Figure 6-9. In order to limit the bremsstrahlung losses to theoretically bearable levels (less than half the fusion power), it would be necessary to reduce the ion-electron energy transfer rate by at least one order of magnitude for ^{3}He-^{3}He, two orders of magnitude for p-^{11}B, and three orders of magnitude for p-^{6}Li. Chapter 4 surveyed all known techniques for reducing the ion-electron energy transfer or otherwise circumventing this problem, and no useful methods were found. Furthermore, it is not possible to alleviate the bremsstrahlung losses for the proton-based fuels by decoupling the energies of the two ion species in the plasma and thereby boosting the fusion rate; the failure of such approaches was discussed in Chapter 5. Even if feasible techniques are eventually found, it is very unlikely that they will work

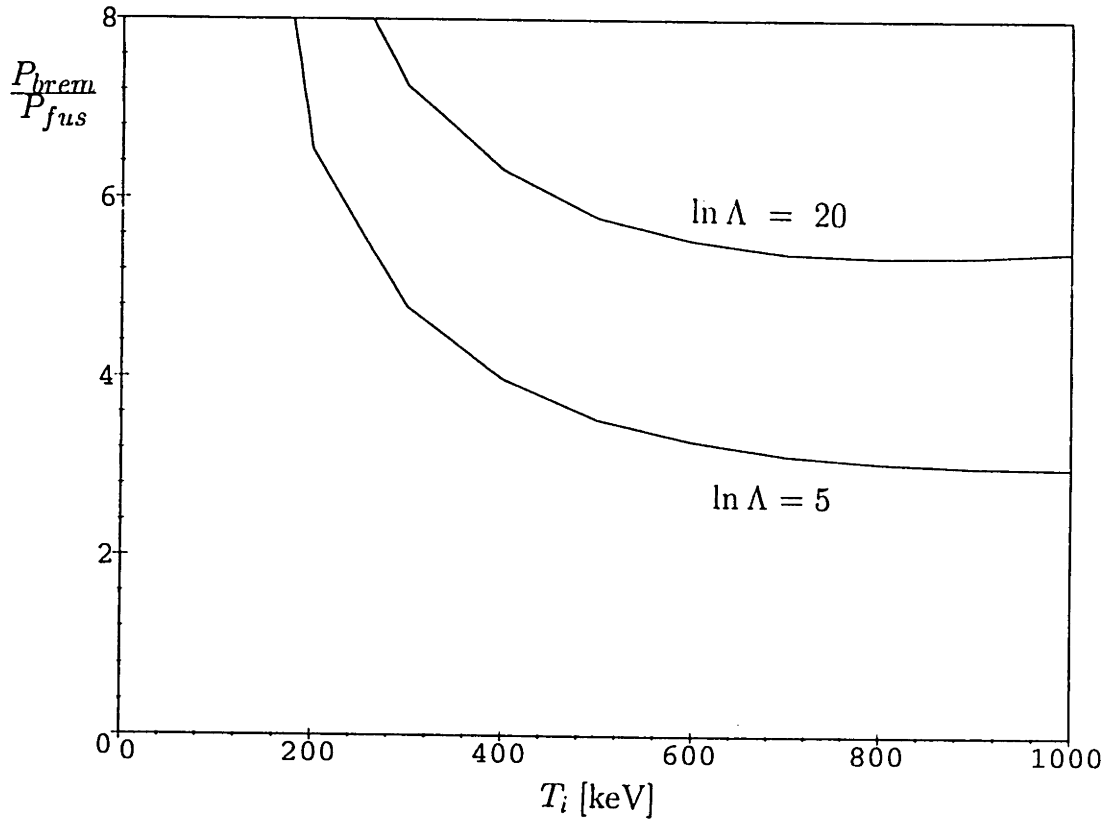

Figure 6-6: Ratio of bremsstrahlung losses to fusion power for p-^{6}Li with various ion temperatures. (T_e determined from $P_{ie} = P_{brem}$; $n_p/n_{Li-6} = 3$.)

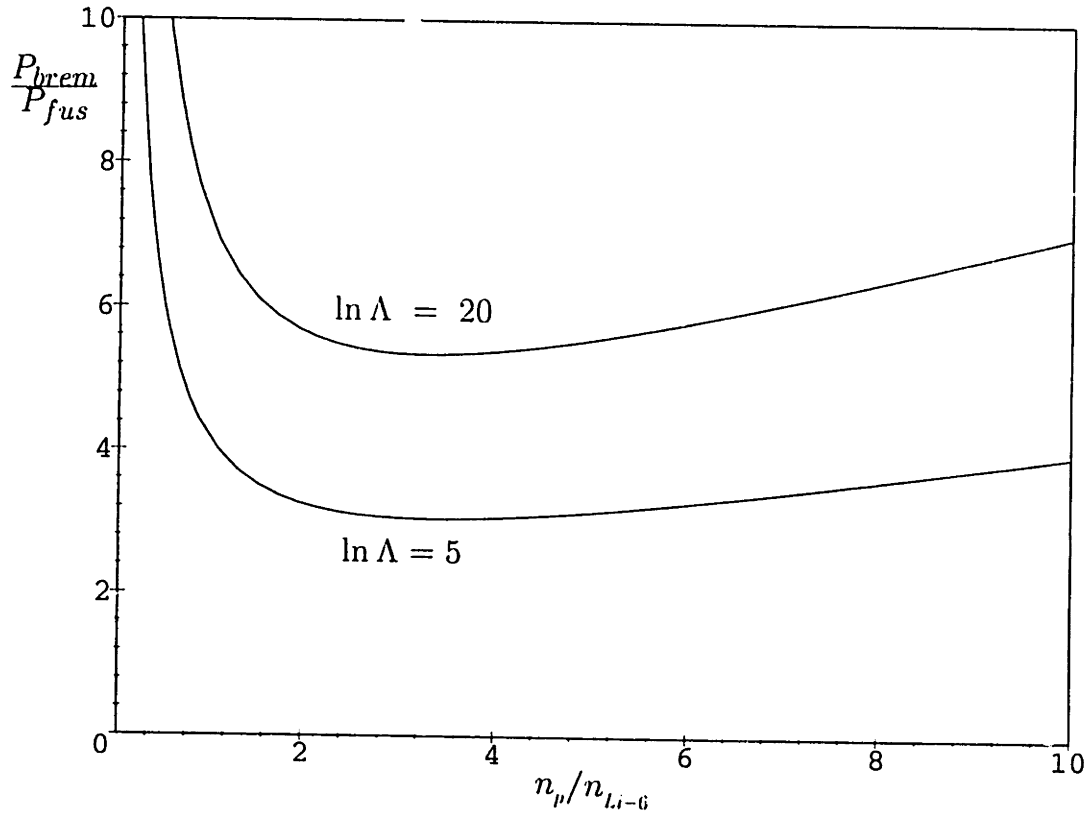

Figure 6-7: Ratio of bremsstrahlung losses to fusion power for p-^{6}Li with various fuel mixtures. (T_i = 800 keV; T_e determined from $P_{ie} = P_{brem}$.)

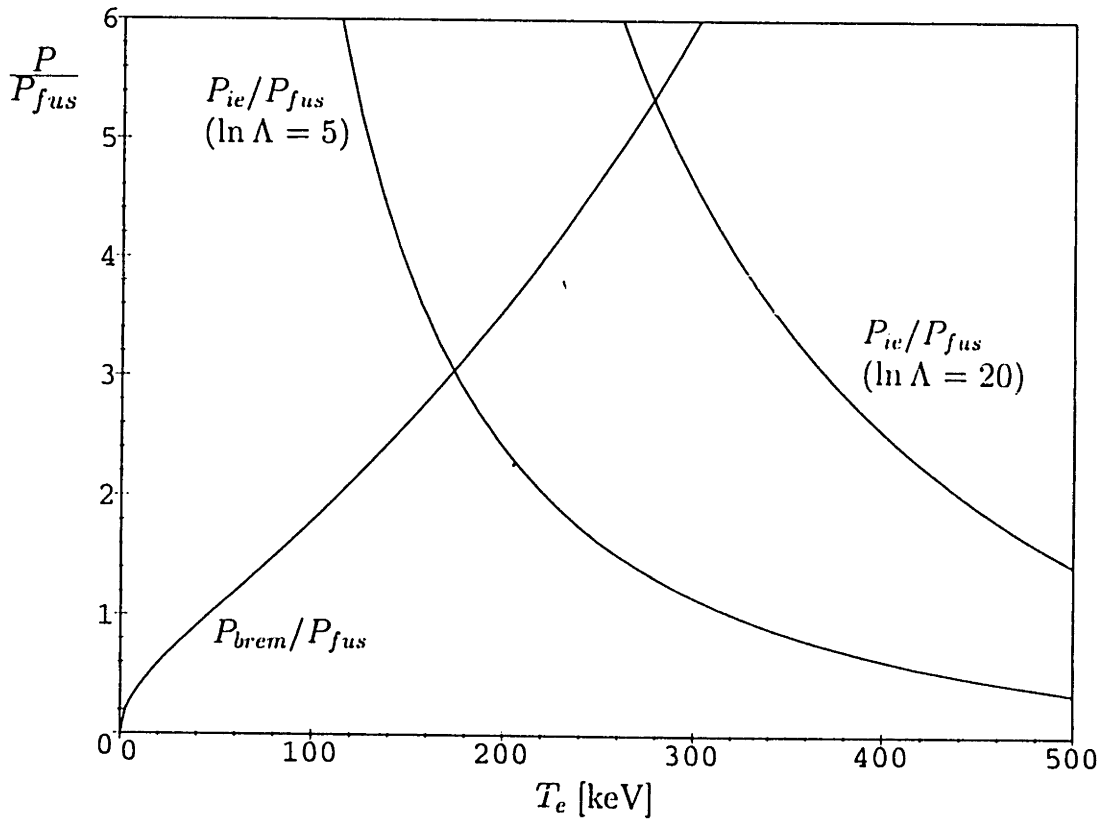

Figure 6-8: Ion-electron energy transfer and bremsstrahlung compared with fusion power for p-^{6}Li with various electron temperatures. (T_i = 800 keV; $n_p/n_{Li-6} = 3$.)

well enough to lower the energy transfer rate as drastically as is required. Therefore, it appears highly doubtful that the advanced aneutronic fuels can ever serve as the basis for power-producing reactors.

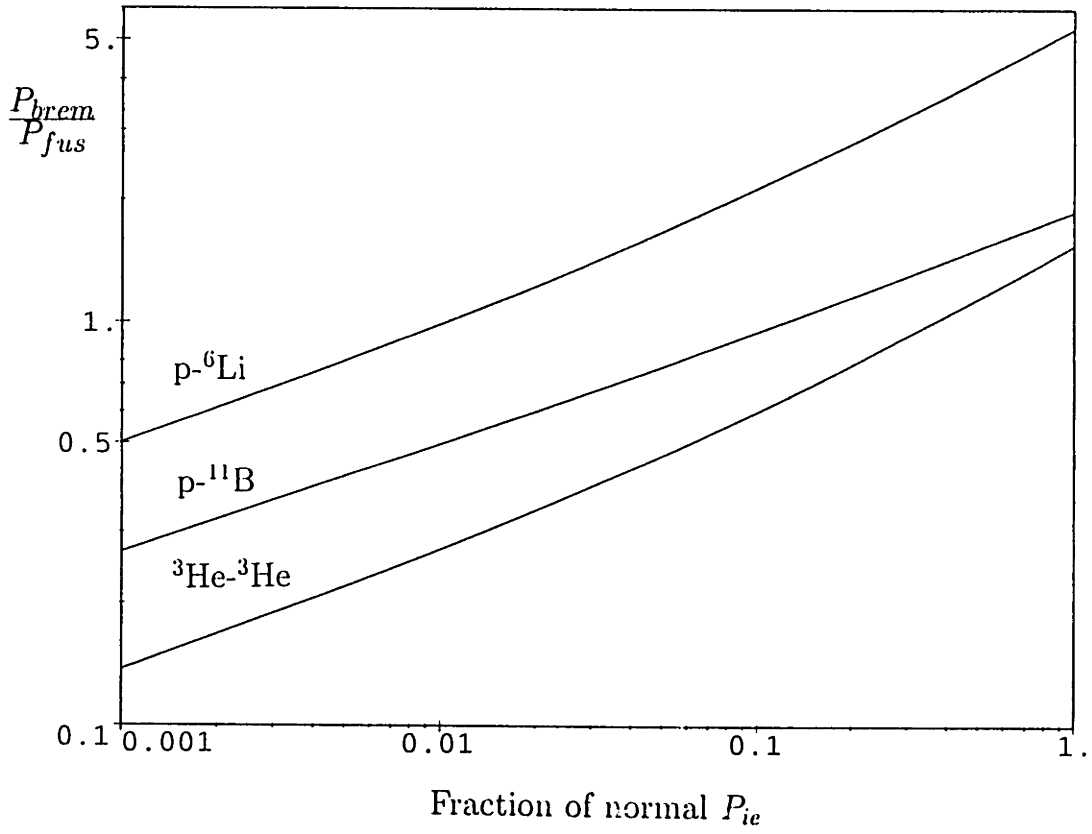

Figure 6-9: Ratio of bremsstrahlung losses to fusion power versus the necessary reduction of ion-electron energy transfer for ^{3}He-^{3}He, p-^{11}B, and p-^{6}Li plasmas under approximately optimum conditions (T_i = 1 MeV for ^{3}He-^{3}He, 300 keV for p-^{11}B [with a 5:1 fuel mixture], and 800 keV for p-^{6}Li [with a 3:1 fuel mixture]; $\ln \Lambda = 20$ throughout.)

Chapter 7

Reduction of D-D Side Reactions from D-^{3}He Plasmas

If one were able to maintain a significantly nonequilibrium plasma, it might be possible to operate D-^{3}He reactors with substantially fewer D-D reactions (and hence neutrons and tritium) than reactors employing equilibrium plasmas would have. This reduction in D-D reactions could be accomplished by decoupling the electron energy to lower the bremsstrahlung losses and permit net power production with more ^{3}He-rich fuel mixtures or by decoupling the two ion species so that the deuterons could be kept at very low energies. Yet to accomplish either of these tasks would require prohibitively large amounts of recirculating power, as the previous chapters have shown. It therefore becomes of interest to determine the maximum extent to which the D-D reactions and their consequences (the production of neutrons and tritium) can be suppressed in a plasma which is in thermodynamic equilibrium.

After examining in Section 7.1 the best performance which can be obtained from D-^{3}He reactors, Section 7.2 will give the results of similar analyses for D-D and D-T reactors, for the purpose of comparison.

As with the results in Chapter 6, the $\ln \Lambda = 5$ results are inherently quite optimistic, since the only source of heat to the electrons is collisional friction with the ions. The electrons in realistic ICF plasmas would experience a great deal of additional heating during the implosion process, so T_e and P_{brem} would be substantially larger than the values which have been calculated here. Thus these results serve to set a lower bound on the power losses.

Although the results in this chapter are expressed in terms of the ratio P_{brem}/P_{fus}, one should also recall the point made in Chapter 6 regarding the importance of bremsstrahlung losses in reactors which use thermal cycles to convert the fusion power into electrical power. If the fusion product energy and bremsstrahlung radiation are converted into electricity by thermal cycles with efficiencies of approximately 1/3, the ratio of the net radiation loss power to the fusion-generated electrical power will be $P_{loss}/P_{gen} \approx 2P_{brem}/P_{fus}$.

Preferential fusion product heating of ions (without heating the electrons) via nuclear elastic scattering [10, 88, 89, 90] or other mechanisms does not improve these calculations; it is already assumed that the ion energy distribution is held fixed and that the *only* source of electron heating is Coulomb friction with ions. Furthermore, since the fusion reactivity is nearly independent of the ion velocity distribution shape for a given mean ion energy (as shown in Appendix A), enhancement of the fast tail of the ion distribution due to nuclear elastic scattering would not substantially alter the results given here.

7.1 Results for Equilibrium D-^{3}He Plasmas

Although one is constrained to operate with plasmas which are essentially in thermodynamic equilibrium, at least theoretically one still has the luxury of removing the reaction products before they undergo further reactions. This choice leads to D-^{3}He reactors which operate with or without burnup of the tritium produced via D-D reactions; these two types of reactor designs will be considered separately below.

While D-D reactions and the burnup of D-D reaction products would create a sizeable number of neutrons, they would add comparatively little to the total fusion reactor power, and so the bremsstrahlung power loss fraction is not greatly altered if only D-^{3}He fusion power is considered. Therefore, for simplicity in all of the D-^{3}He graphs, P_{brem}/P_{fus} has been computed by considering only D-^{3}He fusion power. (In computing neutron power fractions, however, all reactions are in fact taken into account.)

7.1.1 No Tritium Burnup

It is assumed that all of the tritium produced by D-D reactions is removed from the plasma before it has a chance to react with the deuterons. The T could be stored in a "wine cellar" and allowed to decay into ^{3}He for future use in the reactor. This method offers the advantage that there would be no 14 MeV D-T neutrons produced in the reactor, so the neutron power would represent a much smaller fraction of the total fusion power than it otherwise would.

There are several ways in which the tritium removal might be accomplished, since the tritons would have an energy of 1.0 MeV, far greater than the 150 keV mean energy of fuel ions if $T_i = 100$ keV. One method would be fairly similar to the migma configuration with a ring magnet [25, 39]; a properly designed magnetic field configuration can theoretically cause the orbits of particles within specific energy ranges to be unstable, leading to the ejection of the particles from the confinement system. Another technique would be to use electrostatic confinement [18] with a well depth that traps the fuel ions but allows the fusion products, including tritons, to escape; separate means of confining the electrons would also have to be present, of course. One might also devise other methods as well.

Bremsstrahlung and Neutron Power Fractions

Figure 7-1 indicates that the ratio of bremsstrahlung power to fusion power is minimized for T_i between 100 keV and 150 keV, depending on the exact value of $\ln \Lambda$. In particular,

for $\ln \Lambda = 20$ the minimum of $P_{brem}/P_{fus} = 18\%$ occurs at $T_i = 140$ keV, and for $\ln \Lambda = 5$ the minimum is $P_{brem}/P_{fus} = 13\%$ and occurs at $T_i = 160$ keV.

Assuming that there is no burnup of the D-D reaction products (T and ^{3}He), the fraction of the total power which is produced as neutron kinetic energy may be found from the equation,

$$\left(\frac{P_{neutrons}}{P_{fus}}\right)_{\text{no T burnup}} = \left[(1/2)n_D^2 \langle\sigma v\rangle_{D+D\rightarrow n\,+\,He-3}(2.45\text{ MeV})\right] \times \left\{n_D n_{He-3}\langle\sigma v\rangle_{D\,+\,He-3}(18.3\text{ MeV}) + (1/2)n_D^2\left[\langle\sigma v\rangle_{D+D\rightarrow n\,+\,He-3}(3.27\text{ MeV}) + \langle\sigma v\rangle_{D+D\rightarrow T+p}(4.03\text{ MeV})\right]\right\}^{-1} . \tag{7.1}$$

As shown in Figure 7-2, the neutron power fraction is minimized near the same temperature as the bremsstrahlung loss fraction, specifically reaching a minimum of $P_{neutrons}/P_{fus} = 1.1\%$ for $T_i = 100$ keV.

Clearly the neutrons can be reduced by burning with an excess of ^{3}He, but the problem is that then the bremsstrahlung losses will increase, since the fusion power density falls and the effective Z of the plasma rises. Figure 7-3 illustrates this trade-off. If one makes the restriction $P_{brem}/P_{fus} \leq 0.5$, the maximum allowable fuel ratio is $n_{He-3}/n_D \approx 5$, at which point the neutrons constitute about 0.2% of the total power, or roughly one order of magnitude smaller than in a fission reactor. More realistically, bremsstrahlung losses would almost certainly have to be kept much lower, and it is doubtful that the reactor could produce net power under conditions where the D-D neutrons would constitute much less than 1% of the total power.

The effect of electron temperature on ion-electron energy transfer and bremsstrahlung losses is shown in Figure 7-4. It may be seen from the figure that if the electrons were actively refrigerated to a temperature substantially below their equilibrium value, the interspecies energy transfer rate (and necessary recirculating power) would become quite

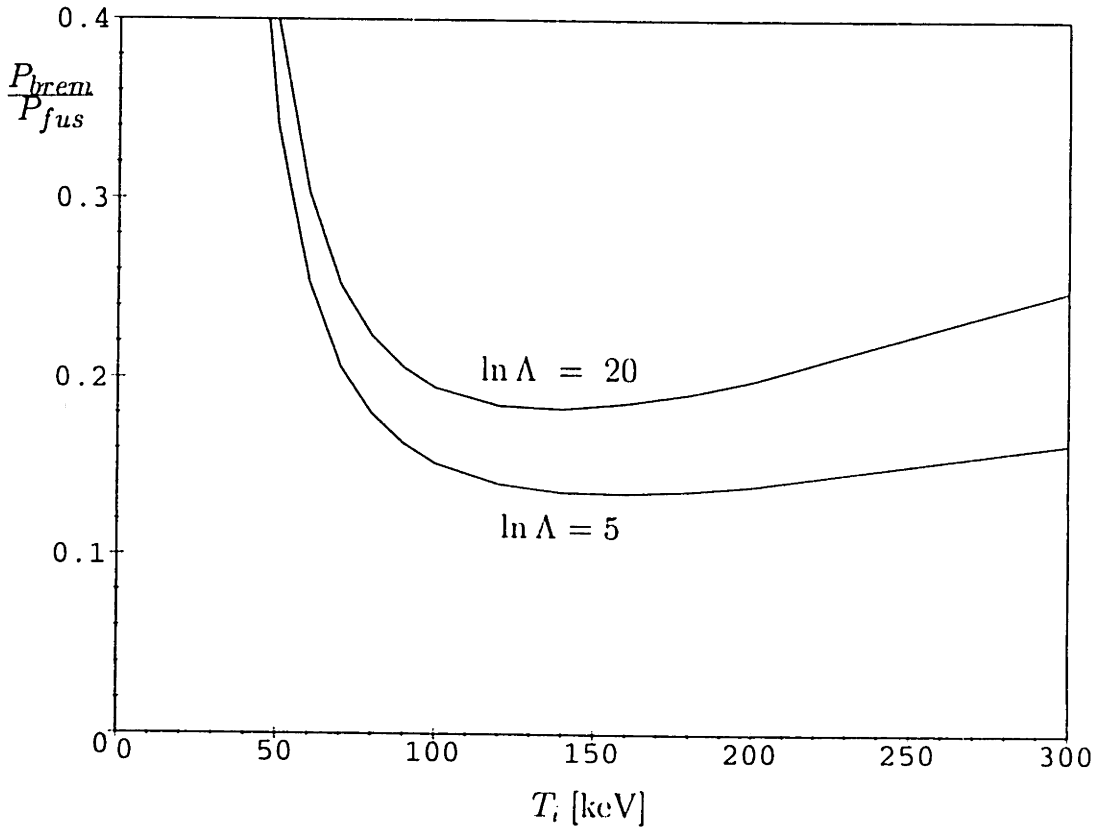

Figure 7-1: Bremsstrahlung power loss fraction for D-^{3}He with various ion temperatures. (T_e determined from $P_{ie} = P_{brem}$; $n_D/n_{He-3} = 1$.)

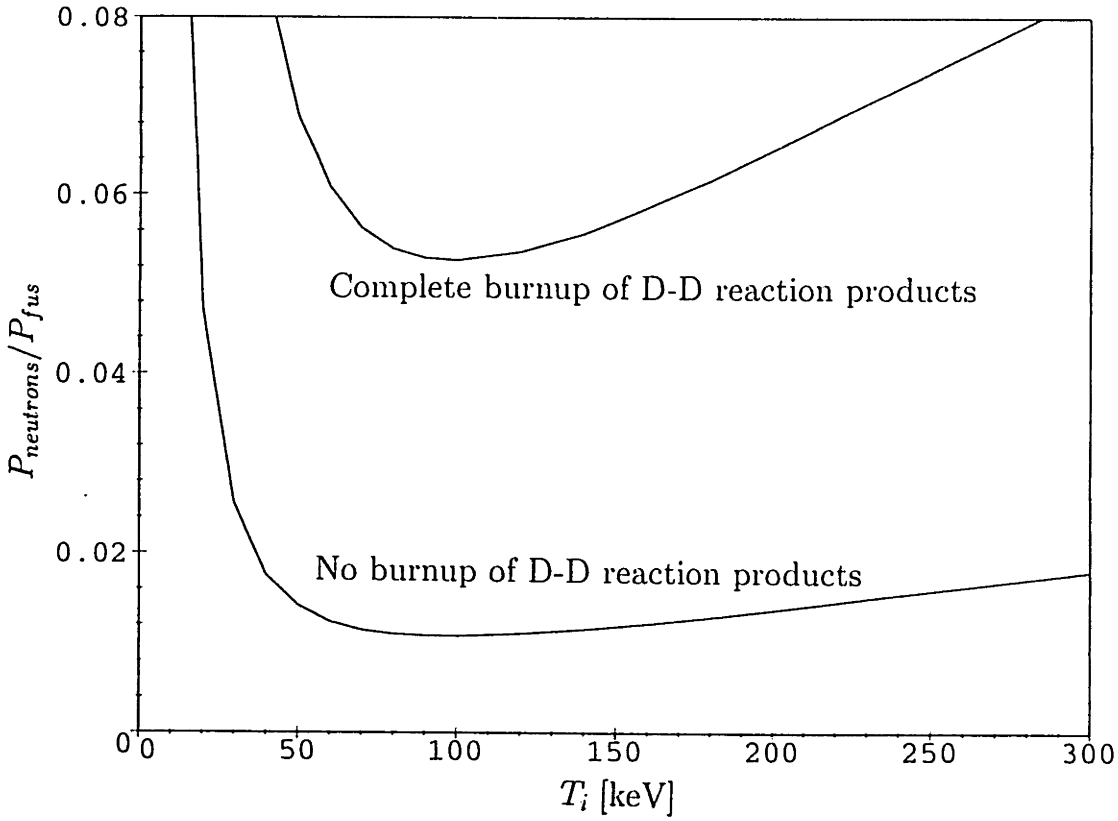

Figure 7-2: Neutron power fraction for D-^{3}He with various ion temperatures. (T_e determined from $P_{ie} = P_{brem}$; $n_D/n_{He-3} = 1$.)

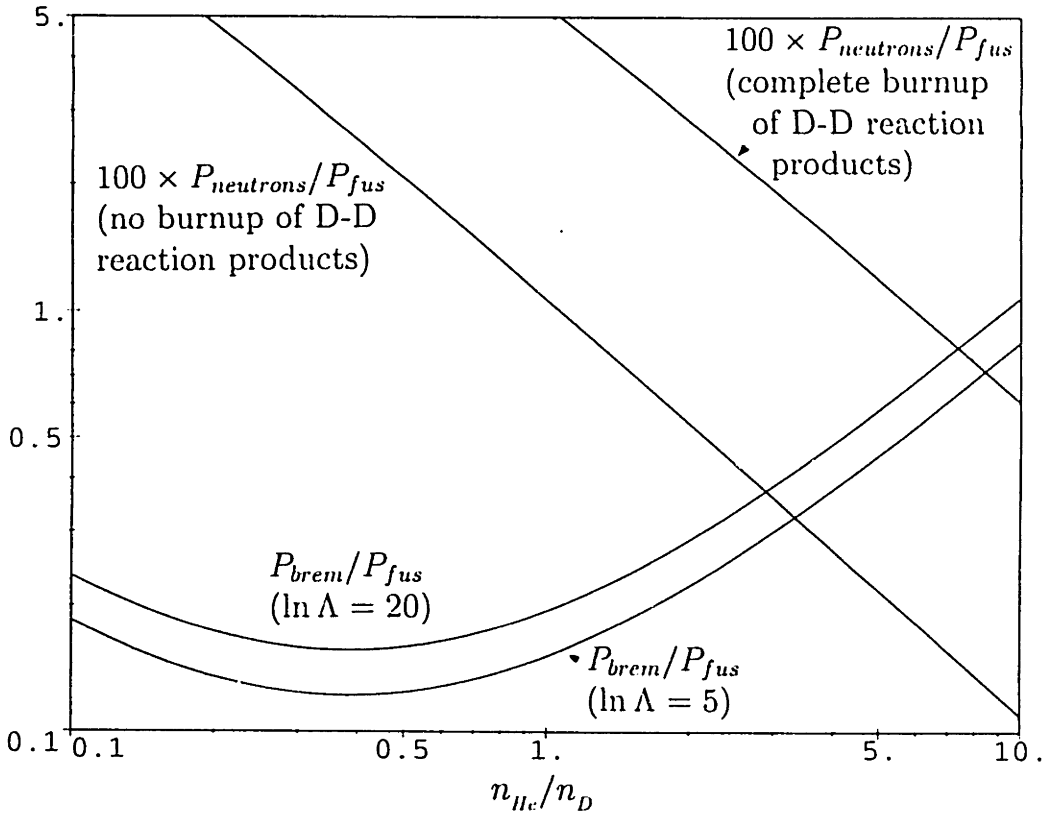

Figure 7-3: Bremsstrahlung power loss fraction and neutron power fraction for D-^{3}He with various fuel mixtures. (T_i = 100 keV; T_e determined from $P_{ie} = P_{brem}$.)

large; this observation confirms the findings discussed in Chapter 4.

Steady-State Tritium Inventory

The steady-state tritium inventory of the reactor may be calculated by noting that the rate of tritium production from D-D side reactions must balance the rate of tritium decay into ^{3}He. Assuming that the reactor is in operation for a fraction η of the time (due to down time for repairs, refueling, etc.), the time-averaged tritium production rate will be

$$\left(\frac{dn_T}{dt}\right)_{production} = \frac{1}{2} n_D^2 \eta \langle \sigma v \rangle_{D+D \rightarrow T+p} \ . \tag{7.2}$$

The tritium decay rate will be

$$\left(\frac{dn_T}{dt}\right)_{decay} = \frac{n_T}{\tau} \ , \tag{7.3}$$

where the base-e time constant τ may be found from the half-life $\tau_{1/2}$, $\tau = \tau_{1/2}/\ln 2 = 5.60 \cdot 10^8$ sec (since $\tau_{1/2} = 12.3$ years).

Thus for the operation of a D-^{3}He reactor with a plasma volume of V, the steady-state number of tritium atoms will be

$$N_T = \frac{1}{2} \eta \tau V n_D^2 \langle \sigma v \rangle_{D+D \rightarrow T+p} \ . \tag{7.4}$$

Neglecting the relatively small amount of D-D fusion power in comparison with the D-^{3}He fusion power, the total power produced by the reactor will be

$$P_{fus} = n_D n_{He-3} \langle \sigma v \rangle_{D\,+\,He-3} V (18.3 \cdot 10^6)(1.6022 \cdot 10^{-19}) \text{ Watts}, \tag{7.5}$$

so the steady-state total mass of tritium per GW of total reactor power can be expressed

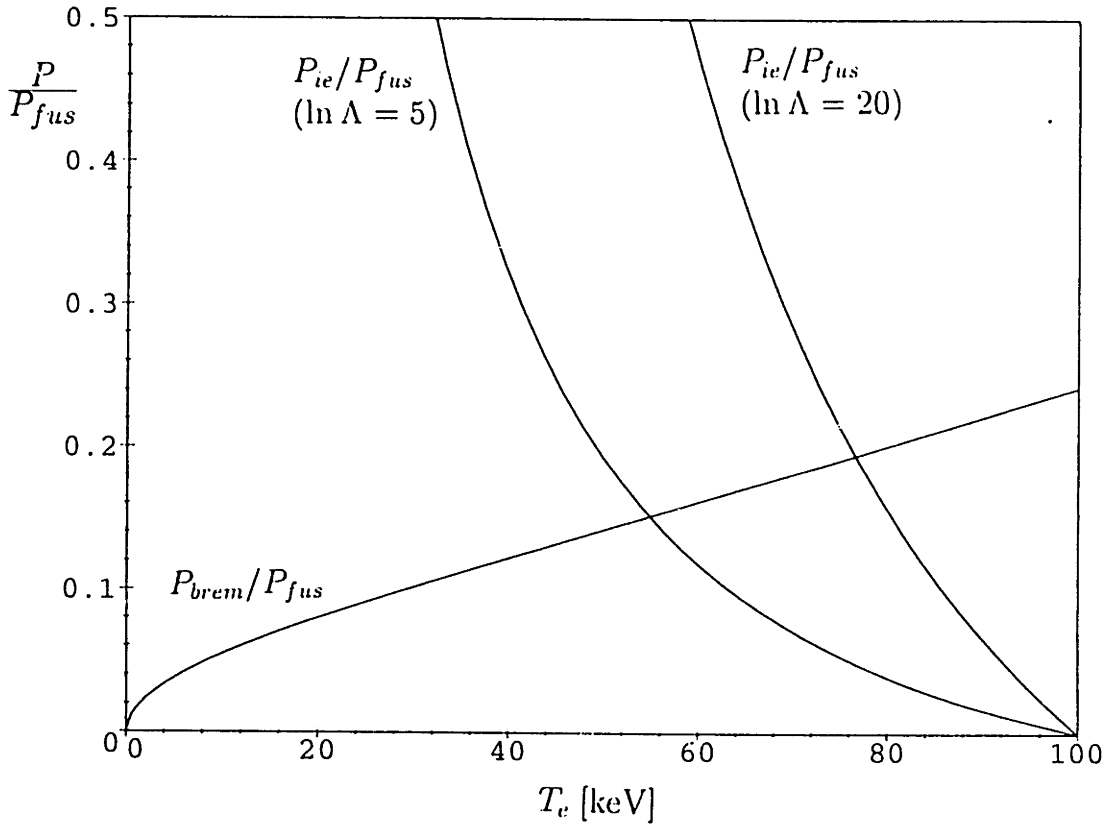

Figure 7-4: Ion-electron energy transfer and bremsstrahlung compared with fusion power for D-^{3}He with various electron temperatures. (T_i = 100 keV; $n_D/n_{He-3} = 1$.)

as

$$M_T = 478\eta \frac{n_D}{n_{He-3}} \frac{\langle \sigma v \rangle_{D+D \rightarrow T+p}}{\langle \sigma v \rangle_{D+He-3}} \frac{\text{kg tritium}}{\text{GW}_t} . \quad (7.6)$$

For $T_i = 100$ keV, $\langle \sigma v \rangle_{D+D \rightarrow T+p} / \langle \sigma v \rangle_{D+He-3} \approx 0.13$ [33]. Taking realistic power losses and conversion efficiency limitations into account, it seems highly probably that a D-^{3}He reactor which produces 1 GW_e of net electrical power would have to have a total power of at least 3 GW_t.

For a 3 GW_t reactor operating essentially full-time ($\eta \approx 1$), one finds that in the steady-state there will be about 190 kg of tritium, or about $1.8 \cdot 10^9$ Curies of radioactivity. While the reactor may not actually be operating 100% of the time, if it is to "earn its keep" for the electric utility company which operates it, the reactor will almost certainly be in operation for the majority of the time ($\eta \geq 0.5$), so the tritium levels will be at least half of the values just quoted for full-time operation. It is important to realize that these levels of radioactivity are only one order of magnitude smaller than those found in a fission reactor core shortly after shutdown [24], and yet only the tritium has been taken into account. Other sources of radioactivity in the D-^{3}He reactor (wall activation, etc.) would also have to be considered in evaluating the total radioactive inventory of the reactor. (Of course, the tritium would at least have the advantage that once the reactor was permanently decommissioned, its levels would decay far more rapidly than those of many of the radionuclides found in a fission core.) The presence of such large amounts of tritium would also pose a serious proliferation hazard.

Clearly the tritium levels in this type of reactor are far higher than one would like, but the alternative of burning the tritium to produce 14 MeV neutrons which will degrade and activate the reactor structure does not appear to be particularly attractive either.

7.1.2 Complete Tritium Burnup

In the calculations above, it was assumed that none of the tritium was burned up in the plasma. An estimate of the opposite case, in which all of the tritium is burned up, will serve to illustrate how much larger the neutron power fraction might be.

D-D reactions can directly produce either 2.45 MeV neutrons or tritium; if each triton is reacted with another deuteron it will yield a 14.1 MeV neutron. Therefore, the fraction of the total power which is produced as neutron kinetic energy if there is complete burnup of the produced T (and ^{3}He) is

$$\left(\frac{P_{neutrons}}{P_{fus}}\right)_{\text{complete T burnup}} =$$
$$\left\{(1/2)n_D^2\left[\langle\sigma v\rangle_{D+D\rightarrow n\,+\,He-3}(2.45\text{ MeV}) + \langle\sigma v\rangle_{D+D\rightarrow T+p}(14.1\text{ MeV})\right]\right\}$$
$$\times\left\{(1/2)n_D^2\left[\langle\sigma v\rangle_{D+D\rightarrow n\,+\,He-3}(3.27+18.3)\text{MeV} + \langle\sigma v\rangle_{D+D\rightarrow T+p}(4.03+17.6)\text{MeV}\right]\right.$$
$$\left.+n_D n_{He-3}\langle\sigma v\rangle_{D\,+\,He-3}(18.3\text{ MeV})\right\}^{-1}. \qquad (7.7)$$

Because the average reactivities for the two possible D-D reactions are nearly equal and because D-^{3}He reactions will still produce the majority of the total power, one may estimate the neutron power fraction with complete tritium burnup as

$$\left(\frac{P_{neutrons}}{P_{fus}}\right)_{\text{complete T burnup}} \approx \frac{(14.1\text{ MeV} + 2.45\text{ MeV})}{2.45\text{ MeV}}\left(\frac{P_{neutrons}}{P_{fus}}\right)_{\text{no T burnup}}$$
$$\approx 7\left(\frac{P_{neutrons}}{P_{fus}}\right)_{\text{no T burnup}}. \qquad (7.8)$$

Thus if the tritium is not promptly removed from the plasma, the neutron power fraction could be up to seven times larger than the values found without tritium burnup.

More precise calculations of the neutron production from D-^{3}He plasmas in which all of the tritium (and also ^{3}He) resulting from D-D reactions is burned up were performed by using the full form of Eq. (7.7), and the results are presented as additional curves in

Figures 7-2 and 7-3. Specifically, for complete burnup of the D-D reaction products, the minimum neutron power fraction occurs for $T_i = 100$ keV, at which point $P_{neutrons}/P_{fus} =$ 5.3% for a 1:1 fuel mixture. The neutron production could be reduced by changing to a more ^{3}He-rich fuel mixture, but then the bremsstrahlung power loss fraction would increase, as has already been discussed.

For a full-size power reactor with a total power of 3 GW_t, a 5.3% neutron power fraction would represent 160 MW of neutron power, most of which would be in the form of very destructive 14.1-MeV neutrons. If the reactor is made to be large so that the neutron power will be spread out over a large wall area, the power density will be very low, and consequently (because of the sophistication and "price per cubic meter" of the hardware components) the reactor will not be particularly attractive in economic terms. On the other hand, if the reactor is designed to have a fairly high power density, the extensive neutron damage to the first wall and other inner components of the reactor will necessitate frequent replacement of many of the key reactor components. Because these inner components will be highly radioactive, technologically very sophisticated, and possibly quite difficult to access from the outside of the reactor, the costs will again be very high. It is unclear at present whether a "happy medium" between these two extremes can be found, and if so then what particular reactor design would embody those optimum qualities.

7.2 Comparison with Results for D-D and D-T

For the purpose of comparison with the other graphs presented in this chapter and in the previous one, the bremsstrahlung calculations have also been performed for D-D and D-T reactors.

7.2.1 D-D

As shown in Figure 7-5, the bremsstrahlung losses in pure D-D reactors would be quite sizeable. For $\ln \Lambda = 20$, the losses reach a minimum of $P_{brem}/P_{fus} = 39\%$; this minimum is quite broad and flat and extends from $T_i = 300$ keV up to $T_i = 600$ keV. The minimum bremsstrahlung power loss fraction for $\ln \Lambda = 5$ is $P_{brem}/P_{fus} = 23\%$, which occurs over the broad range $T_i = 500 - 1000$ keV. As was stated in Table 1.1, without the burnup of the D-D reaction products, the neutron power fraction for D-D is $P_{neutrons}/P_{fus} = 0.36$.

The energy gain could be improved considerably by burning the tritium and helium-3 produced by the D-D reactions, but burnup of the tritium would cause a large increase in the neutron power fraction (and the added 14-MeV neutrons would be much more of a problem than the 2.45-MeV D-D neutrons).

For these reasons, if one seriously wanted to build an attractive D-D fusion reactor, it would be desirable to make do without tritium burning by lowering the electron temperature and bremsstrahlung losses. Figure 7-6 indicates how low the electron temperature would have to be in order to reduce the bremsstrahlung losses by a certain amount. As with all of the other fuels which have been analyzed so far, a reduction in the electron temperature large enough to be truly useful would produce a power flow from the ions to the electrons comparable to or greater than the fusion power.

7.2.2 D-T

Figure 7-7 makes it clear why the fusion research program has concentrated on D-T fuel despite all of its shortcomings in terms of radioactivity and neutron production. The power-producing capability of D-T is staggeringly large in comparison with that of all the other fuels, and it achieves this performance at far lower ion temperatures. Specifically, for $\ln \Lambda = 20$, the minimum bremsstrahlung loss of $P_{brem}/P_{fus} = 0.7\%$ occurs at $T_i = 40$ keV; for $\ln \Lambda = 5$, the minimum bremsstrahlung loss also occurs at $T_i = 40$ keV, and it

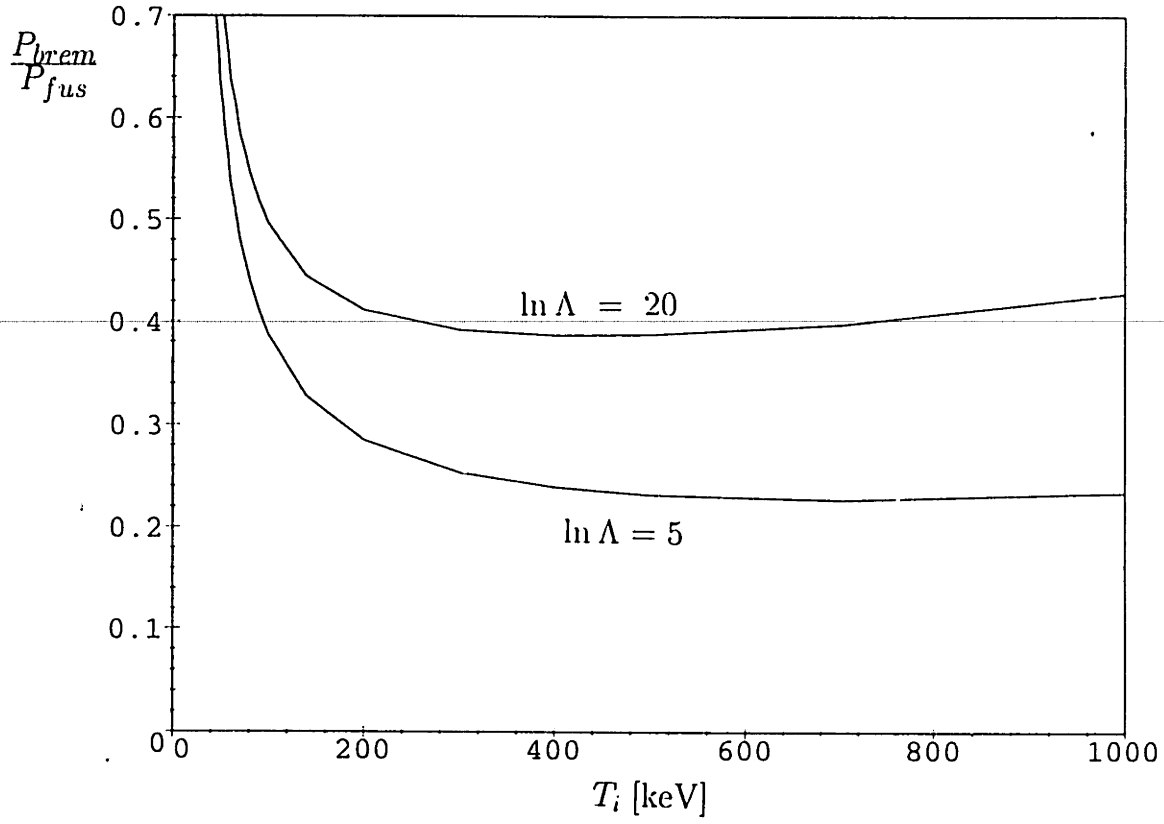

Figure 7-5: Bremsstrahlung power loss fraction for D-D with various ion temperatures. (T_e determined from $P_{ic} = P_{brem}$.)

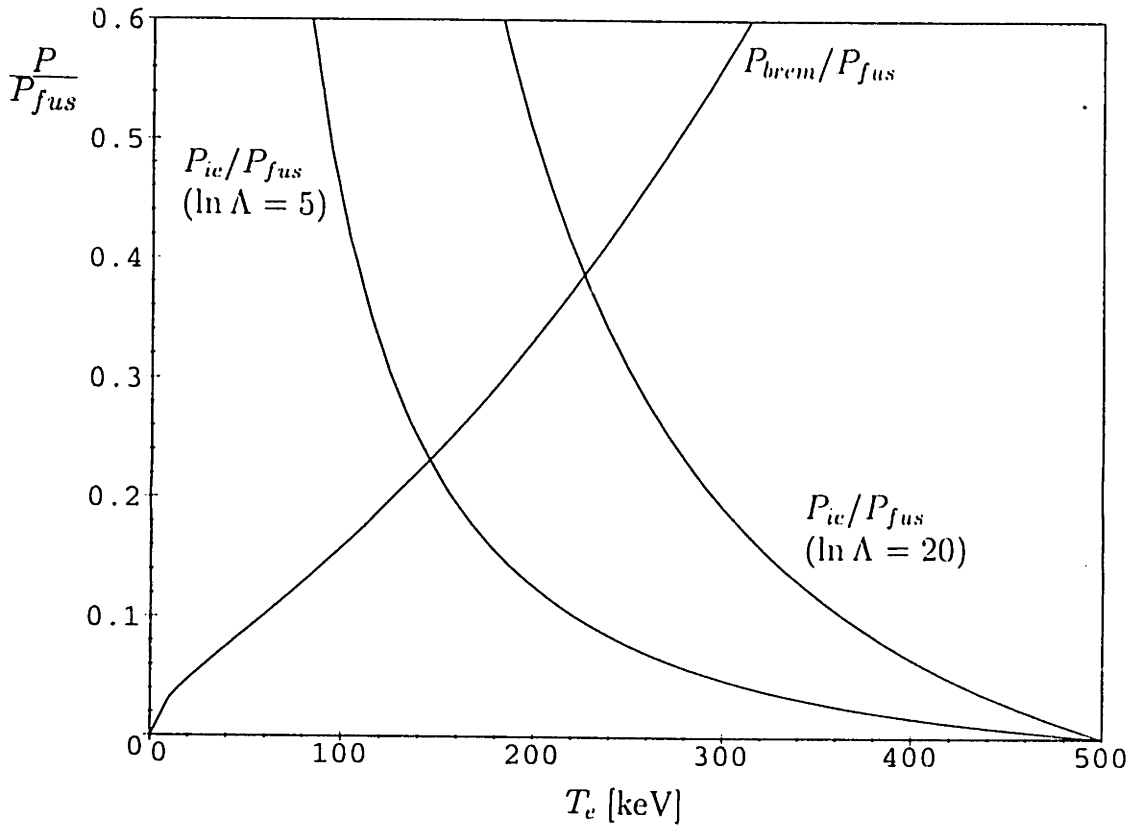

Figure 7-6: Ion-electron energy transfer and bremsstrahlung compared with fusion power for D-D with various electron temperatures. (T_i = 500 keV.)

is $P_{brem}/P_{fus} = 0.6\%$. As was stated in Table 1.1, the neutron power fraction for D-T is $P_{neutrons}/P_{fus} = 0.80$.

It is sobering to realize the implications of the difference between the miniscule ideal losses for D-T which are shown in Figure 7-7 and the large "real-world" losses which have plagued the experimental controlled fusion program for the last half-century and kept D-T from generating net power when all losses were taken into account. The reason this difference is so important (and depressing) is that a similarly large gap will exist between the (far greater) ideal losses calculated for the advanced fuels in Chapter 6 and 7 and the realistic losses which would be found if a large-scale reactor-development program were undertaken for any of these fuels.

7.3 Summary

As D-^{3}He reactors appear to be constrained to operate with equilibrium plasmas, it is fortunate that net energy gains can theoretically be attained with such systems. However, the bremsstrahlung losses even in the ideal case are far from negligible, and the reactors will have to contend with very appreciable levels of neutron and tritium production.

For the purpose of comparison, similar analyses of bremsstrahlung losses for D-D and D-T reactors were also conducted. The results are summarized in Figure 7-8, which may be compared with Figure 6-9 in the previous chapter.

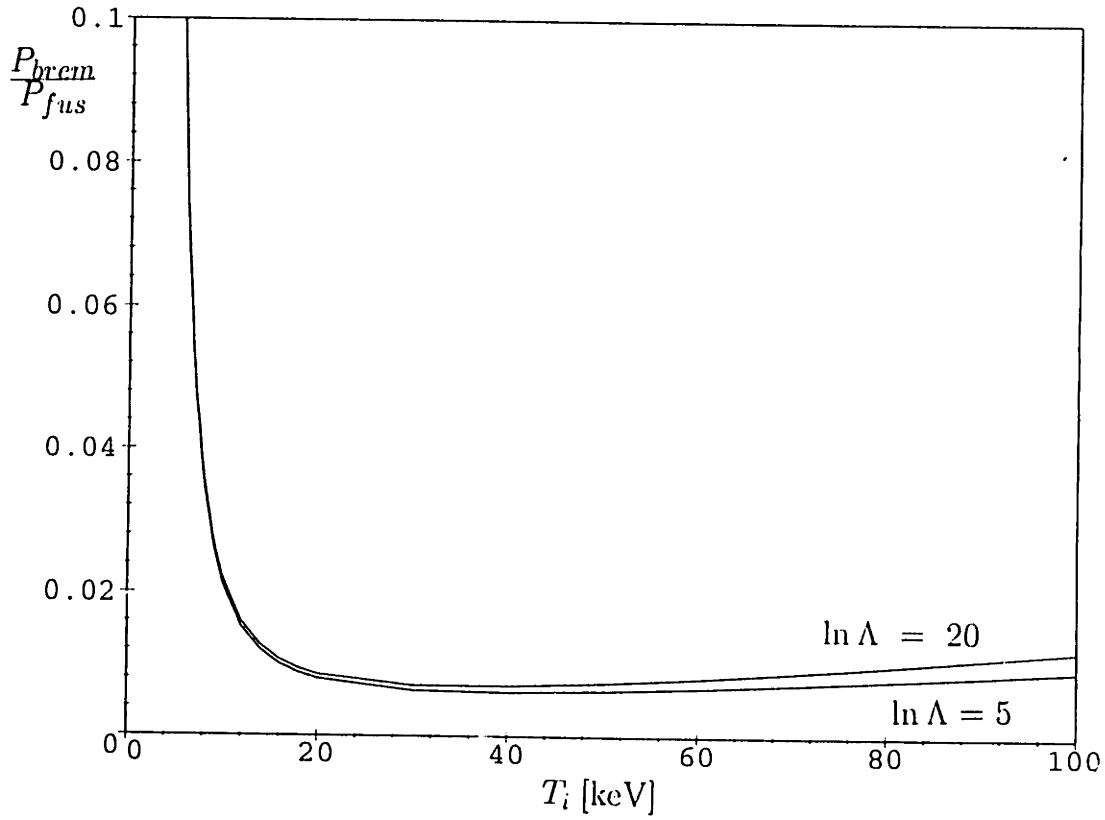

Figure 7-7: Bremsstrahlung power loss fraction for D-T with various ion temperatures. (T_e determined from $P_{ie} = P_{brem}$; $n_D = n_T$.)

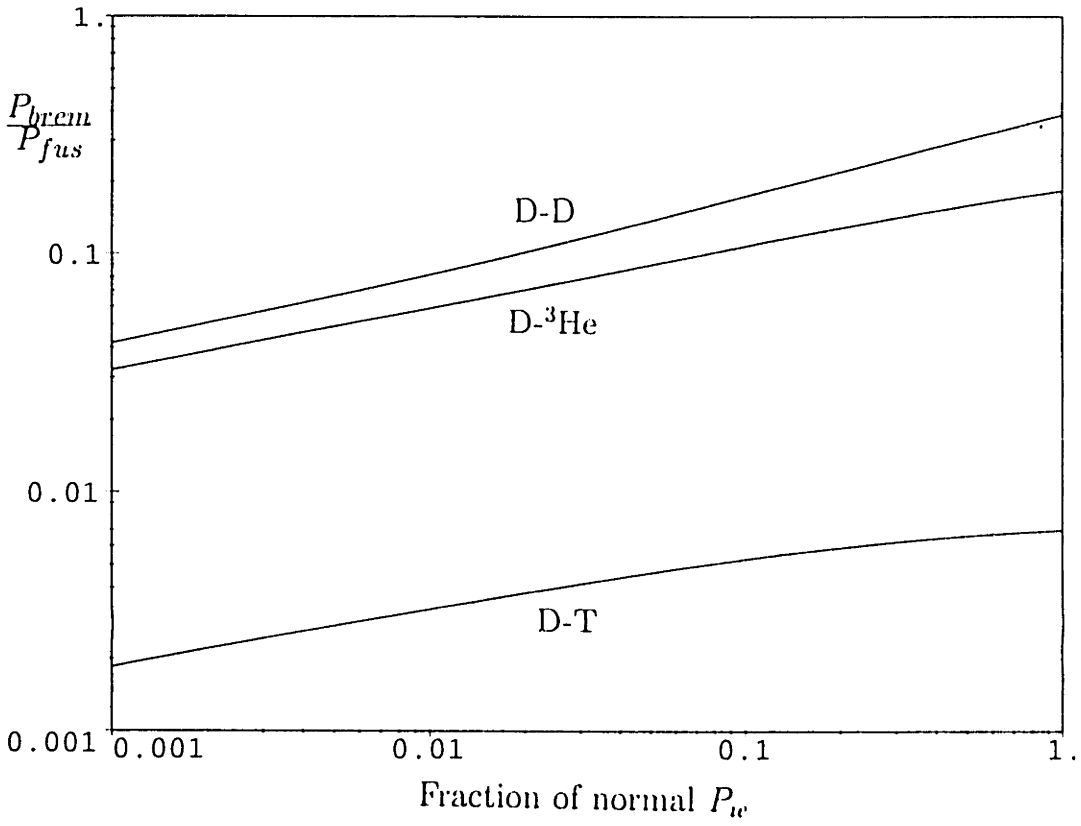

Figure 7-8: Ratio of bremsstrahlung losses to fusion power versus the necessary reduction of ion-electron energy transfer for D-T, D-D, and D-^{3}He plasmas under approximately optimum conditions (T_i = 40 keV for D-T [with a 1:1 fuel mixture], 400 keV for D-D, and 140 keV for D-^{3}He [with a 1:1 fuel mixture]; $\ln \Lambda = 20$ throughout.)

Chapter 8

Conclusions

This work has derived several fundamental limitations that apply to plasma fusion systems which are not in thermodynamic equilibrium, specifically (1) systems which have non-Maxwellian velocity distributions for the ions or the electrons, and (2) systems in which two particle species, such as electrons and fuel ions or two fuel ion species, are at radically different mean energies. The need to remove the entropy generated by collisions in the plasma produces two minimum power values required to keep such a system out of thermodynamic equilibrium. First of all, there is a theoretical minimum power loss which is incurred by venting the generated entropy to room-temperature surroundings by way of a Carnot cycle. For all systems which were considered, this power loss is small enough that the plasma can be kept far from equilibrium without allowing the minimum loss to exceed the fusion power. The second and much more stringent constraint is the minimum recirculating power that must be removed from the plasma after collisional scattering events and returned to the desired region of plasma's phase space in order to keep the system out of thermodynamic equilibrium.

If the recirculating power becomes much larger than the fusion power, the reactor design will be undesirable due to practical considerations, and unless the recirculating

power is handled with extremely high efficiencies, the reactor will probably not even be capable of producing net power. This recirculating power constraint was found to impose severe limitations on all types of nonequilibrium systems which were examined.

It is very important to keep in mind that the calculations determined the *minimum* recirculating power required of *any* mechanism for maintaining a nonequilibrium plasma. There are few presently available mechanisms for recirculating the power at all, and most of the mechanisms which exist will have recirculating power levels far higher and efficiencies far lower than those calculated here for an ideal system.

8.1 Main Results of the Thesis

The results which were obtained for specific types of nonequilibrium plasma systems will now be summarized.

8.1.1 Modification of Ion-Electron Energy Transfer Rate For Large Ratios of Ion to Electron Temperatures

Corrections to the classical Spitzer energy transfer rate between ions and electrons were calculated for the case when the ion temperature T_i is significantly higher than the electron temperature T_e. It was found that slow electrons are partially depleted by their interactions with the ions, resulting in a decrease in the energy transfer in comparison with the Spitzer rate, which assumes perfectly Maxwellian electrons. Since a thorough calculation of this effect had never been done before, it was hoped that the "passive" depletion of slow electrons in this manner might lead to very sizeable decreases in the ion-electron energy transfer rate, especially for large values of T_i/T_e. Although the energy transfer was in fact found to decrease steadily from the classical value as T_i/T_e increases, the reduction did not prove to be large enough to be especially useful. For example, even for T_i/T_e values of several hundred, the energy transfer rate is still around 60-80% of the

Spitzer result.

Nevertheless, the calculation did at least result in a useful expression for the energy transfer correction factor for use by future researchers. In the case in which all of the ion species are at the temperature T_i, the correction factor to the interspecies energy transfer rate P_{ie} was found to be

$$\frac{P_{ie}}{(P_{ie})_{\text{Spitzer}}} \approx \left(1 + \frac{m_e}{m_i}\frac{T_i}{T_e}\right)^{3/2} \exp\left\{-\left(3.5\sum_i \frac{Z_i^2 n_i}{n_e}\frac{m_e}{m_i}\frac{T_i}{T_e}\right)^{2/3}\right\}.$$

This expression is quite accurate for values of $\sum_i (Z_i^2 n_i/n_e)(m_p/m_i)(T_i/T_e)$ less than about 50 (where m_p is the proton mass), although it underestimates the energy transfer rate for larger values of T_i/T_e, and one must resort to the more accurate but more complex analytical results derived and graphed in Chapter 2. It was shown that in the event that the ion distribution is non-Maxwellian, T_i in the correction factor should be replaced by $2\langle E_i\rangle/3$, where $\langle E_i\rangle$ is the mean ion energy.

8.1.2 Power Requirements for Maintaining Non-Maxwellian Velocity Distributions

Chapter 3 presented a calculation of the minimum recirculating power required to keep either the electrons or the ions of a plasma in a non-Maxwellian state, and the chapter then applied the calculation to a number of fuels ranging from D-T to the advanced aneutronic fuels.

In order to reduce ion-electron energy transfer (and thus also bremsstrahlung radiation) for D-^{3}He and the more advanced fuels, it would be desirable to actively deplete most of the electrons moving more slowly than the ions, while keeping the remainder of the electrons in an essentially unperturbed Maxwellian distribution. However, the calculations of Chapter 3 showed that without requiring much more recirculating power than fusion power, it is not possible to maintain such electron distribution shapes.

An even more difficult task would be to hold the entire electron distribution in a substantially non-Maxwellian shape, such as the isotropic, beamlike distribution with a thermal spread which was considered in Chapter 3. Barring prohibitively large amounts of recirculating power, these types of modifications of the electron velocity distribution cannot even be done for D-T, let alone the more advanced fuels.

Similarly, to maintain the fuel ions in a reasonably non-Maxwellian state would require recirculating power levels at least on the order of the fusion power for D-T and significantly greater than the fusion power for all other fuels.

Finally, virtually all methods of alleviating these problems, such as using anisotropic velocity distributions or employing electromagnetic fields in an attempt to remove the collisionally generated entropy from the plasma, were shown not to work.

8.1.3 Power Requirements for Maintaining Particle Species at Radically Different Mean Energies

The other major type of nonequilibrium plasma system which was examined was that in which two or more of the plasma's major particle species are at radically different mean energies. It was shown that if the two species (ions and electrons or two fuel ion species) are somehow actively held at significantly different mean energies, the minimum recirculating power for an ideal system will be the interspecies energy transfer rate, since that power must be continually extracted from the less energetic species and returned to the more energetic species. By applying the standard interspecies energy transfer rate to fuels ranging from D-^{3}He to the advanced aneutronic fuels (there is no reason to use D-T in such systems), the minimum recirculating power required to keep one ion species at a much lower mean energy than the other was shown to be significantly greater than the fusion power. In the same types of plasmas, the recirculating power needed to refrigerate the electrons enough to reduce bremsstrahlung losses by a useful amount was also found to exceed the fusion power by a significant margin.

Numerous methods of reducing the interspecies energy transfer rate were explored. One possible technique, primarily of use for ion-electron energy decoupling, would be to make the velocity distributions of one or both particle species substantially non-Maxwellian, but as has been discussed, this cannot be done to a useful degree. Anisotropy and several other methods were also investigated, but all of these techniques were shown to be inadequate or impractical. While it cannot be claimed that an exhaustive search of all possible methods for reducing the energy transfer rate has been performed, at least all presently known techniques have been investigated to no avail, and the outlook for finding a new method which works well enough and can be implemented in a practical fashion does not look at all promising.

8.1.4 Outlook for Advanced Aneutronic Fuels

The most important concern with advanced aneutronic fuels (^{3}He-^{3}He, p-^{11}B, and p-^{6}Li) is the bremsstrahlung radiation loss which occurs when the mean electron energy becomes too large; all other losses can at least in theory be held to manageable levels by choosing an appropriate confinement system. It was shown that even by assuming that the only source of energy to the electrons is Coulomb friction with the ions and by incorporating all necessary corrections for relativistic effects, variations in the Coulomb logarithm, and the ion-induced partial depletion of slow electrons derived in Chapter 2, the bremsstrahlung losses exceed the fusion power for all three of the advanced aneutronic fuels.

In order to reduce the bremsstrahlung losses to theoretically bearable levels (say no more than half of the fusion power), the ion-electron energy transfer rate would have to be reduced by at least one order of magnitude for the case of ^{3}He-^{3}He, at least two orders of magnitude for p-^{11}B, and at least three orders of magnitude for p-^{6}Li. Nonequilibrium plasmas cannot be used to help in this matter because they would require too much recirculating power to sustain. All other known methods of alleviating this problem have also been shown to be insufficient or impractical. The reductions in ion-electron energy transfer which are required for break-even with the advanced aneutronic fuels

are such stunningly large figures (especially since they were obtained by using extremely optimistic assumptions and parameters) that even if some novel yet practical method could be devised to help, it would almost certainly not be able to help as much as would be required. Thus there is very little hope of ever being able to produce net power with any of these fuels.

8.1.5 Minimum Neutron Output from Feasible D-^{3}He Reactors

Although D-^{3}He can theoretically produce net power when burned in plasmas which are in thermodynamic equilibrium, there is a certain limit to how effectively the D-D side reactions (with their attendant neutron and tritium production difficulties) can be suppressed in such a system without incurring prohibitive levels of bremsstrahlung and other losses. It was hoped that nonequilibrium plasmas could be employed either to lower the electron temperature and thereby permit more ^{3}He-rich fuel mixtures to be used without excessive radiation losses, or else to lower the D temperature below the ^{3}He temperature and thus directly suppress D-D reactions. However, the large amounts of recirculating power which would be required for these schemes make them infeasible.

Therefore, neutron production is limited by the performance attainable with an equilibrium plasma: with minimum bremsstrahlung losses of at least half the fusion power, D-D neutrons would constitute at least 0.2% of the total fusion power, which is about one order of magnitude lower than the same figure for fission. Realistic systems would almost certainly have higher electron temperatures and more bremsstrahlung radiation, as well as other losses with which to contend, so it appears that at best they would be able to attain $P_{neutrons}/P_{fus} \approx 1\%$ (for a 1:1 fuel mixture). Even this figure is still optimistic, because it assumes that the tritons produced in D-D fusion events are somehow removed from the system before they can react with the deuterons to produce extremely unpleasant 14-MeV neutrons. If the tritons do burn up in the plasma, the neutron power fraction would be at least $P_{neutrons}/P_{fus} \approx 5\%$, which is equivalent to 150 MW of neutrons for a reactor with a gross fusion power of 3 GW_t. As a further complication, if the tritium is removed

without burning it, it will build up to sizeable steady-state levels which must be stored safely. For a reactor with a gross fusion power of 3 GW_t, in the steady state there would be approximately 200 kg, or $2 \cdot 10^9$ Ci, of tritium. This level of radioactivity is only about one order of magnitude smaller than that found in a fission reactor core shortly after the core has been shut down.

The bottom line is that realistic D-^{3}He reactors will be limited to at best a neutron power fraction of the same order as fission reactors, and the D-^{3}He reactors will also produce substantial amounts of tritium. Of course, this information must be considered together with the other properties of such fusion reactors and compared with the properties of fission reactors. As an advantage, the fusion reactors would not produce anything like the level of very long-lived, high-level radioactive waste which current fission reactors generate in the form of spent fuel rods. On the other hand, considering the complexity of the fusion problem, as illustrated by the long history of fusion research, fusion reactors will probably be much more technologically sophisticated than fission reactors, and as a corollary they will almost certainly be more costly in economic terms as well.

8.1.6 Summary

In order to summarize the results of the thesis and to emphasize the broad extent and powerful implications of these findings, some specific examples of fusion systems which have been ruled out by this work should be given. In particular, the following systems cannot operate without having to recirculate a prohibitively large amount of power in comparison with the fusion power:

- Systems which attempt to maintain highly non-Maxwellian particle velocity distributions without explicit means of keeping the particles non-Maxwellian despite Coulomb collisions (eg. inertial-electrostatic confinement [19] and migma [38]).
- Systems which attempt to maintain non-Maxwellian distributions through the removal and direct conversion of particles with improper velocities and the reinjection

of particles with the correct velocity (eg. multipolar traps with electrons removed before they thermalize [37]).

- Systems which attempt to maintain non-Maxwellian distributions through the selective heating of slow particles, even if the heating energy comes from a direct converter which selectively decelerates particles that are too fast.

- Systems which attempt to keep two of the plasma's major particle species (ions and electrons or two different species of fuel ions) at radically different mean energies by actively cooling one of the species in any way (synchrotron radiation, active particle removal, ion loss to fusion events, etc.).

- Systems relying on the effects of having anisotropic velocity distributions (for example, counter-propagating beams, nearly radial velocity distributions [19], or beam-plasma interactions) in order to facilitate the maintenance of non-Maxwellian velocity distributions or energy decoupling between two particle species. (The sole exception is that D-T is reactive enough that high-energy beams of D or T can successfully be used to boost the fusion rates in D-T reactors without requiring too much power input to maintain [70].)

- Systems relying on the effects of spatial inhomogeneities in the particle density or the electrostatic potential in order to facilitate the maintenance of non-Maxwellian velocity distributions or energy decoupling between two particle species.

- Systems which attempt to use electric fields, magnetic fields, electrostatic waves, or electromagnetic waves to extract collisionally generated entropy from the plasma and hold the plasma out of thermodynamic equilibrium (barring a very small number of rather wild ideas which have not yet been ruled out and are discussed in Appendix E).

- Transient nonequilibrium burning systems which try to produce enough fusion power before the particle distributions equilibrate. (The power flowing to make the system

equilibrate significantly exceeds the fusion power, so the system could never be operated for a sufficiently short time to "win.")

- Reactors burning advanced aneutronic fuels (^{3}He-^{3}He, p-^{11}B, and p-^{6}Li) in thermodynamic equilibrium [10, 17], even if the bremsstrahlung radiation could somehow be collected and directly converted into electrical energy at relatively high efficiencies.

- Reactors which attempt to burn advanced aneutronic fuels in a plasma which is not in thermodynamic equilibrium, such as plasmas in which the electrons or ions are non-Maxwellian, the mean electron energy is far lower than the mean ion energy, or the mean energy of one fuel ion species is substantially lower than that of the other fuel ion species.

- D-^{3}He reactors which attempt to make the neutron power fraction much smaller than that found in fission reactors–for example, by operating particularly ^{3}He-rich or by attempting to make the mean energy of the ^{3}He ions much larger than the mean energy of the deuterons.

Many other examples could also be given, but those presented above should serve as an indicator of the scope of the results which have been found in this work.

8.2 Proposed Directions for Future Research

There are several directions which should be explored in the course of future fusion research. First of all, emphasis should be placed on the development of reactor designs which are capable of burning D-^{3}He in thermodynamic equilibrium and are as attractive as possible; one of the main priorities of this research area should be the expansion of the currently woefully deficient experimental knowledge base concerning conditions appropriate for ignited D-^{3}He plasmas. Workable and efficient direct electric converters which could function with such reactors should also be seriously pursued. In addition, it would be desirable to explore the few remaining approaches which, although admittedly

quite speculative, may yet allow nonequilibrium plasma fusion and advanced aneutronic fuel reactors to become a reality (see Appendix E for more details). Similarly, it would be prudent to search for radical new physics ideas which could fundamentally improve the fusion problem on a nuclear level (as has been attempted with proposals for muon-catalyzed [105, 106] and antiproton-catalyzed [107] fusion, spin-polarized [106, 108] and nuclear-shape-polarized [107] fusion, fusion in ultra-dense matter [109], and coherent neutron transfer reactions in solid state lattices [110]) and yet would demonstrably work well enough that they could serve as the basis for large power reactors.

As a final point, it is very important that the ultimate goal of this entire field of research should not be forgotten. The stated goal of fusion for over half a century has been to produce large quantities of clean, safe, affordable, and essentially limitless power for the world. If, after a detailed examination of all foreseeable approaches to fusion, it does not seem at all likely that the technologically feasible types of fusion reactors can meet this goal, then energy research should instead concentrate on improving other power generation methods such as fission reactors, solar energy conversion, and fossil fuels.

Appendices

Appendix A

Effect of Non-Maxwellian or Anisotropic Ion Velocity Distributions on Averaged Fusion Reaction Rates

A.1 Comparison of Average Fusion Reactivity Values for Maxwellian Ion Distributions and for Isotropic Monoenergetic Ion Distributions

At several points in the thesis it has been stated that the average fusion reactivity $\langle \sigma v \rangle_{fus}$ for a given mean ion energy is essentially the same regardless of the shape of the ion velocity distributions, provided that the ion velocity distributions are isotropic and that the two fuel ion species (if there are two) have the same mean energy. This assertion will now be explicitly proved.

First of all, an expression for the average fusion reactivity of a plasma with monoenergetic, isotropic ion distributions will be derived. This case represents the extreme limit of non-Maxwellian ion distributions. Then the average fusion reactivity as a function of the mean ion energy will be evaluated for several fuels of interest and compared with the results for purely Maxwellian ions. These two extremes should serve to give an idea of how much variation in the reactivity one might find in examining a wide variety of plasmas with different isotropic ion distribution shapes.

The fusion cross section as a function of energy can be written as [30, 33, 111]

$$\sigma_{fus}(E) = 10^{-24}\,\frac{A_5 + A_2[(A_4 - A_3E)^2 + 1]^{-1}}{E\,[\exp(A_1/\sqrt{E}) - 1]}\ \mathrm{cm}^2, \tag{A.1}$$

in which E is the kinetic energy (in keV) of the lighter ion in the frame in which the heavier ion is at rest, and the Duane coefficients A_1 through A_5 for various fuels are given in Table A.1.

Reaction	A_1	A_2	A_3	A_4	A_5
T(d,n)^{4}He	45.95	50200	$1.368 \cdot 10^{-2}$	1.076	409
D(d,p)T	46.097	372	$4.36 \cdot 10^{-4}$	1.220	0
D(d,n)^{3}He	47.88	482	$3.08 \cdot 10^{-4}$	1.177	0
^{3}He(d,p)^{4}He	89.27	25900	$3.98 \cdot 10^{-3}$	1.297	647

Table A.1: Duane coefficients for calculating the fusion cross sections for T(d,n)^{4}He, D(d,p)T, D(d,n)^{3}He, and ^{3}He(d,p)^{4}He reactions using Eq. (A.1). (Coefficients are from Refs. [30, 33].)

In the laboratory frame of realistic plasmas, both ions are moving, so one must change reference frames in order to find the proper value of E. If it is assumed that the $i1$ ions are the lighter ions of the two species and that θ is the angle between the velocity vectors of colliding ions of the two species, then E is found to be

$$\begin{aligned} E &= \frac{1}{2} m_{i1} |\mathbf{v_{i1}} - \mathbf{v_{i2}}|^2 \\ &= \frac{1}{2} m_{i1} \left(v_{i1}^2 + v_{i2}^2 - 2 v_{i1} v_{i2} \cos\theta \right) . \end{aligned} \tag{A.2}$$

By making the further assumption that both ion species are monoenergetic at the same energy E_i (in keV) and by defining $u \equiv \cos\theta$, the energy becomes

$$E = E_i \left(1 + \frac{m_{i1}}{m_{i2}} - 2u\sqrt{\frac{m_{i1}}{m_{i2}}} \right) . \tag{A.3}$$

The relative collision velocity Δv between the two ions may be found from E:

$$\Delta v = \sqrt{\frac{2E_{ergs}}{m_{i1}}} = 4.377 \cdot 10^7 \sqrt{\frac{E_{keV}}{\mu_{i1}}} \ \frac{\text{cm}}{\text{sec}} , \tag{A.4}$$

where the subscripts on E indicate the change of units and the ion mass has been written in terms of the proton mass, $\mu_{i1} \equiv m_{i1}/m_p$.

For monoenergetic but isotropic ions, the fusion reactivity (in cm^3/sec) averaged over all angles is

$$\begin{aligned} \langle \sigma v \rangle_{fus} &= \frac{1}{2} \int_0^\pi d\theta \ \sin\theta \ \sigma_{fus}(E) \ \Delta v \\ &= \frac{1}{2} \int_{-1}^1 du \ \sigma_{fus}(E) \ \Delta v \ . \end{aligned} \tag{A.5}$$

Using the Duane coefficients in Table A.1, Eq. (A.5) has been used to calculate the values of the average fusion reactivity for T(d,n)^{4}He, D(d,p)T, D(d,n)^{3}He, and ^{3}He(d,p)^{4}He reactions. In each case, the results have been compared with the average reactivity of a Maxwellian ion distribution with the same mean ion energy (or temperature $T_i \equiv (2/3)\langle E_i \rangle$), as shown in Tables A.2 through A.5 and Figures A-1 through A-4. As may be seen from the tables and graphs, for a given mean ion energy, the values of $\langle \sigma v \rangle_{fus}$ for each reaction are very similar for Maxwellian ions and for monoenergetic ions (to within roughly $10 - 30\%$) when the ion energies are in the regime of interest for fusion reactors. The peak values of the reactivity for each case are even closer to each other. These results are in agreement with those of similar calculations which have been performed by Nevins [87] and Santarius [20]. The effect of these corrections on the calculations presented earlier in the thesis is quite small in comparison with the magnitude of change which would

be necessary to alter the fundamental conclusions about the inviability of nonequilibrium fusion plasmas and very clean reactors.

The effects of non-Maxwellian ion distributions on other reactions have not been examined, since suitable Duane coefficients could not be found. (The fit for the p-^{11}B cross section given in [33] does not appear to be that good, in light of more recent data [34, 35].) However, an analysis of other reactions should lead to the same conclusion: for isotropic velocity distributions in which the two ion species (if there are two) have the same mean energy, even very drastic changes in the velocity distribution shape (eg. monoenergetic vs. Maxwellian) cause only small corrections ($\sim 10 - 30\%$ at a given energy, even smaller in terms of the maximum for each curve) in the average fusion reactivity for the temperature regimes of interest. Such small corrections are not enough to alter the conclusions stated earlier in this thesis, where the recirculating power for nonequilibrium plasmas and the bremsstrahlung losses from advanced aneutronic fuels were shown to be too large by factors of two or more.

The results which have been obtained thus far in this appendix should be used to clear up one possible point of confusion. In the past, researchers have contended that nuclear elastic scattering or knock-on processes could significantly improve the fusion reactivity by transferring energy from fusion products to fuel ions and thereby making the ion velocity distribution deviate somewhat from a Maxwellian shape [10, 12, 88, 89, 90]. Yet as has been explicitly shown here, even drastic deviations of the ion distribution shape from equilibrium (in the present case, a monoenergetic distribution) only affect the reactivity for a given mean ion energy by a small amount. Presumably a distribution which is closer to thermodynamic equilibrium would have a reactivity which deviates from the Maxwellian quantity by an even smaller amount. Thus one is led to conclude that processes such as nuclear elastic scattering enhance the fusion rate mainly by boosting the mean energy of the fuel ions, not primarily by altering the ion distribution shape. Indeed, the literature on nuclear elastic scattering generally compares the reactivity of Maxwellian ions with that of an ion distribution which is the sum of a Maxwellian distribution at the same mean

T_i [keV]	$\langle \sigma v \rangle_{fus}$ [cm^3/sec] for Maxwellian ions	$\langle \sigma v \rangle_{fus}$ [cm^3/sec] for monoenergetic ions
1	$5.484 \cdot 10^{-21}$	$3.359 \cdot 10^{-23}$
2	$2.628 \cdot 10^{-19}$	$1.460 \cdot 10^{-20}$
3	$1.713 \cdot 10^{-18}$	$2.199 \cdot 10^{-19}$
5	$1.289 \cdot 10^{-17}$	$3.474 \cdot 10^{-18}$
7	$3.980 \cdot 10^{-17}$	$1.563 \cdot 10^{-17}$
10	$1.089 \cdot 10^{-16}$	$6.195 \cdot 10^{-17}$
20	$4.243 \cdot 10^{-16}$	$4.733 \cdot 10^{-16}$
30	$6.653 \cdot 10^{-16}$	$8.620 \cdot 10^{-16}$
50	$8.705 \cdot 10^{-16}$	$1.020 \cdot 10^{-15}$
70	$9.002 \cdot 10^{-16}$	$9.437 \cdot 10^{-16}$
100	$8.488 \cdot 10^{-16}$	$8.048 \cdot 10^{-16}$
200	$6.278 \cdot 10^{-16}$	$5.405 \cdot 10^{-16}$
300	$4.954 \cdot 10^{-16}$	$4.280 \cdot 10^{-16}$
500	$3.668 \cdot 10^{-16}$	$3.326 \cdot 10^{-16}$
700	$3.087 \cdot 10^{-16}$	$2.919 \cdot 10^{-16}$
1000	$2.672 \cdot 10^{-16}$	$2.620 \cdot 10^{-16}$

Table A.2: T(d,n)^{4}He reaction: comparison of values of $\langle \sigma v \rangle_{fus}$ vs. $T_i \equiv (2/3) \langle E_i \rangle$ for a Maxwellian ion velocity distribution [33] and for a monoenergetic, isotropic ion velocity distribution. See also Figure A-1.

energy and a high-energy tail which is not included in computing the mean energy. If one were to compare ion distributions in which the overall mean energy for each distribution is the same, the fusion rates would be much more similar.

A.2 Fusion Reactivity Values for Systems Operating Precisely at the Peaks of the Reaction Cross Sections

It is also of interest to determine the effect of making essentially all of the ion collisions occur at the optimum net collision velocity corresponding to the peak in the reaction cross section. Hypothetically this situation might be arranged by having two linear, counter-propagating ion beams collide with each other or by utilizing a plasma containing

T_i [keV]	$\langle \sigma v \rangle_{fus}$ [cm^3/sec] for Maxwellian ions	$\langle \sigma v \rangle_{fus}$ [cm^3/sec] for monoenergetic ions
1	$8.300 \cdot 10^{-23}$	$1.230 \cdot 10^{-24}$
2	$2.820 \cdot 10^{-21}$	$2.939 \cdot 10^{-22}$
3	$1.501 \cdot 10^{-20}$	$3.294 \cdot 10^{-21}$
5	$8.774 \cdot 10^{-20}$	$3.685 \cdot 10^{-20}$
7	$2.346 \cdot 10^{-19}$	$1.323 \cdot 10^{-19}$
10	$5.816 \cdot 10^{-19}$	$4.111 \cdot 10^{-19}$
20	$2.434 \cdot 10^{-18}$	$2.219 \cdot 10^{-18}$
30	$4.757 \cdot 10^{-18}$	$4.665 \cdot 10^{-18}$
50	$9.660 \cdot 10^{-18}$	$9.894 \cdot 10^{-18}$
70	$1.444 \cdot 10^{-17}$	$1.492 \cdot 10^{-17}$
100	$2.120 \cdot 10^{-17}$	$2.187 \cdot 10^{-17}$
200	$4.136 \cdot 10^{-17}$	$4.211 \cdot 10^{-17}$
300	$5.850 \cdot 10^{-17}$	$6.086 \cdot 10^{-17}$
500	$8.178 \cdot 10^{-17}$	$9.371 \cdot 10^{-17}$
700	$9.240 \cdot 10^{-17}$	$1.087 \cdot 10^{-16}$
1000	$9.508 \cdot 10^{-17}$	$1.029 \cdot 10^{-16}$

Table A.3: D(d,p)T reaction: comparison of values of $\langle \sigma v \rangle_{fus}$ vs. $T_i \equiv (2/3) \langle E_i \rangle$ for a Maxwellian ion velocity distribution [33] and for a monoenergetic, isotropic ion velocity distribution. See also Figure A-2.

T_i [keV]	$\langle \sigma v \rangle_{fus}$ [cm^3/sec] for Maxwellian ions	$\langle \sigma v \rangle_{fus}$ [cm^3/sec] for monoenergetic ions
1	$6.921 \cdot 10^{-23}$	$7.749 \cdot 10^{-25}$
2	$2.600 \cdot 10^{-21}$	$2.294 \cdot 10^{-22}$
3	$1.453 \cdot 10^{-20}$	$2.825 \cdot 10^{-21}$
5	$8.942 \cdot 10^{-20}$	$3.473 \cdot 10^{-20}$
7	$2.461 \cdot 10^{-19}$	$1.311 \cdot 10^{-19}$
10	$6.262 \cdot 10^{-19}$	$4.257 \cdot 10^{-19}$
20	$2.725 \cdot 10^{-18}$	$2.447 \cdot 10^{-18}$
30	$5.412 \cdot 10^{-18}$	$5.275 \cdot 10^{-18}$
50	$1.112 \cdot 10^{-17}$	$1.141 \cdot 10^{-17}$
70	$1.663 \cdot 10^{-17}$	$1.730 \cdot 10^{-17}$
100	$2.431 \cdot 10^{-17}$	$2.533 \cdot 10^{-17}$
200	$4.625 \cdot 10^{-17}$	$4.746 \cdot 10^{-17}$
300	$6.498 \cdot 10^{-17}$	$6.641 \cdot 10^{-17}$
500	$9.466 \cdot 10^{-17}$	$1.013 \cdot 10^{-16}$
700	$1.136 \cdot 10^{-16}$	$1.295 \cdot 10^{-16}$
1000	$1.267 \cdot 10^{-16}$	$1.469 \cdot 10^{-16}$

Table A.4: D(d,n)^{3}He reaction: comparison of values of $\langle \sigma v \rangle_{fus}$ vs. $T_i \equiv (2/3) \langle E_i \rangle$ for a Maxwellian ion velocity distribution [33] and for a monoenergetic, isotropic ion velocity distribution. See also Figure A-3.

T_i [keV]	$\langle \sigma v \rangle_{fus}$ [cm^3/sec] for Maxwellian ions	$\langle \sigma v \rangle_{fus}$ [cm^3/sec] for monoenergetic ions
1	$3.023 \cdot 10^{-26}$	$2.622 \cdot 10^{-32}$
2	$1.420 \cdot 10^{-23}$	$3.326 \cdot 10^{-27}$
3	$2.751 \cdot 10^{-22}$	$6.086 \cdot 10^{-25}$
5	$6.660 \cdot 10^{-21}$	$1.140 \cdot 10^{-22}$
7	$4.090 \cdot 10^{-20}$	$1.863 \cdot 10^{-21}$
10	$2.273 \cdot 10^{-19}$	$2.279 \cdot 10^{-20}$
20	$3.791 \cdot 10^{-18}$	$1.041 \cdot 10^{-18}$
30	$1.452 \cdot 10^{-17}$	$6.055 \cdot 10^{-18}$
50	$5.441 \cdot 10^{-17}$	$3.887 \cdot 10^{-17}$
70	$1.017 \cdot 10^{-16}$	$1.045 \cdot 10^{-16}$
100	$1.614 \cdot 10^{-16}$	$2.082 \cdot 10^{-16}$
200	$2.437 \cdot 10^{-16}$	$2.788 \cdot 10^{-16}$
300	$2.500 \cdot 10^{-16}$	$2.501 \cdot 10^{-16}$
500	$2.258 \cdot 10^{-16}$	$2.049 \cdot 10^{-16}$
700	$2.029 \cdot 10^{-16}$	$1.813 \cdot 10^{-16}$
1000	$1.805 \cdot 10^{-16}$	$1.639 \cdot 10^{-16}$

Table A.5: ^{3}He(d,p)^{4}He reaction: comparison of values of $\langle \sigma v \rangle_{fus}$ vs. $T_i \equiv (2/3) \langle E_i \rangle$ for a Maxwellian ion velocity distribution [33] and for a monoenergetic, isotropic ion velocity distribution. See also Figure A-4.

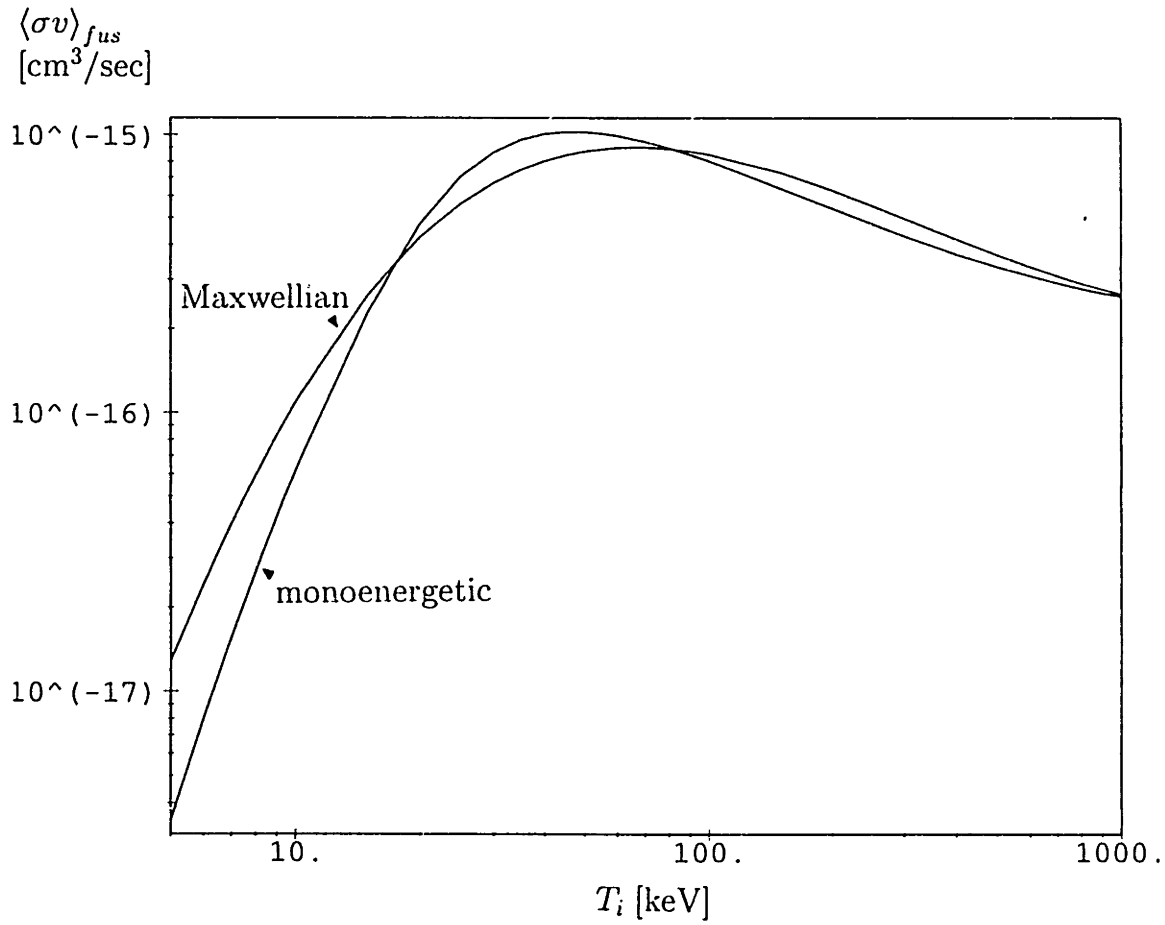

Figure A-1: T(d,n)^{4}He reaction: comparison of plots of $\langle \sigma v \rangle_{fus}$ vs. $T_i \equiv (2/3) \langle E_i \rangle$ for a Maxwellian ion velocity distribution [33] and for a monoenergetic, isotropic ion velocity distribution. See also Table A.2.

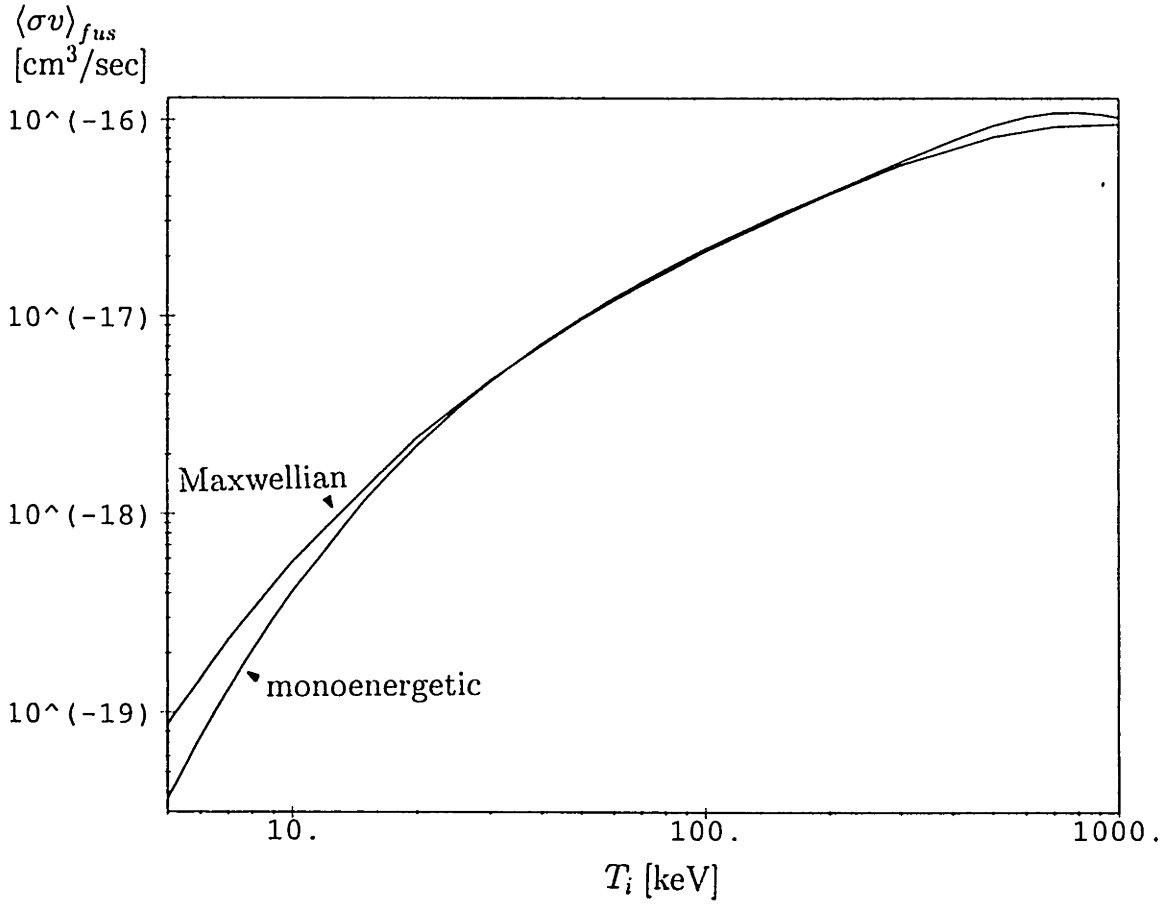

Figure A-2: D(d,p)T reaction: comparison of plots of $\langle \sigma v \rangle_{fus}$ vs. $T_i \equiv (2/3)\langle E_i \rangle$ for a Maxwellian ion velocity distribution [33] and for a monoenergetic, isotropic ion velocity distribution. See also Table A.3.

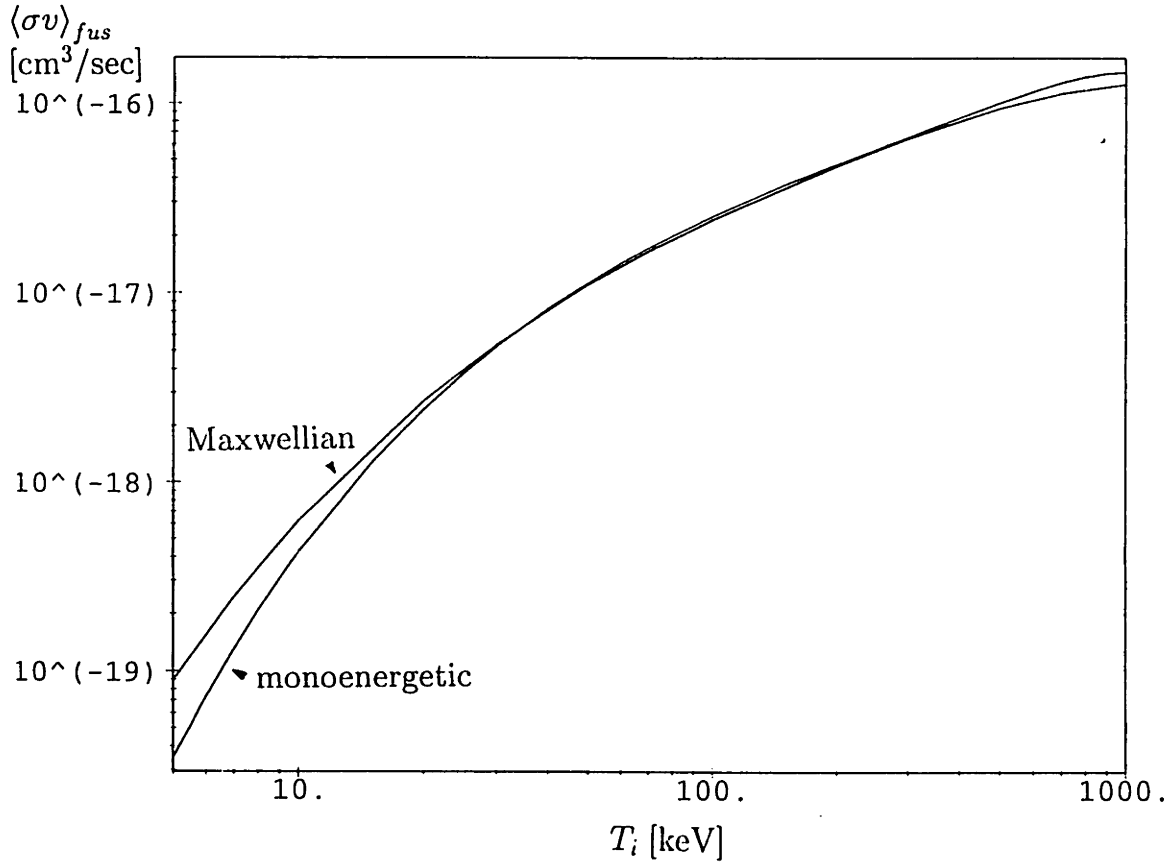

Figure A-3: D(d,n)^{3}He reaction: comparison of plots of $\langle \sigma v \rangle_{fus}$ vs. $T_i \equiv (2/3)\langle E_i \rangle$ for a Maxwellian ion velocity distribution [33] and for a monoenergetic, isotropic ion velocity distribution. See also Table A.4.

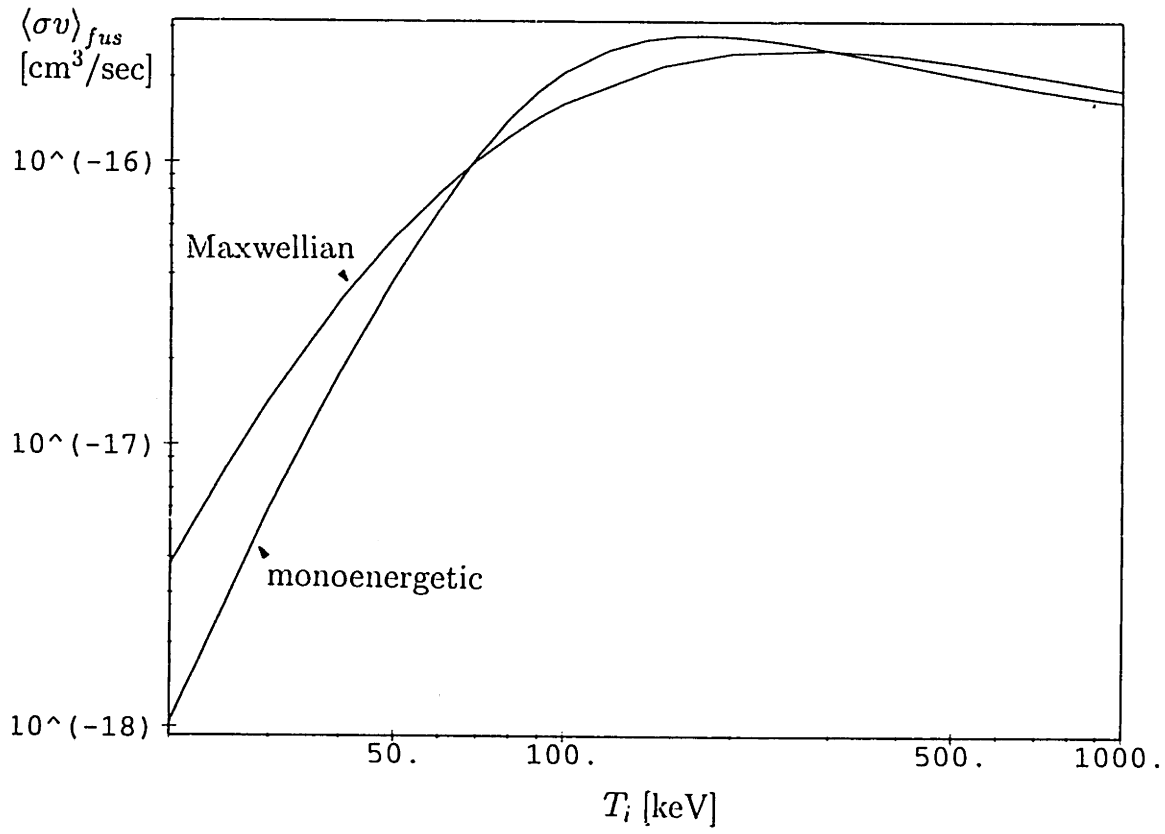

Figure A-4: ^{3}He(d,p)^{4}He reaction: comparison of plots of $\langle \sigma v \rangle_{fus}$ vs. $T_i \equiv (2/3)\langle E_i \rangle$ for a Maxwellian ion velocity distribution [33] and for a monoenergetic, isotropic ion velocity distribution. See also Table A.5.

monoenergetic, high-energy ions of one fuel species and essentially motionless ions of the other fuel species. (Except for D-T, which is reactive enough to permit a certain degree of success with such schemes, these methods cannot be implemented because of the large recirculating power requirements they would entail, as discussed in Chapters 3 and 5. However, it is worthwhile to check how much the fusion rate could be enhanced if such methods could be employed successfully.)

For D-T reactions with Maxwellian ions, the maximum value of $\langle \sigma v \rangle_{fus}$ is $9.01 \cdot 10^{-16}$ cm^3/sec and occurs for $T_i = 65$ keV [33]. If the reactivity is computed for monoenergetic deuterons interacting with essentially motionless tritons (or vice versa – interchange of the two ion species does not affect the reactivity), then the maximum value of $\langle \sigma v \rangle_{fus}$ is $1.67 \cdot 10^{-15}$ cm^3/sec and occurs at a deuteron energy of 130 keV, which is also approximately the energy corresponding to the peak in the fusion cross section [33].

Similarly, D(d,p)T reactions achieve a peak Maxwellian $\langle \sigma v \rangle_{fus}$ value of $9.53 \cdot 10^{-17}$ cm^3/sec for $T_i = 900$ keV [33]. For monoenergetic deuterons striking a target plasma of essentially motionless deuterons, the maximum beam-plasma $\langle \sigma v \rangle_{fus}$ value is $1.58 \cdot 10^{-16}$ cm^3/sec and occurs for an incident deuteron energy of approximately 3 MeV [33]. This energy is only slightly higher than the energy corresponding to the peak in the reaction cross section, which is about 2.5 MeV.

D(d,n)^{3}He reactions have a maximum Maxwellian-averaged reactivity of $\langle \sigma v \rangle_{fus} = 1.27 \cdot 10^{-16}$ cm^3/sec at $T_i = 1.5$ MeV and a peak beam-plasma reactivity of $\langle \sigma v \rangle_{fus} = 2.08 \cdot 10^{-16}$ cm^3/sec for 4-MeV deuterons striking a target plasma of motionless deuterons [33]. Again the optimum beam-plasma energy lies near the energy corresponding to the peak in the reaction cross section, which in this case is approximately 3.5 MeV.

For D-^{3}He reactions with Maxwellian ions, the maximum value of $\langle \sigma v \rangle_{fus}$ is $2.51 \cdot 10^{-16}$ cm^3/sec and occurs for $T_i = 250$ keV [33]. If the reactivity is computed for monoenergetic deuterons interacting with essentially motionless ^{3}He ions (or vice versa), the maximum value of $\langle \sigma v \rangle_{fus}$ is $4.73 \cdot 10^{-16}$ cm^3/sec and occurs at a deuteron energy of 450 keV, which is also the energy of the peak in the fusion cross section [33].

For p-^{11}B, the Maxwellian-averaged value of $\langle \sigma v \rangle_{fus}$ at $T_i = 1$ MeV (where the available graphs end [34, 35]) is $3.65 \cdot 10^{-16}$ cm^3/sec and is still rising as the temperature is increased further. According to Ref. [35], the maximum cross section is approximately $8 \cdot 10^{-25}$ cm^2 and occurs for protons with an energy of roughly 620 keV striking a plasma of essentially motionless boron ions. Based on the results for the other fuels discussed above, this energy should also correspond to the approximate location of the peak beam-plasma reactivity, yielding a maximum $\langle \sigma v \rangle_{fus} \approx 8.7 \cdot 10^{-16}$ cm^3/sec for 620-keV monoenergetic protons and very low-energy boron ions.

The ^{3}He-^{3}He Maxwellian-averaged reactivity is still rising with increasing ion temperature at $T_i = 1$ MeV (where the available graphs end [34, 35]), where it is $\langle \sigma v \rangle_{fus} = 1.25 \cdot 10^{-16}$ cm^3/sec. The peak beam-Maxwellian reactivity is difficult to compute, and would be rather academic even if it were known, since the peak in the reaction cross section occurs for ^{3}He ions with an energy of greater than 30 MeV incident on a target plasma of motionless ^{3}He ions [35]. However, one may calculate the reactivity for two monoenergetic linear beams of ^{3}He ions colliding head-on such that the energy of each beam is 1.5 MeV, the same value as the mean ion energy in the Maxwellian case just discussed. Such a colliding beam arrangement is equivalent to a beam-target system with a beam energy of 6 MeV, so the cross section is approximately $1.5 \cdot 10^{-25}$ cm^2 [35], yielding a reactivity of $\langle \sigma v \rangle_{fus} \approx 5.1 \cdot 10^{-16}$ cm^3/sec.

From this analysis, one may conclude that if all of the ion-ion collisions in a system could be made to occur at the peak in the reaction cross section, the value of $\langle \sigma v \rangle_{fus}$ could be enhanced over that of the Maxwellian-averaged case by a factor of between approximately 2 and 4, depending on the particular fuel involved. Unfortunately, the exploitation of this mechanism for boosting the fusion rate would require the maintenance of highly non-Maxwellian ion distributions, strong velocity anisotropy, and/or energy decoupling between the two ion species. As has been shown in Chapters 3 and 5, these things cannot be accomplished to even a moderate degree for fuels other than D-T.

Appendix B

Useful Integrals

This appendix contains integrals which are useful at several points in the thesis, but especially in Chapter 3. Although one might look them up in a table of integrals or work them out by oneself, these integrals are used with such wild abandon in the thesis that it has been decided to provide them here for the convenience of the reader who actually feels inclined to check some of the calculations which have been presented.

B.1 Integrals from 0 to ∞

$$\int_0^\infty dw e^{-w^2} = \frac{\sqrt{\pi}}{2} . \tag{B.1}$$

$$\int_0^\infty dw w e^{-w^2} = \frac{1}{2} . \tag{B.2}$$

$$\int_0^\infty dw w^2 e^{-w^2} = \frac{\sqrt{\pi}}{4} . \tag{B.3}$$

$$\int_0^\infty dw w^3 e^{-w^2} = \frac{1}{2} \,. \tag{B.4}$$

$$\int_0^\infty dw w^4 e^{-w^2} = \frac{3\sqrt{\pi}}{8} \,. \tag{B.5}$$

B.2 Integrals from 0 to x

$$\int_0^x dw e^{-w^2} \equiv \frac{\sqrt{\pi}}{2} \mathrm{erf}(x) \,. \tag{B.6}$$

$$\begin{aligned} \int_0^x dw w e^{-w^2} &= -\frac{1}{2} \int_0^x \frac{d}{dw}(e^{-w^2}) dw \\ &= \frac{1}{2}\left(1 - e^{-x^2}\right) \,. \end{aligned} \tag{B.7}$$

$$\begin{aligned} \int_0^x dw w^2 e^{-w^2} &= -\frac{1}{2} \int_0^x w \frac{d}{dw}(e^{-w^2}) dw \\ &= -\frac{1}{2} x e^{-x^2} + \frac{1}{2} \int_0^x dw e^{-w^2} \\ &= -\frac{1}{2} x e^{-x^2} + \frac{\sqrt{\pi}}{4} \mathrm{erf}(x) \,. \end{aligned} \tag{B.8}$$

$$\begin{aligned} \int_0^x dw w^3 e^{-w^2} &= -\frac{1}{2} \int_0^x w^2 \frac{d}{dw}(e^{-w^2}) dw \\ &= -\frac{1}{2} x^2 e^{-x^2} + \int_0^x dw w e^{-w^2} \\ &= \frac{1}{2} - \frac{1}{2}\left(x^2 + 1\right) e^{-x^2} \,. \end{aligned} \tag{B.9}$$

$$\begin{aligned}\int_0^x dw w^4 e^{-w^2} &= -\frac{1}{2}\int_0^x w^3 \frac{d}{dw}(e^{-w^2})dw \\ &= -\frac{1}{2}x^3 e^{-x^2} + \frac{3}{2}\int_0^x dw w^2 e^{-w^2} \\ &= \frac{1}{2}\left[-x\left(x^2+\frac{3}{2}\right)e^{-x^2} + \frac{3}{2}\int_0^x dw e^{-w^2}\right] \\ &= \frac{1}{2}\left[-x\left(x^2+\frac{3}{2}\right)e^{-x^2} + \frac{3\sqrt{\pi}}{4}\mathrm{erf}(x)\right] . \end{aligned} \tag{B.10}$$

B.3 Integrals from x to ∞

$$\begin{aligned}\int_x^\infty dw e^{-w^2} &= \int_0^\infty dw e^{-w^2} - \int_0^x dw e^{-w^2} \\ &= \frac{\sqrt{\pi}}{2}\left[1-\mathrm{erf}(x)\right] . \end{aligned} \tag{B.11}$$

$$\begin{aligned}\int_x^\infty dw w e^{-w^2} &= \int_0^\infty dw w e^{-w^2} - \int_0^x dw w e^{-w^2} \\ &= \frac{1}{2}e^{-x^2} . \end{aligned} \tag{B.12}$$

$$\begin{aligned}\int_x^\infty dw w^2 e^{-w^2} &= \int_0^\infty dw w^2 e^{-w^2} - \int_0^x dw w^2 e^{-w^2} \\ &= \frac{\sqrt{\pi}}{4}\left[1-\mathrm{erf}(x)\right] + \frac{1}{2}x e^{-x^2} . \end{aligned} \tag{B.13}$$

$$\int_x^\infty dw w^3 e^{-w^2} = \int_0^\infty dw w^3 e^{-w^2} - \int_0^x dw w^3 e^{-w^2}$$

$$= \frac{1}{2}\left(x^2+1\right)e^{-x^2}\,. \tag{B.14}$$

$$\begin{aligned}\int_x^\infty dw w^4 e^{-w^2} &= \int_0^\infty dw w^4 e^{-w^2} - \int_0^x dw w^4 e^{-w^2} \\ &= \frac{3\sqrt{\pi}}{8}\left[1-\mathrm{erf}(x)\right] + \frac{1}{2}x\left(x^2+\frac{3}{2}\right)e^{-x^2}\,. \end{aligned} \tag{B.15}$$

B.4 Composite integrals

In the integrals below, the definitions $u \equiv v/v_t$, $u_o \equiv v_o/v_t$, and $w \equiv u - u_o$ have been made.

$$\begin{aligned}\int_0^\infty dv v^2 \exp\left\{-\frac{(v-v_o)^2}{v_t^2}\right\} &= v_t^3 \int_0^\infty du u^2 \exp\left\{-(u-u_o)^2\right\} \\ &= v_t^3 \int_{-u_o}^\infty dw (w+u_o)^2 e^{-w^2} \\ &= v_t^3 \left[\int_0^\infty dw w^2 e^{-w^2} + \int_0^{u_o} dw w^2 e^{-w^2} + 2u_o \int_{u_o}^\infty dw w e^{-w^2}\right. \\ &\qquad \left. + u_o^2 \int_0^\infty dw e^{-w^2} + u_o^2 \int_0^{u_o} dw e^{-w^2}\right] \\ &= \frac{\sqrt{\pi}}{4} v_t^3 \left\{(2u_o^2+1)[1+\mathrm{erf}(u_o)] + \frac{2}{\sqrt{\pi}} u_o e^{-u_o^2}\right\}\,. \end{aligned} \tag{B.16}$$

$$\begin{aligned}\int_{v_o}^\infty dv v^2 \exp\left\{-\frac{(v-v_o)^2}{v_t^2}\right\} &= v_t^3 \int_{u_o}^\infty du u^2 \exp\left\{-(u-u_o)^2\right\} \\ &= v_t^3 \int_0^\infty dw (w^2 + 2u_o w + u_o^2) e^{-w^2} \\ &= \frac{\sqrt{\pi}}{4} v_t^3 \left(2u_o^2 + 1 + \frac{4}{\sqrt{\pi}} u_o\right)\,. \end{aligned} \tag{B.17}$$

$$\int_0^{v_o} dv v^2 \exp\left\{-\frac{(v-v_o)^2}{v_t^2}\right\}$$
$$= \int_0^{\infty} dv v^2 \exp\left\{-\frac{(v-v_o)^2}{v_t^2}\right\} - \int_{v_o}^{\infty} dv v^2 \exp\left\{-\frac{(v-v_o)^2}{v_t^2}\right\}$$
$$= \frac{\sqrt{\pi}}{4} v_t^3 \left\{(2u_o^2+1)\mathrm{erf}(u_o) + \frac{2}{\sqrt{\pi}} u_o \left(e^{-u_o^2} - 2\right)\right\} . \qquad \text{(B.18)}$$

$$\int_0^{\infty} dv v^4 \exp\left\{-\frac{(v-v_o)^2}{v_t^2}\right\}$$
$$= v_t^5 \int_0^{\infty} du u^4 \exp\left\{-(u-u_o)^2\right\}$$
$$= v_t^5 \int_{-u_o}^{\infty} dw (w+u_o)^4 e^{-w^2}$$
$$= v_t^5 \int_{-u_o}^{\infty} dw (w^4 + 4u_o w^3 + 6u_o^2 w^2 + 4u_o^3 w + u_o^4) e^{-w^2}$$
$$= v_t^5 \left\{\int_0^{\infty} dw w^4 e^{-w^2} + \int_0^{u_o} dw w^4 e^{-w^2} + 4u_o \int_{u_o}^{\infty} dw w^3 e^{-w^2}\right.$$
$$+6u_o^2 \left(\int_0^{\infty} dw w^2 e^{-w^2} + \int_0^{u_o} dw w^2 e^{-w^2}\right) + 4u_o^3 \int_{u_o}^{\infty} dw w e^{-w^2}$$
$$\left.+u_o^4 \left(\int_0^{\infty} dw e^{-w^2} + \int_0^{u_o} dw e^{-w^2}\right)\right\}$$
$$= \frac{\sqrt{\pi}}{2} v_t^5 \left\{\left(u_o^4 + 3u_o^2 + \frac{3}{4}\right)[1 + \mathrm{erf}(u_o)] + \frac{u_o}{\sqrt{\pi}} e^{-u_o^2} \left(u_o^2 + \frac{5}{2}\right)\right\} .$$
$$\text{(B.19)}$$

$$\int_{v_o}^{\infty} dv v^4 \exp\left\{-\frac{(v-v_o)^2}{v_t^2}\right\} = v_t^5 \int_{u_o}^{\infty} du u^4 \exp\left\{-(u-u_o)^2\right\}$$
$$= v_t^5 \int_0^{\infty} dw (w+u_o)^4 e^{-w^2}$$
$$= v_t^5 \int_0^{\infty} dw (w^4 + 4u_o w^3 + 6u_o^2 w^2 + 4u_o^3 w + u_o^4) e^{-w^2}$$
$$= \frac{\sqrt{\pi}}{2} v_t^5 \left\{\left(u_o^4 + 3u_o^2 + \frac{3}{4}\right) + \frac{4}{\sqrt{\pi}} u_o (u_o^2 + 1)\right\} . \qquad \text{(B.20)}$$

$$\int_0^{v_o} dv v^4 \exp\left\{-\frac{(v-v_o)^2}{v_t^2}\right\}$$
$$= \int_0^{\infty} dv v^4 \exp\left\{-\frac{(v-v_o)^2}{v_t^2}\right\} - \int_{v_o}^{\infty} dv v^4 \exp\left\{-\frac{(v-v_o)^2}{v_t^2}\right\}$$
$$= \frac{\sqrt{\pi}}{2} v_t^5 \left\{ \left(u_o^4 + 3u_o^2 + \frac{3}{4}\right) \mathrm{erf}(u_o) + \frac{u_o}{\sqrt{\pi}} e^{-u_o^2} \left(u_o^2 + \frac{5}{2}\right) \right.$$
$$\left. -\frac{4}{\sqrt{\pi}} u_o (u_o^2 + 1) \right\} . \qquad \text{(B.21)}$$

Appendix C

Algebraic Expressions for the Collision Operators from Chapter 3, and Other Things That Go Bump in the Night

In this appendix there will be presented rather ghastly looking but nonetheless analytical algebraic expressions for the collision operators and other functions relevant to the calculations discussed in Chapter 3.

A number of model velocity distributions have been used to perform the calculations for this thesis. Each distribution has a section in this chapter devoted to it, and the sections go in order of increasing complexity of the distribution functions. The first model distribution function to be considered is actually one which is simpler than any of the distributions which were used in the main body of the thesis. As a result of this relative simplicity, all of the work for this first distribution can be done by hand (up to the point of the final numerical integrations to get the recirculating power levels and

entropy generation rates). Maple was used to manipulate all of the more complicated distributions.

The reader should note that all quantities such as K_1, $\langle E \rangle$, and $(\partial f/\partial t)_{col}$ must be recalculated for each distribution function, so expressions given for them in the case of one distribution should not be mistakenly applied to a different distribution.

C.1 Simple Isotropic Beamlike Distribution

C.1.1 Distribution Function

One of the simplest non-Maxwellian velocity distributions which could be considered is an isotropic, beamlike distribution that has the same "thermal velocity" v_t on each side of the velocity v_o of the peak and that does not include a term to account for the tail of the unseen peak on the negative side of $v = 0$:

$$f(v) = nK_1 \exp\left\{-\frac{m(v-v_o)^2}{2T_o}\right\} = nK_1 \exp\left\{-\frac{(v-v_o)^2}{v_t^2}\right\}, \tag{C.1}$$

in which K_1 is a constant included to normalize the distribution, and the "thermal velocity" has been defined as

$$v_t \equiv \sqrt{\frac{2k_B T_o}{m}}. \tag{C.2}$$

In dealing with this distribution, it is frequently convenient to switch to dimensionless velocity variables $u \equiv v/v_t$ and $u_o \equiv v_o/v_t$.

One may find K_1 from the normalization condition:

$$n = \int_0^\infty dv 4\pi v^2 n K_1 \exp\left\{-\frac{(v-v_o)^2}{v_t^2}\right\}. \tag{C.3}$$

$$\frac{1}{K_1} = \pi^{3/2} v_t^3 \left\{ (2u_o^2 + 1)[1 + \mathrm{erf}(u_o)] + \frac{2}{\sqrt{\pi}} u_o e^{-u_o^2} \right\} . \tag{C.4}$$

It may be seen that in the Maxwellian limit, $u_o = 0$, K_1 reduces to its usual Maxwellian value, yielding

$$f(v) = n \left(\frac{m}{2\pi k_B T_o} \right)^{3/2} \exp\left\{ -\frac{mv^2}{2k_B T_o} \right\} = \frac{n}{\pi^{3/2} v_t^3} \exp\left\{ -\frac{v^2}{v_t^2} \right\} . \tag{C.5}$$

In the opposite limiting case, that of monoenergetic particles with $u_o \gg 1$, one finds that

$$f(v) = \frac{n}{4\pi v_o^2} \frac{1}{\sqrt{\pi}\, v_t} \exp\left\{ -\frac{(v - v_o)^2}{v_t^2} \right\} . \tag{C.6}$$

As $v_t \to 0$ for truly monoenergetic particles, this expression for the distribution function assumes its proper limiting form,

$$f(v) \to \frac{n}{4\pi v_o^2} \delta(v - v_o) . \tag{C.7}$$

C.1.2 Mean Energy

The mean energy of the particles is defined to be:

$$\begin{aligned}
\langle E \rangle &\equiv \frac{1}{n} \int_0^\infty dv 4\pi v^2 \left(\frac{1}{2} m v^2 \right) f(v) \\
&= \frac{1}{n} \int_0^\infty dv 4\pi v^2 \left(\frac{1}{2} m v^2 \right) n K_1 \exp\left\{ -\frac{(v - v_o)^2}{v_t^2} \right\} \\
&= T_o 2\pi^{3/2} v_t^3 K_1 \left\{ \left(u_o^4 + 3u_o^2 + \frac{3}{4} \right) [1 + \mathrm{erf}(u_o)] + \frac{u_o}{\sqrt{\pi}} e^{-u_o^2} \left(u_o^2 + \frac{5}{2} \right) \right\} \\
&= T_o \frac{\left\{ \left(u_o^4 + 3u_o^2 + \frac{3}{4} \right) [1 + \mathrm{erf}(u_o)] + \frac{u_o}{\sqrt{\pi}} e^{-u_o^2} \left(u_o^2 + \frac{5}{2} \right) \right\}}{\left\{ \left(u_o^2 + \frac{1}{2} \right) [1 + \mathrm{erf}(u_o)] + \frac{u_o}{\sqrt{\pi}} e^{-u_o^2} \right\}} .
\end{aligned} \tag{C.8}$$

It is satisfying to note that in the Maxwellian limit, $u_o = 0$, the mean energy reduces to its usual value, $\langle E \rangle = (3/2) T_o$. Similarly, in the monoenergetic limit, $u_o \gg 1$, the mean

energy also assumes its expected value, $\langle E \rangle = mv_o^2/2 \equiv E_o$.

C.1.3 Depletion of Slow Particles

It is useful to note how heavily populated the slow-velocity region of the distribution function is compared with the case of a Maxwellian distribution with the same mean particle energy. (In other words, the Maxwellian has a temperature $T_{Maxw.} \equiv 2\langle E \rangle /3$, where $\langle E \rangle$ is the mean particle energy of the non-Maxwellian.) Dividing the non-Maxwellian distribution function by the Maxwellian one, it is found that

$$\frac{f(v=0)}{f_{Maxwellian}(v=0)} = \frac{\sqrt{2}e^{-u_o^2}\left\{\left(u_o^4+3u_o^2+\frac{3}{4}\right)[1+\mathrm{erf}(u_o)]+\frac{u_o}{\sqrt{\pi}}e^{-u_o^2}\left(u_o^2+\frac{5}{2}\right)\right\}^{3/2}}{3^{3/2}\left\{\left(u_o^2+\frac{1}{2}\right)[1+\mathrm{erf}(u_o)]+\frac{u_o}{\sqrt{\pi}}e^{-u_o^2}\right\}^{5/2}} . \qquad \text{(C.9)}$$

C.1.4 Collision Operator

The Fokker-Planck collision operator for this distribution function may be written (with $w \equiv u - u_o$, $u \equiv v/v_t$, and $u_o \equiv v_o/v_t$),

$$\left(\frac{\partial f}{\partial t}\right)_{col.} = \frac{16\pi^2(Ze)^4 \ln\Lambda n^2 K_1^2}{3m^2} C(u,u_o) , \qquad \text{(C.10)}$$

in which $C(u,u_o)$ has been defined as

$$\begin{aligned} C(u,u_o) \equiv\ & 2e^{-w^2}\left(2w^2+\frac{w}{u}-1\right)\frac{1}{u^3}\int_0^u du' u'^4 e^{-w'^2} \\ & +2e^{-w^2}\left(2w^2-\frac{2w}{u}-1\right)\int_u^\infty du' u' e^{-w'^2} \\ & -6e^{-w^2}\frac{w}{u^2}\int_0^u du' u'^2 e^{-w'^2} + 3e^{-2w^2} \\ =\ & e^{-w^2}\left\{\left(2w^2+\frac{w}{u}-1\right)\frac{1}{u^3}\left[\sqrt{\pi}\left(u_o^4+3u_o^2+\frac{3}{4}\right)(\mathrm{erf}(w)+\mathrm{erf}(u_o))\right.\right. \\ & \left.\left.-\left(w^3+4w^2u_o+6wu_o^2+\frac{3}{2}w+4u_o^3+4u_o\right)e^{-w^2}\right.\right. \end{aligned}$$

$$+\left(u_o^2+\frac{5}{2}\right)u_o e^{-u_o^2}\Bigg]$$
$$-\frac{3w}{u^2}\left(u_o^2+\frac{1}{2}\right)\sqrt{\pi}\left(\mathrm{erf}(w)+\mathrm{erf}(u_o)\right)$$
$$+\left(2w^2-\frac{2w}{u}-1\right)u_o\sqrt{\pi}\left(1-\mathrm{erf}(w)\right)$$
$$+\left(2w^2+\frac{3w^2}{u^2}+\frac{6u_o w}{u^2}-\frac{2w}{u}+2\right)e^{-w^2}-\frac{3u_o w}{u^2}e^{-u_o^2}\Bigg\}\,. \qquad \text{(C.11)}$$

For a Maxwellian distribution with $u_o = 0$, $C(u,0) = 0$ for all u, so $(\partial f/\partial t)_{col.} = 0$ for all u, as expected; a Maxwellian distribution is a stationary solution of the Fokker-Planck equation. Even for non-Maxwellian distributions, it can be shown by numerical integration that this collision operator conserves particles and energy, as required.

C.1.5 Minimum Recirculating Power

The minimum recirculating power required to maintain the non-Maxwellian distribution may be found by using the method discussed in Chapter 3, so that

$$P_{recirc} \equiv -\int_0^{v_d}\left(dv4\pi v^2\right)\left(\frac{1}{2}mv^2\right)\left(\frac{\partial f}{\partial t}\right)_{col}\,, \qquad \text{(C.12)}$$

where the "dividing velocity" v_d is defined as being finite and satisfying the relation:

$$\int_0^{v_d}\left(dv4\pi v^2\right)\left(\frac{\partial f}{\partial t}\right)_{col}=0\,. \qquad \text{(C.13)}$$

The usual definition of the like particle collision time is of use here:

$$\begin{aligned}\tau_{col} &\equiv \frac{\sqrt{m}<E>^{3/2}}{2\sqrt{3\pi}(Ze)^4 n\ln\Lambda}\\ &= \frac{m^2 v_t^3}{4\sqrt{6\pi}(Ze)^4 n\ln\Lambda}\\ &\quad\times\left\{\frac{\left(u_o^4+3u_o^2+\frac{3}{4}\right)\left[1+\mathrm{erf}(u_o)\right]+\frac{u_o}{\sqrt{\pi}}e^{-u_o^2}\left(u_o^2+\frac{5}{2}\right)}{\left(u_o^2+\frac{1}{2}\right)\left[1+\mathrm{erf}(u_o)\right]+\frac{u_o}{\sqrt{\pi}}e^{-u_o^2}}\right\}^{3/2}\,. \qquad \text{(C.14)}\end{aligned}$$

Upon numerical integration of Eq. (C.12) for the particular non-Maxwellian distribution of interest, it is found that the recirculating power may be expressed as

$$P_{recirc} = R_1'(v_o/v_t)\left(\frac{v_o}{v_t}\right)\frac{n\langle E\rangle}{\tau_{col}}\,, \tag{C.15}$$

where $R_1'(u_o)$ is a slowly varying function as given in Table C.1.

u_o	$R_1'(u_o)$		u_o	$R_1'(u_o)$
0.01	0.0634		3	0.148
0.1	0.0657		4	0.168
0.5	0.0764		5	0.183
1	0.0913		10	0.221
1.5	0.107		30	0.253
2	0.122		100	0.265

Table C.1: Selected values of the function $R_1'(u_o)$ from Eq. (C.15) for the recirculating power required to maintain an isotropic, beamlike velocity distribution.

Comparing this function R_1' with the analogous function R_1 given in Table 3.2 for an isotropic, beamlike function in which the tail from the distribution peak on the negative side of $v = 0$ is taken into account, it may be seen that the two functions are essentially identical except at small u_o, where the additional term can actually make a difference.

C.1.6 Entropy Generation Rate

The rate of entropy generation per volume due to particle collisions is given in [63] as

$$\frac{dS}{dt} = -\int_0^\infty dv 4\pi v^2 \ln[f(v)]\left(\frac{\partial f}{\partial t}\right)_{col}\,. \tag{C.16}$$

For the distribution function under consideration, the entropy generation rate is

$$\begin{aligned}\frac{dS}{dt} &= 4\pi \int_0^\infty dv v^2 \left(\frac{\partial f}{\partial t}\right)_{col.} \left[\frac{(v-v_o)^2}{v_t^2} - \ln(nK_1)\right] \\ &= 4\pi v_t^3 \int_0^\infty du u^2 w^2 \left(\frac{\partial f}{\partial t}\right)_{col.} \\ &= \frac{64\pi^3 (Ze)^4 n^2 \ln\Lambda K_1^2 v_t^3}{3m^2} \int_0^\infty du u^2 w^2 C(u, u_o) \, . \end{aligned} \tag{C.17}$$

The entropy generation rate can be cast in a dimensionless form:

$$\begin{aligned}\frac{dS/dt}{n/\tau_{col}} &= \frac{2^{3/2}\left\{\left(u_o^4 + 3u_o^2 + \frac{3}{4}\right)[1 + \mathrm{erf}(u_o)] + \frac{u_o}{\sqrt{\pi}} e^{-u_o^2}\left(u_o^2 + \frac{5}{2}\right)\right\}^{3/2}}{3^{3/2}\sqrt{\pi}\left\{\left(u_o^2 + \frac{1}{2}\right)[1 + \mathrm{erf}(u_o)] + \frac{u_o}{\sqrt{\pi}} e^{-u_o^2}\right\}^{7/2}} \\ &\quad \times \int_0^\infty du u^2 w^2 C(u, u_o) \, . \end{aligned} \tag{C.18}$$

This expression was integrated numerically with Maple. The result of the numerical calculation is that the entropy production may be described by the equation,

$$\frac{dS}{dt} = R_2'(v_o/v_t) \left(\frac{v_o}{v_t}\right)^2 \frac{n}{\tau_{col}} \, , \tag{C.19}$$

in which $R_2'(u_o)$ is a slowly varying function whose values are given in Table C.2.

Except at small values of u_o, where the presence or absence of the term corresponding to the tail of the unseen distribution peak on the negative side of $v = 0$ makes a difference, this function R_2' is essentially identical to the analogous function R_2 given in Table 3.3.

C.2 More Complex Isotropic Beamlike Distribution from Chapter 3

The beamlike but isotropic distribution which was considered in Chapter 3 was more complex than the one which has just been examined. In particular, the beamlike distribution

u_o	$R_2'(u_o)$		u_o	$R_2'(u_o)$
0	0.117		4	0.310
0.1	0.123		5	0.332
0.2	0.129		10	0.390
0.4	0.142		30	0.447
0.6	0.156		100	0.471
0.8	0.169		300	0.479
1	0.183		1000	0.481
1.5	0.214		3000	0.482
2	0.241		10000	0.482
3	0.282		30000	0.482

Table C.2: Selected values of the function $R_2'(u_o)$ from Eq. (C.19) for the entropy generation rate of an isotropic, beamlike velocity distribution.

in Chapter 3 included an extra term to account for the tail of the unseen peak on the negative side of $v = 0$:

$$f(v) = nK_1 \left\{ \exp\left[-\frac{(v - v_o)^2}{v_t^2} \right] + \exp\left[-\frac{(v + v_o)^2}{v_t^2} \right] \right\} . \tag{C.20}$$

This corresponds to the distribution in Eq. (3.11) for the special case of $v_t = v_{ts} = v_{tf}$.

Chapter 3 gave the normalization, mean energy, recirculating power, and entropy generation rates for this distribution function. However, because of length constraints that chapter did not give an explicit algebraic result for the collision operator appropriate for this distribution, so the collision operator will be given here.

The collision operator has been expressed in an essentially dimensionless form (apart from the dimensions of the velocities) by multiplying it by τ_{col}/n. The results presented in this section and in the following sections were obtained by using Maple. (The author was not *quite* crazy enough to do these calculations by hand.) In Maple-ese, the subscripts are not lowered, so one must make mental translations such as $v0 \equiv v_o$, $vts \equiv v_{ts}$, $vtf \equiv v_{tf}$, and $vt \equiv v_t$. The strange-looking factors like %1 stand for short expressions which are given at the end of the equation.

For the faint of heart who would rather look at pictures, graphs of this collision operator for various parameters are given in Figures C-1 through C-3.

$$\left(\frac{\partial f}{\partial t}\right)_{col} \cdot \left(\frac{\tau_{col}}{n}\right) =$$

$$\frac{1}{288} v0 \left(10\, vt^5\, v0\, \mathrm{e}^{\left(-2\frac{(v+v0)^2}{vt^2}\right)} + 10\, vt^5\, v0\, \mathrm{e}^{\left(-2\frac{(v-v0)^2}{vt^2}\right)} - 8\, vt^3\, v0^3\, \%1 \right.$$

$$- 20\, vt^5\, v0\, \%1 + 4\, vt^3\, v0^3\, \mathrm{e}^{\left(-2\frac{(v+v0)^2}{vt^2}\right)} - 8\, v^5\, vt\, \mathrm{e}^{\left(-2\frac{(v-v0)^2}{vt^2}\right)}$$

$$- 6\, v\, vt^5\, \mathrm{e}^{\left(-2\frac{(v+v0)^2}{vt^2}\right)} + 8\, v^5\, vt\, \mathrm{e}^{\left(-2\frac{(v+v0)^2}{vt^2}\right)} - 16\, vt^3\, v^3\, \mathrm{e}^{\left(-2\frac{(v+v0)^2}{vt^2}\right)}$$

$$+ 6\, v\, vt^5\, \mathrm{e}^{\left(-2\frac{(v-v0)^2}{vt^2}\right)} + 16\, vt^3\, v^3\, \mathrm{e}^{\left(-2\frac{(v-v0)^2}{vt^2}\right)} + 4\, vt^3\, v0^3\, \mathrm{e}^{\left(-2\frac{(v-v0)^2}{vt^2}\right)}$$

$$+ 8\, \mathrm{e}^{\left(-\frac{(v+v0)^2}{vt^2}\right)} v^6 \sqrt{\pi}\, \mathrm{erf}\left(\frac{v+v0}{vt}\right)$$

$$+ 8\, \mathrm{e}^{\left(-\frac{(v+v0)^2}{vt^2}\right)} v^3\, v0^3 \sqrt{\pi}\, \mathrm{erf}\left(\frac{v+v0}{vt}\right)$$

$$+ 4\, \mathrm{e}^{\left(-\frac{(v+v0)^2}{vt^2}\right)} v^3\, v0\, vt^2 \sqrt{\pi}\, \mathrm{erf}\left(\frac{v+v0}{vt}\right)$$

$$- 36\, \mathrm{e}^{\left(-\frac{(v-v0)^2}{vt^2}\right)} v0^2\, v^2\, vt^2 \sqrt{\pi}\, \mathrm{erf}\left(\frac{v-v0}{vt}\right)$$

$$+ 12\, \mathrm{e}^{\left(-\frac{(v+v0)^2}{vt^2}\right)} vt^2\, v^4 \sqrt{\pi}\, \mathrm{erf}\left(\frac{v-v0}{vt}\right)$$

$$- 36\, \mathrm{e}^{\left(-\frac{(v-v0)^2}{vt^2}\right)} v0^2\, v^2\, vt^2 \sqrt{\pi}\, \mathrm{erf}\left(\frac{v+v0}{vt}\right)$$

$$+ 16\, \mathrm{e}^{\left(-\frac{(v+v0)^2}{vt^2}\right)} v0^4\, v^2 \sqrt{\pi}\, \mathrm{erf}\left(\frac{v+v0}{vt}\right)$$

$$- 16\, \mathrm{e}^{\left(-\frac{(v-v0)^2}{vt^2}\right)} v0^4\, v^2 \sqrt{\pi}\, \mathrm{erf}\left(\frac{v+v0}{vt}\right)$$

$$+ 6\, v\, \mathrm{e}^{\left(-\frac{(v+v0)^2}{vt^2}\right)} vt^4\, v0 \sqrt{\pi}\, \mathrm{erf}\left(\frac{v-v0}{vt}\right)$$

$$+ 16\, \mathrm{e}^{\left(-\frac{(v+v0)^2}{vt^2}\right)} v0^4\, v^2 \sqrt{\pi}\, \mathrm{erf}\left(\frac{v-v0}{vt}\right)$$

$$+ 6\, \mathrm{e}^{\left(-\frac{(v+v0)^2}{vt^2}\right)} v^2\, vt^4 \sqrt{\pi}\, \mathrm{erf}\left(\frac{v+v0}{vt}\right)$$

$$\left. - 16\, \mathrm{e}^{\left(-\frac{(v-v0)^2}{vt^2}\right)} v0^4\, v^2 \sqrt{\pi}\, \mathrm{erf}\left(\frac{v-v0}{vt}\right) + 20\, vt^3\, v0\, v^2\, \mathrm{e}^{\left(-2\frac{(v-v0)^2}{vt^2}\right)} \right)$$

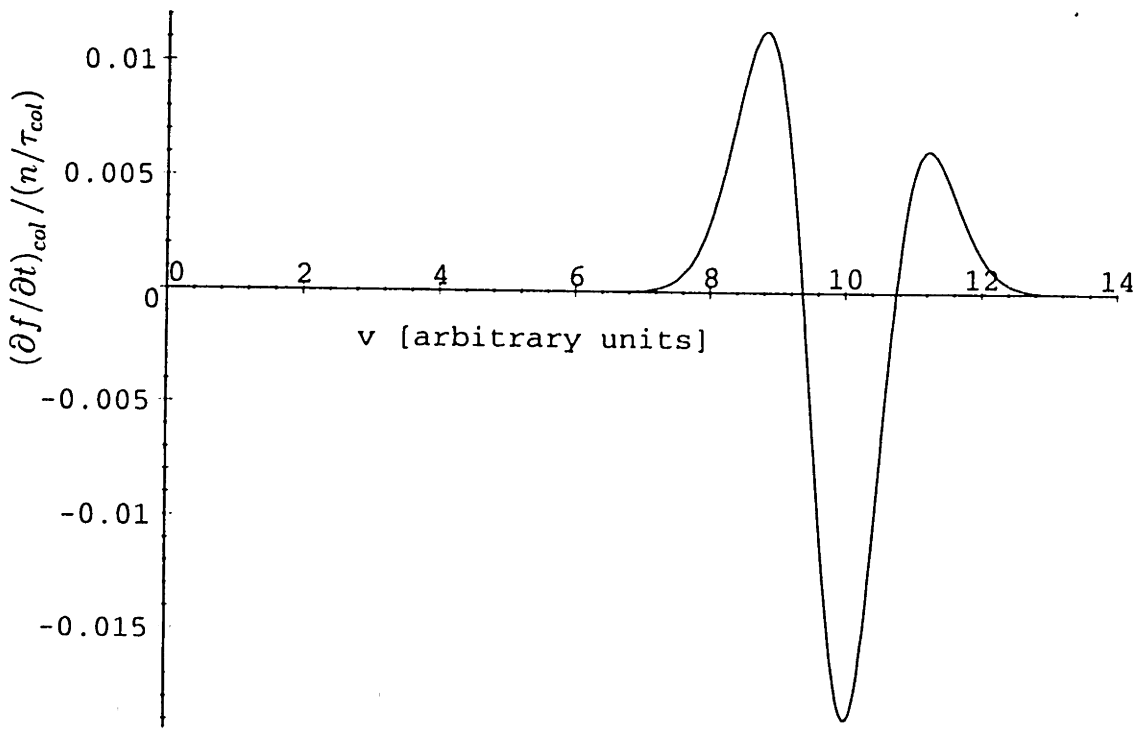

Figure C-1: Collision operator appropriate for the distribution function of Eq. (3.11) with $v_o = 10$ and $v_{ts} = v_{tf} = 1$ (velocities in arbitrary units).

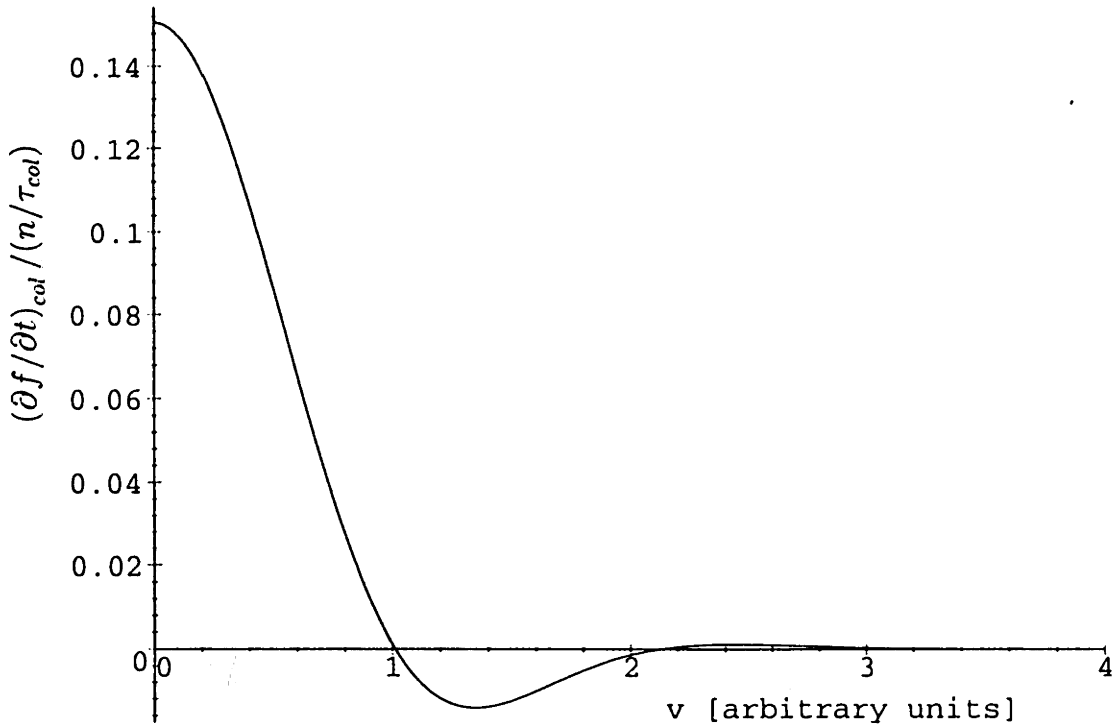

Figure C-2: Collision operator appropriate for the distribution function of Eq. (3.11) with $v_o = 1$ and $v_{ts} = v_{tf} = 1$ (velocities in arbitrary units).

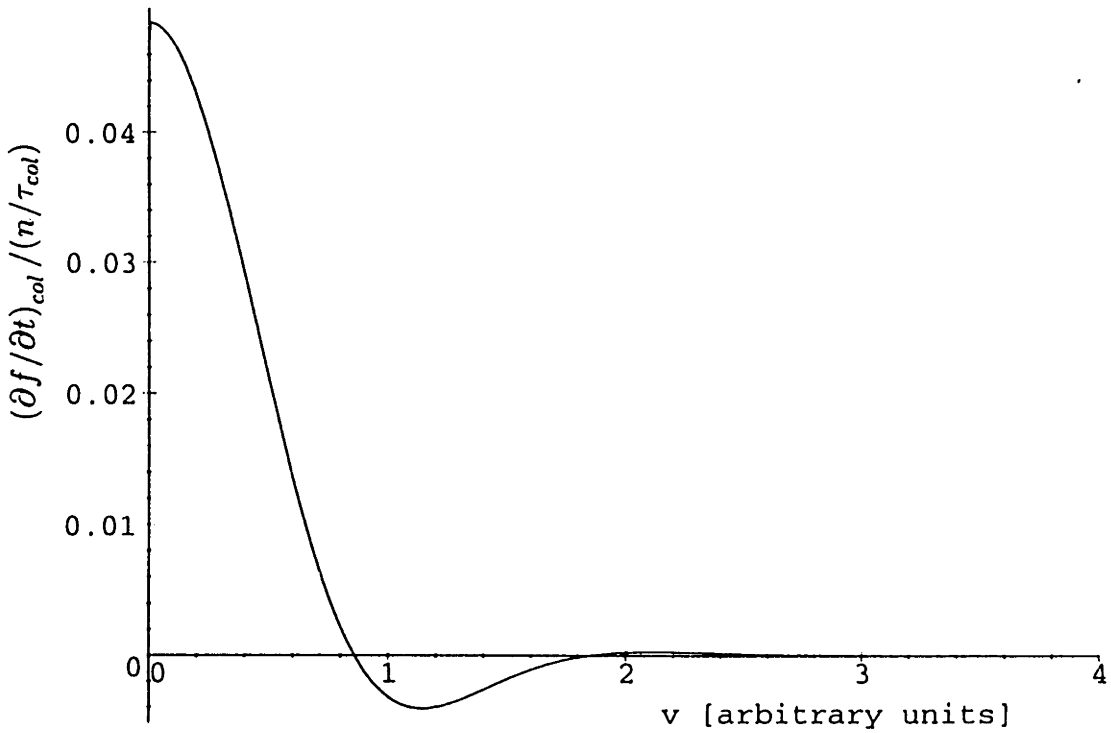

Figure C-3: Collision operator appropriate for the distribution function of Eq. (3.11) with $v_o = 0.5$ and $v_{ts} = v_{tf} = 1$ (velocities in arbitrary units).

$$+ 8\,e^{\left(-\frac{(v+v0)^2}{vt^2}\right)}\,v0^2\,v^4\,\sqrt{\pi}\,\mathrm{erf}\left(\frac{v+v0}{vt}\right)$$

$$- 6\,e^{\left(-\frac{(v-v0)^2}{vt^2}\right)}\,v^2\,vt^4\,\sqrt{\pi}\,\mathrm{erf}\left(\frac{v+v0}{vt}\right) + 8\,v^4\,v0\,vt\,e^{\left(-2\frac{(v+v0)^2}{vt^2}\right)}$$

$$+ 24\,v\,e^{\left(-\frac{(v+v0)^2}{vt^2}\right)}\,vt^2\,v0^3\,\sqrt{\pi}\,\mathrm{erf}\left(\frac{v-v0}{vt}\right)$$

$$+ 8\,v\,e^{\left(-\frac{(v+v0)^2}{vt^2}\right)}\,v0^5\,\sqrt{\pi}\,\mathrm{erf}\left(\frac{v-v0}{vt}\right)$$

$$- 4\,vt^2\,e^{\left(-\frac{(v-v0)^2}{vt^2}\right)}\,v0^4\,\sqrt{\pi}\,\mathrm{erf}\left(\frac{v-v0}{vt}\right)$$

$$- 12\,vt^4\,e^{\left(-\frac{(v-v0)^2}{vt^2}\right)}\,v0^2\,\sqrt{\pi}\,\mathrm{erf}\left(\frac{v+v0}{vt}\right)$$

$$- 4\,vt^2\,e^{\left(-\frac{(v-v0)^2}{vt^2}\right)}\,v0^4\,\sqrt{\pi}\,\mathrm{erf}\left(\frac{v+v0}{vt}\right)$$

$$- 3\,vt^6\,e^{\left(-\frac{(v-v0)^2}{vt^2}\right)}\,\sqrt{\pi}\,\mathrm{erf}\left(\frac{v-v0}{vt}\right)$$

$$- 3\,vt^6\,e^{\left(-\frac{(v-v0)^2}{vt^2}\right)}\,\sqrt{\pi}\,\mathrm{erf}\left(\frac{v+v0}{vt}\right)$$

$$- 12\,vt^4\,e^{\left(-\frac{(v-v0)^2}{vt^2}\right)}\,v0^2\,\sqrt{\pi}\,\mathrm{erf}\left(\frac{v-v0}{vt}\right)$$

$$+ 6\,v\,e^{\left(-\frac{(v-v0)^2}{vt^2}\right)}\,vt^4\,v0\,\sqrt{\pi}\,\mathrm{erf}\left(\frac{v+v0}{vt}\right) + 16\,v\,vt^3\,v0^2\,e^{\left(-2\frac{(v+v0)^2}{vt^2}\right)}$$

$$+ 8\,v\,v0^4\,vt\,e^{\left(-2\frac{(v+v0)^2}{vt^2}\right)} + 20\,e^{\left(-\frac{(v+v0)^2}{vt^2}\right)}\,v^3\,v0\,vt^2\,\sqrt{\pi}\,\mathrm{erf}\left(-\frac{v-v0}{vt}\right)$$

$$- 8\,e^{\left(-\frac{(v+v0)^2}{vt^2}\right)}\,v^6\,\sqrt{\pi}\,\mathrm{erf}\left(\frac{v-v0}{vt}\right)$$

$$- 12\,e^{\left(-\frac{(v+v0)^2}{vt^2}\right)}\,vt^2\,v^4\,\sqrt{\pi}\,\mathrm{erf}\left(\frac{v+v0}{vt}\right)$$

$$+ 16\,e^{\left(-\frac{(v+v0)^2}{vt^2}\right)}\,v0\,v^5\,\sqrt{\pi}\,\mathrm{erf}\left(\frac{v+v0}{vt}\right)$$

$$+ 16\,e^{\left(-\frac{(v-v0)^2}{vt^2}\right)}\,v0\,v^5\,\sqrt{\pi}\,\mathrm{erf}\left(\frac{v-v0}{vt}\right)$$

$$+ 8\,e^{\left(-\frac{(v-v0)^2}{vt^2}\right)}\,v0^2\,v^4\,\sqrt{\pi}\,\mathrm{erf}\left(\frac{v+v0}{vt}\right)$$

$$- 8\,e^{\left(-\frac{(v+v0)^2}{vt^2}\right)}\,v0^2\,v^4\,\sqrt{\pi}\,\mathrm{erf}\left(\frac{v-v0}{vt}\right)$$

$$
\begin{aligned}
&- 8\,\mathrm{e}^{\left(-\frac{(v-v0)^2}{vt^2}\right)}\,v0^2\,v^4\,\sqrt{\pi}\,\mathrm{erf}\left(\frac{v-v0}{vt}\right)\\
&- 6\,\mathrm{e}^{\left(-\frac{(v-v0)^2}{vt^2}\right)}\,v^2\,vt^4\,\sqrt{\pi}\,\mathrm{erf}\left(\frac{v-v0}{vt}\right)\\
&+ 8\,\mathrm{e}^{\left(-\frac{(v-v0)^2}{vt^2}\right)}\,v^3\,v0^3\,\sqrt{\pi}\,\mathrm{erf}\left(\frac{v-v0}{vt}\right)\\
&+ 8\,\mathrm{e}^{\left(-\frac{(v-v0)^2}{vt^2}\right)}\,v^3\,v0^3\,\sqrt{\pi}\,\mathrm{erf}\left(\frac{v+v0}{vt}\right) + 20\,vt^3\,v0\,v^2\,\mathrm{e}^{\left(-2\,\frac{(v+v0)^2}{vt^2}\right)}\\
&- 8\,v\,v0^4\,vt\,\mathrm{e}^{\left(-2\,\frac{(v-v0)^2}{vt^2}\right)} - 16\,v\,vt^3\,v0^2\,\mathrm{e}^{\left(-2\,\frac{(v-v0)^2}{vt^2}\right)}\\
&+ 8\,v0^3\,vt\,v^2\,\mathrm{e}^{\left(-2\,\frac{(v-v0)^2}{vt^2}\right)} + 12\,\mathrm{e}^{\left(-\frac{(v-v0)^2}{vt^2}\right)}\,vt^2\,v^4\,\sqrt{\pi}\,\mathrm{erf}\left(\frac{v-v0}{vt}\right)\\
&+ 4\,vt^2\,\mathrm{e}^{\left(-\frac{(v+v0)^2}{vt^2}\right)}\,v0^4\,\sqrt{\pi}\,\mathrm{erf}\left(\frac{v+v0}{vt}\right)\\
&+ 12\,vt^4\,\mathrm{e}^{\left(-\frac{(v+v0)^2}{vt^2}\right)}\,v0^2\,\sqrt{\pi}\,\mathrm{erf}\left(\frac{v-v0}{vt}\right)\\
&+ 12\,vt^4\,\mathrm{e}^{\left(-\frac{(v+v0)^2}{vt^2}\right)}\,v0^2\,\sqrt{\pi}\,\mathrm{erf}\left(\frac{v+v0}{vt}\right)\\
&- 16\,\mathrm{e}^{\left(-\frac{(v+v0)^2}{vt^2}\right)}\,v0\,v^5\,\sqrt{\pi}\,\mathrm{erf}\left(\frac{v-v0}{vt}\right)\\
&+ 8\,v\,\mathrm{e}^{\left(-\frac{(v+v0)^2}{vt^2}\right)}\,v0^5\,\sqrt{\pi}\,\mathrm{erf}\left(\frac{v+v0}{vt}\right)\\
&+ 6\,v\,\mathrm{e}^{\left(-\frac{(v+v0)^2}{vt^2}\right)}\,vt^4\,v0\,\sqrt{\pi}\,\mathrm{erf}\left(\frac{v+v0}{vt}\right)\\
&+ 8\,v\,\mathrm{e}^{\left(-\frac{(v-v0)^2}{vt^2}\right)}\,v0^5\,\sqrt{\pi}\,\mathrm{erf}\left(\frac{v+v0}{vt}\right)\\
&+ 8\,v\,\mathrm{e}^{\left(-\frac{(v-v0)^2}{vt^2}\right)}\,v0^5\,\sqrt{\pi}\,\mathrm{erf}\left(\frac{v-v0}{vt}\right)\\
&- 8\,\mathrm{e}^{\left(-\frac{(v-v0)^2}{vt^2}\right)}\,v^6\,\sqrt{\pi}\,\mathrm{erf}\left(\frac{v-v0}{vt}\right) + 8\,\mathrm{e}^{\left(-\frac{(v-v0)^2}{vt^2}\right)}\,v^6\,\sqrt{\pi}\,\mathrm{erf}\left(\frac{v+v0}{vt}\right)\\
&- 48\,v^4\,v0\,vt\,\%1 - 16\,\mathrm{e}^{\left(-\frac{(v-v0)^2}{vt^2}\right)}\,v0\,v^5\,\sqrt{\pi}\,\mathrm{erf}\left(\frac{v+v0}{vt}\right)\\
&+ 8\,v0^3\,vt\,v^2\,\mathrm{e}^{\left(-2\,\frac{(v+v0)^2}{vt^2}\right)} + 24\,v\,\mathrm{e}^{\left(-\frac{(v+v0)^2}{vt^2}\right)}\,vt^2\,v0^3\,\sqrt{\pi}\,\mathrm{erf}\left(\frac{v+v0}{vt}\right)\\
&+ 3\,vt^6\,\mathrm{e}^{\left(-\frac{(v+v0)^2}{vt^2}\right)}\,\sqrt{\pi}\,\mathrm{erf}\left(\frac{v+v0}{vt}\right)\\
&+ 36\,\mathrm{e}^{\left(-\frac{(v+v0)^2}{vt^2}\right)}\,v0^2\,v^2\,vt^2\,\sqrt{\pi}\,\mathrm{erf}\left(\frac{v-v0}{vt}\right)
\end{aligned}
$$

$$
\begin{aligned}
&+ 6\,\mathrm{e}^{\left(-\frac{(v+v0)^2}{vt^2}\right)}\, v^2\, vt^4\, \sqrt{\pi}\,\mathrm{erf}\left(\frac{v-v0}{vt}\right) \\
&+ 36\,\mathrm{e}^{\left(-\frac{(v+v0)^2}{vt^2}\right)}\, v0^2\, v^2\, vt^2\, \sqrt{\pi}\,\mathrm{erf}\left(\frac{v+v0}{vt}\right) \\
&+ 24\, v\,\mathrm{e}^{\left(-\frac{(v-v0)^2}{vt^2}\right)}\, vt^2\, v0^3\, \sqrt{\pi}\,\mathrm{erf}\left(\frac{v+v0}{vt}\right) \\
&+ 24\, v\,\mathrm{e}^{\left(-\frac{(v-v0)^2}{vt^2}\right)}\, vt^2\, v0^3\, \sqrt{\pi}\,\mathrm{erf}\left(\frac{v-v0}{vt}\right) \\
&+ 6\, v\,\mathrm{e}^{\left(-\frac{(v-v0)^2}{vt^2}\right)}\, vt^4\, v0\, \sqrt{\pi}\,\mathrm{erf}\left(\frac{v-v0}{vt}\right) \\
&+ 20\,\mathrm{e}^{\left(-\frac{(v-v0)^2}{vt^2}\right)}\, v^3\, v0\, vt^2\, \sqrt{\pi}\,\mathrm{erf}\left(\frac{v+v0}{vt}\right) \\
&+ 4\,\mathrm{e}^{\left(-\frac{(v-v0)^2}{vt^2}\right)}\, v^3\, v0\, vt^2\, \sqrt{\pi}\,\mathrm{erf}\left(\frac{v-v0}{vt}\right) \\
&- 12\,\mathrm{e}^{\left(-\frac{(v-v0)^2}{vt^2}\right)}\, vt^2\, v^4\, \sqrt{\pi}\,\mathrm{erf}\left(\frac{v+v0}{vt}\right) - 48\, v0^3\, vt\, v^2\, \%1 \\
&+ 3\, vt^6\,\mathrm{e}^{\left(-\frac{(v+v0)^2}{vt^2}\right)}\, \sqrt{\pi}\,\mathrm{erf}\left(\frac{v-v0}{vt}\right) \\
&+ 4\, vt^2\,\mathrm{e}^{\left(-\frac{(v+v0)^2}{vt^2}\right)}\, v0^4\, \sqrt{\pi}\,\mathrm{erf}\left(\frac{v-v0}{vt}\right) - 88\, vt^3\, v0\, v^2\, \%1 \\
&+ 8\, v^4\, v0\, vt\,\mathrm{e}^{\left(-2\,\frac{(v-v0)^2}{vt^2}\right)} + 8\,\mathrm{e}^{\left(-\frac{(v+v0)^2}{vt^2}\right)}\, v^3\, v0^3\, \sqrt{\pi}\,\mathrm{erf}\left(\frac{v-v0}{vt}\right)\Bigg)\sqrt{4} \\
&\left(\frac{4\, v0^4 + 12\, vt^2\, v0^2 + 3\, vt^4}{2\, v0^2 + vt^2}\right)^{3/2} \sqrt{3}\Big/\left(vt^5\, \pi^{3/2}\, (2\, v0^2 + vt^2)^2\, v^4\right) \\
&\%1 := \mathrm{e}^{\left(-2\,\frac{v^2+v0^2}{vt^2}\right)}\,.
\end{aligned}
$$

C.3 Complete Distribution Function of Eq. (3.11) with Arbitrary Values of v_o, v_{ts}, and v_{tf}

The distribution which was used in the previous section was a special case of the velocity distribution given in Eq. (3.11). The collision operator can also be worked out for the more general case in which v_o, v_{ts}, and v_{tf} have arbitrary values, so that the distribution

is

$$f(v) = \begin{cases} nK_1\{\exp[-(v-v_o)^2/v_{ts}^2] + \exp[-(v+v_o)^2/v_{ts}^2]\} & \text{for } v < v_o \\ nK_1\{\exp[-(v-v_o)^2/v_{tf}^2] + \exp[-(v+v_o)^2/v_{ts}^2]\} & \text{for } v \geq v_o, \end{cases} \tag{C.21}$$

A graph of the collision operator for the particular case in which $v_o = 3$, $v_{ts} = 1$, and $v_{tf} = 9$ is shown in Figure C-4 to illustrate the qualitative appearance of the collision operator for a class of distribution functions which is of particular interest, as described in Chapter 3.

In the general case, the collision operator for $v < v_o$ is

$$\left(\frac{\partial f}{\partial t}\right)_{col} \cdot \left(\frac{\tau_{col}}{n}\right) =$$

$$-\frac{1}{72}\left(20\, vts^6\, v0^2\, \%1 + 8\, e^{\left(-\frac{(v+v0)^2}{vts^2}\right)} v^6\, vts^2 - 12\, e^{\left(-\frac{(v+v0)^2}{vts^2}\right)} vts^4\, v^4\right.$$

$$- 8\, e^{\left(-\frac{(v-v0)^2}{vts^2}\right)} v^6\, vtf^2 + 8\, e^{\left(-\frac{(v-v0)^2}{vts^2}\right)} v^6\, vts^2 - 8\, v^5\, v0\, vts^2\, e^{\left(-2\frac{(v+v0)^2}{vts^2}\right)}$$

$$- 8\, e^{\left(-\frac{(v-v0)^2}{vts^2}\right)} v^6\, vts\, v0\, \sqrt{\pi}\, \mathrm{erf}\left(\frac{v+v0}{vts}\right)$$

$$- 8\, e^{\left(-\frac{(v-vC)^2}{vts^2}\right)} v^3\, vts\, v0^4\, \sqrt{\pi}\, \mathrm{erf}\left(\frac{v-v0}{vts}\right)$$

$$- 20\, e^{\left(-\frac{(v-v0)^2}{vts^2}\right)} v^3\, v0^2\, vts^3\, \sqrt{\pi}\, \mathrm{erf}\left(\frac{v+v0}{vts}\right)$$

$$- 8\, e^{\left(-\frac{(v+v0)^2}{vts^2}\right)} v^3\, vts\, v0^4\, \sqrt{\pi}\, \mathrm{erf}\left(\frac{v-v0}{vts}\right)$$

$$- 4\, e^{\left(-\frac{(v+v0)^2}{vts^2}\right)} v^3\, v0^2\, vts^3\, \sqrt{\pi}\, \mathrm{erf}\left(\frac{v+v0}{vts}\right)$$

$$- 8\, e^{\left(-\frac{(v+v0)^2}{vts^2}\right)} v^3\, vts\, v0^4\, \sqrt{\pi}\, \mathrm{erf}\left(\frac{v+v0}{vts}\right)$$

$$- 20\, e^{\left(-\frac{(v+v0)^2}{vts^2}\right)} v^3\, v0^2\, vts^3\, \sqrt{\pi}\, \mathrm{erf}\left(\frac{v-v0}{vts}\right)$$

$$- 8\, e^{\left(-\frac{(v-v0)^2}{vts^2}\right)} v^3\, vts\, v0^4\, \sqrt{\pi}\, \mathrm{erf}\left(\frac{v+v0}{vts}\right)$$

$$\left. - 4\, e^{\left(-\frac{(v-v0)^2}{vts^2}\right)} v^3\, v0^2\, vts^3\, \sqrt{\pi}\, \mathrm{erf}\left(\frac{v-v0}{vts}\right) - 8\, e^{\left(-\frac{(v-v0)^2}{vts^2}\right)} v0^2\, vtf^2\, v^4\right.$$

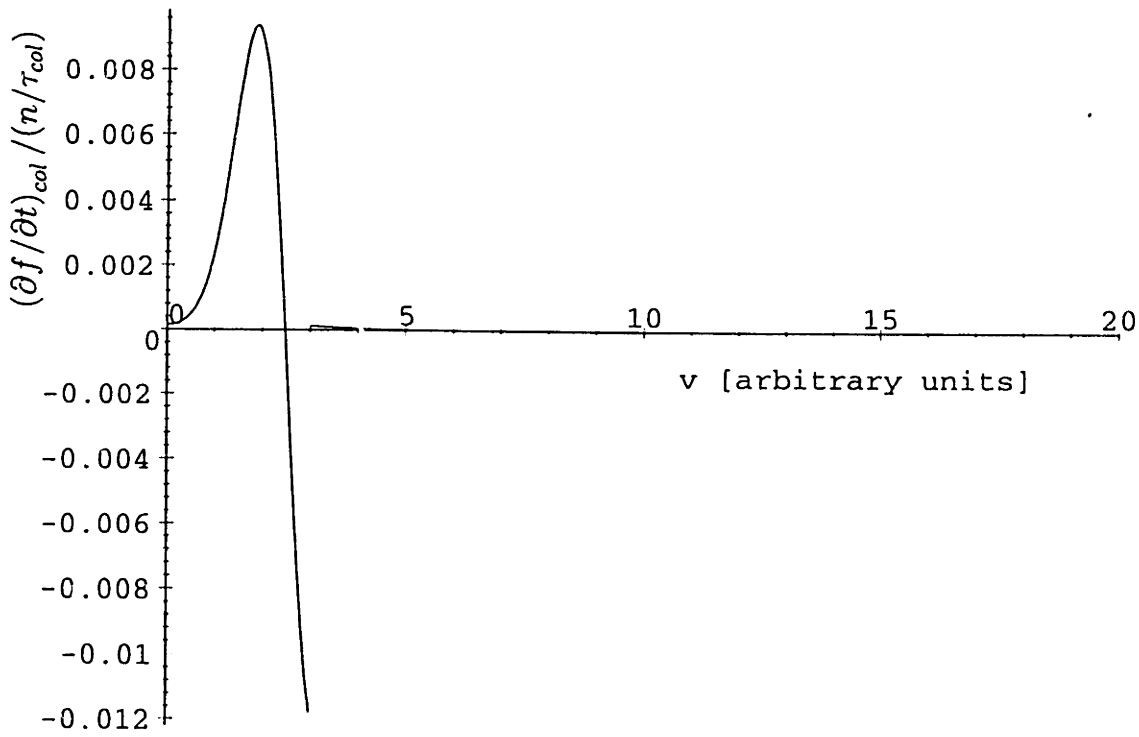

Figure C-4: Collision operator appropriate for the distribution function of Eq. (3.11) with $v_o = 3$, $v_{ts} = 1$, and $v_{tf} = 9$ (velocities in arbitrary units).

$$
\begin{aligned}
&- 8\,e^{\left(-\frac{(v-v0)^2}{vts^2}\right)}\, v0^3\, vtf\, \sqrt{\pi}\, v^4 \\
&+ 8\,e^{\left(-\frac{(v-v0)^2}{vts^2}\right)}\, v0^3\, vts\, \sqrt{\pi}\, \mathrm{erf}\left(\frac{v-v0}{vts}\right) v^4 \\
&- 8\,e^{\left(-\frac{(v-v0)^2}{vts^2}\right)}\, v0^3\, vts\, \sqrt{\pi}\, \mathrm{erf}\left(\frac{v+v0}{vts}\right) v^4 \\
&+ 8\,e^{\left(-\frac{(v-v0)^2}{vts^2}\right)}\, v0^3\, vts\, \sqrt{\pi}\, v^4 \\
&+ 6\,e^{\left(-\frac{(v-v0)^2}{vts^2}\right)}\, v0\, v^2\, vts^5\, \sqrt{\pi}\, \mathrm{erf}\left(\frac{v-v0}{vts}\right) \\
&+ 6\,e^{\left(-\frac{(v-v0)^2}{vts^2}\right)}\, v0\, v^2\, vts^5\, \sqrt{\pi}\, \mathrm{erf}\left(\frac{v+v0}{vts}\right) \\
&+ 12\,e^{\left(-\frac{(v-v0)^2}{vts^2}\right)}\, vts^2\, vtf^2\, v^4 + 12\,e^{\left(-\frac{(v-v0)^2}{vts^2}\right)}\, vts^2\, vtf\, v0\, \sqrt{\pi}\, v^4 \\
&- 12\,e^{\left(-\frac{(v-v0)^2}{vts^2}\right)}\, vts^3\, v0\, \sqrt{\pi}\, \mathrm{erf}\left(\frac{v-v0}{vts}\right) v^4 \\
&+ 12\,e^{\left(-\frac{(v-v0)^2}{vts^2}\right)}\, vts^3\, v0\, \sqrt{\pi}\, \mathrm{erf}\left(\frac{v+v0}{vts}\right) v^4 \\
&- 12\,e^{\left(-\frac{(v-v0)^2}{vts^2}\right)}\, vts^3\, v0\, \sqrt{\pi}\, v^4 \\
&- 24\,v\,e^{\left(-\frac{(v+v0)^2}{vts^2}\right)}\, vts^3\, v0^4\, \sqrt{\pi}\, \mathrm{erf}\left(\frac{v-v0}{vts}\right) \\
&+ 8\,e^{\left(-\frac{(v+v0)^2}{vts^2}\right)}\, v0^2\, vts^2\, v^4 - 8\,e^{\left(-\frac{(v+v0)^2}{vts^2}\right)}\, v0^2\, vtf^2\, v^4 \\
&- 8\,e^{\left(-\frac{(v+v0)^2}{vts^2}\right)}\, v0^3\, vtf\, \sqrt{\pi}\, v^4 \\
&+ 8\,e^{\left(-\frac{(v+v0)^2}{vts^2}\right)}\, v0^3\, vts\, \sqrt{\pi}\, \mathrm{erf}\left(\frac{v-v0}{vts}\right) v^4 \\
&- 8\,e^{\left(-\frac{(v+v0)^2}{vts^2}\right)}\, v0^3\, vts\, \sqrt{\pi}\, \mathrm{erf}\left(\frac{v+v0}{vts}\right) v^4 \\
&+ 8\,e^{\left(-\frac{(v+v0)^2}{vts^2}\right)}\, v0^3\, vts\, \sqrt{\pi}\, v^4 \\
&- 6\,e^{\left(-\frac{(v+v0)^2}{vts^2}\right)}\, v0\, v^2\, vts^5\, \sqrt{\pi}\, \mathrm{erf}\left(\frac{v-v0}{vts}\right) - 8\,e^{\left(-\frac{(v-v0)^2}{vts^2}\right)}\, v^6\, vtf\, v0\, \sqrt{\pi} \\
&+ 8\,e^{\left(-\frac{(v-v0)^2}{vts^2}\right)}\, v^6\, vts\, v0\, \sqrt{\pi} \\
&+ 8\,e^{\left(-\frac{(v-v0)^2}{vts^2}\right)}\, v^6\, vts\, v0\, \sqrt{\pi}\, \mathrm{erf}\left(\frac{v-v0}{vts}\right) - 8\,e^{\left(-\frac{(v+v0)^2}{vts^2}\right)}\, v^6\, vtf\, v0\, \sqrt{\pi} \\
&+ 8\,e^{\left(-\frac{(v+v0)^2}{vts^2}\right)}\, v^6\, vts\, v0\, \sqrt{\pi}\, \mathrm{erf}\left(\frac{v-v0}{vts}\right)
\end{aligned}
$$

$$
\begin{aligned}
&+ 8\,e^{\left(-\frac{(v+v0)^2}{vts^2}\right)}\, v^6\, vts\, v0\, \sqrt{\pi} + 16\,e^{\left(-\frac{(v-v0)^2}{vts^2}\right)}\, v0^2\, v^5\, vtf\, \sqrt{\pi} \\
&+ 16\,e^{\left(-\frac{(v+v0)^2}{vts^2}\right)}\, v0\, v^5\, vts^2 \\
&- 36\,e^{\left(-\frac{(v+v0)^2}{vts^2}\right)}\, v0^3\, v^2\, vts^3\, \sqrt{\pi}\, \mathrm{erf}\left(\frac{v+v0}{vts}\right) \\
&- 16\,e^{\left(-\frac{(v+v0)^2}{vts^2}\right)}\, v0^5\, v^2\, vts\, \sqrt{\pi}\, \mathrm{erf}\left(\frac{v+v0}{vts}\right) \\
&- 36\,e^{\left(-\frac{(v+v0)^2}{vts^2}\right)}\, v0^3\, v^2\, vts^3\, \sqrt{\pi}\, \mathrm{erf}\left(\frac{v-v0}{vts}\right) \\
&+ 12\,e^{\left(-\frac{(v+v0)^2}{vts^2}\right)}\, vts^2\, vtf\, v0\, \sqrt{\pi}\, v^4 \\
&- 12\,e^{\left(-\frac{(v+v0)^2}{vts^2}\right)}\, vts^3\, v0\, \sqrt{\pi}\, \mathrm{erf}\left(\frac{v-v0}{vts}\right) v^4 \\
&+ 12\,e^{\left(-\frac{(v+v0)^2}{vts^2}\right)}\, vts^3\, v0\, \sqrt{\pi}\, \mathrm{erf}\left(\frac{v+v0}{vts}\right) v^4 \\
&- 12\,e^{\left(-\frac{(v+v0)^2}{vts^2}\right)}\, vts^3\, v0\, \sqrt{\pi}\, v^4 - 12\,e^{\left(-\frac{(v-v0)^2}{vts^2}\right)}\, vts^4\, v^4 \\
&- 8\,e^{\left(-\frac{(v+v0)^2}{vts^2}\right)}\, v^6\, vtf^2 - 16\,e^{\left(-\frac{(v-v0)^2}{vts^2}\right)}\, v0\, v^5\, vts^2 \\
&+ 16\,e^{\left(-\frac{(v-v0)^2}{vts^2}\right)}\, v0\, v^5\, vtf^2 - 16\,e^{\left(-\frac{(v-v0)^2}{vts^2}\right)}\, v0^2\, v^5\, vts\, \sqrt{\pi}\, \mathrm{erf}\left(\frac{v-v0}{vts}\right) \\
&+ 16\,e^{\left(-\frac{(v-v0)^2}{vts^2}\right)}\, v0^2\, v^5\, vts\, \sqrt{\pi}\, \mathrm{erf}\left(\frac{v+v0}{vts}\right) \\
&- 16\,e^{\left(-\frac{(v-v0)^2}{vts^2}\right)}\, v0^2\, v^5\, vts\, \sqrt{\pi} \\
&+ 16\,e^{\left(-\frac{(v-v0)^2}{vts^2}\right)}\, v0^5\, v^2\, vts\, \sqrt{\pi}\, \mathrm{erf}\left(\frac{v-v0}{vts}\right) \\
&+ 36\,e^{\left(-\frac{(v-v0)^2}{vts^2}\right)}\, v0^3\, v^2\, vts^3\, \sqrt{\pi}\, \mathrm{erf}\left(\frac{v+v0}{vts}\right) \\
&+ 16\,e^{\left(-\frac{(v-v0)^2}{vts^2}\right)}\, v0^5\, v^2\, vts\, \sqrt{\pi}\, \mathrm{erf}\left(\frac{v+v0}{vts}\right) \\
&+ 36\,e^{\left(-\frac{(v-v0)^2}{vts^2}\right)}\, v0^3\, v^2\, vts^3\, \sqrt{\pi}\, \mathrm{erf}\left(\frac{v-v0}{vts}\right) \\
&+ 12\,e^{\left(-\frac{(v+v0)^2}{vts^2}\right)}\, vts^2\, vtf^2\, v^4 - 8\,e^{\left(-\frac{(v+v0)^2}{vts^2}\right)}\, v^6\, vts\, v0\, \sqrt{\pi}\, \mathrm{erf}\left(\frac{v+v0}{vts}\right) \\
&+ 48\, v^4\, v0^2\, vts^2\, \%1 - 6\,e^{\left(-\frac{(v+v0)^2}{vts^2}\right)}\, v0\, v^2\, vts^5\, \sqrt{\pi}\, \mathrm{erf}\left(\frac{v+v0}{vts}\right) \\
&- 16\,e^{\left(-\frac{(v+v0)^2}{vts^2}\right)}\, v0\, v^5\, vtf^2 - 16\,e^{\left(-\frac{(v+v0)^2}{vts^2}\right)}\, v0^2\, v^5\, vtf\, \sqrt{\pi}
\end{aligned}
$$

$$
\begin{aligned}
&+ 16\,e^{\left(-\frac{(v+v0)^2}{vts^2}\right)}\, v0^2\, v^5\, vts\, \sqrt{\pi}\, \mathrm{erf}\left(\frac{v - v0}{vts}\right) \\
&- 16\,e^{\left(-\frac{(v+v0)^2}{vts^2}\right)}\, v0^2\, v^5\, vts\, \sqrt{\pi}\, \mathrm{erf}\left(\frac{v + v0}{vts}\right) \\
&+ 16\,e^{\left(-\frac{(v+v0)^2}{vts^2}\right)}\, v0^2\, v^5\, vts\, \sqrt{\pi} \\
&- 16\,e^{\left(-\frac{(v+v0)^2}{vts^2}\right)}\, v0^5\, v^2\, vts\, \sqrt{\pi}\, \mathrm{erf}\left(\frac{v - v0}{vts}\right) \\
&- 8\, vts^2\, e^{\left(-\frac{(v-v0)^2}{vts^2}\right)}\, v0\, vtf^2\, v^3 - 8\, vts^2\, e^{\left(-\frac{(v-v0)^2}{vts^2}\right)}\, v0^2\, vtf\, \sqrt{\pi}\, v^3 \\
&+ 8\, vts^3\, e^{\left(-\frac{(v-v0)^2}{vts^2}\right)}\, v0^2\, \sqrt{\pi}\, v^3 \\
&+ 4\, vts^3\, e^{\left(-\frac{(v-v0)^2}{vts^2}\right)}\, v0^5\, \sqrt{\pi}\, \mathrm{erf}\left(\frac{v - v0}{vts}\right) \\
&+ 12\, vts^5\, e^{\left(-\frac{(v-v0)^2}{vts^2}\right)}\, v0^3\, \sqrt{\pi}\, \mathrm{erf}\left(\frac{v + v0}{vts}\right) \\
&+ 4\, vts^3\, e^{\left(-\frac{(v-v0)^2}{vts^2}\right)}\, v0^5\, \sqrt{\pi}\, \mathrm{erf}\left(\frac{v + v0}{vts}\right) \\
&+ 12\, vts^5\, e^{\left(-\frac{(v-v0)^2}{vts^2}\right)}\, v0^3\, \sqrt{\pi}\, \mathrm{erf}\left(\frac{v - v0}{vts}\right) \\
&- 3\, vts^7\, e^{\left(-\frac{(v+v0)^2}{vts^2}\right)}\, v0\, \sqrt{\pi}\, \mathrm{erf}\left(\frac{v - v0}{vts}\right) \\
&- 3\, vts^7\, e^{\left(-\frac{(v+v0)^2}{vts^2}\right)}\, v0\, \sqrt{\pi}\, \mathrm{erf}\left(\frac{v + v0}{vts}\right) - 8\, vts^4\, e^{\left(-\frac{(v+v0)^2}{vts^2}\right)}\, v0\, v^3 \\
&+ 8\, vts^2\, e^{\left(-\frac{(v+v0)^2}{vts^2}\right)}\, v0\, vtf^2\, v^3 + 8\, vts^2\, e^{\left(-\frac{(v+v0)^2}{vts^2}\right)}\, v0^2\, vtf\, \sqrt{\pi}\, v^3 \\
&- 8\, vts^3\, e^{\left(-\frac{(v+v0)^2}{vts^2}\right)}\, v0^2\, \sqrt{\pi}\, v^3 \\
&- 4\, vts^3\, e^{\left(-\frac{(v+v0)^2}{vts^2}\right)}\, v0^5\, \sqrt{\pi}\, \mathrm{erf}\left(\frac{v - v0}{vts}\right) \\
&- 12\, vts^5\, e^{\left(-\frac{(v+v0)^2}{vts^2}\right)}\, v0^3\, \sqrt{\pi}\, \mathrm{erf}\left(\frac{v + v0}{vts}\right) + 8\, vts^4\, e^{\left(-\frac{(v-v0)^2}{vts^2}\right)}\, v0\, v^3 \\
&+ 3\, vts^7\, e^{\left(-\frac{(v-v0)^2}{vts^2}\right)}\, v0\, \sqrt{\pi}\, \mathrm{erf}\left(\frac{v - v0}{vts}\right) \\
&+ 3\, vts^7\, e^{\left(-\frac{(v-v0)^2}{vts^2}\right)}\, v0\, \sqrt{\pi}\, \mathrm{erf}\left(\frac{v + v0}{vts}\right) \\
&- 24\, v\, e^{\left(-\frac{(v-v0)^2}{vts^2}\right)}\, vts^3\, v0^4\, \sqrt{\pi}\, \mathrm{erf}\left(\frac{v - v0}{vts}\right)
\end{aligned}
$$

$$
\begin{aligned}
&- 8\,v\,\mathrm{e}^{\left(-\frac{(v+v0)^2}{vts^2}\right)}\,v0^6\,vts\,\sqrt{\pi}\,\mathrm{erf}\left(\frac{v-v0}{vts}\right)\\
&- 8\,v\,\mathrm{e}^{\left(-\frac{(v+v0)^2}{vts^2}\right)}\,v0^6\,vts\,\sqrt{\pi}\,\mathrm{erf}\left(\frac{v+v0}{vts}\right)\\
&- 24\,v\,\mathrm{e}^{\left(-\frac{(v-v0)^2}{vts^2}\right)}\,vts^3\,v0^4\,\sqrt{\pi}\,\mathrm{erf}\left(\frac{v+v0}{vts}\right)\\
&- 6\,v\,\mathrm{e}^{\left(-\frac{(v-v0)^2}{vts^2}\right)}\,vts^5\,v0^2\,\sqrt{\pi}\,\mathrm{erf}\left(\frac{v-v0}{vts}\right)\\
&- 6\,v\,\mathrm{e}^{\left(-\frac{(v-v0)^2}{vts^2}\right)}\,vts^5\,v0^2\,\sqrt{\pi}\,\mathrm{erf}\left(\frac{v+v0}{vts}\right)\\
&- 8\,v\,\mathrm{e}^{\left(-\frac{(v-v0)^2}{vts^2}\right)}\,v0^6\,vts\,\sqrt{\pi}\,\mathrm{erf}\left(\frac{v-v0}{vts}\right)\\
&- 8\,v\,\mathrm{e}^{\left(-\frac{(v-v0)^2}{vts^2}\right)}\,v0^6\,vts\,\sqrt{\pi}\,\mathrm{erf}\left(\frac{v+v0}{vts}\right)\\
&- 6\,v\,\mathrm{e}^{\left(-\frac{(v+v0)^2}{vts^2}\right)}\,vts^5\,v0^2\,\sqrt{\pi}\,\mathrm{erf}\left(\frac{v+v0}{vts}\right)\\
&- 24\,v\,\mathrm{e}^{\left(-\frac{(v+v0)^2}{vts^2}\right)}\,vts^3\,v0^4\,\sqrt{\pi}\,\mathrm{erf}\left(\frac{v+v0}{vts}\right)\\
&- 6\,v\,\mathrm{e}^{\left(-\frac{(v+v0)^2}{vts^2}\right)}\,vts^5\,v0^2\,\sqrt{\pi}\,\mathrm{erf}\left(\frac{v-v0}{vts}\right)\\
&- 4\,vts^3\,\mathrm{e}^{\left(-\frac{(v+v0)^2}{vts^2}\right)}\,v0^5\,\sqrt{\pi}\,\mathrm{erf}\left(\frac{v+v0}{vts}\right)\\
&- 12\,vts^5\,\mathrm{e}^{\left(-\frac{(v+v0)^2}{vts^2}\right)}\,v0^3\,\sqrt{\pi}\,\mathrm{erf}\left(\frac{v-v0}{vts}\right) + 8\,\mathrm{e}^{\left(-\frac{(v-v0)^2}{vts^2}\right)}\,v0^2\,vts^2\,v^4\\
&- 8\,v^4\,v0^2\,vts^2\,\mathrm{e}^{\left(-2\frac{(v+v0)^2}{vts^2}\right)} - 8\,v0^4\,vts^2\,v^2\,\mathrm{e}^{\left(-2\frac{(v+v0)^2}{vts^2}\right)}\\
&- 8\,v0^4\,vts^2\,v^2\,\mathrm{e}^{\left(-2\frac{(v-v0)^2}{vts^2}\right)} + 48\,v0^4\,vts^2\,v^2\,\%1\\
&- 8\,v^4\,v0^2\,vts^2\,\mathrm{e}^{\left(-2\frac{(v-v0)^2}{vts^2}\right)} - 20\,vts^4\,v0^2\,v^2\,\mathrm{e}^{\left(-2\frac{(v-v0)^2}{vts^2}\right)}\\
&+ 88\,vts^4\,v0^2\,v^2\,\%1 - 16\,vts^4\,v0\,v^3\,\mathrm{e}^{\left(-2\frac{(v-v0)^2}{vts^2}\right)} + 8\,vts^4\,v0^4\,\%1\\
&- 4\,vts^4\,v0^4\,\mathrm{e}^{\left(-2\frac{(v+v0)^2}{vts^2}\right)} - 20\,vts^4\,v0^2\,v^2\,\mathrm{e}^{\left(-2\frac{(v+v0)^2}{vts^2}\right)}\\
&+ 16\,vts^4\,v0\,v^3\,\mathrm{e}^{\left(-2\frac{(v+v0)^2}{vts^2}\right)} - 10\,vts^6\,v0^2\,\mathrm{e}^{\left(-2\frac{(v+v0)^2}{vts^2}\right)}\\
&- 10\,vts^6\,v0^2\,\mathrm{e}^{\left(-2\frac{(v-v0)^2}{vts^2}\right)} - 4\,vts^4\,v0^4\,\mathrm{e}^{\left(-2\frac{(v-v0)^2}{vts^2}\right)}\\
&+ 6\,v\,vts^6\,v0\,\mathrm{e}^{\left(-2\frac{(v+v0)^2}{vts^2}\right)} - 6\,v\,vts^6\,v0\,\mathrm{e}^{\left(-2\frac{(v-v0)^2}{vts^2}\right)}\\
&+ 8\,v\,v0^5\,vts^2\,\mathrm{e}^{\left(-2\frac{(v-v0)^2}{vts^2}\right)} + 8\,v^5\,v0\,vts^2\,\mathrm{e}^{\left(-2\frac{(v-v0)^2}{vts^2}\right)}
\end{aligned}
$$

$$
\begin{aligned}
&+ 16\,v\,vts^4\,v0^3\,\mathrm{e}^{\left(-2\frac{(v-v0)^2}{vts^2}\right)} - 8\,v\,v0^5\,vts^2\,\mathrm{e}^{\left(-2\frac{(v+v0)^2}{vts^2}\right)} \\
&- 16\,v\,vts^4\,v0^3\,\mathrm{e}^{\left(-2\frac{(v+v0)^2}{vts^2}\right)}\Bigg)\sqrt{4}\left(\left(3\sqrt{\pi}\,vtf^4 + 16\,vtf^3\,v0\right.\right. \\
&- 3\,vtf^3\,vts\sqrt{\pi} + 12\,vtf^2\,v0^2\sqrt{\pi} - 16\,vtf^2\,vts\,v0 + 3\,vtf^2\sqrt{\pi}\,vts^2 \\
&+ 16\,vtf\,v0^3 - 12\,vtf\,v0^2\,vts\sqrt{\pi} + 16\,vtf\,vts^2\,v0 - 3\,vtf\,vts^3\sqrt{\pi} \\
&\left.\left.+ 4\,v0^4\sqrt{\pi} - 16\,vts\,v0^3 + 12\,vts^2\,v0^2\sqrt{\pi} - 16\,vts^3\,v0 + 3\sqrt{\pi}\,vts^4\right)\right. \\
&\left/\left(\sqrt{\pi}\,vtf^2 + 4\,vtf\,v0 - vtf\,vts\sqrt{\pi} + 2\,v0^2\sqrt{\pi} - 4\,vts\,v0 + \sqrt{\pi}\,vts^2\right)\right) \\
&{}^{3/2}\sqrt{3}\left/\left(\left(2\,v0^2\,vts\sqrt{\pi} + vts^3\sqrt{\pi} - 4\,vts^2\,v0 + 2\,v0^2\,vtf\sqrt{\pi}\right.\right.\right. \\
&\left.\left.\left.+ vtf^3\sqrt{\pi} + 4\,vtf^2\,v0\right)^2 vts^4\,v^4\sqrt{\pi}\right) \\
&\%1 := \mathrm{e}^{\left(-2\frac{v^2+v0^2}{vts^2}\right)}\,.
\end{aligned}
$$

Likewise, the collision operator for $v \geq v_o$ is

$$
\begin{aligned}
&\left(\frac{\partial f}{\partial t}\right)_{col}\cdot\left(\frac{\tau_{col}}{n}\right) = \\
&\quad\frac{1}{72}\left(8\,vtf^4\,v^5\,v0\,vts^2\,\mathrm{e}^{\left(-2\frac{(v+v0)^2}{vts^2}\right)} - 6\,v\,vtf^4\,vts^6\,v0\,\mathrm{e}^{\left(-2\frac{(v+v0)^2}{vts^2}\right)}\right. \\
&\quad+ 8\,vts^6\,v^5\,v0\,\%1 + 6\,v\,vtf^2\,vts^8\,v0\,\%1 \\
&\quad+ 20\,vtf^4\,vts^4\,v0^2\,v^2\,\mathrm{e}^{\left(-2\frac{(v-v0)^2}{vtf^2}\right)} - 12\,vtf^2\,vts^6\,v0\,v^3\,\%1 \\
&\quad- 6\,v\,vtf^8\,vts^2\,v0\,\%1 - 16\,v\,vtf^4\,vts^4\,v0^3\,\mathrm{e}^{\left(-2\frac{(v-v0)^2}{vtf^2}\right)} \\
&\quad+ 6\,v\,vtf^6\,vts^4\,v0\,\mathrm{e}^{\left(-2\frac{(v-v0)^2}{vtf^2}\right)} + 6\,\mathrm{e}^{\left(-\frac{(v-v0)^2}{vtf^2}\right)}\,vts^9\,v^3\sqrt{\pi}\,\mathrm{erf}\left(\frac{v+v0}{vts}\right) \\
&\quad+ 8\,\mathrm{e}^{\left(-\frac{(v-v0)^2}{vtf^2}\right)}\,vts^4\,v^3\,vtf\,v0^4\sqrt{\pi}\,\mathrm{erf}\left(\frac{v-v0}{vtf}\right) \\
&\quad+ 24\,v\,\mathrm{e}^{\left(-\frac{(v+v0)^2}{vts^2}\right)}\,vtf^4\,vts^3\,v0^4\sqrt{\pi}\,\mathrm{erf}\left(\frac{v+v0}{vts}\right) \\
&\quad+ 8\,v\,\mathrm{e}^{\left(-\frac{(v+v0)^2}{vts^2}\right)}\,vtf^4\,v0^6\,vts\sqrt{\pi}\,\mathrm{erf}\left(\frac{v+v0}{vts}\right) \\
&\quad- 32\,v\,\mathrm{e}^{\left(-\frac{(v+v0)^2}{vts^2}\right)}\,vtf^4\,vts^4\,v0^3 + 8\,\mathrm{e}^{\left(-\frac{(v-v0)^2}{vtf^2}\right)}\,vts^4\,v^6\,vtf\,v0\sqrt{\pi} \\
&\quad\left.- 8\,\mathrm{e}^{\left(-\frac{(v-v0)^2}{vtf^2}\right)}\,vts^5\,v^6\,v0\sqrt{\pi} + 32\,v\,\mathrm{e}^{\left(-\frac{(v+v0)^2}{vts^2}\right)}\,vtf^8\,v0^3\right)
\end{aligned}
$$

$$+ 24\,\mathrm{e}^{\left(-\frac{(v-v0)^2}{vtf^2}\right)}\, vts^7\, v^3\, v0^2\, \sqrt{\pi}\,\mathrm{erf}\left(\frac{v+v0}{vts}\right)$$
$$+ 8\,\mathrm{e}^{\left(-\frac{(v-v0)^2}{vtf^2}\right)}\, vts^4\, v^3\, v0\, vtf^4$$
$$+ 4\,\mathrm{e}^{\left(-\frac{(v-v0)^2}{vtf^2}\right)}\, vts^4\, v^3\, v0^2\, vtf^3\, \sqrt{\pi}\,\mathrm{erf}\left(\frac{v-v0}{vtf}\right)$$
$$- 8\,\mathrm{e}^{\left(-\frac{(v-v0)^2}{vtf^2}\right)}\, vts^5\, v0^3\, \sqrt{\pi}\, v^4 - 32\, v\,\mathrm{e}^{\left(-\frac{(v+v0)^2}{vts^2}\right)}\, vtf^4\, v0^5\, vts^2$$
$$+ 24\, v\,\mathrm{e}^{\left(-\frac{(v+v0)^2}{vts^2}\right)}\, vtf^7\, v0^4\, \sqrt{\pi}\,\mathrm{erf}\left(\frac{v-v0}{vtf}\right)$$
$$+ 8\, v\,\mathrm{e}^{\left(-\frac{(v+v0)^2}{vts^2}\right)}\, vtf^5\, v0^6\, \sqrt{\pi}\,\mathrm{erf}\left(\frac{v-v0}{vtf}\right)$$
$$+ 8\, v\, vtf^4\, v0^5\, vts^2\,\mathrm{e}^{\left(-2\,\frac{(v+v0)^2}{vts^2}\right)} - 20\, v\, vtf^8\, v0^3\, \%1$$
$$+ 16\, v\, vtf^4\, vts^4\, v0^3\,\mathrm{e}^{\left(-2\,\frac{(v+v0)^2}{vts^2}\right)}$$
$$+ 6\, v\,\mathrm{e}^{\left(-\frac{(v+v0)^2}{vts^2}\right)}\, vtf^4\, vts^5\, v0^2\, \sqrt{\pi}\,\mathrm{erf}\left(\frac{v+v0}{vts}\right)$$
$$+ 6\, v\,\mathrm{e}^{\left(-\frac{(v+v0)^2}{vts^2}\right)}\, vtf^9\, v0^2\, \sqrt{\pi}\,\mathrm{erf}\left(\frac{v-v0}{vtf}\right)$$
$$+ 8\, v\,\mathrm{e}^{\left(-\frac{(v-v0)^2}{vtf^2}\right)}\, vts^5\, v0^6\, \sqrt{\pi}\,\mathrm{erf}\left(\frac{v+v0}{vts}\right)$$
$$+ 24\, v\,\mathrm{e}^{\left(-\frac{(v-v0)^2}{vtf^2}\right)}\, vts^7\, v0^4\, \sqrt{\pi}\,\mathrm{erf}\left(\frac{v+v0}{vts}\right)$$
$$+ 32\, v\,\mathrm{e}^{\left(-\frac{(v+v0)^2}{vts^2}\right)}\, vtf^6\, v0^5$$
$$+ 8\, v\,\mathrm{e}^{\left(-\frac{(v-v0)^2}{vtf^2}\right)}\, vts^4\, v0^6\, vtf\, \sqrt{\pi}\,\mathrm{erf}\left(\frac{v-v0}{vtf}\right)$$
$$+ 24\, v\,\mathrm{e}^{\left(-\frac{(v-v0)^2}{vtf^2}\right)}\, vtf^3\, vts^4\, v0^4\, \sqrt{\pi}\,\mathrm{erf}\left(\frac{v-v0}{vtf}\right)$$
$$+ 6\, v\,\mathrm{e}^{\left(-\frac{(v-v0)^2}{vtf^2}\right)}\, vts^9\, v0^2\, \sqrt{\pi}\,\mathrm{erf}\left(\frac{v+v0}{vts}\right)$$
$$- 64\,\mathrm{e}^{\left(-\frac{(v+v0)^2}{vts^2}\right)}\, vtf^4\, v0^4\, v^2\, vts^2 - 40\,\mathrm{e}^{\left(-\frac{(v+v0)^2}{vts^2}\right)}\, vtf^4\, v0^2\, v^2\, vts^4$$
$$+ 36\,\mathrm{e}^{\left(-\frac{(v+v0)^2}{vts^2}\right)}\, vtf^4\, v0^3\, v^2\, vts^3\, \sqrt{\pi}\,\mathrm{erf}\left(\frac{v+v0}{vts}\right)$$
$$- 12\,\mathrm{e}^{\left(-\frac{(v-v0)^2}{vtf^2}\right)}\, vtf^2\, vts^5\, v^4\, v0\, \sqrt{\pi}\,\mathrm{erf}\left(\frac{v+v0}{vts}\right)$$
$$+ 64\,\mathrm{e}^{\left(-\frac{(v+v0)^2}{vts^2}\right)}\, vtf^6\, v0^4\, v^2 + 64\,\mathrm{e}^{\left(-\frac{(v+v0)^2}{vts^2}\right)}\, vtf^8\, v0^2\, v^2$$

$$
\begin{aligned}
&- 32\,v\,\mathrm{e}^{\left(-\frac{(v-v0)^2}{vtf^2}\right)}\,vts^6\,v0^5 + 32\,v\,\mathrm{e}^{\left(-\frac{(v-v0)^2}{vtf^2}\right)}\,vts^4\,v0^5\,vtf^2 \\
&- 8\,vts^4\,v^5\,v0\,vtf^2\,\mathrm{e}^{\left(-2\frac{(v-v0)^2}{vtf^2}\right)} \\
&+ 16\,\mathrm{e}^{\left(-\frac{(v+v0)^2}{vts^2}\right)}\,vtf^4\,v0^2\,v^5\,vts\,\sqrt{\pi}\,\mathrm{erf}\left(\frac{v+v0}{vts}\right) \\
&- 16\,\mathrm{e}^{\left(-\frac{(v+v0)^2}{vts^2}\right)}\,vtf^5\,v0^2\,v^5\,\sqrt{\pi}\,\mathrm{erf}\left(\frac{v-v0}{vtf}\right) \\
&- 8\,vtf^5\,vts^2\,\mathrm{e}^{\left(-\frac{(v+v0)^2}{vts^2}\right)}\,v0^2\,\sqrt{\pi}\,v^3 - 16\,vtf^4\,vts^6\,\mathrm{e}^{\left(-\frac{(v+v0)^2}{vts^2}\right)}\,v0^2 \\
&+ 24\,vtf^2\,vts^6\,\mathrm{e}^{\left(-\frac{(v-v0)^2}{vtf^2}\right)}\,v^3\,v0 + 16\,vtf^2\,vts^8\,\mathrm{e}^{\left(-\frac{(v-v0)^2}{vtf^2}\right)}\,v0^2 \\
&+ 6\,\mathrm{e}^{\left(-\frac{(v+v0)^2}{vts^2}\right)}\,vtf^4\,v0\,v^2\,vts^5\,\sqrt{\pi}\,\mathrm{erf}\left(\frac{v+v0}{vts}\right) \\
&+ 16\,\mathrm{e}^{\left(-\frac{(v+v0)^2}{vts^2}\right)}\,vtf^5\,v0^2\,v^5\,\sqrt{\pi} - 16\,\mathrm{e}^{\left(-\frac{(v+v0)^2}{vts^2}\right)}\,vtf^4\,v0^2\,v^5\,vts\,\sqrt{\pi} \\
&+ 32\,\mathrm{e}^{\left(-\frac{(v+v0)^2}{vts^2}\right)}\,vtf^8\,v^3\,v0 + 8\,vts^4\,v^4\,v0^2\,vtf^2\,\mathrm{e}^{\left(-2\frac{(v-v0)^2}{vtf^2}\right)} \\
&- 24\,vts^6\,v^4\,v0^2\,\%1 + 20\,v\,vts^8\,v0^3\,\%1 - 8\,v\,vts^4\,v0^5\,vtf^2\,\mathrm{e}^{\left(-2\frac{(v-v0)^2}{vtf^2}\right)} \\
&+ 8\,v\,vts^6\,v0^5\,\%1 - 12\,vtf^5\,vts^2\,\mathrm{e}^{\left(-\frac{(v+v0)^2}{vts^2}\right)}\,v0^3\,v^2\,\sqrt{\pi}\,\mathrm{erf}\left(\frac{v-v0}{vtf}\right) \\
&+ 32\,v\,\mathrm{e}^{\left(-\frac{(v-v0)^2}{vtf^2}\right)}\,vtf^4\,vts^4\,v0^3 \\
&+ 6\,v\,\mathrm{e}^{\left(-\frac{(v-v0)^2}{vtf^2}\right)}\,vtf^5\,vts^4\,v0^2\,\sqrt{\pi}\,\mathrm{erf}\left(\frac{v-v0}{vtf}\right) - 8\,v\,vtf^6\,v0^5\,\%1 \\
&- 16\,vtf^4\,vts^4\,\mathrm{e}^{\left(-\frac{(v+v0)^2}{vts^2}\right)}\,v0^4 \\
&+ 4\,vtf^5\,vts^2\,\mathrm{e}^{\left(-\frac{(v+v0)^2}{vts^2}\right)}\,v0^5\,\sqrt{\pi}\,\mathrm{erf}\left(\frac{v-v0}{vtf}\right) \\
&+ 4\,vtf^4\,vts^3\,\mathrm{e}^{\left(-\frac{(v+v0)^2}{vts^2}\right)}\,v0^5\,\sqrt{\pi}\,\mathrm{erf}\left(\frac{v+v0}{vts}\right) \\
&+ 12\,vtf^4\,vts^5\,\mathrm{e}^{\left(-\frac{(v+v0)^2}{vts^2}\right)}\,v0^3\,\sqrt{\pi}\,\mathrm{erf}\left(\frac{v+v0}{vts}\right) \\
&- 6\,vtf^7\,vts^2\,\mathrm{e}^{\left(-\frac{(v+v0)^2}{vts^2}\right)}\,v0\,v^2\,\sqrt{\pi}\,\mathrm{erf}\left(\frac{v-v0}{vtf}\right) - 4\,v\,vtf^6\,vts^2\,v0^3\,\%1 \\
&+ 12\,vtf^7\,vts^2\,\mathrm{e}^{\left(-\frac{(v+v0)^2}{vts^2}\right)}\,v0^3\,\sqrt{\pi}\,\mathrm{erf}\left(\frac{v-v0}{vtf}\right) \\
&+ 3\,vtf^4\,vts^7\,\mathrm{e}^{\left(-\frac{(v+v0)^2}{vts^2}\right)}\,v0\,\sqrt{\pi}\,\mathrm{erf}\left(\frac{v+v0}{vts}\right)
\end{aligned}
$$

$$
\begin{aligned}
&- 16\, vtf^6\, vts^4\, e^{\left(-\frac{(v-v0)^2}{vtf^2}\right)}\, v0^2 - 24\, vtf^6\, vts^2\, e^{\left(-\frac{(v+v0)^2}{vts^2}\right)}\, v^3\, v0 \\
&- 16\, vtf^4\, vts^4\, e^{\left(-\frac{(v-v0)^2}{vtf^2}\right)}\, v0^4 + 8\, vtf^4\, vts^3\, e^{\left(-\frac{(v+v0)^2}{vts^2}\right)}\, v0^2\, \sqrt{\pi}\, v^3 \\
&+ 3\, vtf^9\, vts^2\, e^{\left(-\frac{(v+v0)^2}{vts^2}\right)}\, v0\, \sqrt{\pi}\, \mathrm{erf}\left(\frac{v - v0}{vtf}\right) \\
&- 24\, vtf^6\, vts^2\, e^{\left(-\frac{(v+v0)^2}{vts^2}\right)}\, v0^2\, v^2 \\
&- 6\, vtf^2\, vts^7\, e^{\left(-\frac{(v-v0)^2}{vtf^2}\right)}\, v^3\, \sqrt{\pi}\, \mathrm{erf}\left(\frac{v + v0}{vts}\right) \\
&+ 16\, vtf^8\, vts^2\, e^{\left(-\frac{(v+v0)^2}{vts^2}\right)}\, v0^2 \\
&- 12\, vtf^5\, vts^4\, e^{\left(-\frac{(v-v0)^2}{vtf^2}\right)}\, v0^3\, \sqrt{\pi}\, \mathrm{erf}\left(\frac{v - v0}{vtf}\right) \\
&- 4\, vtf^3\, vts^4\, e^{\left(-\frac{(v-v0)^2}{vtf^2}\right)}\, v0^5\, \sqrt{\pi}\, \mathrm{erf}\left(\frac{v - v0}{vtf}\right) \\
&- 4\, vtf^2\, vts^5\, e^{\left(-\frac{(v-v0)^2}{vtf^2}\right)}\, v0^5\, \sqrt{\pi}\, \mathrm{erf}\left(\frac{v + v0}{vts}\right) \\
&+ 16\, vtf^2\, vts^6\, e^{\left(-\frac{(v-v0)^2}{vtf^2}\right)}\, v0^4 \\
&- 12\, vtf^2\, vts^7\, e^{\left(-\frac{(v-v0)^2}{vtf^2}\right)}\, v0^3\, \sqrt{\pi}\, \mathrm{erf}\left(\frac{v + v0}{vts}\right) \\
&- 3\, vtf^7\, vts^4\, e^{\left(-\frac{(v-v0)^2}{vtf^2}\right)}\, v0\, \sqrt{\pi}\, \mathrm{erf}\left(\frac{v - v0}{vtf}\right) \\
&- 4\, vtf^2\, vts^5\, e^{\left(-\frac{(v-v0)^2}{vtf^2}\right)}\, v^3\, v0^2\, \sqrt{\pi}\, \mathrm{erf}\left(\frac{v + v0}{vts}\right) \\
&- 3\, vtf^2\, vts^9\, e^{\left(-\frac{(v-v0)^2}{vtf^2}\right)}\, v0\, \sqrt{\pi}\, \mathrm{erf}\left(\frac{v + v0}{vts}\right) \\
&- 24\, vtf^2\, vts^6\, e^{\left(-\frac{(v-v0)^2}{vtf^2}\right)}\, v0^2\, v^2 + 8\, vtf^3\, vts^4\, e^{\left(-\frac{(v-v0)^2}{vtf^2}\right)}\, v0^2\, \sqrt{\pi}\, v^3 \\
&- 6\, vtf^7\, vts^2\, e^{\left(-\frac{(v+v0)^2}{vts^2}\right)}\, v^3\, \sqrt{\pi}\, \mathrm{erf}\left(\frac{v - v0}{vtf}\right) \\
&+ 12\, e^{\left(-\frac{(v-v0)^2}{vtf^2}\right)}\, vtf^3\, vts^4\, v^4\, v0\, \sqrt{\pi}\, \mathrm{erf}\left(\frac{v - v0}{vtf}\right) \\
&- 8\, vtf^2\, vts^5\, e^{\left(-\frac{(v-v0)^2}{vtf^2}\right)}\, v0^2\, \sqrt{\pi}\, v^3 \\
&+ 12\, vtf^2\, vts^5\, e^{\left(-\frac{(v-v0)^2}{vtf^2}\right)}\, v0^3\, v^2\, \sqrt{\pi}\, \mathrm{erf}\left(\frac{v + v0}{vts}\right) \\
&- 4\, vtf^5\, vts^2\, e^{\left(-\frac{(v+v0)^2}{vts^2}\right)}\, v^3\, v0^2\, \sqrt{\pi}\, \mathrm{erf}\left(\frac{v - v0}{vtf}\right)
\end{aligned}
$$

$$
\begin{aligned}
&+ 16\, vtf^6\, vts^2\, \mathrm{e}^{\left(-\frac{(v+v0)^2}{vts^2}\right)}\, v0^4 \\
&+ 6\, vtf^2\, vts^7\, \mathrm{e}^{\left(-\frac{(v-v0)^2}{vtf^2}\right)}\, v0\, v^2\, \sqrt{\pi}\, \mathrm{erf}\left(\frac{v+v0}{vts}\right) \\
&+ 16\, \mathrm{e}^{\left(-\frac{(v+v0)^2}{vts^2}\right)}\, vtf^5\, v0^5\, v^2\, \sqrt{\pi}\, \mathrm{erf}\left(\frac{v-v0}{vtf}\right) \\
&+ 16\, \mathrm{e}^{\left(-\frac{(v+v0)^2}{vts^2}\right)}\, vtf^4\, v0^5\, v^2\, vts\, \sqrt{\pi}\, \mathrm{erf}\left(\frac{v+v0}{vts}\right) \\
&+ 8\, \mathrm{e}^{\left(-\frac{(v+v0)^2}{vts^2}\right)}\, vtf^5\, v0^3\, \sqrt{\pi}\, v^4 + 8\, \mathrm{e}^{\left(-\frac{(v+v0)^2}{vts^2}\right)}\, vtf^5\, v^6\, v0\, \sqrt{\pi} \\
&+ 8\, \mathrm{e}^{\left(-\frac{(v+v0)^2}{vts^2}\right)}\, vtf^4\, v^6\, vts\, v0\, \sqrt{\pi}\, \mathrm{erf}\left(\frac{v+v0}{vts}\right) \\
&+ 24\, \mathrm{e}^{\left(-\frac{(v+v0)^2}{vts^2}\right)}\, vtf^7\, v^3\, v0^2\, \sqrt{\pi}\, \mathrm{erf}\left(\frac{v-v0}{vtf}\right) \\
&+ 8\, \mathrm{e}^{\left(-\frac{(v+v0)^2}{vts^2}\right)}\, vtf^5\, v^3\, v0^4\, \sqrt{\pi}\, \mathrm{erf}\left(\frac{v-v0}{vtf}\right) \\
&+ 8\, \mathrm{e}^{\left(-\frac{(v+v0)^2}{vts^2}\right)}\, vtf^4\, v^3\, vts\, v0^4\, \sqrt{\pi}\, \mathrm{erf}\left(\frac{v+v0}{vts}\right) \\
&- 8\, \mathrm{e}^{\left(-\frac{(v+v0)^2}{vts^2}\right)}\, vtf^4\, v^6\, vts\, v0\, \sqrt{\pi} \\
&+ 48\, \mathrm{e}^{\left(-\frac{(v+v0)^2}{vts^2}\right)}\, vtf^7\, v0^3\, v^2\, \sqrt{\pi}\, \mathrm{erf}\left(\frac{v-v0}{vtf}\right) \\
&+ 12\, \mathrm{e}^{\left(-\frac{(v+v0)^2}{vts^2}\right)}\, vtf^9\, v0\, v^2\, \sqrt{\pi}\, \mathrm{erf}\left(\frac{v-v0}{vtf}\right) \\
&- 8\, \mathrm{e}^{\left(-\frac{(v+v0)^2}{vts^2}\right)}\, vtf^5\, v0^3\, v^4\, \sqrt{\pi}\, \mathrm{erf}\left(\frac{v-v0}{vtf}\right) \\
&+ 8\, \mathrm{e}^{\left(-\frac{(v+v0)^2}{vts^2}\right)}\, vtf^4\, v0^3\, v^4\, vts\, \sqrt{\pi}\, \mathrm{erf}\left(\frac{v+v0}{vts}\right) \\
&+ 32\, \mathrm{e}^{\left(-\frac{(v+v0)^2}{vts^2}\right)}\, vtf^6\, v^3\, v0^3 - 12\, \mathrm{e}^{\left(-\frac{(v-v0)^2}{vtf^2}\right)}\, vtf^3\, vts^4\, v0\, \sqrt{\pi}\, v^4 \\
&+ 12\, \mathrm{e}^{\left(-\frac{(v-v0)^2}{vtf^2}\right)}\, vtf^2\, vts^5\, v0\, \sqrt{\pi}\, v^4 + 64\, \mathrm{e}^{\left(-\frac{(v-v0)^2}{vtf^2}\right)}\, vts^6\, v0^4\, v^2 \\
&- 8\, \mathrm{e}^{\left(-\frac{(v+v0)^2}{vts^2}\right)}\, vtf^5\, v^6\, v0\, \sqrt{\pi}\, \mathrm{erf}\left(\frac{v-v0}{vtf}\right) \\
&+ 6\, \mathrm{e}^{\left(-\frac{(v+v0)^2}{vts^2}\right)}\, vtf^9\, v^3\, \sqrt{\pi}\, \mathrm{erf}\left(\frac{v-v0}{vtf}\right) \\
&- 48\, \mathrm{e}^{\left(-\frac{(v-v0)^2}{vtf^2}\right)}\, vts^7\, v0^3\, v^2\, \sqrt{\pi}\, \mathrm{erf}\left(\frac{v+v0}{vts}\right)
\end{aligned}
$$

$$
\begin{aligned}
&- 32\,e^{\left(-\frac{(v+v0)^2}{vts^2}\right)}\, vtf^4\, v^3\, vts^2\, v0^3 - 8\,e^{\left(-\frac{(v+v0)^2}{vts^2}\right)}\, vtf^4\, v^3\, v0\, vts^4 \\
&+ 4\,e^{\left(-\frac{(v+v0)^2}{vts^2}\right)}\, vtf^4\, v^3\, v0^2\, vts^3\, \sqrt{\pi}\,\mathrm{erf}\left(\frac{v+v0}{vts}\right) \\
&- 8\,e^{\left(-\frac{(v+v0)^2}{vts^2}\right)}\, vtf^4\, v0^3\, vts\, \sqrt{\pi}\, v^4 - 12\,e^{\left(-\frac{(v+v0)^2}{vts^2}\right)}\, vtf^5\, vts^2\, v0\, \sqrt{\pi}\, v^4 \\
&- 64\,e^{\left(-\frac{(v-v0)^2}{vtf^2}\right)}\, vts^4\, v0^4\, v^2\, vtf^2 - 40\,e^{\left(-\frac{(v-v0)^2}{vtf^2}\right)}\, vts^4\, v0^2\, v^2\, vtf^4 \\
&+ 12\,e^{\left(-\frac{(v+v0)^2}{vts^2}\right)}\, vtf^4\, vts^3\, v0\, \sqrt{\pi}\, v^4 \\
&+ 12\,e^{\left(-\frac{(v+v0)^2}{vts^2}\right)}\, vtf^5\, vts^2\, v^4\, v0\, \sqrt{\pi}\,\mathrm{erf}\left(\frac{v-v0}{vtf}\right) \\
&+ 16\,e^{\left(-\frac{(v-v0)^2}{vtf^2}\right)}\, vts^5\, v0^2\, v^5\, \sqrt{\pi} \\
&- 12\,e^{\left(-\frac{(v-v0)^2}{vtf^2}\right)}\, vts^9\, v0\, v^2\, \sqrt{\pi}\,\mathrm{erf}\left(\frac{v+v0}{vts}\right) \\
&- 16\,e^{\left(-\frac{(v-v0)^2}{vtf^2}\right)}\, vts^4\, v0^2\, v^5\, vtf\, \sqrt{\pi} + 64\,e^{\left(-\frac{(v-v0)^2}{vtf^2}\right)}\, vts^8\, v0^2\, v^2 \\
&+ 16\,e^{\left(-\frac{(v-v0)^2}{vtf^2}\right)}\, vts^4\, v0^2\, v^5\, vtf\, \sqrt{\pi}\,\mathrm{erf}\left(\frac{v-v0}{vtf}\right) \\
&- 36\,e^{\left(-\frac{(v-v0)^2}{vtf^2}\right)}\, vts^4\, v0^3\, v^2\, vtf^3\, \sqrt{\pi}\,\mathrm{erf}\left(\frac{v-v0}{vtf}\right) \\
&- 8\,e^{\left(-\frac{(v-v0)^2}{vtf^2}\right)}\, vts^4\, v^6\, vtf\, v0\, \sqrt{\pi}\,\mathrm{erf}\left(\frac{v-v0}{vtf}\right) \\
&- 6\,e^{\left(-\frac{(v-v0)^2}{vtf^2}\right)}\, vts^4\, v0\, v^2\, vtf^5\, \sqrt{\pi}\,\mathrm{erf}\left(\frac{v-v0}{vtf}\right) \\
&- 12\,e^{\left(-\frac{(v+v0)^2}{vts^2}\right)}\, vtf^4\, vts^3\, v^4\, v0\, \sqrt{\pi}\,\mathrm{erf}\left(\frac{v+v0}{vts}\right) \\
&- 16\,e^{\left(-\frac{(v-v0)^2}{vtf^2}\right)}\, vts^5\, v0^2\, v^5\, \sqrt{\pi}\,\mathrm{erf}\left(\frac{v+v0}{vts}\right) \\
&- 16\,e^{\left(-\frac{(v-v0)^2}{vtf^2}\right)}\, vts^4\, v0^5\, v^2\, vtf\, \sqrt{\pi}\,\mathrm{erf}\left(\frac{v-v0}{vtf}\right) \\
&- 16\,e^{\left(-\frac{(v-v0)^2}{vtf^2}\right)}\, vts^5\, v0^5\, v^2\, \sqrt{\pi}\,\mathrm{erf}\left(\frac{v+v0}{vts}\right) \\
&+ 8\,e^{\left(-\frac{(v-v0)^2}{vtf^2}\right)}\, vts^4\, v0^3\, vtf\, \sqrt{\pi}\, v^4 \\
&- 8\,e^{\left(-\frac{(v-v0)^2}{vtf^2}\right)}\, vts^4\, v0^3\, v^4\, vtf\, \sqrt{\pi}\,\mathrm{erf}\left(\frac{v-v0}{vtf}\right) \\
&+ 8\,e^{\left(-\frac{(v-v0)^2}{vtf^2}\right)}\, vts^5\, v0^3\, v^4\, \sqrt{\pi}\,\mathrm{erf}\left(\frac{v+v0}{vts}\right)
\end{aligned}
$$

$$
\begin{aligned}
&- 32\,\mathrm{e}^{\left(-\frac{(v-v0)^2}{vtf^2}\right)}\,vts^6\,v^3\,v0^3 - 32\,\mathrm{e}^{\left(-\frac{(v-v0)^2}{vtf^2}\right)}\,vts^8\,v^3\,v0 \\
&+ 8\,\mathrm{e}^{\left(-\frac{(v-v0)^2}{vtf^2}\right)}\,vts^5\,v^3\,v0^4\,\sqrt{\pi}\,\mathrm{erf}\left(\frac{v+v0}{vts}\right) - 32\,v\,\mathrm{e}^{\left(-\frac{(v-v0)^2}{vtf^2}\right)}\,vts^8\,v0^3 \\
&+ 32\,\mathrm{e}^{\left(-\frac{(v-v0)^2}{vtf^2}\right)}\,vts^4\,v^3\,vtf^2\,v0^3 \\
&+ 8\,\mathrm{e}^{\left(-\frac{(v-v0)^2}{vtf^2}\right)}\,vts^5\,v^6\,v0\,\sqrt{\pi}\,\mathrm{erf}\left(\frac{v+v0}{vts}\right) - 10\,vtf^8\,vts^2\,v0^2\,\%1 \\
&+ 10\,vtf^4\,vts^6\,v0^2\,\mathrm{e}^{\left(-2\frac{(v+v0)^2}{vts^2}\right)} + 4\,vtf^4\,vts^4\,v0^4\,\mathrm{e}^{\left(-2\frac{(v-v0)^2}{vtf^2}\right)} \\
&+ 4\,vtf^4\,vts^4\,v0^4\,\mathrm{e}^{\left(-2\frac{(v+v0)^2}{vts^2}\right)} - 4\,vtf^6\,vts^2\,v0^4\,\%1 \\
&- 16\,vts^4\,v^3\,v0\,vtf^4\,\mathrm{e}^{\left(-2\frac{(v+v0)^2}{vts^2}\right)} - 12\,vtf^8\,v^4\,\%1 \\
&+ 8\,vtf^4\,v0^4\,v^2\,vts^2\,\mathrm{e}^{\left(-2\frac{(v+v0)^2}{vts^2}\right)} + 10\,vtf^6\,vts^4\,v0^2\,\mathrm{e}^{\left(-2\frac{(v-v0)^2}{vtf^2}\right)} \\
&- 10\,vtf^2\,vts^8\,v0^2\,\%1 - 4\,vtf^2\,vts^6\,v0^4\,\%1 + 24\,vtf^4\,vts^4\,v^4\,\%1 \\
&- 24\,vtf^6\,v0^4\,v^2\,\%1 + 8\,vtf^4\,v^4\,v0^2\,vts^2\,\mathrm{e}^{\left(-2\frac{(v+v0)^2}{vts^2}\right)} \\
&- 44\,vtf^8\,v^3\,v0\,\%1 - 32\,vtf^6\,v^3\,v0^3\,\%1 - 8\,vtf^6\,v^5\,v0\,\%1 \\
&- 52\,vtf^8\,v0^2\,v^2\,\%1 + 20\,vtf^4\,vts^4\,v0^2\,v^2\,\mathrm{e}^{\left(-2\frac{(v+v0)^2}{vts^2}\right)} \\
&- 52\,vts^8\,v0^2\,v^2\,\%1 + 8\,vtf^6\,vts^2\,v0^2\,v^2\,\%1 - 24\,vtf^6\,v^4\,v0^2\,\%1 \\
&+ 8\,vtf^2\,vts^6\,v0^2\,v^2\,\%1 + 16\,vts^4\,v^3\,v0\,vtf^4\,\mathrm{e}^{\left(-2\frac{(v-v0)^2}{vtf^2}\right)} \\
&+ 32\,vts^6\,v^3\,v0^3\,\%1 - 12\,vts^8\,v^4\,\%1 + 8\,vts^4\,v0^4\,v^2\,vtf^2\,\mathrm{e}^{\left(-2\frac{(v-v0)^2}{vtf^2}\right)} \\
&+ 12\,vtf^6\,vts^2\,v^3\,v0\,\%1 - 24\,vts^6\,v0^4\,v^2\,\%1 + 4\,v\,vtf^2\,vts^6\,v0^3\,\%1 \\
&+ 44\,vts^8\,v^3\,v0\,\%1\Big)\,\sqrt{4}\,\Big(\Big(3\,\sqrt{\pi}\,vtf^4 + 16\,vtf^3\,v0 - 3\,vtf^3\,vts\,\sqrt{\pi} \\
&+ 12\,vtf^2\,v0^2\,\sqrt{\pi} - 16\,vtf^2\,vts\,v0 + 3\,vtf^2\,\sqrt{\pi}\,vts^2 + 16\,vtf\,v0^3 \\
&- 12\,vtf\,v0^2\,vts\,\sqrt{\pi} + 16\,vtf\,vts^2\,v0 - 3\,vtf\,vts^3\,\sqrt{\pi} + 4\,v0^4\,\sqrt{\pi} \\
&- 16\,vts\,v0^3 + 12\,vts^2\,v0^2\,\sqrt{\pi} - 16\,vts^3\,v0 + 3\,\sqrt{\pi}\,vts^4\Big)\Big/\Big(\\
&\sqrt{\pi}\,vtf^2 + 4\,vtf\,v0 - vtf\,vts\,\sqrt{\pi} + 2\,v0^2\,\sqrt{\pi} - 4\,vts\,v0 + \sqrt{\pi}\,vts^2\Big)\Big)^{3/2} \\
&\sqrt{3}\Big/\Big(\Big(2\,v0^2\,vts\,\sqrt{\pi} + vts^3\,\sqrt{\pi} - 4\,vts^2\,v0 + 2\,v0^2\,vtf\,\sqrt{\pi} + vtf^3\,\sqrt{\pi} \\
&+ 4\,vtf^2\,v0\Big)^2\,vtf^4\,vts^4\,v^4\,\sqrt{\pi}\Big)
\end{aligned}
$$

$$\%1 := e^{\left(-\frac{vts^2\,v^2+vts^2\,v0^2-2\,vts^2\,v0\,v+vtf^2\,v^2+vtf^2\,v0^2+2\,vtf^2\,v0\,v}{vtf^2\,vts^2}\right)}.$$

C.4 Improved Model Distribution from Chapter 3

Chapter 3 went on to consider an even more general distribution, Eq. (3.53), which is repeated here for the reader's convenience:

$$f(v) = \begin{cases} nK_1 \exp[-(v-v_{o1})^2/v_{ts}^2] & \text{for } v < v_o \\ nK_1\{(1-A)\exp[-(v-v_{o1})^2/v_{tf1}^2] + A\exp[-(v-v_{o2})^2/v_{tf2}^2]\} & \text{for } v \geq v_o. \end{cases}$$

This improved distribution function was used in further optimizations of the electron velocity distribution in ^{3}He plasmas. The distribution has six independently adjustable parameters: v_{o1}, v_{o2}, v_{ts}, v_{tf1}, v_{tf2}, and A. It is assumed that $v_{o2} \geq v_{o1}$. Based on the optimization of the earlier model distribution function to minimize the recirculating power, one can safely choose to set v_{ts} to be as small as allowed by the numerical integration, which turned out to be $v_{ts} = 0.1v_{ti}$, where $v_{ti} \equiv \sqrt{2T_i/m_i}$.

Two local minima of the recirculating power have been found; for one A is small and positive (corresponding to a relatively small positive perturbation of the model distribution function which was previously used), while for the other, A is small and negative (corresponding to a small negative perturbation of the previously used distribution function).

Figures C-5, C-6, and C-7 show the distribution function, collision operator, and collisionally induced velocity-space particle flux, respectively, for the case of the optimum positive perturbation. One should recall that velocities corresponding to zero particle flux are dividing velocities, as discussed in Chapter 3. The graphs only show these functions for velocities v such that $v > v_{o1}$. Below the point $v = v_{o1}$, the distribution function drops off precipitously to zero (with a width of $v_{ts} = 0.01v_{ti}$), causing spikes in the collision operator and particle flux just below the point $v = v_{o1}$; these spikes cannot be shown in

a useful manner in graphs of the present scale.

For comparison, Figures C-8, C-9, and C-10 show the distribution function, collision operator, and collisionally induced velocity-space particle flux, respectively, for the case of the optimum negative perturbation. One should note the qualitative similarities between these graphs and their counterparts for the case of the optimum positive perturbation.

What appears to be happening is that the electrons displaced from $v < v_o$ "prefer" (energetically speaking) to remain relatively close to the velocity region from which they have been removed; however, if the displaced electrons are trying to diffuse back downward in velocity into the relatively small depleted region, there must also be a considerable number of electrons which will diffuse upward in velocity into the (much larger) velocity space volume which surrounds the perturbation. Thus it is reasonable that the optimum of the new distribution function occurs when the perturbation is fairly concentrated at small velocities and contains several times the number of displaced slow electrons.

The appropriate normalization constant is

$$
\begin{aligned}
K1 = 1 \Big/ \Bigg(\pi \Bigg(& -4\,vts^2\,v01 + 4\,vts^2\,v01\,A - 4\,vts^2\,v01\,A\,\mathrm{e}^{\left(-\frac{(-v01+v02)^2}{vtf2^2}\right)} \\
& + 2\,vts^2\,v01\,\mathrm{e}^{\left(-\frac{v01^2}{vts^2}\right)} - 2\,vts^2\,v01\,\mathrm{e}^{\left(-\frac{v01^2}{vts^2}\right)}\,A \\
& + 2\,vts^2\,v01\,A\,\mathrm{e}^{\left(-\frac{v01^2\,vtf2^2+vts^2\,v01^2+vts^2\,v02^2-2\,vts^2\,v02\,v01}{vts^2\,vtf2^2}\right)} \\
& + 2\,vts\,\sqrt{\pi}\,v01^2\,\mathrm{erf}\left(\frac{v01}{vts}\right) - 2\,vts\,\sqrt{\pi}\,v01^2\,\mathrm{erf}\left(\frac{v01}{vts}\right)A \\
& + 2\,vts\,\sqrt{\pi}\,v01^2\,\mathrm{erf}\left(\frac{v01}{vts}\right)A\,\mathrm{e}^{\left(-\frac{(-v01+v02)^2}{vtf2^2}\right)} + vts^3\,\sqrt{\pi}\,\mathrm{erf}\left(\frac{v01}{vts}\right) \\
& - vts^3\,\sqrt{\pi}\,\mathrm{erf}\left(\frac{v01}{vts}\right)A + vts^3\,\sqrt{\pi}\,\mathrm{erf}\left(\frac{v01}{vts}\right)A\,\mathrm{e}^{\left(-\frac{(-v01+v02)^2}{vtf2^2}\right)} \\
& + 2\,v01^2\,vtf1\,\sqrt{\pi} - 2\,\sqrt{\pi}\,v01^2\,vtf1\,A + vtf1^3\,\sqrt{\pi} - \sqrt{\pi}\,vtf1^3\,A \\
& + 2\,\sqrt{\pi}\,A\,v02^2\,vtf2 + \sqrt{\pi}\,A\,vtf2^3 + 4\,vtf1^2\,v01 \\
& + 2\,A\,v02\,vtf2^2\,\mathrm{e}^{\left(-\frac{(-v01+v02)^2}{vtf2^2}\right)} - 4\,vtf1^2\,v01\,A \\
& + 2\,\sqrt{\pi}\,A\,vtf2\,v02^2\,\mathrm{erf}\left(\frac{-v01+v02}{vtf2}\right)
\end{aligned}
$$

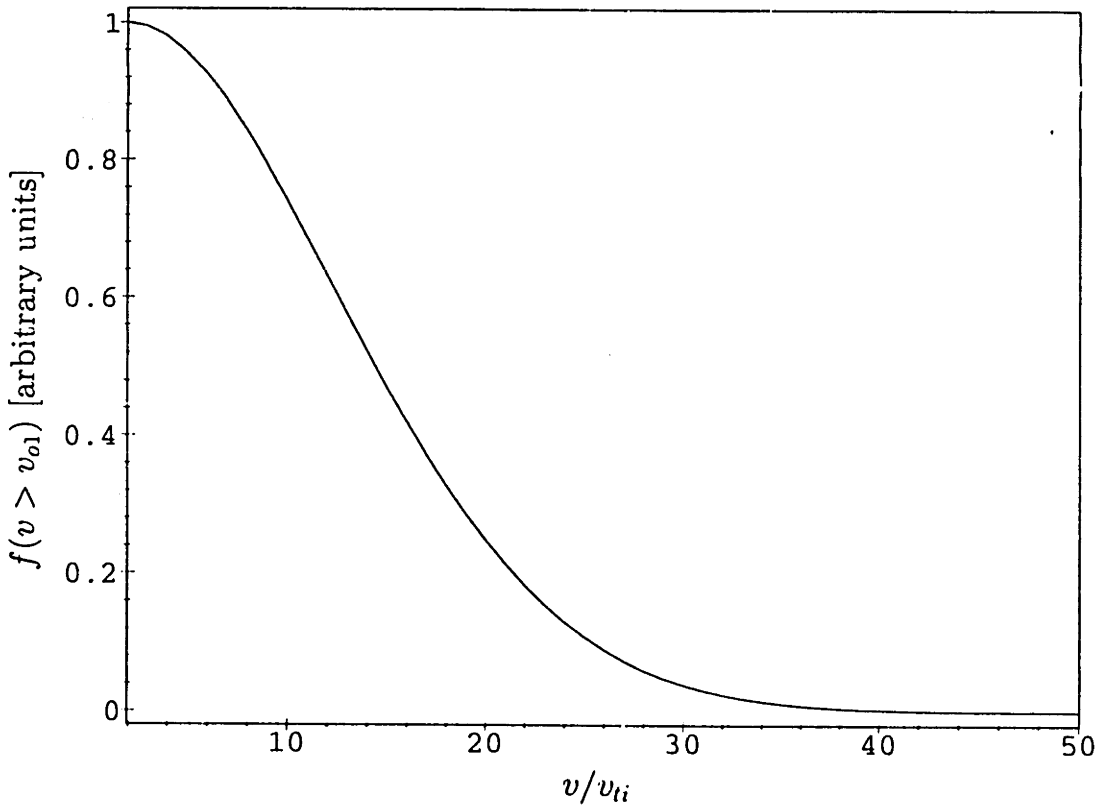

Figure C-5: Distribution function from Eq. (3.53) with parameters chosen to minimize P_{recirc} for electrons in a pure ^{3}He plasma ($T_i = 1$ MeV and $\ln\Lambda = 20$) subject to the constraints that $A > 0$, $\langle E_e \rangle = 73.5$ keV, and $P_{ie}/(P_{ie})_{Spitzer} = 0.01$. Parameters are: $v_{o1} \approx v_{o2} \approx 1.923 v_{ti}$, $v_{ts} = 0.01 v_{ti}$, $v_{tf1} \approx 15.788 v_{ti}$, $v_{tf2} \approx 8.8 v_{ti}$, and $A \approx 0.0883$ (where $v_{ti} \equiv \sqrt{2T_i/m_i}$).

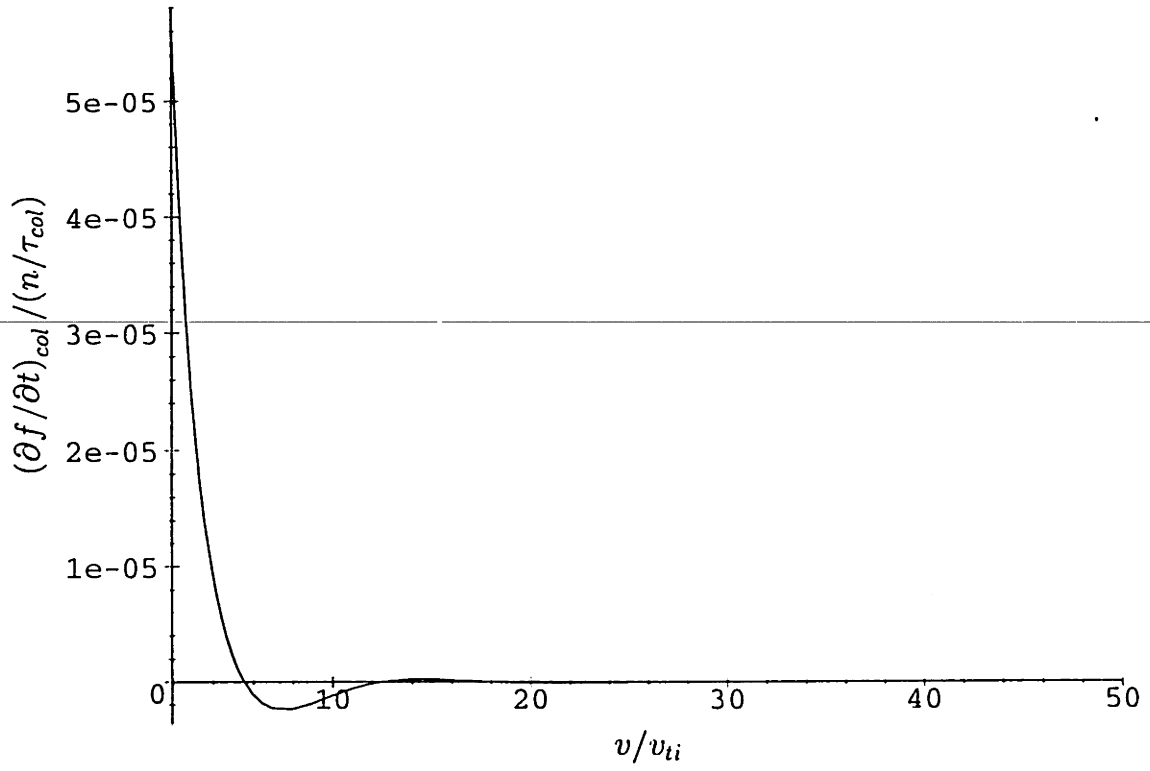

Figure C-6: Collision operator corresponding to the distribution function from Eq. (3.53) with parameters chosen to minimize P_{recirc} for electrons in a pure ^{3}He plasma ($T_i = 1$ MeV and $\ln\Lambda = 20$) subject to the constraints that $A > 0$, $\langle E_e \rangle = 73.5$ keV, and $P_{ie}/(P_{ie})_{Spitzer} = 0.01$. Parameters are: $v_{o1} \approx v_{o2} \approx 1.923 v_{ti}$, $v_{ts} = 0.01 v_{ti}$, $v_{tf1} \approx 15.788 v_{ti}$, $v_{tf2} \approx 8.8 v_{ti}$, and $A \approx 0.0883$.

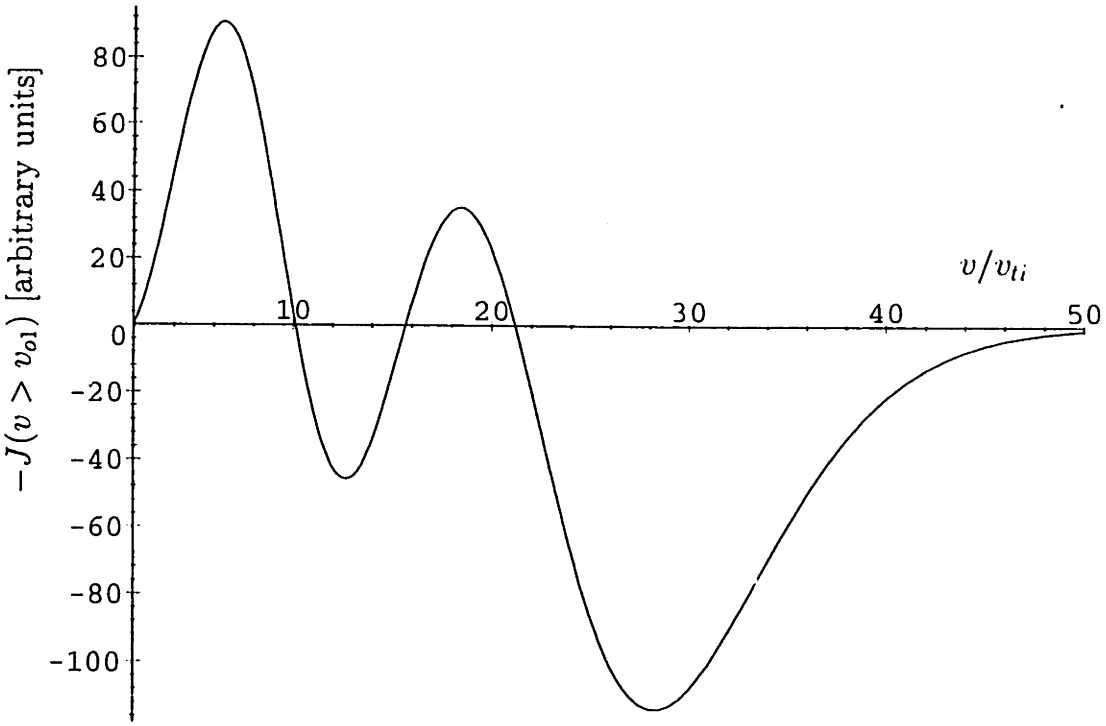

Figure C-7: Particle flux in velocity space corresponding to the distribution function from Eq. (3.53) with parameters chosen to minimize P_{recirc} for electrons in a pure ^{3}He plasma ($T_i = 1$ MeV and $\ln\Lambda = 20$) subject to the constraints that $A > 0$. $\langle E_e \rangle = 73.5$ keV, and $P_{ie}/(P_{ie})_{Spitzer} = 0.01$. Parameters are: $v_{o1} \approx v_{o2} \approx 1.923 v_{ti}$, $v_{ts} = 0.01 v_{ti}$, $v_{tf1} \approx 15.788 v_{ti}$, $v_{tf2} \approx 8.8 v_{ti}$, and $A \approx 0.0883$.

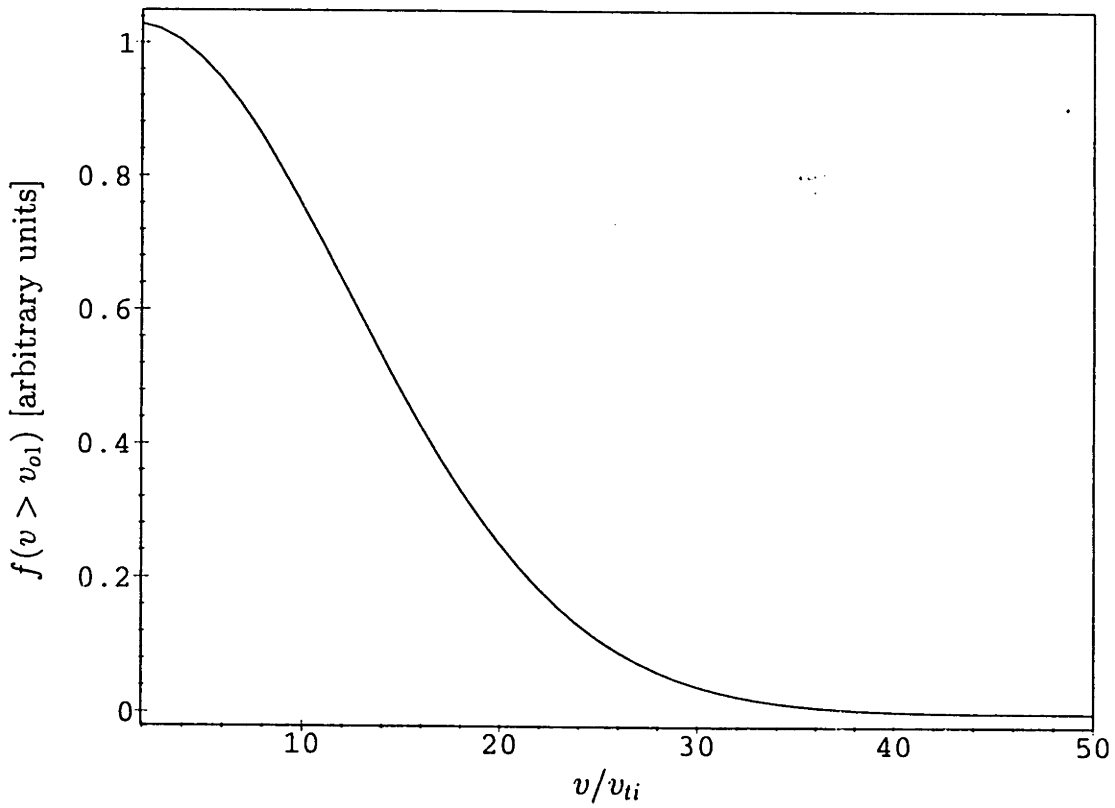

Figure C-8: Distribution function from Eq. (3.53) with parameters chosen to minimize P_{recirc} for electrons in a pure ^{3}He plasma ($T_i = 1$ MeV and $\ln\Lambda = 20$) subject to the constraints that $A < 0$, $\langle E_e \rangle = 73.5$ keV, and $P_{ie}/(P_{ie})_{Spitzer} = 0.01$. Parameters are: $v_{o1} \approx 1.926 v_{ti}$, $v_{o2} \approx 12 v_{ti}$, $v_{ts} = 0.01 v_{ti}$, $v_{tf1} \approx 15.683 v_{ti}$, $v_{tf2} \approx 10.912 v_{ti}$, and $A \approx -0.05$.

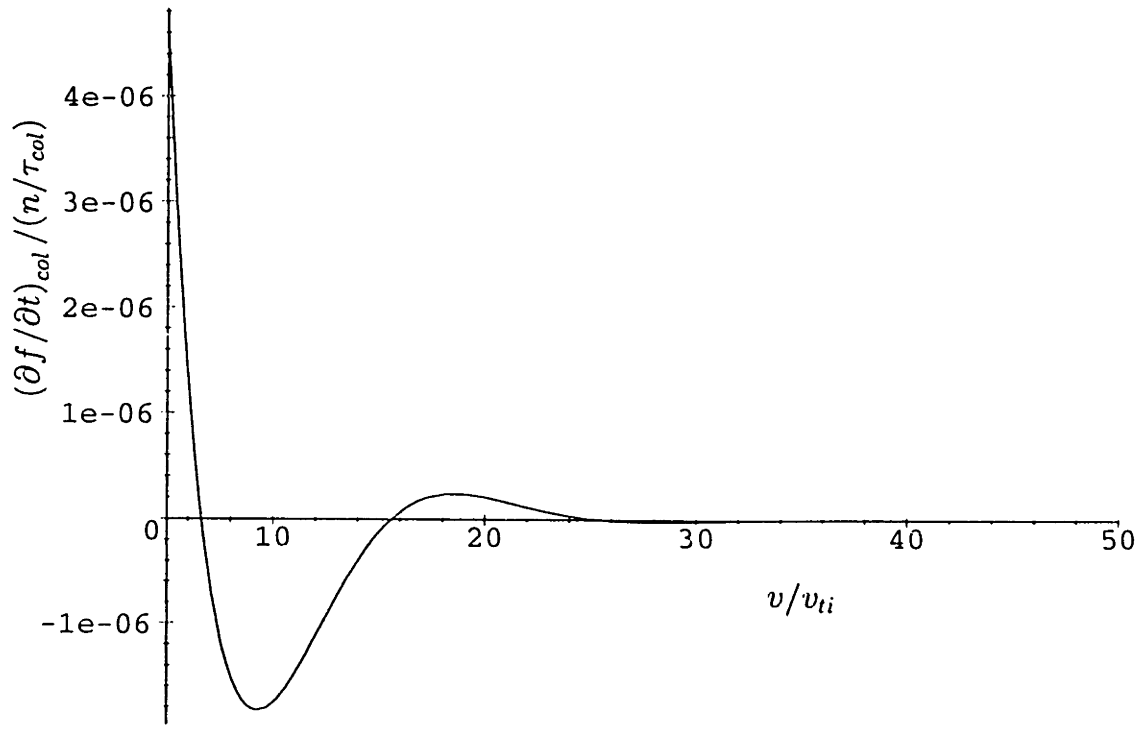

Figure C-9: Collision operator corresponding to the distribution function from Eq. (3.53) with parameters chosen to minimize P_{recirc} for electrons in a pure ^{3}He plasma ($T_i = 1$ MeV and $\ln\Lambda = 20$) subject to the constraints that $A < 0$, $\langle E_e \rangle = 73.5$ keV, and $P_{ie}/(P_{ie})_{Spitzer} = 0.01$. Parameters are: $v_{o1} \approx 1.926 v_{ti}$, $v_{o2} \approx 12 v_{ti}$, $v_{ts} = 0.01 v_{ti}$, $v_{tf1} \approx 15.683 v_{ti}$, $v_{tf2} \approx 10.912 v_{ti}$, and $A \approx -0.05$.

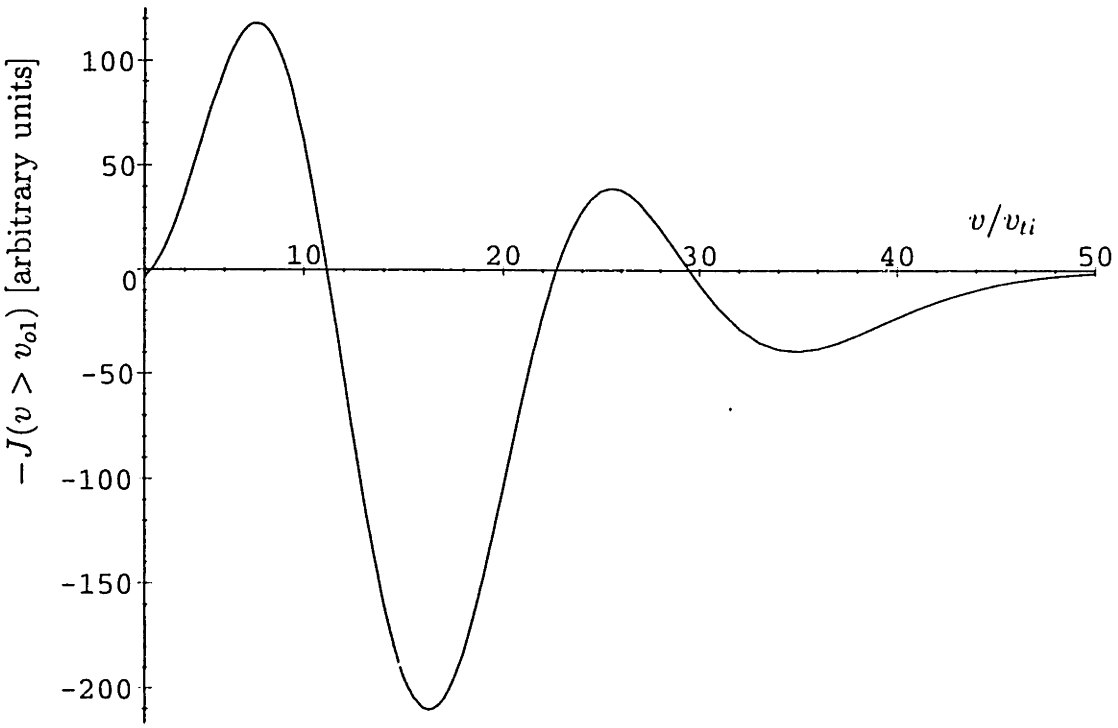

Figure C-10: Particle flux in velocity space corresponding to the distribution function from Eq. (3.53) with parameters chosen to minimize P_{recirc} for electrons in a pure ^{3}He plasma ($T_i = 1$ MeV and $\ln\Lambda = 20$) subject to the constraints that $A < 0$, $\langle E_e \rangle = 73.5$ keV, and $P_{ie}/(P_{ie})_{Spitzer} = 0.01$. Parameters are: $v_{o1} \approx 1.926 v_{ti}$, $v_{o2} \approx 12 v_{ti}$, $v_{ts} = 0.01 v_{ti}$, $v_{tf1} \approx 15.683 v_{ti}$, $v_{tf2} \approx 10.912 v_{ti}$, and $A \approx -0.05$.

$$+\sqrt{\pi}\,A\,vtf2^3\,\mathrm{erf}\left(\frac{-v01+v02}{vtf2}\right)+2\,A\,vtf2^2\,\mathrm{e}^{\left(-\frac{(-v01+v02)^2}{vtf2^2}\right)}\,v01\Bigg)\Bigg)\ .$$

The mean particle energy for this distribution is

$$\begin{aligned}\langle E\rangle = \frac{1}{4}m\Bigg(&4\,vtf2\,A\,v02^4\sqrt{\pi}\,\mathrm{erf}\left(\frac{-v01+v02}{vtf2}\right)+3\,A\,vtf2^5\sqrt{\pi}\,\mathrm{erf}\left(\frac{-v01+v02}{vtf2}\right)\\
&+12\,A\,v02^2\,vtf2^3\sqrt{\pi}\,\mathrm{erf}\left(\frac{-v01+v02}{vtf2}\right)+3\,vts^5\sqrt{\pi}\,\mathrm{erf}\left(\frac{v01}{vts}\right)\\
&+4\,vts^2\,v01^3\,\mathrm{e}^{\left(-\frac{v01^2}{vts^2}\right)}+16\,v01^3\,vtf1^2+16\,v01\,vtf1^4\\
&-16\,v01\,vtf1^4\,A-16\,v01^3\,vtf1^2\,A-4\,vts^2\,v01^3\,\mathrm{e}^{\left(-\frac{v01^2}{vts^2}\right)}\,A\\
&-10\,v01\,vts^4\,\mathrm{e}^{\left(-\frac{v01^2}{vts^2}\right)}\,A+12\,vts^3\,v01^2\sqrt{\pi}\,\mathrm{erf}\left(\frac{v01}{vts}\right)\\
&-12\,vts^3\,v01^2\sqrt{\pi}\,\mathrm{erf}\left(\frac{v01}{vts}\right)A\\
&+12\,vts^3\,v01^2\sqrt{\pi}\,\mathrm{erf}\left(\frac{v01}{vts}\right)A\,\mathrm{e}^{\left(-\frac{(-v01+v02)^2}{vtf2^2}\right)}\\
&+4\,vts\,v01^4\sqrt{\pi}\,\mathrm{erf}\left(\frac{v01}{vts}\right)-4\,vts\,v01^4\sqrt{\pi}\,\mathrm{erf}\left(\frac{v01}{vts}\right)A\\
&+4\,vts\,v01^4\sqrt{\pi}\,\mathrm{erf}\left(\frac{v01}{vts}\right)A\,\mathrm{e}^{\left(-\frac{(-v01+v02)^2}{vtf2^2}\right)}-4\,v01^4\,vtf1\sqrt{\pi}\,A\\
&-12\,vtf1^3\,v01^2\sqrt{\pi}\,A+4\,A\,v02^4\,vtf2\sqrt{\pi}+12\,A\,vtf2^3\,v02^2\sqrt{\pi}\\
&-16\,vts^2\,v01^3\,A\,\mathrm{e}^{\left(-\frac{(-v01+v02)^2}{vtf2^2}\right)}-16\,vts^4\,v01\,A\,\mathrm{e}^{\left(-\frac{(-v01+v02)^2}{vtf2^2}\right)}\\
&+3\,vts^5\sqrt{\pi}\,\mathrm{erf}\left(\frac{v01}{vts}\right)A\,\mathrm{e}^{\left(-\frac{(-v01+v02)^2}{vtf2^2}\right)}+16\,vts^2\,v01^3\,A\\
&+16\,vts^4\,v01\,A+10\,v01\,vts^4\,\mathrm{e}^{\left(-\frac{v01^2}{vts^2}\right)}+4\,v01^4\,vtf1\sqrt{\pi}\\
&+12\,vtf1^3\,v01^2\sqrt{\pi}-3\,vtf1^5\sqrt{\pi}\,A+3\,A\,vtf2^5\sqrt{\pi}-16\,vts^2\,v01^3\\
&-16\,vts^4\,v01+3\,vtf1^5\sqrt{\pi}-3\,vts^5\sqrt{\pi}\,\mathrm{erf}\left(\frac{v01}{vts}\right)A\\
&+4\,A\,vtf2^2\,\mathrm{e}^{\left(-\frac{(-v01+v02)^2}{vtf2^2}\right)}\,v01^3+4\,A\,v02\,vtf2^2\,\mathrm{e}^{\left(-\frac{(-v01+v02)^2}{vtf2^2}\right)}\,v01^2\\
&+6\,vtf2^4\,A\,\mathrm{e}^{\left(-\frac{(-v01+v02)^2}{vtf2^2}\right)}\,v01+10\,A\,v02\,vtf2^4\,\mathrm{e}^{\left(-\frac{(-v01+v02)^2}{vtf2^2}\right)}\\
&+4\,v02^2\,A\,vtf2^2\,\mathrm{e}^{\left(-\frac{(-v01+v02)^2}{vtf2^2}\right)}\,v01+4\,A\,v02^3\,vtf2^2\,\mathrm{e}^{\left(-\frac{(-v01+v02)^2}{vtf2^2}\right)}\end{aligned}$$

$$+ 4\,vts^2\,v01^3\,A\,\%1 + 10\,vts^4\,v01\,A\,\%1\Big) \Big/ \Big(-4\,vts^2\,v01$$
$$+ 4\,vts^2\,v01\,A - 4\,vts^2\,v01\,A\,\mathrm{e}^{\left(-\frac{(-v01+v02)^2}{vtf2^2}\right)} + 2\,vts^2\,v01\,\mathrm{e}^{\left(-\frac{v01^2}{vts^2}\right)}$$
$$- 2\,vts^2\,v01\,\mathrm{e}^{\left(-\frac{v01^2}{vts^2}\right)}\,A + 2\,vts^2\,v01\,A\,\%1 + 2\,vts\,\sqrt{\pi}\,v01^2\,\mathrm{erf}\left(\frac{v01}{vts}\right)$$
$$- 2\,vts\,\sqrt{\pi}\,v01^2\,\mathrm{erf}\left(\frac{v01}{vts}\right)\,A$$
$$+ 2\,vts\,\sqrt{\pi}\,v01^2\,\mathrm{erf}\left(\frac{v01}{vts}\right)\,A\,\mathrm{e}^{\left(-\frac{(-v01+v02)^2}{vtf2^2}\right)} + vts^3\,\sqrt{\pi}\,\mathrm{erf}\left(\frac{v01}{vts}\right)$$
$$- vts^3\,\sqrt{\pi}\,\mathrm{erf}\left(\frac{v01}{vts}\right)\,A + vts^3\,\sqrt{\pi}\,\mathrm{erf}\left(\frac{v01}{vts}\right)\,A\,\mathrm{e}^{\left(-\frac{(-v01+v02)^2}{vtf2^2}\right)}$$
$$+ 2\,v01^2\,vtf1\,\sqrt{\pi} - 2\,\sqrt{\pi}\,v01^2\,vtf1\,A + vtf1^3\,\sqrt{\pi} - \sqrt{\pi}\,vtf1^3\,A$$
$$+ 2\,\sqrt{\pi}\,A\,v02^2\,vtf2 + \sqrt{\pi}\,A\,vtf2^3 + 4\,vtf1^2\,v01$$
$$+ 2\,A\,v02\,vtf2^2\,\mathrm{e}^{\left(-\frac{(-v01+v02)^2}{vtf2^2}\right)} - 4\,vtf1^2\,v01\,A$$
$$+ 2\,\sqrt{\pi}\,A\,vtf2\,v02^2\,\mathrm{erf}\left(\frac{-v01+v02}{vtf2}\right)$$
$$+ \sqrt{\pi}\,A\,vtf2^3\,\mathrm{erf}\left(\frac{-v01+v02}{vtf2}\right) + 2\,A\,vtf2^2\,\mathrm{e}^{\left(-\frac{(-v01+v02)^2}{vtf2^2}\right)}\,v01\Big)$$
$$\%1 := \mathrm{e}^{\left(-\frac{v01^2\,vtf2^2+vts^2\,v01^2+vts^2\,v02^2-2\,vts^2\,v02\,v01}{vts^2\,vtf2^2}\right)}.$$

The complete expression for the collision operator appropriate for this distribution function would have been given here as well, but it was so long and unpleasant that even LaTeX could not digest it.

Appendix D

Raw Data from Numerical Integrations for Properties of Non-Maxwellian Distributions of Chapter 3

This appendix contains some of the raw data from the numerical integrations which were used to determine the minimum recirculating power and entropy generation rates of non-Maxwellian velocity distributions for Chapter 3. The data is given in Tables D.1 through D.4.

All quantities are expressed in dimensionless units. The recirculating power density P_{recirc} and the entropy density generation rate dS/dt are written in terms of $n\langle E\rangle/\tau_{col}$ and n/τ_{col}, respectively. Velocities are expressed in arbitrary units, since only their relative values matter here. The entry "N.D." indicates that a particular quantity was not determined.

Some comments about the visible implications of these results (and the motivation for choosing the particular parameters of each trial) are in order.

Trials 1-19 cover the case $v_{ts} = v_{tf} = v_t$. For $v_o \ll v_t$, the dividing velocity v_d approaches an asymptotic value of roughly 1.37 v_t; in the opposite limit, $v_o \gg v_t$, v_d approaches the value of v_o, but it is always slightly larger than v_o. The dimensionless recirculating power $P_{recirc}/(n\langle E\rangle/\tau_{col})$ generally scales like $(v_o/v_t)^4$ for $v_o/v_t \ll 1$ and like (v_o/v_t) for $v_o/v_t \gg 1$. The dimensionless entropy generation rate $(dS/dt)/(n/\tau_{col})$ scales approximately like $(v_o/v_t)^2$ for $v_o/v_t \gg 1$.

Trials 20-28 cover the case in which $v_{ts} \ll v_o \ll v_{tf}$.

The relative lack of sensitivity to the precise value of v_{ts}, provided that $v_{ts} \ll v_o \ll v_{tf}$, is illustrated by the results of Trials 26-28.

Trials 29-32 serve as "sanity checks." These trials show that the results only depend on the *relative* values of the input velocity parameters v_o, v_{ts}, and v_{tf}, not on the absolute magnitude of the velocities. This behavior confirms what was expected.

The purpose of Trials 33-46 was to check how sensitive the recirculating power was to small changes in v_d. In these trials the value of the dividing velocity used in computing the recirculating power was truncated by one digit in each successive calculation. Because the recirculating power does not appear to be especially sensitive to the truncation of v_d by one or even two digits, one should not have to worry about whether the accuracy to which v_d has been found will affect the results for P_{recirc}.

In Chapter 3, the distribution function of Eq. (3.11) was optimized to minimize the recirculating power for the particular case of a pure ^{3}He plasma with $T_i = 1$ MeV and $\ln\Lambda = 20$, subject to the constraints that $\langle E_e\rangle = (3/2)\cdot 49$ keV$= 73.5$ keV and $P_{ie}/(P_{ie})_{Spitzer} = 0.01$. This optimization was shown graphically in Figure 3-5. Trials 47-50 in Table D.3 give the data which was used to make that graph. Unlike the earlier tables, where velocities were given in arbitrary units, Table D.3 gives the velocities in multiples of the ion thermal velocity for 1-MeV ^{3}He ions, $v_{ti} \equiv \sqrt{2T_i/m_i}$.

Finally, Table D.4 gives the parameters of the distribution from Eq. (3.53) which specify local minima with respect to the recirculating power for electrons in a pure ^{3}He plasma with $T_i = 1$ MeV, $\ln\Lambda = 20$, $\langle E_e \rangle = 73.5$ keV, and $P_{ie}/(P_{ie})_{Spitzer} = 0.01$. As with Table D.3, velocities here are expressed in multiples of the ion thermal velocity. For these calculations, the value of v_{ts} was fixed at $0.01 v_{ti}$.

Each local minimum in Table D.4 has several dividing velocities, which must be taken into account in calculating the recirculating power, in accordance with the methods discussed in Chapter 3. These dividing velocities correspond to the zeros in the velocity-space particle flux curves shown in Figures C-7 and C-10.

A third local minimum also exists but is not shown, since it is physically identical to the distribution of Trial 51 with the trivial substitutions $v_{tf1} \leftrightarrow v_{tf2}$ and $A \leftrightarrow (1 - A)$. Because the definition of the distribution in Eq. (3.53) is not fully symmetric under the interchange of v_{o1} and v_{o2}, there is no similar "mirror image" of the local minimum found in Trial 52.

Trial no.	v_o	v_{ts}	v_{tf}	v_d	$P_{recirc}/(n\langle E\rangle/\tau_{col})$	$(dS/dt)/(n/\tau_{col})$
1	0.01	1	1	1.36904	$5.81017 \cdot 10^{-9}$	$2.23307 \cdot 10^{-14}$
2	0.03	1	1	1.36926	$4.69423 \cdot 10^{-7}$	$4.90486 \cdot 10^{-12}$
3	0.1	1	1	1.37175	$5.62992 \cdot 10^{-5}$	$6.87249 \cdot 10^{-8}$
4	0.3	1	1	1.39394	$3.58273 \cdot 10^{-3}$	$2.45074 \cdot 10^{-4}$
5	0.5	1	1	1.43952	$1.82379 \cdot 10^{-2}$	$5.98831 \cdot 10^{-3}$
6	1	1	1	1.66200	$8.53637 \cdot 10^{-2}$	0.138279
7	1.5	1	1	2.00409	0.159856	0.466585
8	2	1	1	2.40128	0.244401	0.963270
9	3	1	1	3.27534	0.445065	2.53780
10	4	1	1	4.20563	0.672513	4.96789
11	5	1	1	5.16298	0.914655	8.29900
12	10	1	1	10.07882	2.20761	39.0448
13	30	1	1	30.02545	7.59835	402.142
14	100	1	1	N.D.	N.D.	4711.27
15	300	1	1	N.D.	N.D.	$4.30724 \cdot 10^4$
16	1000	1	1	N.D.	N.D.	$4.81249 \cdot 10^5$
17	3000	1	1	N.D.	N.D.	$4.33815 \cdot 10^6$
18	10000	1	1	N.D.	N.D.	$4.82285 \cdot 10^7$
19	30000	1	1	N.D.	N.D.	$4.34126 \cdot 10^8$
20	10	1	10	13.4015	0.183356	N.D.
21	10	1	30	33.6106	$3.19056 \cdot 10^{-2}$	3.23869
22	10	1	60	66.8951	$1.24848 \cdot 10^{-2}$	2.02711
23	10	1	100	110.779	$6.86938 \cdot 10^{-3}$	1.34608
24	10	1	300	327.620	$2.14724 \cdot 10^{-3}$	N.D.
25	10	1	600	651.662	$1.06223 \cdot 10^{-3}$	N.D.
26	3	1	30	33.4922	$6.72447 \cdot 10^{-3}$	N.D.
27	10	1	100	110.779	$6.86938 \cdot 10^{-3}$	1.34608
28	30	1	300	331.256	$6.93049 \cdot 10^{-3}$	N.D.

Table D.1: Minimum recirculating power and entropy generation rates for non-Maxwellian velocity distributions described by Eq. (3.11).

Trial no.	v_o	v_{ts}	v_{tf}	v_d	$P_{recirc}/(n\langle E\rangle/\tau_{col})$	$(dS/dt)/(n/\tau_{col})$
29	1	1	1	1.66200	$8.53637 \cdot 10^{-2}$	0.138279
30	2	2	2	3.32400	$8.53637 \cdot 10^{-2}$	0.138279
31	3	1	1	3.27534	0.445065	2.53780
32	6	2	2	6.55069	0.445065	2.53780
33	10	1	1	10.07882	2.20761	39.0448
34	10	1	1	10.0788	2.20714	39.0448
35	10	1	1	10.078	2.18836	39.0448
36	10	1	1	10.07	2.00048	39.0448
37	10	1	1	10.0	0.367930	39.0448
38	0.5	1	1	1.43952	$1.82379 \cdot 10^{-2}$	$5.98831 \cdot 10^{-3}$
39	0.5	1	1	1.4395	$1.82367 \cdot 10^{-2}$	$5.98831 \cdot 10^{-3}$
40	0.5	1	1	1.439	$1.82069 \cdot 10^{-2}$	$5.98831 \cdot 10^{-3}$
41	0.5	1	1	1.43	$1.76688 \cdot 10^{-2}$	$5.98831 \cdot 10^{-3}$
42	0.5	1	1	1.4	$1.58530 \cdot 10^{-2}$	$5.98831 \cdot 10^{-3}$
43	10	1	100	110.779	$6.86938 \cdot 10^{-3}$	1.34608
44	10	1	100	110.77	$6.86769 \cdot 10^{-3}$	1.34608
45	10	1	100	110.7	$6.85454 \cdot 10^{-3}$	1.34608
46	10	1	100	110	$6.72255 \cdot 10^{-3}$	1.34608

Table D.2: "Sanity checks" of minimum recirculating power and entropy generation rates for non-Maxwellian velocity distributions described by Eq. (3.11).

Trial no.	v_o	v_{ts}	v_{tf}	v_d	$P_{recirc}/(n\langle E\rangle/\tau_{col})$
47	3	0.962	15.240	17.4194	$1.44557 \cdot 10^{-2}$
48	2.5	0.5745	15.448	17.4140	$1.16796 \cdot 10^{-2}$
49	2	0.11	15.646	17.3332	$9.16803 \cdot 10^{-3}$
50	1.9094	0.01	15.683	17.3024	$8.74258 \cdot 10^{-3}$

Table D.3: Optimization of v_o, v_{ts}, and v_{tf} from Eq. (3.11) for electrons in a pure ^{3}He plasma ($T_i = 1$ MeV and $\ln\Lambda = 20$) to minimize P_{recirc} subject to the constraints that $\langle E_e\rangle = (3/2) \cdot 49$ keV$= 73.5$ keV and $P_{ie}/(P_{ie})_{Spitzer} = 0.01$. Velocities are given in multiples of $v_{ti} \equiv \sqrt{2T_i/m_i}$. These points are graphed in Figure 3-5.

Trial	v_{o1}	v_{o2}	v_{tf1}	v_{tf2}	A	v_d	$P_{recirc}/(n\langle E\rangle/\tau_{col})$
51	1.9232	1.9232	15.788	8.8	0.08832	10.1196 15.6592 21.1837	$3.39050 \cdot 10^{-3}$
52	1.926	12	15.683	10.9117	-0.05	11.1491 22.6637 29.4762	$3.83160 \cdot 10^{-3}$

Table D.4: Parameters of the distribution from Eq. (3.53) which specify local minima with respect to P_{recirc} for electrons in a pure ^{3}He plasma ($T_i = 1$ MeV and $\ln\Lambda = 20$) subject to the constraints that $\langle E_e\rangle = 73.5$ keV and $P_{ie}/(P_{ie})_{Spitzer} = 0.01$. Velocities are given in multiples of $v_{ti} \equiv \sqrt{2T_i/m_i}$. The value of v_{ts} was fixed at $0.01v_{ti}$. Note that each local minimum has several dividing velocities.

Appendix E

Potential New Approaches for Nonequilibrium and Aneutronic Fusion Reactors

Mark Twain once offered some advice about the potential pitfalls of being part of a "Consensus" and saying that something cannot work:

> I have been a Consensus more than once myself, and I know the business– and its vicissitudes... Thirty-five years ago I was an expert precious-metal quartz-miner. There was an outcrop in my neighborhood that assayed $600 a ton–gold. But every fleck of gold in it was shut up tight and fast in an intractable and impersuadable base-metal shell. Acting as a Consensus, I delivered the finality verdict that no human ingenuity would ever be able to set free two dollars' worth of gold out of a ton of that rock. The fact is, I did not foresee the cyanide process... These sorrows have made me suspicious of Consensuses. Do you know, I tremble and the goose flesh rises on my skin every time I encounter one, now. I sheer warily off and get behind something,

saying to myself, "It looks innocent and all right, but no matter, ten to one there's a cyanide process under that thing somewhere." [112]

After demonstrating that there are very rigorous limitations on fusion schemes which attempt to operate out of thermodynamic equilibrium or with very small neutron power fractions, it would be wise to examine the issue of whether these limitations could be circumvented by some radical "cyanide process" which has not been taken into account. Therefore, in this appendix will be presented several new approaches which may be suitable for nonequilibrium or aneutronic fusion reactors. The ideas which will be discussed are put forward solely as a guide to the types of directions one might want to consider if further research on this topic is performed. The list of ideas is not intended to be exhaustive, and those which are discussed are still far from being proven feasible.

Assuming that any of these techniques can truly lead to a practical method of extracting entropy from the plasma in order to maintain non-Maxwellian velocity distributions or to keep particle species at widely differing mean energies, the final product might be used in the manner illustrated in Figure E-1. As shown in the figure, particle beams collide in the dense central region, resulting in fusion events for a few of the ions and appreciable amounts of phase-space scattering (at least in comparison with the fusion rate) for all of the other particles. Therefore, after each pass (or perhaps every few passes), the particles are run through entropy extraction devices which restore the desired nonequilibrium character to the plasma. Although it would be preferable to have the entropy extraction devices operate directly on the dense, bulk region of the plasma, if there are practical limitations (density, proximity of effect, etc.) on the entropy extraction devices, they can at least be used in the fashion illustrated in Figure E-1.

Section E.1 will investigate the possibility of using waves to recirculate power and remove entropy from a plasma which is not in thermodynamic equilibrium. Then Section E.2 will outline some ideas regarding how electromagnetic fields might affect the collisional process in a useful fashion without the fields' actually having to extract entropy directly from the plasma particles. Other methods for attacking the entropy problem will be

discussed in Section E.3. Since one of the main problems with aneutronic fusion is the bremsstrahlung radiation power loss, Section E.4 will address the issue of directly reducing the bremsstrahlung, rather than simply reducing the ion-electron energy transfer rate (as described in Chapters 2-4). Some of these ideas might also be applied to the design of new direct electric converters; this will be the topic of discussion in Section E.5. Finally, Section E.6 will use the formalism of the Fokker-Planck calculational techniques from Chapter 2 in order to analyze the behavior of particles in systems which use velocity-dependent forces to maintain nonequilibrium plasmas.

E.1 Wave-Based Systems for Maintaining Nonequilibrium Plasmas

In Section 3.5, it was shown that quasilinear interactions between particles and electromagnetic or electrostatic waves cannot extract entropy from a plasma. This prevents the use of such wave-particle interactions for maintaining non-Maxwellian velocity distributions or for decoupling the mean energies of two of the plasma's major particle species. However, there might be other types of wave-particle interactions which could successfully keep a plasma out of thermodynamic equilibrium. Two examples are highly nonlinear phenomena and coupled cyclotron radiation emission and absorption.

If entropy could actually be transferred from the plasma to a wave, this ability might be used in the following manner. A wave with a certain energy might be injected into the plasma, and after interacting with the particles and removing their entropy, the wave would have the same energy but a broader frequency linewidth. The wave could then be direct-converted to recover nearly all of its energy, but due to the linewidth broadening a small fraction of the wave's energy could not be converted back into electrical energy and would have to be dissipated as heat in the wave-receiving system.

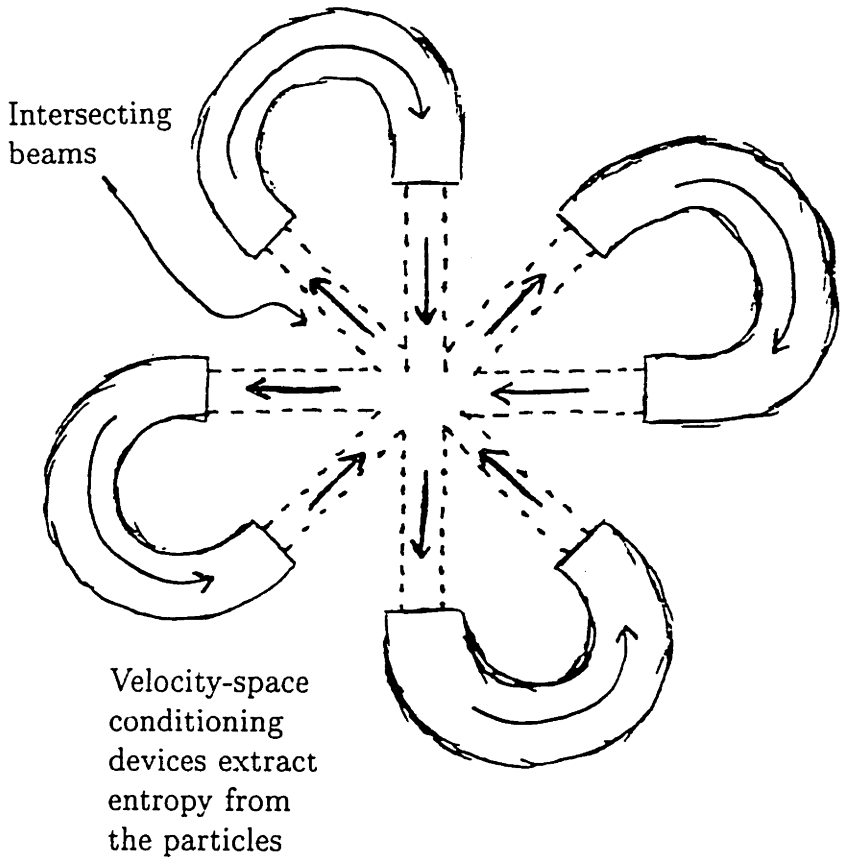

Figure E-1: Idealized system for maintaining a nonequilibrium plasma. The entropy extraction devices counteract the effects of collisions and restore the particle distributions to the desired state.

E.1.1 Cyclotron Radiation Emission and Absorption

As was discussed in Section 3.5, synchrotron or cyclotron radiation by itself would not be a useful mechanism for extracting entropy from a plasma, since the power removed by the radiation would have to be replaced by some other mechanism, leading back to the recirculating power arguments which were made in Chapter 3.

This objection could be overcome, however, if the cyclotron radiation itself were used to "close the loop" and recirculate the necessary amount of power at very high efficiencies. In other words, it might be possible for particle species or subpopulations of particle species which have acquired too much energy via collisions to be induced to emit cyclotron radiation; the emitted radiation would have the right frequency so that it would be efficiently reabsorbed via cyclotron absorption processes by particle species or subpopulations thereof which have lost energy due to collisions. It might be necessary for the emission and reabsorption to take place in different spatial regions of the plasma with different local properties (magnetic field strength, density, electron energy, etc.). In principle this technique could be used for maintaining non-Maxwellian distributions, ion-electron decoupling, or decoupling between ion species.

Further work should be done to investigate whether this or similar techniques could actually succeed.

E.1.2 Highly Nonlinear Phenomena

Since the derivation in Section 3.5 was only a quasilinear treatment of the problem, it may still be possible that highly nonlinear wave-particle interactions could allow waves to remove entropy from a plasma. More sophisticated types of wave-based nonequilibrium plasma devices are also imaginable. For instance, one might use not only the wave's qualities but also the configuration of externally applied electric or magnetic fields to control the effect of interactions with the wave for particles in various regions of phase space. Mul-

tiple waves with different frequencies or other properties might also be coupled together by nonlinear processes within the plasma to help maintain the desired particle distributions, the internal recirculating power, or the degree of energy coupling or decoupling between particle species.

E.2 Useful Effects Which Might Be Induced by Electromagnetic Fields Without Requiring the Fields Themselves to Carry Entropy

Although it was shown in Section 3.5 that hardly any type of electromagnetic field is capable of extracting entropy from a plasma in a particularly useful manner, methods of potentially circumventing this proof were noted there. At least hypothetically, fields might be able to modify the rate of collisional entropy generation or the process of transferring entropy between different groups of particles without the fields themselves actually having to carry the entropy at any point.

E.2.1 Background – The Magnetic Corkscrew

One concept which could possibly prove useful for the present purpose is the technique of using electric and/or magnetic fields which are resonant with particles of particular velocities, so that particles with different velocities would respond to the fields in different ways. A bit of explanation about velocity-resonant fields is in order, as this concept may not seem immediately clear.

The prototypical example of a velocity-resonant plasma system is the aptly named "magnetic corkscrew" [113, 114, 115, 116, 117]. Basically, the magnetic corkscrew is a device for creating a helical magnetic field of increasing or decreasing spatial periodicity, or in other words with a pitch angle which varies along the length of the corkscrew. Due to

interactions between its helical magnetic field and gyrating particles which pass through the system, the corkscrew is able to exert a net effect on particles with the velocity for which the corkscrew was designed, while on average not altering the velocities of nonresonant particles. Specifically, the corkscrew can transfer a resonant particle's energy from the transverse direction to the longitudinal direction ($v_\perp^2$ to $v_\parallel^2$) if the corkscrew is of the accelerating type, or in the opposite direction ($v_\parallel^2$ to $v_\perp^2$) if the corkscrew is of the decelerating type. Unlike the interconversion between parallel and perpendicular particle kinetic energy which occurs in a conventional magnetic mirror, in a corkscrew the conversion between the two components of the kinetic energy occurs in a unidirectional manner. The original purpose for such systems was to facilitate the trapping of particles injected into mirror machines by "herding" particles out of the mirror's loss cone.

The fundamental problem with the corkscrew was found to be that while on average it exerts no *net* effect on nonresonant particles, the *standard deviation* of the corkscrew's effect on nonresonant particles is appreciable. Thus, although the corkscrew actively herds resonant particles out of the mirror loss cone, it also substantially enhances the velocity-space diffusion of nonresonant particles and scatters many of them into the loss cone. This phenomenon may prove a fatal flaw for other types of velocity-resonant systems as well, but as this has not yet been determined for certain, such systems should at least be examined.

The basic idea of velocity-resonant fields will now be utilized to propose a specific new type of device which may be useful for altering the collisional velocity-space diffusion properties of a plasma.

E.2.2 Closed-Orbit, Highly Velocity-Resonant Device

As a simple but concrete example of a potentially useful system of the type under discussion, a device which at least naively appears to keep particles highly non-Maxwellian and focused around some optimum velocity is shown in Figure E-2.

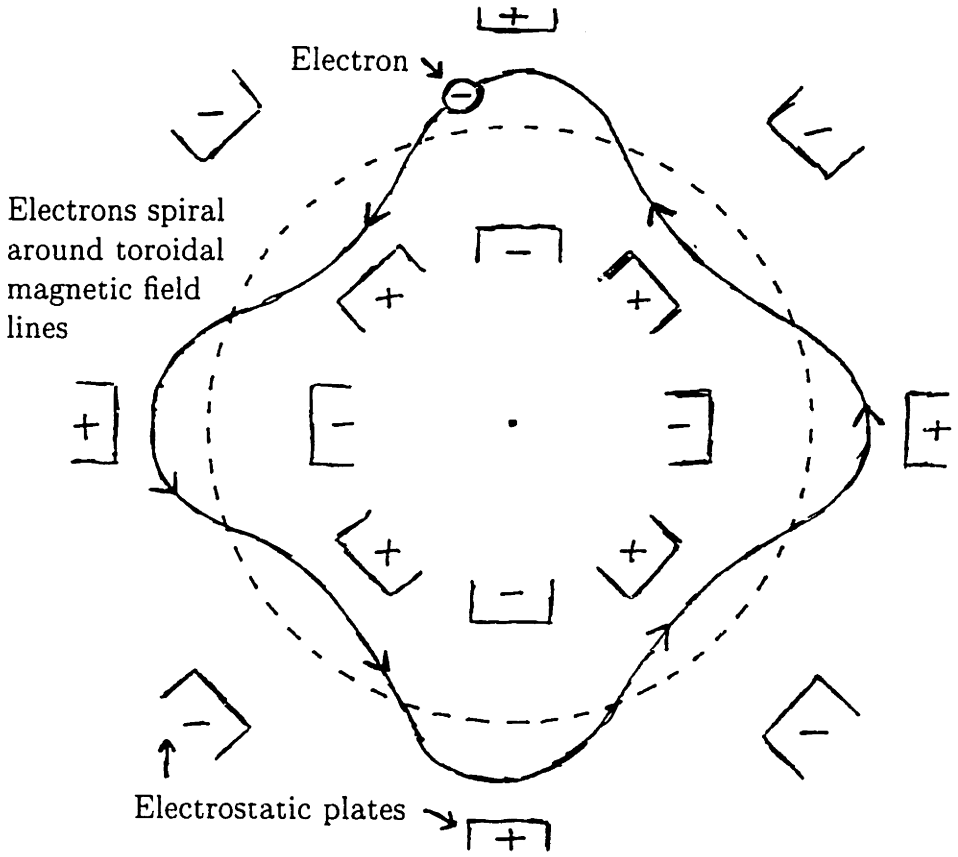

Figure E-2: Closed-orbit, highly velocity-resonant device for possibly maintaining non-Maxwellian particle distributions. Particles of the proper velocity and phase follow closed orbits which keep the particles at the bottom of the electric potential well for each set of electrostatic plates that the particles pass.

In this particular system, the electric field is held static. Particles (say electrons for the sake of argument) spiral around an applied toroidal magnetic field. Those electrons with the optimum velocity v_o have orbits which precisely close on themselves; in other words, resonant electrons follow the exact same spiraling trajectory on each trip around the torus. The spiraling motion of the electrons affects their relative positions in the electric potential gradient between each set of electrostatic plates which they pass. The spacing of the electrostatic plates around the torus is arranged so that electrons with velocity v_o are the same distance from the positive plate for each set of plates that they pass. Obviously it will be energetically favorable for the particles to have a phase which minimizes this distance. Particles which do not have the optimum velocity, or at least follow closed trajectories, will be at random positions between each successive set of electrostatic plates which they pass, so on average they will experience no net effect from the electric fields.

While the electron motion in this type of system is manifestly classical, it possesses many striking parallels with the quantum-mechanical behavior of electrons in solid lattices such as in semiconductors. Among these parallels are:

- The electrons undergo periodic oscillations (analogous to the oscillating quantum wavefunction of the electrons in solids).
- There is a periodic electric potential perturbation (like that created by lattice ions).
- The entire system possesses translation symmetry [around the loop] (analogous to Born-von Karman boundary conditions and Bloch's theorem in solid state lattices [118]).
- There is a net reinforcement or cancellation of effects on each pass of the electrons through the system (analogous to constructive and destructive quantum interference between the forward-propagating and backward-propagating reflected components of an electron's wavefunction in solid lattices).

Because of these many parallels with the physics of electron behavior in solid state lattices, it is conceivable that devices of the type described above might be able to create useful modifications of the velocity-space diffusion or the effective electron mass. In fact, it may even be possible for this system or other such systems to create energy bandgaps, which could serve as strong impediments to collisional diffusion into undesirable regions of phase space.

It is very important to realize that one could produce further potentially beneficial effects by increasing the electric field strength so that for the resonant ($v = v_o$) particles, the magnitude of the electric potential energy would exceed the particles' kinetic energy; resonant particles would thus have even less energy than very slowly moving particles. It might then be possible to inject all of the electrons at the optimum velocity and keep them "trapped" at that velocity in spite of electron-electron collisions, for they would not have enough energy to slow down or speed up.

In reality it would probably be preferable to use a time-varying electric field in order to prevent particles from being drawn to the wall of the vacuum chamber. The discussion here has centered on static fields in order to simplify matters and focus on the basic idea behind these systems.

More elaborate types of closed-orbit, velocity-resonant systems also come to mind when examining this concept. As an example, an additional segment could be inserted in the toroidal loop of the system shown in Figure E-2. At one end of the segment would be an accelerating magnetic corkscrew, and at the other end would be a decelerating corkscrew of the same (but opposite, since it is decelerating) parameters; between the two corkscrews would lie a drift tube without any resonant fields of note. Particles with the desired values of $v_{\|}$ and $v_{\perp}$ would enter this segment, have their relative ratio of $v_{\|}^2/v_{\perp}^2$ temporarily altered and then restored, and finally exit the segment with their original velocity components unchanged and still with the proper phase relative to the resonant electric fields. On the other hand, particles without the desired $v_{\perp}$ (even if they have the correct $v_{\|}$ and phase to be resonant with the electric fields) would undergo a net phase

change in the drift tube, which would affect their behavior on their next pass through the resonant electric fields. If implemented properly this sort of method might ensure phase-space "confinement" in $v_{\|}$, $v_{\perp}$, and phase.

If these techniques for closed-orbit, highly velocity-resonant systems work at all (which they may not, in the sober light of reality), it cannot be because entropy is transferred out of the system, since naively they appear to function even when the fields are static. The only apparent explanation for how they might work is that they might suppress the rate of entropy generation by altering the ground state energy, and hence the preferred stationary minimum-entropy-generating state, of the particles. (Note that this shift appears to be accomplished in a non-trivial way which at least naively could hold true even if the device contains colliding, counter-propagating beams. In contrast, the entropically favored velocity distribution profile of a collection of particles could be shifted in a trivial manner by simply boosting the velocity of a beam which has been sufficiently isolated from collisions and other outside influences.) This behavior would be in accordance with one of the potential loopholes which has been mentioned in Section 3.5.

These types of devices might also be useful for purposes other than those which have been discussed here.

E.2.3 Inducing Soliton-Like Behavior in the Distribution Function

A different and potentially useful manner of viewing the effects induced by the closed-orbit, velocity-resonant device described above is that the perturbing field could cause the stationary (or "solitary") solution of the Fokker-Planck equation to become non-Maxwellian. Mathematically this situation would be quite analogous to the creation of solitons [80, 119], in which nonlinear perturbations added to the wave equation allow the production and maintenance of distinctively shaped waveforms which are not affected by the usual dispersive phenomena. The realization of this analogy may allow the development of other plasma systems in which perturbing fields (and possibly also tailored

density profiles and other techniques) alter the Fokker-Planck equation into a soliton-type equation (for instance, an equation similar to the Korteweg-DeVries equation, nonlinear Schroedinger equation, or sine-Gordon equation [80, 119, 120]), so that certain properly designed non-Maxwellian distributions become stable, solitary solutions, despite the dispersive effects of collisional velocity diffusion.

E.2.4 Forcibly Restricting the Particles' Allowed Phase Space Expansion

The possibility of energy band gaps was briefly mentioned in the context of the closed-orbit, velocity-resonant device discussed above. This general approach, modifying collisional processes by forcibly restricting the region of phase space which the particles are allowed to occupy or to expand into due to collisions, could prove to be a powerful idea. It would be advisable to examine whether this approach could be applied to classes of systems other than the one currently under discussion.

E.2.5 Debye Shielding of Applied Electric Fields

If systems with velocity-resonant electric fields are to operate as intended, it is necessary that the applied electric potential not be screened out too rapidly. In particular, the Debye screening length must be no less than the smaller of the electron gyroradius and the spacing between the alternating electric field plates.

The electron Debye length is [30]

$$\lambda_{De} = \sqrt{\frac{T_e}{4\pi e^4 n_e}} = 743 \sqrt{\frac{T_{e,\,eV}}{n_e}} \text{ cm.} \tag{E.1}$$

For $T_e \equiv \frac{2}{3}\langle E_e \rangle = 40$ keV and $n_e = 10^{10}$ cm^{-3}, the Debye length is

$$\lambda_{De} = 1.5 \text{ cm.} \tag{E.2}$$

As this is probably the smallest theoretically tolerable Debye length, it would appear that velocity conditioners or velocity-space focusing devices with resonant electric fields are limited to operate at densities $n_e \leq 10^{10}$ cm^{-3}.

While such densities are far too low for local fusion reactions to be of interest, there are possible solutions. One potentially useful approach would be to use time-varying fields which have a frequency high enough that the fields would not be screened out. Another solution might be to place low-density velocity conditioners at the edge of a spherically converging/diverging plasma of the sort shown in Figures E-1 and E-3.

The core density of the plasma system shown in Figure E-3 may be determined from the radii of the core (r_{core}) and the entire plasma (R_{edge}). Assuming that the plasma flow converges at constant velocity, one finds [18, 86]:

$$n_{core} = \left(\frac{R_{edge}}{r_{core}}\right)^2 n_{edge} \, . \tag{E.3}$$

Thus for $n_{edge} = 10^{10}$ cm^{-3} and $\frac{R_{edge}}{r_{core}} > 100$, the core density is

$$n_{core} > 10^{14} \text{ cm}^{-3} \, . \tag{E.4}$$

Therefore low-density velocity conditioning devices at the edge of the spherically convergent plasma might be able to keep velocity distributions in the high-density core non-Maxwellian and create useful amounts of fusion power in the core.

However, devices placed at the edge of such a plasma would actually have to extract entropy, rather than merely suppress its generation locally. Otherwise entropy generated by collisions when the particles transit the dense core would build up and the plasma

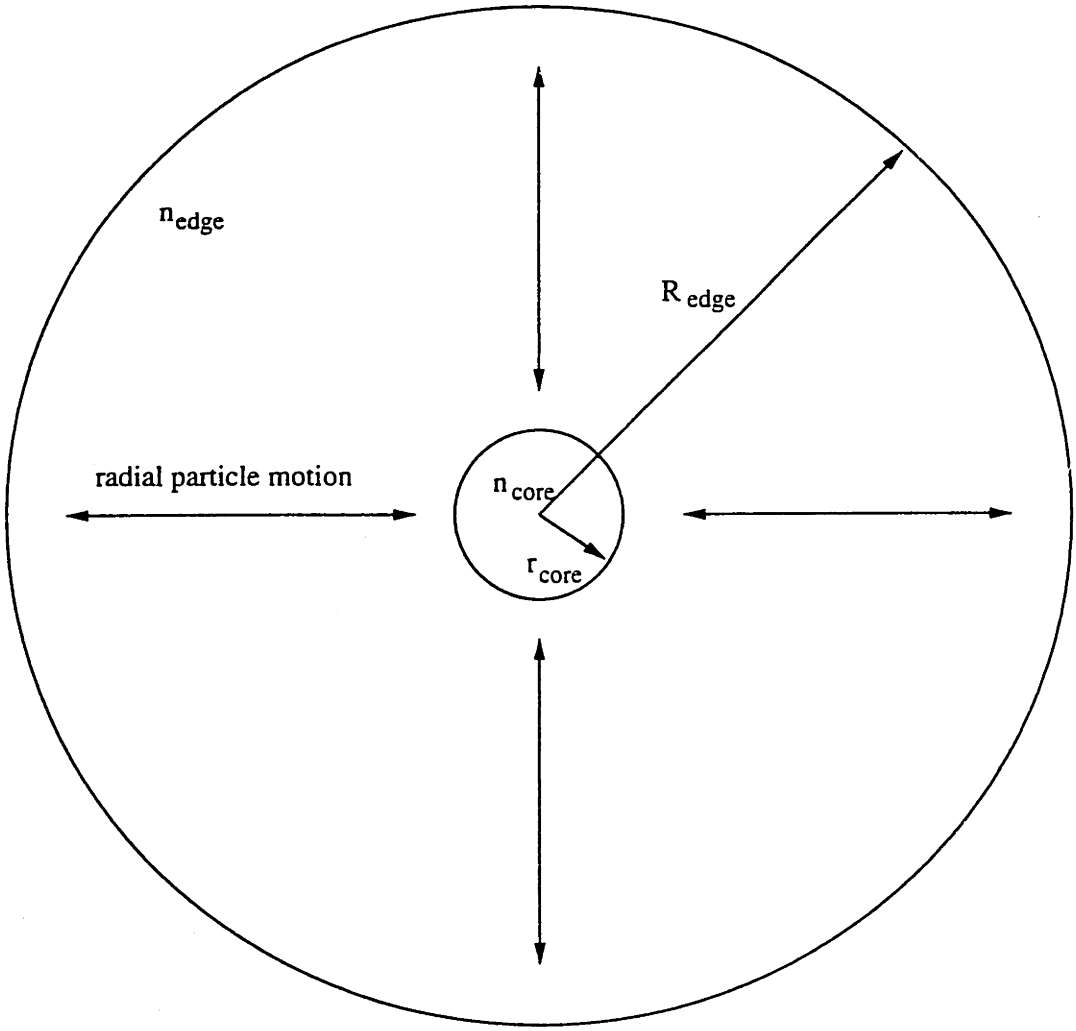

Figure E-3: Spherically converging/diverging plasma with a low-density edge and high-density core.

would rapidly thermalize.

If spherically convergent plasma systems were to be seriously considered further, one would also have to deal with practical limitations such as the maintenance of the central focusing effect [86, 87].

Just as Debye shielding of applied electric fields is a problem, diamagnetic shielding of applied magnetic fields is also a concern, and it would have to be examined further.

E.3 Other Possible Approaches for Keeping Plasmas Out of Thermodynamic Equilibrium

There are other methods which might be investigated as well; some of these are briefly described below.

E.3.1 Transfer of Entropy to Lower-Energy Particles

As has already been mentioned, one potentially useful and feasible approach would be to transfer the collisionally generated entropy of the main plasma particles to a much lower-energy group of particles, which could then be "sacrificed" to a direct electric converter with as little net energy loss as possible. This possibility should be explored further in the future.

E.3.2 Transfer of Entropy to Other Degrees of Freedom

A related idea would be to find other degrees of freedom (not just other particles) to which the collisionally generated entropy could be transferred (in preparation for the eventual removal of the entropy by some mechanism).

This idea is quite similar to the method of adiabatic demagnetization which is employed in cryogenic devices operating near absolute zero [121]. In such systems, the entropy associated with thermal motion in a substance is given to particle spins, resulting in an increased disorder of the alignments of particle spins in the material but a lower temperature due to thermal motion.

If the collisionally generated entropy in the plasma could be transferred to some extra degree of freedom (spin, spatial distribution, ion charge states, etc.) whose increased disorder would not adversely affect the operation of the reactor (and from which the entropy could eventually be extracted and completely removed from the system), the outlook for nonequilibrium plasma systems might brighten considerably.

E.3.3 Stochastic Cooling

An important technique used to cool beams in particle accelerators is stochastic cooling [76]. Although it is unclear whether this method could be implemented with the comparatively high particle densities required for fusion plasmas, this is an issue which should certainly be considered further.

E.4 Direct Reduction of Bremsstrahlung Radiation

Another possible avenue for future work would be to investigate whether bremsstrahlung radiation itself could be directly reduced. For example, this might be accomplished by somehow "artificially" stimulating the inverse bremsstrahlung process (without requiring prohibitively large densities, plasma radii, or reaction energy yields, as discussed in Chapter 4) or by applying electromagnetic fields in some fashion that suppresses the bremsstrahlung emission process.

The net effect of directly reducing the bremsstrahlung radiation is graphed in Figures

E-4 and E-5 for a variety of fusion fuels. These graphs have been calculated by using the methods outlined in Chapters 1, 6, and 7 and assuming that the right-hand side of the usual bremsstrahlung formula, Eq. (1.2), can be reduced by a certain factor.

As shown in Figures E-4 and E-5, a given fractional reduction in the bremsstrahlung power could be more beneficial than the same fractional reduction in the ion-electron energy transfer rate (see Figures 6-9 and 7-8).

E.5 Novel Ideas for Direct Electric Conversion

If the types of devices discussed in the previous sections of this appendix can be constructed, modified versions of them may also be useful as direct electric converters to turn the kinetic energy of charged fusion products into electrical energy. Recent work has indicated that there are considerable problems with previously proposed direct conversion schemes [99]. One of these problems is that magnetic fields which would permit the fusion products to cross and enter a direct converter would also cause intolerably large losses of fuel ions and electrons; another serious problem is that converters for especially high-energy fusion products would suffer from severe arcing problems. These findings seem to rule out the use of some previously developed direct converter designs [100, 101]. By contrast, the advantages of the devices discussed below as direct converters are that they could potentially remove energy from particles in very selective regions of phase space and that they could theoretically act at some reasonable distance so as not to cause problems with arcing or particle losses. Such devices could also be operated in reverse as particle accelerators, if so desired.

E.5.1 Energy Exchange Between Particles and Electric Fields

Before examining specific devices, one should consider the fundamental nature of energy exchange between particles and fields.

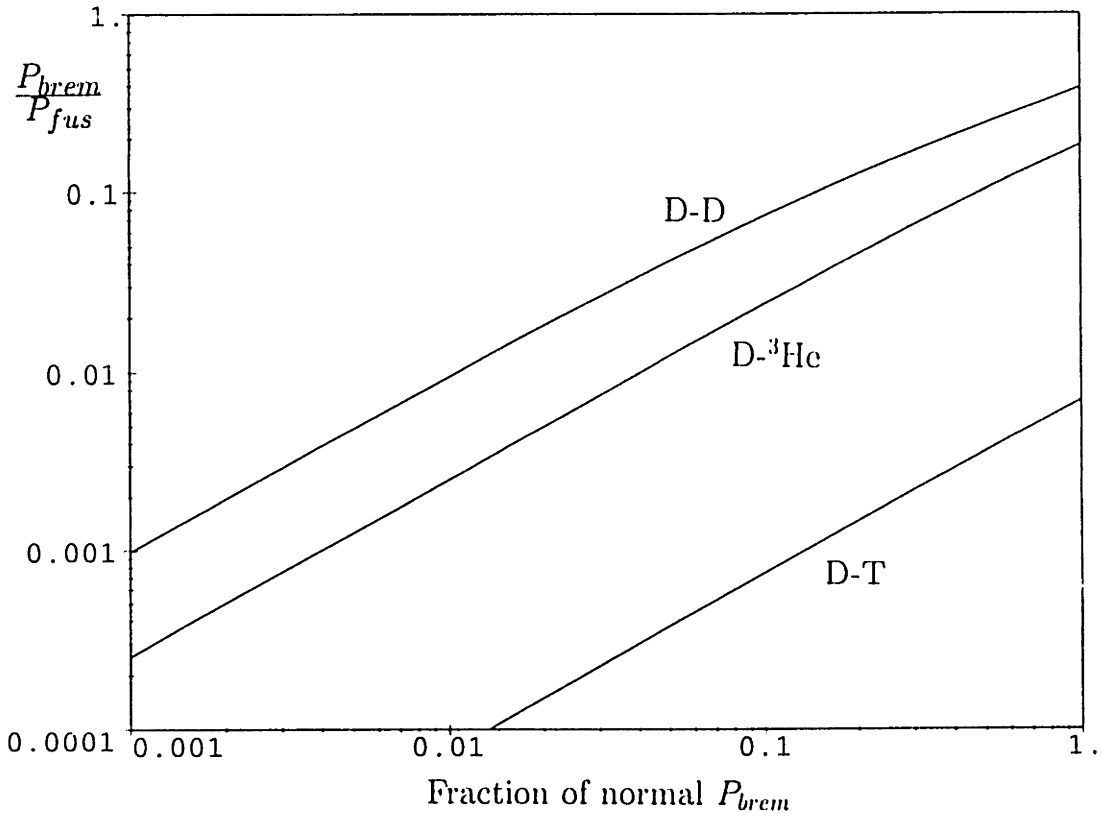

Figure E-4: Ratio of bremsstrahlung losses to fusion power versus the necessary reduction in the usual formula for bremsstrahlung radiation for D-T, D-D, and D-^{3}He plasmas under approximately optimum conditions (T_i = 40 keV for D-T [with a 1:1 fuel mixture], 400 keV for D-D, and 140 keV for D-^{3}He [with a 1:1 fuel mixture]; $\ln \Lambda = 20$ throughout.) Compare with Figure 7-8.

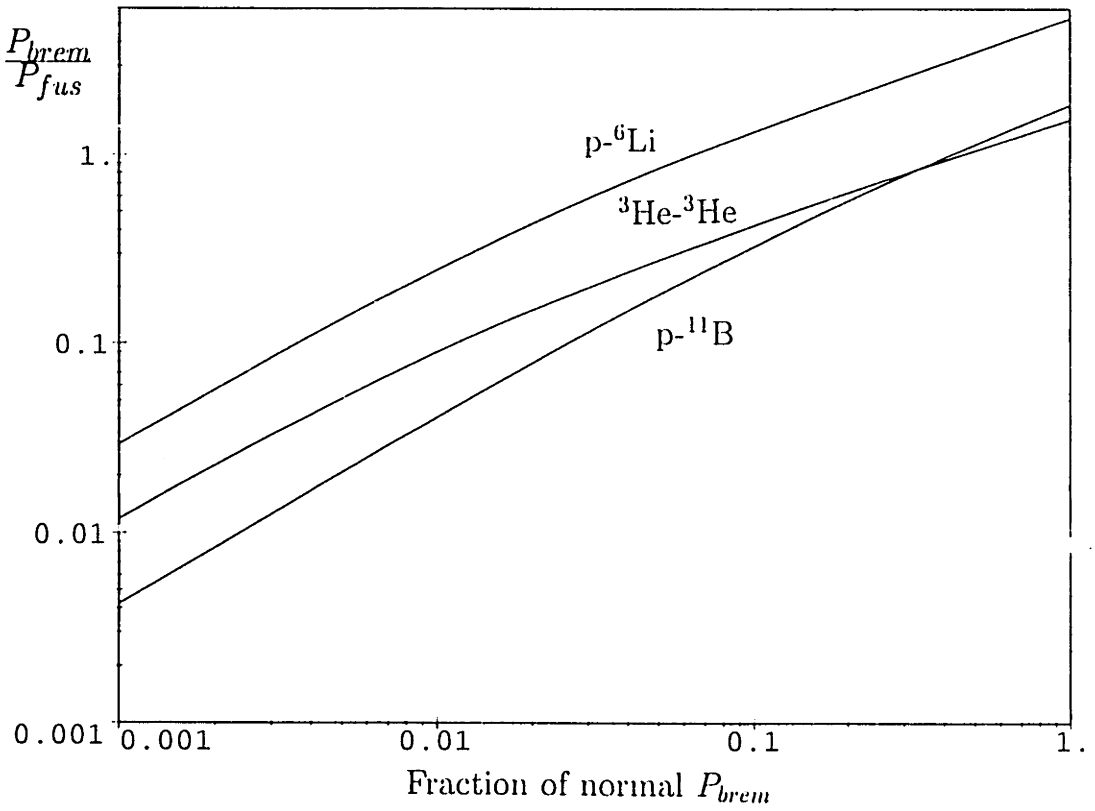

Figure E-5: Ratio of bremsstrahlung losses to fusion power versus the necessary reduction in the usual formula for bremsstrahlung radiation for ^{3}He-^{3}He, p-^{11}B, and p-^{6}Li plasmas under approximately optimum conditions (T_i = 1 MeV for ^{3}He-^{3}He, 300 keV for p-^{11}B [with a 5:1 fuel mixture], and 800 keV for p-^{6}Li [with a 3:1 fuel mixture]; $\ln\Lambda = 20$ throughout.) Compare with Figure 6-9.

While magnetic fields will prove to be useful tools for restricting the accelerating or decelerating forces to certain regions of phase space, electric fields are the only technique for actually applying the accelerating or decelerating forces. The power transferred from an electric field $\mathbf{E}$ to a particle with velocity $\mathbf{v}$ and charge Ze is

$$P = Ze\mathbf{E} \cdot \mathbf{v} \; . \tag{E.5}$$

The best way to ensure that field-particle energy exchange will be confined to particles in a specific location in velocity space is to let the electric field be periodic with respect to time and also make the particle's velocity component parallel to the electric field periodic with time. Specifically, one could choose the time variations of the field (as seen by the particle) and the corresponding parallel velocity component v_E to be the following:

$$\mathbf{E} \equiv \mathbf{E_o} \exp(-i\omega_E t) \; ; \tag{E.6}$$

$$v_E \equiv v_{E\,o} \exp(-i\omega_v t - i\phi) \; . \tag{E.7}$$

The time-averaged power input to the particle will then be

$$\langle P \rangle \; = \; \begin{cases} \frac{1}{2} Ze E_o v_{E\,o} \cos(\phi) & \text{for } \omega_v = \omega_E \\ \\ 0 & \text{otherwise.} \end{cases} \tag{E.8}$$

If ω_v and/or ω_E is a function of the magnitude of the total velocity, only particles in certain regions of velocity space will be able to exchange energy with the electric field.

It would appear that only particles in an infinitesimally small portion of phase space will be resonant with the electric field ($\omega_v = \omega_E$). However, in reality various effects such as the limited physical length or time duration of the perturbing field and the field's spectral purity will produce a certain finite value for the resonance width in phase space; these effects and the resonance width will of course depend on the exact nature of the

system.

Note that the sign of the power input depends on the particle phase; particles within $\pm\pi/2$ of being in phase with the field are accelerated and out-of-phase particles are decelerated. The system should either be designed so that most of the particles have the desired phase relationship with the field (which seems infeasible at densities of interest for fusion reactors) or else provided with an additional mechanism for ensuring that particles of the wrong phase will not stay resonant with the field for long.

E.5.2 Magnetic Corkscrew with Electric Field Wiggler

Electric Field Wiggler System

As a concrete example of a device of the type described above, consider a linear system in which the particles move through a series of spatially alternating transverse electric fields, as shown in Figure E-6a. (The electric fields would ultimately probably have to be time-varying to achieve useful effects, but for the time being it is simpler to think of them as static.) If the spatial period of the alternating electric fields is L, then from the viewpoint of a particle moving through the system, the temporal angular frequency of the field is

$$\omega_E = \frac{2\pi}{L} v_\parallel \,, \tag{E.9}$$

in which $v_\parallel$ is the velocity component of the particle along the longitudinal direction of the system. Such a configuration will be referred to as an electric field wiggler, in analogy with the so-called wiggler magnetic field systems used in free electron lasers [78].

As depicted in Figure E-6a, a static magnetic field in the longitudinal direction is used to produce transverse oscillations of the velocity in the form of cyclotron motion. These motions will have a velocity-independent angular frequency of the usual value [30],

$$\omega_v = \frac{|Ze|B}{mc} \,. \tag{E.10}$$

The system shown in Figure E-6a has the desired property that only particles in a certain region of velocity space, specifically particles for which

$$v_{\|} = \frac{|Ze|B}{mc}\frac{L}{2\pi}\,, \tag{E.11}$$

will be resonant with the electric field and exchange energy with it.

Now one must add a mechanism that will prevent particles of the wrong phase from staying resonant for long enough to be significantly displaced the wrong way in velocity space. The specific device which has been chosen for this purpose is the magnetic corkscrew, for reasons which will become apparent in a moment.

Device for Accelerating Slow Particles

Before considering devices for deceleration and direct electric conversion, the principles of the systems under discussion will be explored by considering an accelerating device.

In order to accelerate slow particles, one may combine an accelerating corkscrew with an electric field wiggler in which the spatial period L of the electric field oscillations is initially small and then increases as a particle proceeds through the device.

Only particles whose longitudinal velocity $v_{\|}$ increases sufficiently rapidly as they move through the system will stay in resonance with the electric field. If a particle is in phase with the electric field, it will gain transverse velocity $v_{\perp}$, which will then be continually transformed by the corkscrew into additional longitudinal velocity, satisfying the condition to keep the particle in resonance with the electric field wiggler.

A particle which is momentarily resonant with the electric field but of the wrong phase will lose a certain amount of its $v_{\perp}$; having less transverse energy to be converted into longitudinal energy by the corkscrew, the particle will not be able to meet the resonance requirement of a rapidly increasing $v_{\|}$, so it will very quickly drop out of resonance with the electric field, and its energy will become constant. If necessary, particles may be

a)

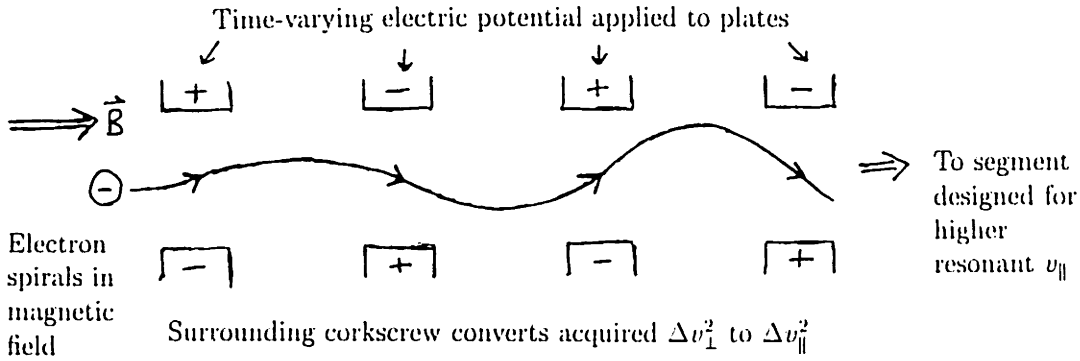

b)

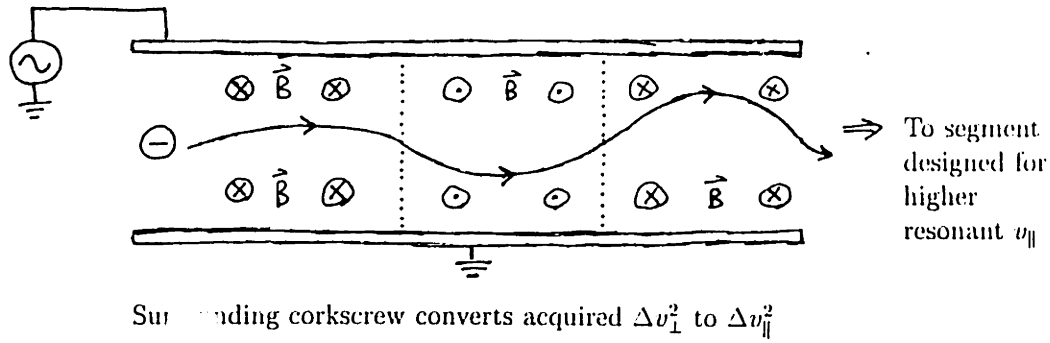

Figure E-6: Particle accelerating devices; similar systems can be used as direct electric converters to decelerate particles. The devices can be designed to interact with a specific particle species (electrons, fuel ions, or charged fusion products). a) Electric field wiggler system (surrounded by a magnetic corkscrew, not shown). b) Magnetic field wiggler system (surrounded by a magnetic corkscrew, not shown).

cycled through the system more than once in order to give them repeated opportunities to have the proper phase and be accelerated.

Particles of the same species which pass through the system in the opposite direction will be gyrating in the wrong direction to be in resonance with the corkscrew. Thus they can be in resonance with the electric field for at most a brief moment, and their energy will therefore be essentially constant.

If other species of particles are present in the device, their different charge or mass will prevent them from resonantly interacting with either the corkscrew or the electric field wiggler.

By designing the system so that the spatial periodicity at its entrance corresponds to a velocity somewhat lower than is expected to be found among the particles and also so that the resonant velocity increases up to a final value of the desired velocity v_o, the device can effectively form a "bucket lift" to sweep slow particles of all initial velocities up to the desired velocity.

Device for Decelerating Fast Particles

The principles just outlined may be used in reverse to create a device which will decelerate fast particles passing through it and directly convert the particles' energy into electrical energy. At the entrance of the device the electric field wiggler has a long spatial period, corresponding to a large resonant particle velocity. The spatial period steadily decreases down the length of the device until the resonant velocity at the exit is the desired value, v_o. Only particles whose $v_{\|}$ decreases sufficiently rapidly (and which have the desired phase) will stay in resonance with the wiggler electric field, which removes transverse energy from the particles. A decelerating corkscrew replenishes the particles' transverse energy at the same rate by drawing on their store of longitudinal energy, thereby slowing them enough to satisfy the electric field's resonance condition. As in the case of the accelerating device, particles which are of the wrong phase, are traveling in the wrong direction, or are of a

different species should at most only momentarily experience a net effect by the electric field, so their energies will remain essentially constant.

E.5.3 Magnetic Wiggler with RF Electric Field and Corkscrew

It is a rather simple task to come up with variations on this general idea. For instance, one could consider a device in which the frequency of the electric field variation is not velocity-dependent but the frequency of transverse velocity oscillations does depend on the longitudinal velocity–this situation corresponds to the opposite case from that considered in the previous section.

For this particular system, the transverse velocity oscillations can be caused by having the particles pass through a free-electron-laser-type magnetic wiggler, as shown in Figure E-6b. Static but spatially alternating transverse magnetic fields cause particles passing longitudinally through the system to wiggle back and forth in a direction perpendicular both to the direction of longitudinal motion and to the alternating magnetic field. If L now denotes the spatial period of the magnetic wiggler, then the angular frequency of the transverse velocity oscillations will be

$$\omega_v = \frac{2\pi}{L} v_{\|} \, . \tag{E.12}$$

If one applies a transverse radio-frequency electric field whose frequency is ω_E, only particles with the corresponding resonant value of $v_{\|}$,

$$v_{\|} = \frac{L}{2\pi} \omega_E \, , \tag{E.13}$$

will be able to exchange energy with the field.

As with the device described in the previous section, by varying L to increase the resonant velocity as a particle proceeds through the system and by adding an accelerating

corkscrew to convert $v_\perp^2$ to $v_\parallel^2$, this system can be made to accelerate slow particles of the desired species and phase while having a minimal effect on all other particles. Conversely, a device with a continually decreasing resonant value of $v_\parallel$ which is accompanied by a decelerating corkscrew may be used to decelerate fast particles and directly convert their energy into electricity.

E.6 Fokker-Planck Equation with a Velocity-Dependent Force

The most obvious way to hold a non-Maxwellian velocity distribution function in the desired shape despite collisional effects is to provide a force which focuses the particles in velocity space. At least hypothetically, such a force might be provided by resonant cyclotron emission and absorption in certain regions of velocity space or by other means. It is therefore of interest to derive the effect of a general velocity-dependent force $\mathbf{F}(\mathbf{v})$ on a particle distribution. This can be done by using the mathematical tools discussed in Chapter 2.

E.6.1 Equilibrium Particle Distribution Function

In order to simplify matters, it will be assumed that the plasma is in a steady state ($\partial f/\partial t = 0$) and that spatial diffusion may be neglected ($\nabla_{\mathbf{x}} f = 0$). With these assumptions , the Fokker Planck equation, Eq. (2.10), becomes

$$\frac{\mathbf{F}(\mathbf{v})}{m_\alpha} \cdot \nabla_{\mathbf{v}} f_\alpha = \left(\frac{\partial f_\alpha}{\partial t}\right)_{col} . \tag{E.14}$$

As a further simplification, the system will be considered to be isotropic; it will be assumed that $\mathbf{F}(\mathbf{v})$ only acts in the "radial" direction $\hat{\mathbf{v}}$ in velocity space and that the distribution functions involved in calculating the collision operator are spherically symmetric

with respect to velocity. While this choice may seem grossly inadequate to describe the systems which are under consideration, it should be a fairly reasonable approximation for studying the behavior of the plasma in the system as a whole, not just in any one section of the device (see for example Figure E-1). Moreover, the velocity-space calculations are made much more tractable by this assumption.

From Chapter 2, one recalls that the Fokker-Planck collision operator due to collisions with multiple particle species is given by

$$\left(\frac{\partial f_\alpha}{\partial t}\right)_{col} = \sum_\beta C_{\alpha\beta} \equiv -\nabla_{\mathbf{v}} \cdot \sum_\beta \mathbf{J}_{\alpha\beta} \,, \tag{E.15}$$

where the terms $\mathbf{J}_{\alpha\beta}$ have been defined as

$$\begin{aligned} \mathbf{J}_{\alpha\beta} \;=\; -\frac{16\pi^2 e^4 \ln\Lambda Z_\alpha^2 Z_\beta^2}{m_\alpha^2} \Bigg\{ \frac{\partial f_\alpha}{\partial v} \frac{1}{3} \left[\frac{1}{v^3} \int_0^v du f_\beta(u) u^4 + \int_v^\infty du f_\beta(u) u \right] \\ + f_\alpha \frac{m_\alpha}{m_\beta} \frac{1}{v^2} \int_0^v du f_\beta(u) u^2 \Bigg\} \hat{\mathbf{v}} \,. \end{aligned} \tag{E.16}$$

Using Equation (E.15) in Equation (E.14) and integrating both sides with respect to velocity, it is found that

$$\begin{aligned} \int d^3\mathbf{v} \mathbf{F}(\mathbf{v}) \cdot \nabla_{\mathbf{v}} f_\alpha &= -m_\alpha \int d^3\mathbf{v} \nabla_{\mathbf{v}} \cdot \mathbf{J}_\alpha(\mathbf{v}) \\ &= -m_\alpha \int_S \mathbf{J}_\alpha(\mathbf{v}) \cdot d\mathbf{v} \,, \end{aligned} \tag{E.17}$$

where the definition $\mathbf{J}_\alpha \equiv \sum_\beta \mathbf{J}_{\alpha\beta}$ has been made and Gauss's theorem has been used to rewrite the right-hand side of the equation as an integral over surface S in velocity space.

In a similar fashion, the left-hand side of this equation may be rewritten by using Green's first identity, so that

$$\int d^3\mathbf{v} \mathbf{F}(\mathbf{v}) \cdot \nabla_{\mathbf{v}} f_\alpha = \int_S f_\alpha(\mathbf{v}) \mathbf{F}(\mathbf{v}) \cdot d\mathbf{v} - \int d^3\mathbf{v} f_\alpha(\mathbf{v}) \nabla_{\mathbf{v}} \cdot \mathbf{F}(\mathbf{v}) \,. \tag{E.18}$$

Therefore the Fokker-Planck equation becomes

$$\int_S f_\alpha(\mathbf{v})\mathbf{F}(\mathbf{v})\cdot d\mathbf{v} - \int d^3\mathbf{v} f_\alpha(\mathbf{v})\nabla_\mathbf{v}\cdot\mathbf{F}(\mathbf{v}) \;=\; -m_\alpha\int_S \mathbf{J}_\alpha(\mathbf{v})\cdot d\mathbf{v}\,, \qquad \text{(E.19)}$$

which for an isotropic system reduces to

$$f_\alpha(v)F(v) - \frac{1}{v^2}\int_0^v dv' f_\alpha(v')\left[2v'F(v') + v'^2\frac{dF(v')}{dv'}\right] \;=\; -m_\alpha J_\alpha(v)\,. \qquad \text{(E.20)}$$

By using the expression for the collisional velocity-space flux J, it is found that

$$\begin{aligned} f_\alpha(v)F(v) \;-\; & \frac{1}{v^2}\int_0^v dv' f_\alpha(v')\left[2v'F(v') + v'^2\frac{dF(v')}{dv'}\right] \\ &= \sum_\beta \frac{16\pi^2 e^4 \ln\Lambda Z_\alpha^2 Z_\beta^2}{m_\alpha}\left\{ f_\alpha\frac{m_\alpha}{m_\beta}\frac{1}{v^2}\int_0^v du f_\beta(u)u^2 \right. \\ &\quad \left. + \frac{\partial f_\alpha}{\partial v}\frac{1}{3}\left[\frac{1}{v^3}\int_0^v du f_\beta(u)u^4 + \int_v^\infty du f_\beta(u)u\right]\right\}\,. \qquad \text{(E.21)} \end{aligned}$$

By specifying a particular velocity-dependent force and using Equation (E.21), the equilibrium particle distribution function may be found.

E.6.2 Power Input from Field to Particles

The power per volume delivered to the particles of the α species by the force $\mathbf{F}(\mathbf{v})$ is

$$P_{input} = \int d^3\mathbf{v} f_\alpha(\mathbf{v})\mathbf{F}(\mathbf{v})\cdot\mathbf{v}\,. \qquad \text{(E.22)}$$

For isotropic functions of velocity, this input power density is

$$P_{input} = \int_0^\infty dv 4\pi v^3 f_\alpha(v)F(v)\,. \qquad \text{(E.23)}$$

Provided that the various possible modes of energy loss are neglected, the required

input power needed to maintain a non-Maxwellian distribution should be zero; the power given to slow particles is compensated by the power extracted from fast particles. Of course, the necessity of pumping collisionally generated entropy out of the system will require that a small amount of heat energy be continually extracted from the plasma (and replaced by work input).

E.6.3 Evaluation for Particular Forms of Velocity-Dependent Forces

If the desired optimum velocity of the particles is v_o, the force should obey the relations,

$$F(v) \begin{cases} > 0 & \text{for } v < v_o \\ < 0 & \text{for } v > v_o. \end{cases} \tag{E.24}$$

One could consider various possible velocity-dependent forces which might be approximately realized by physical systems. As examples, two of the simplest possible functional forms for the force are a step function which jumps from positive to negative at $v = v_o$ and a linear function,

$$F(v) = (v_o - v)F_o \, , \tag{E.25}$$

where F_o is a positive constant.

These methods could be employed if one wished to explore further the remaining potentially feasible methods of maintaining nonequilibrium plasmas.

E.7 Summary

This appendix has discussed several broad categories of mechanisms by which electromagnetic fields might be used to maintain nonequilibrium plasmas or to improve the performance of aneutronic fusion systems. These proposals for new types of plasma systems have not yet been explored in any depth, and indeed there may be fatal flaws lurking

under the bed just about to spring on them. However, it is hoped that these ideas may at least serve as a starting point for future explorations of the few remaining potential pathways to nonequilibrium and aneutronic plasma fusion reactors. There may also be other, currently unforeseen uses for these types of devices, even if they should prove to be incapable of fulfilling any of their originally intended purposes.

Appendix F

Relative Importance of Synchrotron Radiation Losses and Bremsstrahlung Losses

In calculating the electron temperature and bremsstrahlung losses in this thesis, the effects of synchrotron radiation have been optimistically assumed to be negligibly small. While there are measures (such as the use of multipolar configurations [10], ring magnets [25], and plasma diamagnetism [18]) which can be taken in order to minimize the synchrotron losses, a realistic reactor will still have to cope with a certain amount of synchrotron radiation. Therefore, it is important to gain an understanding of the relative importance of synchrotron radiation as opposed to bremsstrahlung radiation in a variety of fusion reactor types.

The power density of emitted synchrotron radiation is given in [98] as:

$$P_{syn} = \frac{4e^4 B^2 n_e}{3m_e^2 c^3} \left(\frac{T_e}{m_e c^2}\right) \left[1 + \frac{5}{2}\left(\frac{T_e}{m_e c^2}\right)\right] . \qquad \text{(F.1)}$$

Evaluating the constants, defining V_{syn} to be the plasma volume which is under the influence of the magnetic field and emitting synchrotron radiation, letting f represent the fraction of the radiation which is actually lost (not reflected back into the plasma and reabsorbed there), and putting the electron temperature and rest energy in eV, the synchrotron power becomes

$$P_{syn} = 6.21 \cdot 10^{-28} B^2 n_e T_e \left[1 + \frac{5}{2}\left(\frac{T_e}{m_e c^2}\right)\right] f V_{syn} \text{ Watts.} \tag{F.2}$$

With the aid of Eq. (1.2), the ratio of the total synchrotron radiation power to the total bremsstrahlung power may be estimated from the expression

$$\frac{P_{syn}}{P_{brem}} \approx 3.67 \cdot 10^4 \, f \, \frac{V_{syn}}{V} \, \frac{B^2 \sqrt{T_e}}{\sum_i Z_i^2 n_i} \, , \tag{F.3}$$

in which V is the total plasma volume and the temperature is in eV. (For this estimate the relativistic corrections to the synchrotron and bremsstrahlung losses have been neglected, since they are roughly comparable.)

Of course, if properties such as the electron temperature, density, and magnetic field strength are not uniform, the above formula must be rewritten in terms of integrals over the plasma volume. The result has been written in the manner above in order to simplify its appearance and emphasize its physical meaning.

As has been shown in Chapters 6 and 7, the minimum bremsstrahlung losses are already quite considerable for all fuels other than D-T, so it would be best not to allow the synchrotron radiation to become a substantial additional loss. In order to ensure that the relationship $P_{syn}/P_{brem} \ll 1$ will be satisfied, one should choose a particular plasma confinement system which maximizes the density but minimizes B, T_e, and V_{syn}/V (the fraction of the volume in which a strong magnetic field is present) and which allows a large majority of the synchrotron radiation to be reflected from the walls and reabsorbed in the plasma ($f \ll 1$).

Because of the characteristic frequency range of synchrotron radiation, any of the radiation which does escape from the plasma system can quite possibly be directly converted into electrical energy at high efficiencies. However, it is still desirable to minimize the synchrotron radiation in order to avoid the unpleasant necessity of recirculating an amount of power which is substantial in comparison with the fusion power.

Energy losses due to the escape of electrons or fuel ions from the confinement system are clearly another important concern, but since they are entirely dependent on the particular configuration which is chosen, they have not been addressed in this thesis.

Bibliography

[1] O. Wilde, "The Ballad of Reading Gaol." (Originally published in 1898.) In *Plays, Prose Writings and Poems* (Alfred A. Knopf, Inc., New York, 1991).

[2] J.R. McNally, Jr., Fusion Chain Reactions [Parts I, II, and III]. *Nuclear Fusion* **11**, 187-193 (1971).

[3] T.A. Weaver, G.B. Zimmerman, and L.L. Wood, Prospects for Exotic Fuel Usage in CTR Systems I. $B^{11}(p,2\alpha)He^4$: A Clean, High Performance CTR Fuel. Lawrence Livermore National Laboratory, Report UCRL-74352, 1972.

[4] T.A. Weaver, G.B. Zimmerman, and L.L. Wood, Exotic CTR Fuels: Non-Thermal Effects and Laser Fusion Applications. Lawrence Livermore National Laboratory, Report UCRL-74938, 1973.

[5] L.L. Wood and T.A. Weaver, Some Direct Conversion Possibilities for Advanced CTR Systems. Lawrence Livermore National Laboratory, Report UCID-16229, 1973.

[6] T.A. Weaver, J.H. Nuckolls, and L.L. Wood, Fusion Microexplosions, Exotic Fusion Fuels, Direct Conversion: Advanced Technology Options for CTR. Lawrence Livermore National Laboratory, Report UCID-16309, 1973.

[7] T.A. Weaver and L.L. Wood, Some Promising Approaches to Advanced CTR Reactor Systems. Report UCID-16870, 1975.

[8] G.W. Shuy, Advanced Fusion Fuel Cycles and Fusion Reaction Kinetics (Ph.D. thesis, University of Wisconsin at Madison, 1980).

[9] G.W. Shuy and R.W. Conn, Charged Particle Cross Section Requirements for Advanced Fusion Fuel Cycles. In *Nuclear Cross Sections for Technology*, Volume 594, edited by J.L. Fowler, C.H. Johnson, and C.D. Bowman (U.S. Government Printing Office, Washington, D.C., 1980).

[10] R.W. Conn, G.W. Shuy, D. Kerst, I.N. Sviatoslavsky, D.K. Sze, D. Arnush, A.J. Cole, J.D. Gordon, L. Heflinger, T. Samec, W. Steele, C.C. Baker, A. Bolon, R.G. Clemmer, J. Jung, D.L. Smith, G.H. Miley, T. Blue, J. DeVeaux, D.E. Driemeyer, J. Gilligan, J. Metzger, and W. Tetley, Alternate Fusion Fuel Cycle Research. In

Plasma Physics and Controlled Nuclear Fusion Research 1980 (International Atomic Energy Agency, Vienna, 1981) Volume II, pp. 621-631.

[11] J.M. Dawson, Advanced Fuel Reactors. In *Fusion Volume 1. Magnetic Confinement Part B*, edited by E. Teller (Academic Press, New York, 1981).

[12] J.R. McNally, Jr., Physics of Fusion Fuel Cycles. *Nuclear Technology/Fusion* **2**, 9-28 (1982).

[13] L.M. Lidsky, End Product Economics and Fusion Research Program Priorities. *Journal of Fusion Energy* **2**, 269-292 (1982).

[14] L.M. Lidsky, The Trouble with Fusion. *Technology Review* **86** (7), 32-44 (October 1983).

[15] C. Powell, J. Nering, B.C. Maglich, and A. Wilmerding, Studies of Physics Conditions for Aneutronic and/or Nonradioactive Nuclear Energy Generation in ^{3}He-Induced Fission of ^{6}Li and ^{3}He Fusion in a Steady State Migma Plasma. *Nuclear Instruments and Methods in Physics Research* **A271**, 41-54 (1988).

[16] J. Golden and R.A. Miller, Monte Carlo Simulation of Energy Balance in a Pure ^{3}He Migma of 4 MeV. *Nuclear Instruments and Methods in Physics Research* **A271**, 79-88 (1988).

[17] G.H. Miley, H. Hora, L. Cicchitelli, G.V. Kasotakis, and R.J. Stening, An Advanced Fuel Laser Fusion and Volume Compression of p-^{11}B Laser-Driven Targets. *Fusion Technology* **19**, 43-51 (1991).

[18] R.W. Bussard, Some Physics Considerations of Magnetic Inertial-Electrostatic Confinement: A New Concept for Spherical Converging-Flow Fusion. *Fusion Technology* **19**, 273-293 (1991).

[19] R.W. Bussard, Preliminary Study of Inertial-Electrostatic-Fusion (IEF) for Electric Utility Power Plants. EPRI Report TR-103394 (February 1994).

[20] J.F. Santarius, K.H. Simmons, and G.A. Emmert, Modelling Inertial-Electrostatic-Confinement Fusion Devices. *Bulletin of the American Physical Society* **39**, 1740 (1994).

[21] H. Momota, Feasibility of Advanced Fuels. *Transactions of Fusion Technology* **27**, 28-31 (1995).

[22] J.D. Gordon, T.K. Samec, B.I. Hauss, S.A. Freije, W.G. Steele, I.N. Sviatoslavsky, D.K. Sze, R. Sanders, L.T. Pong, R.W. Conn, G. Shuy, R.N. Cherdack, J. Wysocki, J. Celnik, *Evaluation of Proton-Based Fuels for Fusion Power Plants* (Reports TRW-FRE-006 and TRW-FRE-007, TRW, Redondo Beach, CA, 1981).

[23] M.E. Sawan and I.N. Sviatoslavsky, Assessment of First Wall Lifetime in D-^{3}He and D-T Reactors with Impact on Reactor Availability. *Fusion Technology* **26**, 1141-1145 (1994).

[24] S. Glasstone and A. Sesonske, *Nuclear Reactor Engineering* (Third Edition, Van Nostrand Reinhold Company, New York, 1981).

[25] J.P. Blewett, Ring Magnets in Migma Systems. *Nuclear Instruments and Methods in Physics Research* **A271**, 214-216 (1988).

[26] L. Spitzer, *Monthly Notices, Royal Astronomical Society* **100**, 396 (London, 1940).

[27] L. Spitzer, *Physics of Fully Ionized Gases* (Interscience Publishers, Inc., New York, 1956; also Second Revised Edition, John Wiley & Sons, 1962).

[28] J.G. Cordey, in *Theory of Magnetically Confined Plasmas: Proceedings of Course and Workshop*, Varenna, Italy, 1977 (Pergamon Press, 1979), p. 307.

[29] J.M. Dawson, Series Lecture on Advanced Fusion Reactors (Research Report IPPJ-623, Institute of Plasma Physics, Nagoya University, Japan, 1983).

[30] D.L. Book, *NRL Plasma Formulary* (Naval Research Laboratory, Washington, revised 1987).

[31] S. Maxon, Bremsstrahlung Rate and Spectra from a Hot Gas (Z=1). *Physical Review A* **5**, 1630-1633 (1972).

[32] J.F. Clarke, Hot-Ion-Mode Ignition in a Tokamak Reactor. *Nuclear Fusion* **20**, 563-570 (1980).

[33] G.H. Miley, H. Towner, and N. Ivich, *Fusion Cross Sections and Reactivities.* University of Illinois, Champaign-Urbana, 1974.

[34] J.R. McNally, Jr., K.E. Rothe, and R.D. Sharp, *Fusion Reactivity Graphs and Tables for Charged Particle Reactions.* Oak Ridge National Laboratory, Report ORNL/TM-6914, 1979.

[35] R. Feldbacher, *The AEP Barnbook DATLIB, INDC(AUS)-12/G.* IAEA International Nuclear Data Committee, Vienna, October 1987.

[36] R. Feldbacher and M. Heindler, Basic Cross Section Data for Aneutronic Reactor. *Nuclear Instruments and Methods in Physics Research* **A271**, 55-64 (1988).

[37] D.C. Barnes, R.A. Nebel, and L. Turner, Production and Application of Dense Penning Trap Plasmas. *Physics of Fluids B* **5**, 3651-3660 (1993).

[38] B.C. Maglich, Time Average Neutralized Migma: A Colliding Beam/Plasma Hybrid Physical State as Aneutronic Energy Source - A Review. *Nuclear Instruments and Methods in Physics Research* **A271**, 13-36 (1988).

[39] B.C. Maglich, T.F. Chuang, C. Powell, J. Nering, and A. Wilmerding, Fokker-Planck Simulation of Strong-Focused D+^{3}He Plasma and Experimental Observation of 725 keV Deuterium Migma Stabilized by Oscillating Electrons. Joint USA-Japan Fusion Workshop: Physics of High Energy Particles in Toroidal Systems (Irvine, CA, August 30-September 1, 1993).

[40] S. Tamor, G.W. Shuy, and P. Stroud, Proton Based Fusion Fuel Cycles with Non-Thermal Distributions. American Nuclear Society Conference (1985).

[41] N. Rostoker, F. Wessel, H. Rahman, B.C. Maglich, B. Spivey, and A. Fisher, Magnetic Fusion with High Energy Self-Colliding Ion Beams. *Physical Review Letters* **70**, 1818-1821 (1993).

[42] E.A. Frieman, M.L. Goldberger, K.M. Watson, S. Weinberg, and M.N. Rosenbluth, Two-Stream Instability in Finite Beams. *Physics of Fluids* **5**, 196-209 (1962).

[43] E.S. Weibel, Spontaneously Growing Transverse Waves in a Plasma Due to an Anisotropic Velocity Distribution. *Physical Review Letters* **2**, 83-84 (1959).

[44] H.P. Furth, Prevalent Instability of Nonthermal Plasmas. *Physics of Fluids* **6**, 48-57 (1963).

[45] M.N. Rosenbluth, Energy Exchange Between Electrons and Ions. Gulf General Atomic Report GAMD-1710 (1960).

[46] M.N. Rosenbluth, Energy Exchange Between Electrons and Ions. *Bulletin of the American Physical Society* **21**, 1114-1115 (1976).

[47] Dante Alighieri, *The Inferno.* In *The Divine Comedy* (originally written circa 1320, translated by H.F. Cary, International Collectors Library, Garden City, New York, 1946).

[48] M.N. Rosenbluth, W.M. MacDonald, and D L. Judd, Fokker-Planck Equation for an Inverse-Square Force. *Physical Review* **107**, 1-6 (1957).

[49] W.M. MacDonald, M.N. Rosenbluth, and W. Chuck, Relaxation of a System of Particles with Coulomb Interactions. *Physical Review* **107**, 350-353 (1957).

[50] J.P. Freidberg, *Theory of Magnetic Confinement I*, MIT class notes (unpublished, 1991).

[51] P.J. Catto (private communication, March 10, 1994).

[52] I.S. Gradshteyn and I.M. Ryzhik, *Table of Integrals, Series, and Products* (Academic Press, Inc., New York, 1980).

[53] P.J. Catto (private communication, June 17, 1994).

[54] Wolfram Research, Inc., *Mathematica,* Version 2.2 (Wolfram Research, Inc., Champaign, IL, 1993).

[55] J.D. Galambos, Effects of Nuclear Elastic Scattering and Modifications of Ion-Electron Equilibration Power on Advanced-Fuel Burns (Ph.D. thesis, University of Illinois at Urbana/Champaign, 1982).

[56] J.D. Galambos (private communication, September 20, 1994).

[57] M.G. McCoy, A.A. Mirin, and J. Killeen, FPPAC: A Two-Dimensional Multispecies Nonlinear Fokker-Planck Package. *Computer Physics Communications* **24**, 37-61 (1981).

[58] A.A. Mirin, M.G. McCoy, G.P. Tomashke, and J. Killeen, FPPAC88: A Two-Dimensional Multispecies Nonlinear Fokker-Planck Package. *Computer Physics Communications* **51**, 373-380 (1988).

[59] D.V. Sivukhin, in *Reviews of Plasma Physics*, edited by M.A. Leontovich (Consultants Bureau, New York, 1966), Vol. 4, pp. 93-241.

[60] W.M. Siebert, *Circuits, Signals, and Systems* (MIT Press, Cambridge, Massachusetts, 1986).

[61] L.D. Landau and E.M. Lifshitz, *Statistical Physics Part 1* (3rd Edition, Pergamon Press, New York, 1980).

[62] Waterloo Maple Software, *Maple V*, Release 3 (Waterloo Maple Software, University of Waterloo, Ontario, Canada, 1994).

[63] R.D. Hazeltine and J.D. Meiss, *Plasma Confinement* (Addison-Wesley Publishing Company, New York, 1992).

[64] J.A. McLennan, *Introduction to Nonequilibrium Statistical Mechanics* (Prentice Hall, Inc., New Jersey, 1989).

[65] S.R. de Groot and P. Mazur, *Non-Equilibrium Thermodynamics* (North-Holland Publishing Company, Amsterdam, 1962).

[66] A.W. Morgenthaler and P.L. Hagelstein, Kinetic Theory of a Nonequilibrium Plasma: Evaluation of the Vectorized Collisional Boltzmann Equation. *Physics of Fluids B* **5**, 1453-1470 (1993).

[67] M. Rosenberg and N.A. Krall, The Effect of Collisions in Maintaining a Non-Maxwellian Plasma Distribution in a Spherically Convergent Ion Focus. *Physics of Fluids B* **4**, 1788-1794 (1992).

[68] D.C. Barnes (private communication, January 11, 1995).

[69] S. Ichimaru, *Basic Principles of Plasma Physics. A Statistical Approach* (Addison-Wesley Publishing Company, New York, 1973).

[70] J.M. Dawson, H.P. Furth, and F.H. Tenney, Production of Thermonuclear Power by Non-Maxwellian Ions in a Closed Magnetic Field Configuration. *Physical Review Letters* **26**, 1156-1160 (1971).

[71] R.F. Post, K.D. Marx, and C.J. Eggens, Creation of Transient High-Density Plasmas by Convergent Neutral Beams. *Nuclear Fusion* **15**, 701-703 (1975).

[72] P.J. Catto and J.R. Myra, Entropy Production Determination of the Ambipolar Solution Nearest Equilibrium. *Plasma Physics and Controlled Fusion* **28**, 959-972 (1986).

[73] J. Oxenius, *Kinetic Theory of Particles and Photons. Theoretical Foundations of Non-LTE Plasma Spectroscopy* (Springer-Verlag, Berlin, 1986).

[74] E.M. Lifshitz and L.P. Pitaevskii, *Physical Kinetics* (3rd Edition, Pergamon Press, New York, 1981).

[75] M.S. Livingston and J.P. Blewett, *Particle Accelerators* (McGraw-Hill Book Company, Inc., New York, 1962).

[76] M. Conte and W.W. MacKay, *An Introduction to the Physics of Particle Accelerators* (World Scientific Publishing Co., New Jersey, 1991).

[77] H. Wiedemann, *Particle Accelerator Physics. Basic Principles and Linear Beam Dynamics* (Springer-Verlag, Berlin, 1993).

[78] A. Yariv, *Quantum Electronics,* third edition (John Wiley & Sons, New York, 1989).

[79] R.C. Davidson, *Methods in Nonlinear Plasma Theory* (Academic Press, Inc., New York, 1972).

[80] D.G. Swanson, *Plasma Waves* (Academic Press, Inc., New York, 1989).

[81] J.R. McNally, Jr., Simple Physical Model for the Effect of a Magnetic Field on the Coulomb Lagarithm for Test Ions Slowing Down on Electrons in a Plasma. *Nuclear Fusion* **15**, 344-346 (1975).

[82] J. Galambos and G.H. Miley, Effects of Enhanced Ion/Electron Equilibration Power on Cat-D Tokamak Ignition. *Nuclear Technology/Fusion* **4**, 241-245 (1983).

[83] S. Ichimaru and M.N. Rosenbluth, Relaxation Processes in Plasmas with Magnetic Field. Temperature Relations. *Physics of Fluids* **13**, 2778-2789 (1970).

[84] R.C. Davidson, *Physics of Nonneutral Plasmas* (Addison-Wesley Publishing Company, New York, 1990).

[85] L. Turner and D.C. Barnes, The Brillouin Limit and Beyond: A Route to Inertial-Electrostatic Confinement of a Single-Species Plasma. *Physical Review Letters* **70**, 798 (1993).

[86] T.H. Rider, A General Critique of Inertial-Electrostatic Confinement Fusion Systems. To appear in *Physics of Plasmas.*

[87] W.M. Nevins, Can Inertial Electrostatic Confinement Work Beyond the Ion-Ion Collisional Time Scale? Submitted to *Physics of Plasmas* (January 1995).

[88] J. Galambos, J. Gilligan, E. Greenspan, P. Stroud, and G.H. Miley, Discrete Nuclear Elastic Scattering Effects in Cat-D and D-^{3}He Fusion Plasmas. *Nuclear Fusion* **24**, 739-750 (1984).

[89] Y. Nakao, M. Ohta, and H. Nakashima, Effects of Nuclear Elastic Scattering on Ignition and Thermal Instability Characteristics of D-D Fusion Reactor Plasmas. *Nuclear Fusion* **21**, 973-979 (1981).

[90] Y. Nakao, K. Kai, H. Matsuura, and K. Kudo, Effect of Nuclear Elastic Scattering on Fusion Reactivity of Self-Sustaining D-^{3}He Plasmas. *Transactions of Fusion Technology* **27**, 555-558 (1995).

[91] E. Greenspan and D. Shvarts, A Multigroup Model for the Slowing Down of Energetic Ions in Plasmas. *Nuclear Fusion* **16**, 295-302 (1976).

[92] F.D. Kantrowitz and R.W. Conn, Kinetic Analysis of Nuclear and Coulomb Scattering in High-Temperature Tandem Mirror Plasmas. *Nuclear Fusion* **24**, 1335-1346 (1984).

[93] N.J. Fisch and J.M. Rax, Interaction of Energetic Alpha Particles with Intense Lower Hybrid Waves. *Physical Review Letters* **69**, 612-615 (1992).

[94] E.J. Valeo and N.J. Fisch, Excitation of Large-k_θ Ion-Bernstein Waves in Tokamaks. *Physical Review Letters* **73**, 3536-3539 (1994).

[95] G.A. Emmert, L.A. El-Guebaly, G.L. Kulcinski, J.F. Santarius, I.N. Sviatoslavsky, and D.M. Meade, Improvement in Fusion Reactor Performance Due to Ion Channeling. *Fusion Technology* **26**, 1158-1162 (1994).

[96] G. Bekefi, *Radiation Processes in Plasmas* (Wiley, New York, 1966).

[97] T.W. Johnston and J.M. Dawson, Correct Values for High-Frequency Power Absorption by Inverse Bremsstrahlung in Plasmas. *Physics of Fluids* **16**, 722 (1973).

[98] K. Miyamoto, *Plasma Physics for Nuclear Fusion* (MIT Press, Cambridge, MA, 1989).

[99] M.N. Rosenbluth and F.L. Hinton, Generic Issues for Direct Conversion of Fusion Energy from Alternative Fuels. *Plasma Physics and Controlled Fusion* **36**, 1255-1268 (1994).

[100] W.L. Barr, R.W. Moir, and G.W. Hamilton, Experimental Results from a Beam Direct Converter at 100 kV. *Journal of Fusion Energy* **2**, 131-143 (1982).

[101] W.L. Barr, and R.W. Moir, Test Results on Plasma Direct Converters. *Nuclear Technology/Fusion* **3**, 98-111 (1983).

[102] H. Momota, A. Ishida, Y. Kohzaki, G.H. Miley, S. Ohi, M. Ohnishi, K. Sato, L.C. Steinhauer, Y. Tomita, and M. Tuszewski, Conceptual Design of the D-^{3}He Reactor Artemis. *Fusion Technology* **21**, 2307-2323 (1992).

[103] L.Y. Syu, G.H. Miley, Y. Tomita, and H. Momota, Analytical Studies on a Traveling Wave Direct Energy Converter for D-^{3}He Fusion. *Transactions of Fusion Technology* **27**, 551-554 (1995).

[104] H. Katayama, K. Sato, and F. Miyawaki, Direct Energy Conversion for D-^{3}He Reactor. *Transactions of Fusion Technology* **27**, 563-566 (1995).

[105] G. Chapline and R. Moir, Some Thoughts on the Production of Muons for Fusion Catalysis. *Journal of Fusion Energy* **5**, 191-200 (1986).

[106] B. Brunelli and G.G. Leotta (eds.), *Muon-Catalyzed Fusion and Fusion with Polarized Nuclei* (Plenum Press, New York, 1987).

[107] L.J. Perkins, J.H. Hammer, S.W. Haney, and D.E. Morgan, Prospects for Fusion with Reduced Coulomb Barriers. *Bulletin of the American Physical Society* **39**, 1760 (1994).

[108] O. Mitarai, H. Hasuyama, and Y. Wakuta, Spin Polarization Effect on Ignition Access Condition for D-T and D-^{3}He Tokamak Fusion Reactors. *Fusion Technology* **21**, 2265-2283 (1992).

[109] S. Ichimaru, Nuclear Fusion in Dense Plasmas. *Reviews of Modern Physics* **65**, 255-305 (1993).

[110] P.L. Hagelstein, Lattice-Induced Atomic and Nuclear Reactions. *Transactions of Fusion Technology* **26**, 461-473 (1994).

[111] B.H. Duane, *Fusion Cross Section Theory.* U.S. Atomic Energy Commission, Report BNWL-1685 (1972).

[112] M. Twain (S. Clemens), "Dr. Loeb's Incredible Discovery." In *The Complete Essays of Mark Twain*, edited by C. Neider (Doubleday & Company, Garden City, N.Y., 1963).

[113] R.C. Wingerson, "Corkscrew" - A Device for Changing the Magnetic Moment of Charged Particles in a Magnetic Field. *Physical Review Letters* **6**, 446-448 (1961).

[114] R.C. Wingerson, T.H. Dupree, and D.J. Rose, Trapping and Loss of Charged Particles in a Perturbed Magnetic Field. *Physics of Fluids* **7**, 1475-1484 (1964).

[115] L.M. Lidsky, Orbit Stability in a Helically Perturbed Magnetic Field. *Physics of Fluids* **7**, 1484-1488 (1964).

[116] J.F. Clarke and L.M. Lidsky, Velocity Diffusion in Resonantly Perturbed Magnetic Field. *Physics of Fluids* **13**, 1580-1585 (1970).

[117] R.W. Moir and L.M. Lidsky, Diffusion Resulting from Nonadiabatic Scattering on a Helically Perturbed Field in a Torus. *Plasma Physics* **13**, 159-171 (1971).

[118] N.W. Ashcroft and N.D. Mermin, *Solid State Physics* (W.B. Saunders Company, Philadelphia, 1976).

[119] D.R. Nicholson, *Introduction to Plasma Theory* (John Wiley & Sons, New York, 1983).

[120] H. Goldstein, Classical Mechanics (2nd Edition, Addison-Wesley Publishing Company, Reading, Massachusetts, 1980).

[121] F. Reif, *Fundamentals of Statistical and Thermal Physics* (McGraw-Hill Book Company, New York, 1965).

[122] M. Shelley, *Frankenstein.* (Originally published in 1818.) In *Classics of Horror* (Longmeadow Press, Stamford, Connecticut, 1991).

Vita

The author is one of Arkansas's few exports, along with Bill Clinton and Tyson chicken. (He is not to blame for Bill Clinton.) In 1986 he was found to be a nerd and was therefore promptly institutionalized at MIT as a freshman, and he didn't manage to escape until June 1995. During his internment, he passed the time by cranking out this tome and collecting three minors for the Ph.D. program: biomedicine, solid state and optical physics, and relativistic quantum field theory. He also picked up a Master's degree in nuclear engineering, took several classes in mechanical engineering, moseyed over to Harvard for various and sundry medical school, physics, and humanities classes, and haunted the foreign languages department for some time, studying French, German, Japanese, and Chinese.

In his free time, the author spent approximately 150 hours as a volunteer in public school classrooms teaching physics to eighth- and ninth-grade students (much to their horror), and as a result of these experiences he produced over 250 pages of physics curriculum material presenting everything from Newton's laws to quantum mechanics on a junior high school level. The author is also rather partial to writing poetry, reading literature, and eating pizza.

Now that he has escaped out into the real world, the author aspires to become a mad scientist. Accordingly, his first major career goal is to be the sinister cause of one of the cases in *The X-Files.*

"As a child I had not been content with the results promised by the modern professors of natural science. With a confusion of ideas only to be accounted for by my extreme youth and my want of a guide on such matters, I had retrod the steps of knowledge along the paths of time and exchanged the discoveries of recent enquirers for the dreams of forgotten alchemists. Besides, I had a contempt for the uses of modern natural philosophy. It was very different when the masters of the science sought immortality and power; such views, although futile, were grand; but now the scene was changed. The ambition of the enquirer seemed to limit itself to the annihilation of those visions on which my interest in science was chiefly founded. I was required to exchange chimeras of boundless grandeur for realities of little worth... [S]oon my mind was filled with one thought, one conception, one purpose. So much has been done, exclaimed the soul of Frankenstein–more, far more, will I achieve; treading in the steps already marked, I will pioneer a new way, explore unknown powers, and unfold to the world the deepest mysteries of creation."

– Mary Shelley's *Frankenstein*, Chapter III (1818) [122]